ANALYSIS OF ELASTIC SHELLS OF REVOLUTION WITH MEMBRANE AND FLEXURE STRESSES UNDER ARBITRARY LOADING USING TRAPEZOIDAL FINITE ELEMENTS

by

KRISHNA MURARI AGRAWAL

B.E. (Hons.) University of Jabalpur, India, 1961
M.E. (Struct.) University of Roorkee, India, 1963

A THESIS SUBMITTED IN PARTIAL FULFILMENT OF

THE REQUIREMENTS FOR THE DEGREE OF

DOCTOR OF PHILOSOPHY

in the Department

of

CIVIL ENGINEERING

We accept this thesis as conforming

to the required standard

THE UNIVERSITY OF BRITISH COLUMBIA

April, 1968

In presenting this thesis in partial fulfilment of the requirements for an advanced degree at the University of British Columbia, I agree that the Library shall make it freely available for reference and study. I further agree that permission for extensive copying of this thesis for scholarly purposes may be granted by the Head of my Department or by his representatives. It is understood that copying or publication of this thesis for financial gain shall not be allowed without my written permission.

K.M. Agrawal

Department of Civil Engineering

The University of British Columbia
Vancouver 8, Canada

Date April, 1968

ABSTRACT

Analysis of a general shell of revolution with arbitrary loading and boundary conditions using the Finite Element approach, well-suited for use with the electronic computer, is presented. The shell is approximated by an assemblage of flat, equilateral trapezoids and isosceles triangles connected to each other at the corners. The assumptions involved in transforming a piece of plate into a finite element are defined. Uncoupled plane stress and flexure stiffness matrices for the above-mentioned shapes of the finite elements are derived from considerations of (i) statics, and (ii) virtual work (energy). Statics matrices are asymmetric with the exception of the triangle plane stress stiffness matrix. However, it is important to note that irrespective of the size of the trapezoid element, in conditions of uniform stress the nodal forces satisfy Betti's reciprocal theorem. When a trapezoid reduces to a rectangle, the asymmetry of plane stress and flexure stiffness matrices disappears.

Asymmetry of the Statics matrix is removed by averaging the matrix and its transpose. This process corresponds to introducing self-equilibrating nodal forces which disappear in conditions of uniform stress.

Suitable direction cosine matrices are derived to transform the displacements and forces from the element coordinate system to the shell coordinate system.

The accuracy of the formulation is demonstrated in several examples by comparing the finite element solution with the elasticity solution. The comparison suggests convergence of the results to the correct solution on reduction of the element size.

DEDICATED TO MY PARENTS SHANTI DEVI AND GOVIND DAS AGRAWAL

TABLE OF CONTENTS

TABLE OF CONTENTS (Cont'd)

TABLE OF CONTENTS (cont'd)

TABLE OF CONTENTS (cont'd)

TABLE OF CONTENTS (cont'd)

LIST OF TABLES

LIST OF TABLES (cont'd)

LIST OF TABLES (cont'd)

LIST OF TABLES (cont'd)

LIST OF FIGURES

LIST OF FIGURES (cont'd)

LIST OF FIGURES (Cont'd)

LIST OF SYMBOLS

Symbol	
a	half of the top side of a trapezoid
$a_1,\ldots,a_{12}$	constant parameters
b_i	constant parameter associated with the i th displacement mode
c	projection of the inclined side of a trapezoid on the X-axis, positive if the bottom side is bigger than the top side; also, half of the base of an isosceles triangle
D_1	$= Et/(1-\mu^2)$, extensional rigidity per unit length of the plate
D_2	$= Et^3/12(1-\mu^2)$, flexural rigidity per unit length of the plate
E	modulus of elasticity
f_i	nodal force in the i th direction
h	half of the height of a trapezoid or a triangle
K	ratio of the bottom side to the top side of a trapezoid; also, ratio of height to base of a triangle
K_1	ratio of height to top side of a trapezoid
$K_{i,j}$	stiffness coefficient belonging to i th row and j th column of the stiffness matrix
M_n	bending moment/length in n-direction (perpendicular to the inclined edge)
M_{nt}	twisting moment/length on n-plane
M_x, M_y	bending moments/length in X and Y directions
M_{xy}, M_{yx}	twisting moments/length on X and Y planes
M_θ, M_ϕ	bending moments/length in θ and ϕ (parallel and meridian) directions
$M_{\theta\phi}, M_{\phi\theta}$	twisting moments/length on θ and ϕ planes
n	no. of corners in a finite element; also, direction normal to the inclined edge
N	total degrees of freedom of corner movements of an element

LIST OF SYMBOLS (cont'd)

Symbol	
N_θ, N_ϕ	membrane direct force/length in θ and ϕ (i.e. parallel and meridian) directions
$N_{\theta\phi}, N_{\phi\theta}$	membrane shear on θ and ϕ planes
p	intensity of the distributed load
P,M,R	shell coordinate directions (tangent to the parallel circle, tangent to the meridian circle and normal to the shell surface)
Q_x, Q_y	transeverse shears on X and Y planes
R	radius of curvature of the shell surface at a point
R_L	radius of the parallel circle containing lower nodes 1 and 2 of an element
R_U	radius of the parallel circle containing upper nodes 3 and 4 of an element
t	thickness of a plate element (assumed same as shell)
u,v	displacements in X and Y directions in the plane of the plate
w	displacement in Z-direction
We_j	external work done by the nodal forces of the finite element due to a virtual displacement $\{\bar{\delta}\}_j$ which is unity in the jth direction and zero in all other directions
Wi_j	internal work done by the internal forces of the plate element due to a virtual displacement $\{\bar{\delta}\}_j$
x,y	coordinates of a point on the plate element
XYZ	element coordinate direction - right hand system
X-Y-Z	shell coordinate directions at the apex
α	accute angle in the plane of the flat element between Y-axis and the inclined side - positive if counter-clockwise
$\alpha_1, \alpha_2, \ldots$	constant coefficients
β	at the lower node, angle between tangent to the meridian and the chord line joining the lower and the upper nodes of the element

LIST OF SYMBOLS (cont'd)

Symbol	
β_1	at the upper nodes, angle between tangent to the meridian and the chord line joining the lower and the upper nodes of the element $(\beta_1 = \phi_u - \phi_L - \beta)$
γ	angle of inclination of the element with the plane of a parallel circle
δ_i	nodal displacement in the ith direction
ε	half the accute angle between the planes of two equal adjacent flat elements intersecting along a common inclined edge
$\varepsilon_x, \varepsilon_y$	direct strains in X and Y directions
ε_{xy}	shear strain
θ	angle between the planes of reference meridian and a meridian passing through a point on the shell; looking from top - counter-clockwise angle positive
θ_e	angle between the adjacent meridian planes which enclose the element
θ_x	horizontal angle between the base of a triangle element and the X-direction at the apex
μ	Poisson's ratio
ξ	horizontal displacement
σ_x, σ_y	direct stresses in X and Y directions
σ_{xy}	shear stress
ϕ	angle between the axis of rotation and tangent to the meridian at a point on the shell
ϕ_e	difference of the angles made by tangents to the meridian at upper and lower nodes of an element with the axis of rotation $(= \phi_U - \phi_L)$
ϕ_L, ϕ_U	angle between the axis of rotation and tangent to a meridian at lower and upper nodes respectively of an element
χ	rotation about P-axis

LIST OF SYMBOLS (cont'd)

MATRIX SYMBOLS

Note: (i) a subscript Δ refers to a triangle element

(ii) a superscript * refers to a flexure element

Symbol	
$[A]$	N x N matrix in terms of nodal coordinates
$\{B\}$	N x 1 matrix of constant parameters; $b_1, b_2, \ldots, b_N$
$[C]$	N x N matrix of statically equivalent corner forces. Entries of the jth column of this matrix correspond to statically equivalent nodal forces due to a displacement mode b_j
$[D]$	3 x 3 symmetric matrix containing elastic constants
$\{f\}$	N x 1 matrix of nodal forces; $f_1, f_2, \ldots, f_N$
$\{f\}_{XYZ}, \{f\}_{PMR}$	forces in element coordinates X-Y-Z and in shell coordinates P-M-R respectively
$[G]$	3 x N matrix in terms of variables x and y
$[H]$	N x N symmetric matrix defined by $\iint_{area} [G]^T [D][G] dxdy$
$[I]$	N x N identity matrix
$[K]$	N x N stiffness matrix of the finite element
$[K]_{XYZ}, [K]_{PMR}$	stiffness matrix in element coordinates X-Y-Z and shell coordinates P-M-R respectively
$\{M^*\}$	3 x 1 moment matrix (M_x, M_y and M_{xy})
$[MT^*]$	3 x N moment matrix in terms of variables x and y
$[Q^*]$	2 x 1 matrix of transeverse shears (Q_x and Q_y)
$[R^*]$	2 x N matrix in terms of variables x and y
$[S]$	entire structure stiffness matrix
$[ST]$	3 x N stress matrix in terms of variables x and y
$[T]$	transformation matrix
$[T^i]$	3 x 3 matrix containing cosines of the angles between P-M-R axes and the XYZ axes at node i

LIST OF SYMBOLS (cont'd)

Symbol

$[T^3_\Delta]$	3 x 3 matrix containing cosines of the angles between X-Y-Z directions of the shell at the apex and X-Y-Z directions of a triangle
$\{We\}$	N x 1 matrix of external work done by the nodal forces of the finite element due to all virtual displacement $\{\bar{\delta}\}_j$, $j = 1,2,\ldots,N$
$\{Wi\}$	N x 1 matrix of internal work done by the internal forces of the plate element due to all virtual displacements $\{\bar{\delta}\}_j$, $j = 1,2,\ldots,N$
$\{\delta\}$	N x 1 matrix of nodal displacements; $\delta_1, \delta_2, \ldots, \delta_N$
$\{\bar{\delta}\}_j$	N x 1 matrix of virtual displacements; here, the displacement in the jth direction is equal to unity and zero in all other directions
$[\bar{\delta}]$	N x N matrix of all virtual displacements; i.e. $\{\bar{\delta}\}_i$, $i = 1,2,\ldots,N$ = N x N identity matrix, [I]
$\{\delta\}_{XYZ}, \{\delta\}_{PMR}$	nodal displacements in element coordinates X-Y-Z and shell coordinates P-M-R respectively
$\{\Delta\}$	structure deformation vector
$\{\varepsilon\}$	3 x 1 matrix of strains (ε_x, ε_y and ε_{xy})
$\{\bar{\varepsilon}\}_j$	3 x 1 matrix of strains due to a virtual displacement, $\{\bar{\delta}\}_j$
$\{\sigma\}$	3 x 1 matrix of stresses (σ_x, σ_y and σ_{xy})
$\{\chi^*\}$	3 x 1 matrix of curvatures $\left(-\frac{\partial^2 w}{\partial x^2}, -\frac{\partial^2 w}{\partial y^2}, 2\frac{\partial^2 w}{\partial x \partial y}\right)$
$\{\bar{\chi}^*\}_j$	3 x 1 matrix of curvatures due to virtual deformations, $\{\bar{\delta}^*\}_j$

ACKNOWLEDGEMENTS

The author is greatly indebted to his thesis director, Dr. A. Hrennikoff for recommending the thesis topic and for offering suggestions and critical checks at various stages of the study. His keen insight into the physical behaviour of finite elements greatly helped the development of the subject.

The author is also grateful to Dr. S. Tezcan, Dr. S. Cherry, Dr. B. Ovunc and other members of his Ph.D. committee with whom he had helpful discussions.

Thanks are also due the University of British Columbia Computing Centre for free use of facilities, Diane Johnson for efficient typing of the thesis, and finally my wife, Christine, whose constant encouragement made this thesis become reality.

CHAPTER I

INTRODUCTION

1.1 General

Shells of revolution are structural forms whose middle surfaces are generated by rotating a plane curve about an axis in its plane. Conical shells and domes are examples of shells of revolution. These structural forms provide a unique feeling of spatial continuity and architectural beauty and are used to enclose large column-free spaces. Due to the curved nature of their surface, shells are capable of carrying external loads mainly by membrane action. In building construction, they are as ancient as the Roman Pantheon of 120 A.D. The Pantheon, built by the Roman Emperor, Hadrian, for the worship of pagan gods, is a massive dome structure over 4 ft. in thickness.[1] Today, however, with better understanding of the inherent strength in shape, shells are being built with thicknesses as little as 2.5 inches.[2]

Rigorous solution for deflections and stresses in shells of revolution are obtainable for very simple geometry and certain specific boundary and loading conditions. However, when complicated geometry and arbitrary boundary and loading conditions are involved, the solution of the governing differential equation becomes extremely complicated and often impossible.

1.2 The Finite Element Method of Solution

Approximate solution of a continuum problem can be obtained by recourse to the Finite Element (F.E.) method. For axisymmetric shells, the finite element method has been suggested using: (1), elements in the form of a frustrum of a cone[3-5], and (2), doubly curved elements in the form of a frustrum of a shell of revolution.[6] The above methods consider axisymmetric deformations only. The extension to unsymmetric deformations, by means of Fourier expansion, is suggested by Percy et al.[7] An extensive survey of the existing methods of analysis of shells of revolution is presented by Jones and Strome.[8] However, these methods are restricted to axisymmetric boundary conditions. It is therefore desirable to have a method of solution which will handle a completely general shell of revolution problem with arbitrary loading and boundary conditions.

1.3 The Flat Polygonal Finite Element

In the present analysis, the restrictions of axisymmetric loading and boundary conditions involved in the use of finite elements in the shape of a frustrum of a cone are removed. The use of polygonal elements, connected to each other at the corners, allows the solution of a general shell of revolution with completely arbitrary boundary and loading conditions. The matrix algebra method of structural analysis, best-suited for use with the high-speed electronic computer, is applicable.

It has, at times, been suggested that the curved shape of polygonal shell elements should be used to avoid difficulty of discontinuities in geometry. This may increase the accuracy of the solution, but will also undoubtedly increase the derivation complications and computational

difficulties of the force-displacement relations of the finite element. The need of curved elements may not arise if it can be shown that good approximation to the true solution can be achieved using flat elements. In a shell problem, the size of subdivision necessary to obtain reasonable accuracy is not obvious, but in the regions of rapidly-changing displacements and stresses, small sized elements must be used. If the ratio of the radius of curvature of the curved element to its side is large, the influence of curvature on the force-displacement properties of the element is small, and in such a case, a curved element essentially behaves as a flat element. Thus, the use of flat element seems to be adequate for the analysis of shells.

1.4 Shape of the Polygonal Finite Element

A model of a shell of arbitrary shape can be made from an assemblage of flat triangular elements.[9,10] However, it has been shown that in general quadrilateral elements provide greater accuracy than the triangular elements.[11,12] Yet, in special circumstances the use of triangular elements cannot be completely avoided. In a shell of revolution, advantage of geometrical symmetry is taken in selecting the shape of quadrilateral finite elements. The shell surface is subdivided by a number of meridian lines and parallel circles. The curved portion of the shell enclosed between two meridian lines and two parallel circles is approximated by a flat surface in the shape of an equilateral trapezoid. The elements joining the apex are in the shape of isosceles triangles. Therefore, the solution of a shell of revolution will involve finite elements in the shape of equilateral trapezoids and isosceles triangles. This approximation introduces some errors in the results apart from those due to the finite size of the elements. However, as the element size decreases, the model approaches the

continuously curved shape, thereby reducing the errors.

1.5 Types of Stresses in a Shell

The scope of the study here is limited to elastic shells of revolution subjected to small deflections. A shell normally has both membrane and flexure stresses induced in it. It is therefore necessary to assign both plane stress and flexure properties to the finite element used in the analysis. For small deflections, the equations of statics are written for an undeformed plate. This permits an independent derivation of the stress-deformation relations of an element in plane stress and flexure which are finally reduced to the combined relations.

1.6 The Nature of a Finite Element

The nature of a plane stress finite element may be explained in the following manner. Consider a homogeneous plate of large dimensions in X-Y plane subjected to a simple stress condition such as uniform unidimensional strain or shearless bending in X-direction. Remove from this plate a polygonal area of the shape of the assumed finite element. It is held in equilibrium by the appropriate edge stresses. Assume now that the edge stresses are replaced by proper statically equivalent nodal forces, the corner displacements remaining unaffected by this operation. This transforms the given piece of plate into the finite element proper which is in effect a body whose corners move in several simple strain conditions through the same distances as the same points on the plate when acted upon by corner-forces statically equivalent to the edge-stresses. Each strain condition may be viewed as an independent displacement mode. The finite element must act in such manner under several simple strain conditions

including uniform strains in X and Y directions and uniform shearing strain. The number of these independent displacement modes including the three rigid body modes is selected to match the total number of possible movements of the corners of the finite element. A displacement expression, obtained by combining these displacement modes in certain proportions through coefficients or parameters, is known as the displacement function. Proper selection of the values of these parameters allows to effect separate X or Y displacements of the corners of the finite element. By converting the combined edge stresses in the element into statically equivalent corner forces, it is possible to formulate the force-displacement relation, i.e., the stiffness matrix of the finite element [K] relating the corner-forces $\{f\}$ with the corner-displacements $\{\delta\}$ by the equation:

$$\{f\} = [K]\{\delta\}$$

The nature of a flexure finite element whose corners are free to deflect and rotate about two axes in its plane is explained in a similar manner. Here, the simple strain conditions are replaced by the simple curvature conditions, and edge stresses by edge moments and transeverse shears. The selected independent curvature modes must include the uniform curvatures in X and Y directions and uniform twist.

There are two distinct methods available for conversion of the edge stresses (or moments) into the nodal forces: the direct statics method, and the energy method. The entries of the stiffness matrix [K], known as the stiffness-coefficients, obtained by these methods are usually different.

It is curious that the energy derivation of the stiffness matrix in the presence of a certain qualifying condition coincides exactly with the result of application of the Rayleigh-Ritz method to the structure as a whole, an approach completely unrelated to the finite element method.

In the analysis of a problem by the finite element method, the results depend on the stiffness matrix used. The stiffness matrix depends on the displacement modes employed and also on the manner of derivation of the corner forces from the edge stresses. Thus, the selection of these displacement modes is important and is based on certain qualifying conditions.

1.7 Criterion for Selecting Displacement Modes

If the displacement modes, related to an element, are so selected that continuity of deflections and slopes is always preserved on the interelement boundaries, then the force-displacement relations can be derived by the Rayleigh-Ritz method. In such a case,the formulation always leads to an underestimate (lower bound) of strain energy of the structure. On successive reduction of the element size, the strain energy of the finite element approximation approaches the true strain energy of the structure monotonically from below.[13-19] However, it should be noted that the criterion of continuity of deformations on the interelement boundaries is a sufficient condition for monotonic convergence of results to the true solution with regard to the strain energy of the entire system but not a necessary condition for monotonic convergence of stresses to their true values. Clough[20] used displacement modes which do not preserve continuity of displacements along element boundaries for his plane stress rectangular finite element and demonstrated convergence of displacements and stresses to their true values.

What interests an engineer is the stresses and to a smaller extent deflections. Energy as such is of no interest to him unless it is a proof of the correctness of solution.

In a general case, selection of displacement functions that will satisfy continuity of all deformations along element boundaries is impossible.[18] Bazely, Cheung, Irons and Zienkiewcz[21] assert that it is possible to achieve convergence without the conformity requirements. They state that the only necessary condition for convergence of the solution to its true value is that of the displacement function being capable of representing rigid body movements and constant strain (curvature) states throughout a finite element irrespective of its size or shape. Thus, if the selected displacement function having discontinuities at the interelement boundaries is such that as the element size decreases continuity at the interelement boundaries tends to be restored, then the formulation must tend to the correct solution. If the constant strain (curvature) criterion is used in the basic derivation of the displacement function then as the elements decrease indefinitely in size, the continuity at the nodes will require a constant strain (curvature) state to be reached in the limit within each element. This state of constant strain (curvature) will automatically require that compatibility of the deformations exist across the interelement boundaries.[21,22]

Hrennikoff[23] demonstrates the necessity and sufficiency of the presence of constant stress states in the formulation of plane stress stiffness matrix, derived using the statics approach, for convergence of the calculated results to its true value. He views the finite elements in the limit, as the molecules of a continuum and defines stresses as in the theory of elasticity. The differential equations of the theory of elasticity

governing the conditions of plane stress are based on statics, continuity of the material and its elasticity properties. He shows that these equations are equally applicable to the model which in the limit becomes in effect a simplified representation of the molecular structure of the plate. This observation is easily extended to finite elements in flexure where the constant strain condition is replaced by the constant curvature condition.

In a shell model, where the continuously curved surface is approximated by flat polygonal elements meeting at an angle, a shell displacement will produce both inplane and out of plane displacements in the flat plate elements and the continuity along the element boundaries would be even harder to satisfy than either in plane stress or flexure of a plate. Thus, the Rayleigh-Ritz sufficiency condition[13-17] appears all but impossible in the application to shells. However, convergence of the results to the true solution can be still claimed by selecting displacement functions that will satisfy the constant strain (curvature) criterion of Bazely et al[21] and Zienkiewicz.[22]

In the following study a piece of plate, whose displacement and stress properties are defined at any point within its boundaries, will be referred to as a plate element whereas when the force and displacement properties are defined only at the nodes, it will be referred to as a finite element.

In Chapter II plane stress and in Chapter III flexure stiffness matrices for equilateral trapezoid and isosceles triangular elements have been derived using statics and virtual work approaches. These matrices refer to the element coordinate directions. In Chapter IV, transformation matrices are derived which transform the stiffness matrices from element

coordinates to shell coordinates.

Several examples demonstrating the suitability of both types of stiffness matrices and convergence of calculated results to the true solution on reduction of the element size are presented in Chapter V.

CHAPTER II

DERIVATION OF PLANE STRESS STIFFNESS MATRICES

2.1 General

The stiffness matrix formulation may be based on the assumption of simple states of stresses or displacements of an element. In the following formulation of plane stress stiffness matrices, assumptions are made on the states of stress in the element. Displacement surfaces are then selected in the form of polynomials in x and y to provide the assumed stress states.

2.2 Selection of Stress Fields for a Quadrilateral Element

In a plane stress problem, a corner or a node of a finite element is allowed to displace independently in two perpendicular directions. Thus, a polygonal plate element having n nodes has 2n degrees of freedom to displace as these nodes move while the element deforms under stress.

However, by rigid body movements three of these displacements may be made zero without interfering in any way with the stresses imposed on the plate element. This leaves (2n-3) independent stress conditions required for the formulation of the force-displacement relations, i.e., stiffness matrix of the finite element irrespective of its actual shape.

For a quadrilateral element with four nodes, the number of these independent stress conditons is (2)(4)-(3)=(5). Three of these stress

conditions must be constant direct stresses in two perpendicular directions and one constant shear.

The two additional conditions of the stresses selected are, shearless bending in the plane of the plate with the direct stresses varying linearly in the two perpendicular directions. In x-y coordinate system, (Fig. (II-1)), this corresponds to the selection of stress states as

$$\begin{array}{ll} \sigma_x & \begin{array}{ll} \text{(i)} & \text{Constant} \\ \text{(ii)} & \text{Linear function of } y \end{array} \\ \sigma_y & \begin{array}{ll} \text{(iii)} & \text{Constant} \\ \text{(iv)} & \text{Linear function of } x \end{array} \\ \sigma_{xy} & \text{(v)} \quad \text{Constant} \end{array} \qquad \text{(II-1)}$$

Here, σ_x, σ_y - direct stresses in x and y directions respectively.

σ_{xy} - shear stress.

Since the plate material obeys Hooke's law, the stresses throughout the element are related to the strains as,[24]

$$\begin{aligned} \sigma_x &= \frac{E}{(1-\mu^2)} (\varepsilon_x + \mu\varepsilon_y) \\ \sigma_y &= \frac{E}{(1-\mu^2)} (\varepsilon_y + \mu\varepsilon_x) \\ \sigma_{xy} &= \frac{E}{2(1+\mu)} \varepsilon_{xy} \end{aligned} \qquad \text{(II-2)}$$

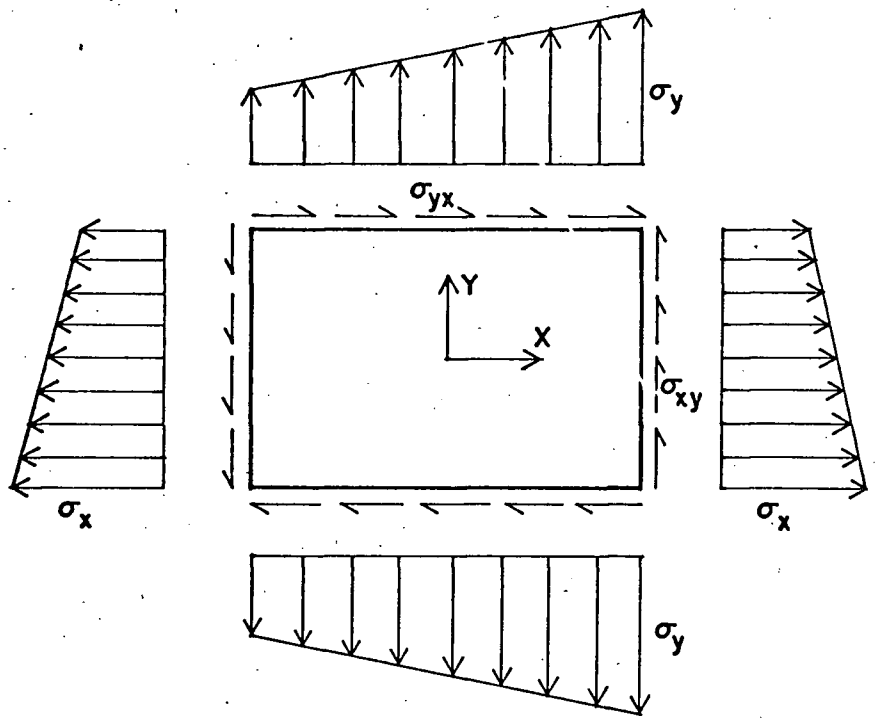

FIG. (II-1) NORMAL AND SHEAR STRESSES IN A PLATE

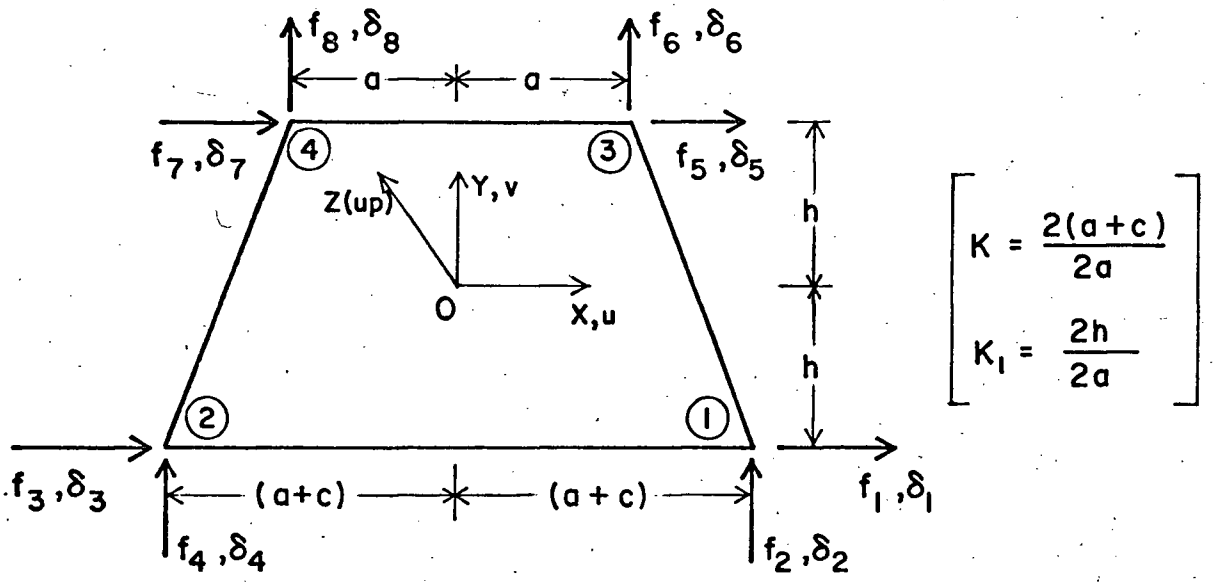

FIG. (II-2) EQUILATERAL TRAPEZOID ELEMENT IN PLANE STRESS. (Positive directions of nodal forces and displacements.)

Here, E = Modulus of elasticity

μ = Poisson's ratio

$\varepsilon_x, \varepsilon_y$ = direct strain in x and y directions respectively

ε_{xy} = shear strain

The strains may be expressed as the partial derivatives of the displacements.

$$\varepsilon_x = \frac{\partial u}{\partial x} \; ; \; \varepsilon_y = \frac{\partial v}{\partial y} \; ; \; \varepsilon_{xy} = \frac{\partial u}{\partial y} + \frac{\partial v}{\partial x} \qquad \text{(II-3)}$$

Here, u and v are displacements in x and y directions respectively.

2.3 Selection of Displacement Functions to Provide the Assumed Stress Fields

A quadratic polynomial in x and y is assumed to represent u and v displacements of a point in the plate element.

$$\begin{aligned} u &= a_1 + a_2 x + a_3 y + a_4 x^2 + a_5 xy + a_6 y^2 \\ v &= a_7 + a_8 x + a_9 y + a_{10} x^2 + a_{11} xy + a_{12} y^2 \end{aligned} \qquad \text{(II-4,a)}$$

Here, $a_1, a_2, \ldots, a_{12}$ are constant parameters.

Substituting the expressions for u and v into the Eqns. (II-3) and (II-2) it is found

$$\begin{aligned} \sigma_x &= \frac{E}{(1-\mu^2)} [(a_2 + \mu a_9) + (2a_4 + \mu a_{11})x + (a_5 + 2\mu a_{12})y] \\ \sigma_y &= \frac{E}{(1-\mu^2)} [(\mu a_2 + a_9) + (2\mu a_4 + a_{11})x + (\mu a_5 + 2a_{12})y] \\ \sigma_{xy} &= \frac{E}{2(1+\mu)} [(a_3 + a_8) + (a_5 + 2a_{10})x + (2a_6 + a_{11})y] \end{aligned} \qquad \text{(II-4,b)}$$

For Eqn. (II-4,b) to agree with Eqn. (II-1), several terms in Eqn. (II-4,b) must vanish. These are:

$$\begin{aligned}
&\text{(i)} \quad 2a_4 + \mu a_{11} = 0; \quad \text{or, } a_{11} = -\frac{2}{\mu} a_4 \\
&\text{(ii)} \quad \mu a_5 + 2a_{12} = 0; \quad \text{or, } a_{12} = -\frac{\mu}{2} a_5 \\
&\text{(iii)} \quad a_5 + 2a_{10} = 0; \quad \text{or, } a_{10} = -\frac{1}{2} a_5 \\
\text{and} \quad &\text{(iv)} \quad 2a_6 + a_{11} = 0; \quad \text{or, } a_6 = -\frac{1}{2} a_{11} = \frac{1}{\mu} a_4
\end{aligned} \tag{II-4,c}$$

Thus, there are only eight independent constants in the quadratic polynomials of Eqn. (II-4,a). Renaming these constants as

$$b_1 = a_1;\ b_2 = a_2;\ b_3 = a_3;\ b_4 = -\frac{a_4}{\mu}$$

$$b_5 = \frac{a_5}{2};\ b_6 = a_9;\ b_7 = a_8;\ b_8 = a_7$$

and rewriting Eqn. (II-4,a) in terms of the eight new constants, one obtains

$$\begin{aligned}
u &= b_1 + b_2 x + b_3 y - b_4(\mu x^2 + y^2) + 2b_5 xy \\
v &= b_8 + b_7 x + b_6 y - b_5(x^2 + \mu y^2) + 2b_4 xy
\end{aligned} \tag{II-5}$$

Constants b_1 and b_8 correspond to the rigid body displacements and $(b_3\text{-}b_7)$ corresponds to rigid body rotation of the plate element. The other constants simply provide five independent stress conditions as given below.

$$\sigma_x = \frac{D_1}{t}\left[\underbrace{(b_2 + \mu b_6)}_{\text{Constant}} + \underbrace{2b_5(1-\mu^2)y}_{\text{Linear function of } y}\right]$$

$$\sigma_y = \frac{D_1}{t}\left[\underbrace{(\mu b_2 + b_6)}_{\text{Constant}} + \underbrace{2b_4(1-\mu^2)x}_{\text{Linear function of } x}\right] \qquad \text{(II-6)}$$

$$\sigma_{xy} = \frac{D_1}{t}\frac{(1-\mu)}{2}\underbrace{(b_3 + b_7)}_{\text{Constant}}$$

Here, $D_1 = \frac{Et}{(1-\mu^2)}$ Extentional rigidity per unit length of the plate

t = thickness of the piece of plate (constant)

The displacement functions of Eqn. (II-5) include constant strain states - a criterion suggested by Bazely et al[21] and Zienkiewicz[22] for the convergence of solution to the true result.

2.4 Evaluation of the Constant Parameters $(b_1, b_2, \ldots, b_8)$ for an Equilateral Trapezoid Finite Element

Equation (II-5) provides displacements at any point (x,y) of the plate element in terms of the eight parameters $(b_1, b_2, \ldots, b_8)$ and the coordinates of that point. Eight independent equations for nodal displacements $\delta_1, \delta_2, \ldots, \delta_8$ are obtained in terms of the eight parameters. These are written in the matrix form in Table (II-1). In short, these can be written as

$$\{\delta\} = [A]\{B\} \qquad \text{(II-7)}$$

Here, $\{\delta\}$ = 8 x 1 column vector of nodal displacements $\delta_1, \delta_2, \ldots, \delta_8$ (Fig. II-2)

$[A]$ = 8 x 8 matrix in terms of nodal coordinates

$\{B\}$ = 8 x 1 column vector of constant parameters, $b_1, \ldots, b_8$.

Table (II-1) Nodal Displacements of an Equilateral Trapezoid Plate Element in Terms of the Eight Constant Parameters Fig. (II-2)

$$\begin{bmatrix} \delta_1 \\ \delta_2 \\ \delta_3 \\ \delta_4 \\ \delta_5 \\ \delta_6 \\ \delta_7 \\ \delta_8 \end{bmatrix} = \begin{bmatrix} 1 & (a+c) & -h & -\{\mu(a+c)^2 + h^2\} & -2(a+c)h & 0 & 0 & 0 \\ 0 & 0 & 0 & -2(a+c)h & -\{(a+c)^2 + \mu h^2\} & -h & (a+c) & 1 \\ 1 & -(a+c) & -h & -\{\mu(a+c)^2 + h^2\} & 2(a+c)h & 0 & 0 & 0 \\ 0 & 0 & 0 & 2(a+c)h & -\{(a+c)^2 + \mu h^2\} & -h & -(a+c) & 1 \\ 1 & a & h & -\{\mu a^2 + h^2\} & 2ah & 0 & 0 & 0 \\ 0 & 0 & 0 & 2ah & -\{a^2 + \mu h^2\} & h & a & 1 \\ 1 & -a & h & -\{\mu a^2 + h^2\} & -2ah & 0 & 0 & 0 \\ 0 & 0 & 0 & -2ah & -\{a^2 + \mu h^2\} & h & -a & 1 \end{bmatrix} \begin{bmatrix} b_1 \\ b_2 \\ b_3 \\ b_4 \\ b_5 \\ b_6 \\ b_7 \\ b_8 \end{bmatrix}$$

$$\{\delta\} = [A]\{B\} \qquad \text{Eqn. (II-7)}$$

Table (II-2) Parameters $\{B\}$ in Terms of the Eight Nodal Displacements

$$\begin{bmatrix} b_1 \\ b_2 \\ b_3 \\ b_4 \\ b_5 \\ b_6 \\ b_7 \\ b_8 \end{bmatrix} = \begin{bmatrix} 1/4 & -\alpha_3\alpha_4 & 1/4 & \alpha_3\alpha_4 & 1/4 & \alpha_3\alpha_5 & 1/4 & -\alpha_3\alpha_5 \\ \alpha_6 & 0 & -\alpha_6 & 0 & \alpha_7 & 0 & -\alpha_7 & 0 \\ -\alpha_8 & -\mu\alpha_2\alpha_4 & -\alpha_8 & \mu\alpha_2\alpha_4 & \alpha_8 & \mu\alpha_2\alpha_5 & \alpha_8 & -\mu\alpha_2\alpha_5 \\ 0 & -\alpha_4 & 0 & \alpha_4 & 0 & \alpha_5 & 0 & -\alpha_5 \\ -\alpha_4 & 0 & \alpha_4 & 0 & \alpha_5 & 0 & -\alpha_5 & 0 \\ -\alpha_2\alpha_4 & -\alpha_8 & \alpha_2\alpha_4 & -\alpha_8 & \alpha_2\alpha_5 & \alpha_8 & -\alpha_2\alpha_5 & \alpha_8 \\ 0 & \alpha_6 & 0 & -\alpha_6 & 0 & \alpha_7 & 0 & -\alpha_7 \\ -\alpha_1\alpha_4 & 1/4 & \alpha_1\alpha_4 & 1/4 & \alpha_1\alpha_5 & 1/4 & -\alpha_1\alpha_5 & 1/4 \end{bmatrix} \begin{bmatrix} \delta_1 \\ \delta_2 \\ \delta_3 \\ \delta_4 \\ \delta_5 \\ \delta_6 \\ \delta_7 \\ \delta_8 \end{bmatrix}$$

$$\{B\} = [A^{-1}]\{\delta\} \qquad \text{Eqn. (II-8)}$$

Here, $\alpha_1 = \left\{\frac{a^2 + (a + c)^2 + 2\mu h^2}{2}\right\}$; $\alpha_2 = \left\{\frac{a^2 - (a + c)^2}{2h}\right\}$; $\alpha_3 = \left[\frac{2h^2 + \mu\{a^2 + (a + c)^2\}}{2}\right]$

$$\alpha_4 = \frac{1}{8h(a + c)} \; ; \; \alpha_5 = \frac{1}{8ha} \; ; \; \alpha_6 = \frac{1}{4(a + c)} \; ; \; \alpha_7 = \frac{1}{4a} \; ; \; \alpha_8 = \frac{1}{4h}$$

The parameters, $\{B\}$, are evaluated in terms of the nodal displacements as

$$\{B\} = [A^{-1}]\{\delta\} \tag{II-8}$$

The $[A^{-1}]$ matrix is given in Table (II-2).

Knowning the corner displacements $\{\delta\}$ of a plate element, the displacements at any point of the element are obtained simply by substituting Eqn. (II-8) in Eqn. (II-5).

2.5 Evaluation of Stresses at Any Point in a Plate Element

Using Eqn. (II-5) for displacements, strains at any point (x,y) of the plate are given by

$$\begin{aligned} \varepsilon_x &= \frac{\partial u}{\partial x} = b_2 - 2\mu b_4 x + 2b_5 y \\ \varepsilon_y &= \frac{\partial v}{\partial y} = b_6 - 2\mu b_5 y + 2b_4 x \\ \varepsilon_{xy} &= \frac{\partial u}{\partial y} + \frac{\partial v}{\partial x} = b_3 + b_7 \end{aligned} \tag{II-9}$$

Writing in the matrix form, these are

$$\{\varepsilon\} = [G]\{B\} \tag{II-10}$$

[G] is a 3 x 8 matrix and is shown in Table (II-3).

Substituting Eqn. (II-8) for $\{B\}$ in Eqn. (II-10) one obtains

$$\{\varepsilon\} = [G][A^{-1}]\{\delta\} \tag{II-11}$$

Table (II-3) Strains at Any Point (x,y) in the Trapezoid Element

$$\begin{bmatrix} \varepsilon_x \\ \varepsilon_y \\ \varepsilon_{xy} \end{bmatrix} = \begin{bmatrix} 0 & 1 & 0 & -2\mu x & 2y & 0 & 0 & 0 \\ 0 & 0 & 0 & 2x & -2\mu y & 1 & 0 & 0 \\ 0 & 0 & 1 & 0 & 0 & 0 & 1 & 0 \end{bmatrix} \begin{bmatrix} b_1 \\ b_2 \\ b_3 \\ b_4 \\ b_5 \\ b_6 \\ b_7 \\ b_8 \end{bmatrix}$$

$$\{\varepsilon\} = [G]\{B\} \qquad \text{Eqn. (II-10)}$$

Table (II-4) Stress-Strain Relationship

$$\begin{bmatrix} \sigma_x \\ \sigma_y \\ \sigma_{xy} \end{bmatrix} = \begin{bmatrix} \frac{E}{(1-\mu 2)} & \frac{\mu E}{(1-\mu 2)} & 0 \\ \frac{\mu E}{(1-\mu 2)} & \frac{E}{(1-\mu 2)} & 0 \\ 0 & 0 & \frac{E}{2(1+\mu)} \end{bmatrix} \begin{bmatrix} \varepsilon_x \\ \varepsilon_y \\ \varepsilon_{xy} \end{bmatrix}$$

$$\{\sigma\} = [D]\{\varepsilon\} \qquad \text{Eqn. (II-12)}$$

Stress-strain relationships of Eqn. (II-2) can be rewritten in matrix form as

$$\{\sigma\} = [D]\{\varepsilon\} \qquad \text{(II-12)}$$

The (3 x 3) symmetrix matrix [D] contains the elastic constants and is shown in Table (II-4). Substituting Eqn. (II-11) for $\{\varepsilon\}$ in Eqn. (II-12) one gets,

$$\{\sigma\} = [D][G][A^{-1}]\{\delta\} \qquad \text{(II-13)}$$

Letting, $$[ST] = [D][G][A^{-1}] \qquad \text{(II-14,a)}$$

Eqn. (II-13) is rewritten as

$$\{\sigma\} = [ST]\{\delta\} \qquad \text{(II-14,b)}$$

(3 x 8) stress matrix [ST] is shown in Table (II-5).

Thus, knowing the nodal displacements for any particular element, stresses at any point within the element may be obtained by simply substituting the coordinates of that point in the matrix Eqn. (II-14,b).

Table (II-5) Stresses at Any Point in the Trapezoid Element in Terms of the Nodal Displacements

$$\begin{bmatrix}\sigma_x\\ \sigma_y\\ \sigma_{xy}\end{bmatrix} \frac{E}{(1-\mu^2)} = \begin{bmatrix} 1 & 2 & 3 & 4 \\ \frac{(2h-\mu\alpha_2) - 2(1-\mu^2)y}{8h(a+c)} & -\frac{\mu}{4h} & -\left\{\frac{(2h-\mu\alpha_2) - 2(1-\mu^2)y}{8h(a+c)}\right\} & -\frac{\mu}{4h} \\ \frac{2\mu h-\alpha_2}{8h(a+c)} & -\left\{\frac{2(1-\mu^2)x + 2(a+c)}{8h(a+c)}\right\} & -\left\{\frac{2\mu h-\alpha_2}{8h(a+c)}\right\} & \left\{\frac{2(1-\mu^2)x - 2(a+c)}{8h(a+c)}\right\} \\ -\frac{(1-\mu)}{8h} & \frac{(1-\mu)(2h-\mu\alpha_2)}{16h(a+c)} & -\frac{(1-\mu)}{8h} & -\frac{(1-\mu)(2h-\mu\alpha_2)}{16h(a+c)} \end{bmatrix}$$

$$\begin{bmatrix} 5 & 6 & 7 & 8 \\ \left\{\frac{(2h+\mu\alpha_2) + 2(1-\mu^2)y}{8ha}\right\} & \frac{\mu}{4h} & -\left\{\frac{(2h+\mu\alpha_2) + 2(1-\mu^2)y}{8ha}\right\} & \frac{\mu}{4h} \\ \frac{2\mu h+\alpha_2}{8ha} & \frac{2a+2(1-\mu^2)x}{8ha} & -\left\{\frac{2\mu h+\alpha_2}{8ha}\right\} & \frac{2a-2(1-\mu^2)x}{8ha} \\ \frac{(1-\mu)}{8h} & \frac{(1-\mu)(2h+\mu\alpha_2)}{16ha} & \frac{(1-\mu)}{8h} & -\frac{(1-\mu)(2h+\mu\alpha_2)}{16ha} \end{bmatrix} \begin{bmatrix}\delta_1\\ \delta_2\\ \delta_3\\ \delta_4\\ \delta_5\\ \delta_6\\ \delta_7\\ \delta_8\end{bmatrix}$$

Here, $\alpha_2 = \frac{-c(2a+c)}{2h}$

$$\{\sigma\} = [ST]\{\delta\} \qquad \text{Eqn. (II-14,b)}$$

2.6 Derivation of Stiffness Matrices

Force-displacement relations or the stiffness matrix of the finite element is obtained by converting the edge stresses corresponding to individual displacement modes into equivalent nodal forces. There are two distinct methods for conversion of the edge stresses into the equivalent nodal forces (i) The distributed edge stresses are transformed into equivalent nodal forces by the simple law of the lever. The stiffness matrix so obtained will be referred to as the Statics Matrix.
and (ii) The principle of virtual work is used for obtaining the equivalent nodal forces. The stiffness matrix so obtained will be referred to as the Energy Matrix.

2.7 Derivation of Plane Stress Statics Stiffness Matrix for an Equilateral Trapezoid.

Each of the component displacement modes is considered separately. The edge stresses are apportioned to the connecting nodes by the simple law of the lever.

In the present case, only linearly distributed direct stresses and constant shear stress in x and y directions are present. Collecting direct stresses by the law of the lever is consistent with statics. For uniformly distributed shear stress, it is only logical to apportion half of the total shear force on the edge to each of the connecting nodes.

The stresses on the inclined sides of the trapezoid act at an angle. It is convenient to replace the inclined sides by infinitesimal steps with horizontal and vertical parts, the stresses on which are respectively vertical and horizontal. The components of corner forces are then found by

transferring the stresses acting on the projected sides in accordance with statics.

2.8 Sample Procedure to Determine the Equivalent Nodal Forces Due to the Displacement Mode $b_4 \neq 0$, All other b_j's = 0

The displacements for this mode are given by $u = -b_4(\mu x^2 + y^2)$; $v = 2b_4 xy$

Corresponding to these displacements, the strains are

$$\varepsilon_x = \frac{\partial u}{\partial x} = -2\mu b_4 x \; ; \; \varepsilon_y = \frac{\partial v}{\partial y} = 2b_4 x$$

$$\varepsilon_{xy} = \frac{\partial u}{\partial y} + \frac{\partial v}{\partial x} = 0$$

Using Eqn. (II-2), the forces/length of the plate are;

Direct force/length in x-direction = $t\sigma_x = 0$

Direct force/length in y-direction = $t\sigma_y = 2Etb_4 x$

Shear force/length = $t\sigma_{xy} = 0$

Here, t = thickness of the plate element.

The distribution of these forces on the element is shown in Fig. (II-3). The equivalent nodal forces are collected for each edge separately using the law of the lever and are shown in Fig. (II-4). Finally, the nodal forces from all edges are combined Fig. (II-5).

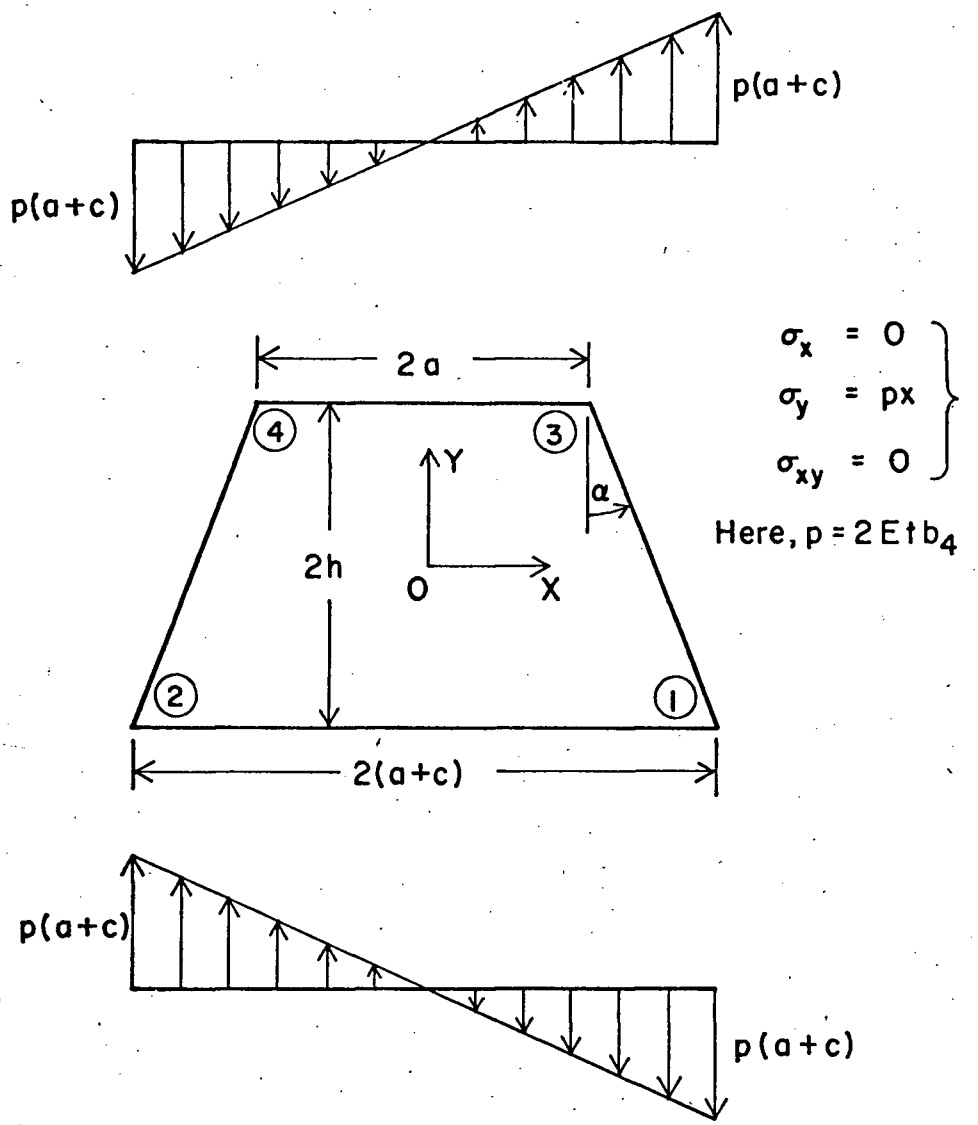

FIG. (II-3) FORCE DISTRIBUTION DUE TO THE DISPLACEMENT MODE, b_4.

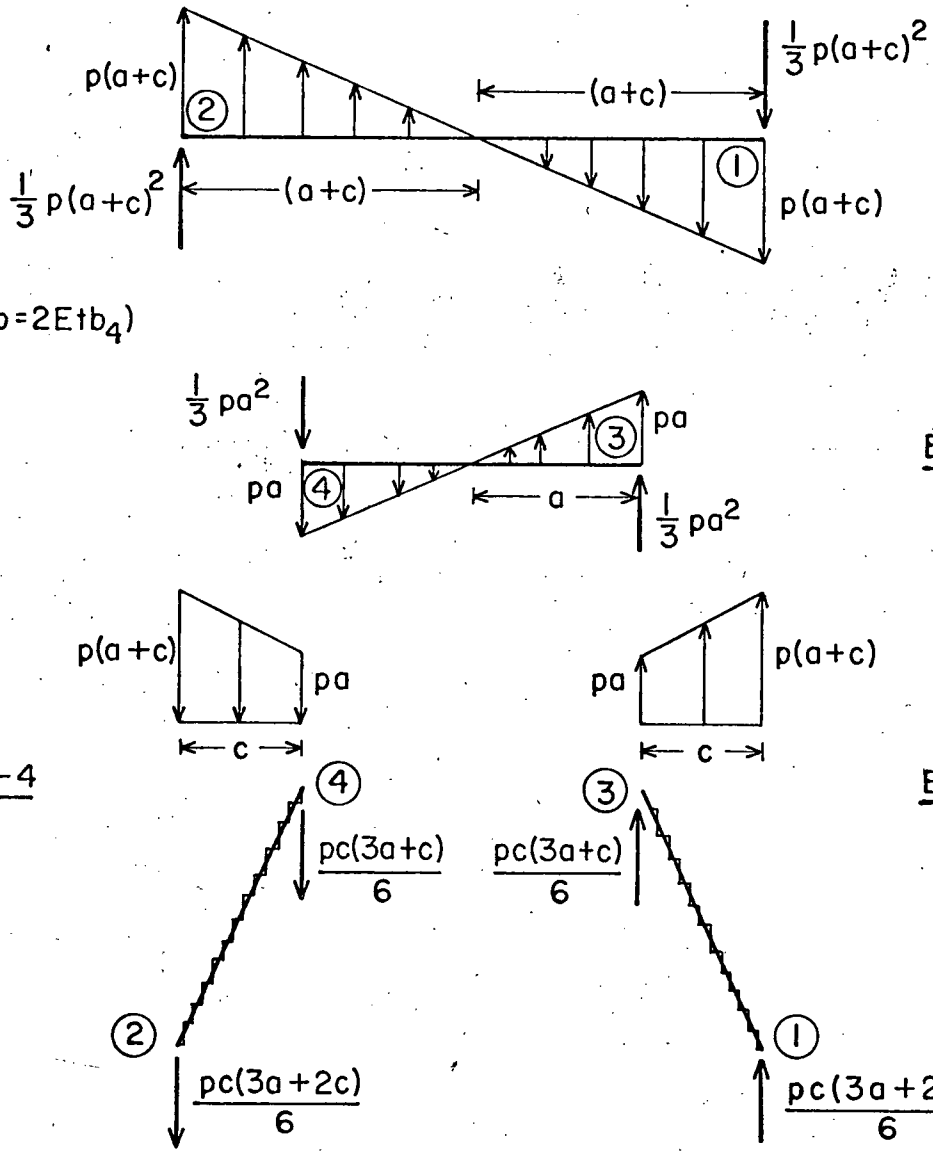

FIG(II-4) EQUIVALENT NODAL FORCE CONTRIBUTIONS FROM INDIVIDUAL EDGES

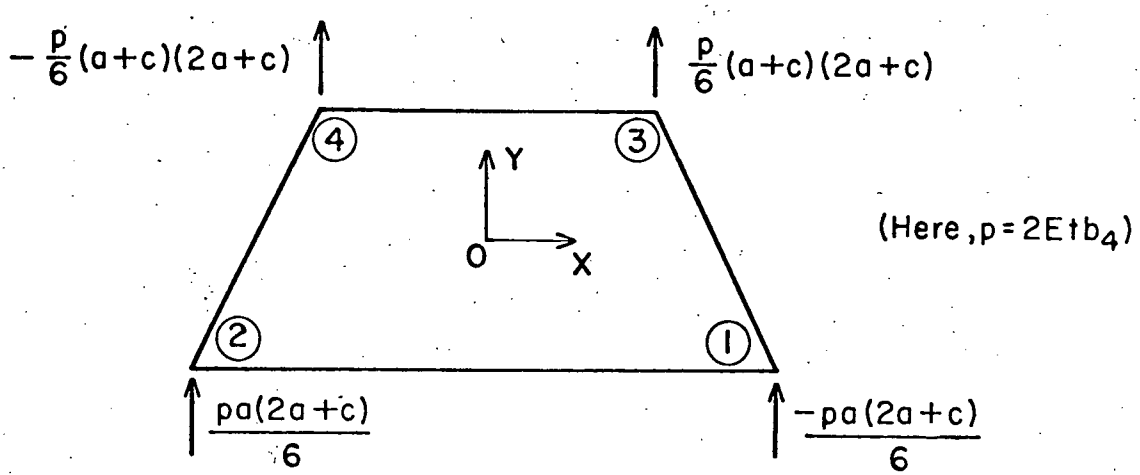

FIG(II-5) EQUIVALENT NODAL FORCES CORRESPONDING TO THE DISPLACEMENT MODE b_4

2.9 Addition of Equivalent Corner Forces from Individual Displacement Modes

For a general deformed state of the plate element given by Eqn. (II-5), the equivalent corner forces are simply the sums of equivalent corner forces from individual displacement modes. Although there are only five independent stress modes, for the purpose of compatible matrix multiplication all the eight displacement modes are considered. The equivalent force contributions from modes corresponding to rigid body motion will be zero.

Collectively, the equivalent forces for all the displacement modes are written in the matrix form as

$$\{f\} = [C]\{B\} \tag{II-15}$$

Here, $\{f\}$ = 8 x 1 column vector of equivalent corner forces in the positive directions of Fig. (II-2).

$[C]$ = 8 x 8 matrix. Jth column of this matrix contains equivalent corner forces in eight positive directions of Fig. (II-2) due to a displacement mode b_j

The matrix Eqn. (II-15) is shown in full in Table (II-6). Using Eqn. (II-8) to substitute for $\{B\}$ in Eqn. (II-15), the nodal forces are:

$$\{f\} = [C][A^{-1}]\{\delta\} \tag{II-16}$$

Thus, Eqn. (II-16) gives the relationship between nodal forces and nodal displacements. This relationship is commonly known in the form

$$\{f\} = [K]\{\delta\} \tag{II-17}$$

Table (II-6) Equivalent Corner Forces in Terms of Constant Parameters ($b_1, b_2, \ldots b_8$)

(equilateral trapezoid element in plane stress)

$$\begin{bmatrix} f_1 \\ f_2 \\ f_3 \\ f_4 \\ f_5 \\ f_6 \\ f_7 \\ f_8 \end{bmatrix} \underset{=}{D_1} \begin{bmatrix} 0 & h & -\frac{1}{4}(1-\mu)(2a+c) & 0 & -\frac{2}{3}(1-\mu^2)h^2 & \mu h & -\frac{1}{4}(1-\mu)(2a+c) & 0 \\ 0 & -\frac{1}{2}\mu(2a+c) & \frac{1}{2}(1-\mu)h & -\frac{1}{3}(1-\mu^2)(2a+c)a & 0 & -\frac{1}{2}(2a+c) & \frac{1}{2}(1-\mu)h & 0 \\ 0 & -h & -\frac{1}{4}(1-\mu)(2a+c) & 0 & \frac{2}{3}(1-\mu^2)h^2 & -\mu h & -\frac{1}{4}(1-\mu)(2a+c) & 0 \\ 0 & -\frac{1}{2}\mu(2a+c) & -\frac{1}{2}(1-\mu)h & \frac{1}{3}(1-\mu^2)(2a+c)a & 0 & -\frac{1}{2}(2a+c) & -\frac{1}{2}(1-\mu)h & 0 \\ 0 & h & \frac{1}{4}(1-\mu)(2a+c) & 0 & \frac{2}{3}(1-\mu^2)h^2 & \mu h & \frac{1}{4}(1-\mu)(2a+c) & 0 \\ 0 & \frac{1}{2}\mu(2a+c) & \frac{1}{2}(1-\mu)h & \frac{1}{3}(1-\mu^2)(2a+c)(a+c) & 0 & \frac{1}{2}(2a+c) & \frac{1}{2}(1-\mu)h & 0 \\ 0 & -h & \frac{1}{4}(1-\mu)(2a+c) & 0 & -\frac{2}{3}(1-\mu^2)h^2 & -\mu h & \frac{1}{4}(1-\mu)(2a+c) & 0 \\ 0 & \frac{1}{2}\mu(2a+c) & -\frac{1}{2}(1-\mu)h & -\frac{1}{3}(1-\mu^2)(2a+c)(a+c) & 0 & \frac{1}{2}(2a+c) & -\frac{1}{2}(1-\mu)h & 0 \end{bmatrix} \begin{bmatrix} b_1 \\ b_2 \\ b_3 \\ b_4 \\ b_5 \\ b_6 \\ b_7 \\ b_8 \end{bmatrix}$$

$$\{f\} = [C]\{B\} \qquad \text{Eqn. (II-15)}$$

Here, $D_1 = \dfrac{Et}{(1-\mu^2)}$ = Extensional rigidity per unit length of the plate

t = thickness of the plate (constant for the element)

Here, [K] = stiffness matrix of the finite element in plane stress. See Table (II-7,a)

Comparing Eqns. (II-16) and (II-17)

$$[K] = [C][A^{-1}] \qquad \text{(II-18)}$$

It may be noted that a force in the ith direction due to a general state of displacements is referred to as f_i whereas, a force in the i th direction due to a unit displacement in the j th direction alone is called $K_{i,j}$ (definition of stiffness coefficient).

Thus, the following relation holds,

$$f_1 = k_{1,1}\delta_1 + K_{1,2}\delta_2 + \ldots + K_{1,8}\delta_8$$
$$f_2 = K_{2,1}\delta_1 + K_{2,2}\delta_2 + \ldots + K_{2,8}\delta_8$$
$$\vdots$$
$$f_i = K_{i,1}\delta_1 + K_{i,2}\delta_2 + \ldots + K_{i,8}\delta_8$$
$$\vdots$$

Due to the geometrical symmetry of the finite element about y-axis, stiffness coefficients belonging to columns 3, 4, 7 and 8 (due to unit displacements at joints 2 and 4) may be obtained simply by inspection from those of columns 1, 2, 5 and 6 (due to unit displacements at joints 1 and 3). This is shown in Table (II-7,b). The explicit expressions for

Table (II-7,A) Plane Stress Stiffness Matrix

$$[K] = \begin{bmatrix} K_{11} & K_{12} & K_{13} & K_{14} & K_{15} & K_{16} & K_{17} & K_{18} \\ K_{21} & K_{22} & K_{23} & K_{24} & K_{25} & K_{26} & K_{27} & K_{28} \\ K_{31} & K_{32} & K_{33} & K_{34} & K_{35} & K_{36} & K_{37} & K_{38} \\ K_{41} & K_{42} & K_{43} & K_{44} & K_{45} & K_{46} & K_{47} & K_{48} \\ K_{51} & K_{52} & K_{53} & K_{54} & K_{55} & K_{56} & K_{57} & K_{58} \\ K_{61} & K_{62} & K_{63} & K_{64} & K_{65} & K_{66} & K_{67} & K_{68} \\ K_{71} & K_{72} & K_{73} & K_{74} & K_{75} & K_{76} & K_{77} & K_{78} \\ K_{81} & K_{82} & K_{83} & K_{84} & K_{85} & K_{86} & K_{87} & K_{88} \end{bmatrix}$$

Table (II-7,B) Equalities in the Stiffness Coefficients due to the Geometrical Symmetry of the Trapezoid about Y-Axis

$$[K] = \begin{bmatrix} K_{11} & K_{12} & K_{31} & -K_{32} & K_{15} & K_{16} & K_{35} & -K_{36} \\ K_{21} & K_{22} & -K_{41} & K_{42} & K_{25} & K_{26} & -K_{45} & K_{46} \\ K_{31} & K_{32} & K_{11} & -K_{12} & K_{35} & K_{36} & K_{15} & -K_{16} \\ K_{41} & K_{42} & -K_{21} & K_{22} & K_{45} & K_{46} & -K_{25} & K_{26} \\ K_{51} & K_{52} & K_{71} & -K_{72} & K_{55} & K_{56} & K_{75} & -K_{76} \\ K_{61} & K_{62} & -K_{81} & K_{82} & K_{65} & K_{66} & -K_{85} & K_{86} \\ K_{71} & K_{72} & K_{51} & -K_{52} & K_{75} & K_{76} & K_{55} & -K_{56} \\ K_{81} & K_{82} & -K_{61} & K_{62} & K_{85} & K_{86} & -K_{65} & K_{66} \end{bmatrix}$$

stiffness coefficients belonging to columns 1, 2, 5 and 6 are given in Table (II-7,c).

The dimensionless ratios of the sides K and K_1 are normally defined as (See Fig. (II-2))

$$K = \frac{2(a + c)}{2a} \; ; \quad K_1 = \frac{2h}{2a}$$

In order to obtain stiffness coefficients belonging to columns 5 and 6 from those of columns 1 and 2, the above dimensionless ratios would have to be written by analogy, as

$$K^{new} = \frac{2a}{2(a + c)} \; ; \quad K_1{}^{new} = \frac{2h}{2(a + c)}$$

which are equal to $1/K$ and K_1/K respectively. Therefore, the values of the stiffness coefficients of columns 5 and 6 may be obtained by inspection from those of columns 1 and 2 by replacing the dimensionless ratios of the sides K and K_1 by $1/K$ and K_1/K respectively.

It may be noted that the stiffness matrix [K] for an equilateral trapezoid obtained from the statics approach is not symmetrical about the main diagonal. However, if the trapezoid reduces to a rectangle, the statics stiffness matrix becomes symmetrical. The statics plane stress stiffness matrix for a rectangle coincides with the one derived by Clough[20] using Energy considerations and based on the same assumption of stress states. Apparently, its lack of symmetry reflects the asymmetry of the element itself about X-axis.

It is more important to note that the stiffness coefficients for a trapezoid element still satisfy reciprocity relations in conditions of uniform stress. Thus when the element decreases in size and the stresses in the vicinity of the element become nearly uniform, the irregularity due to the asymmetry of the statics stiffness matrix will tend to correct itself.

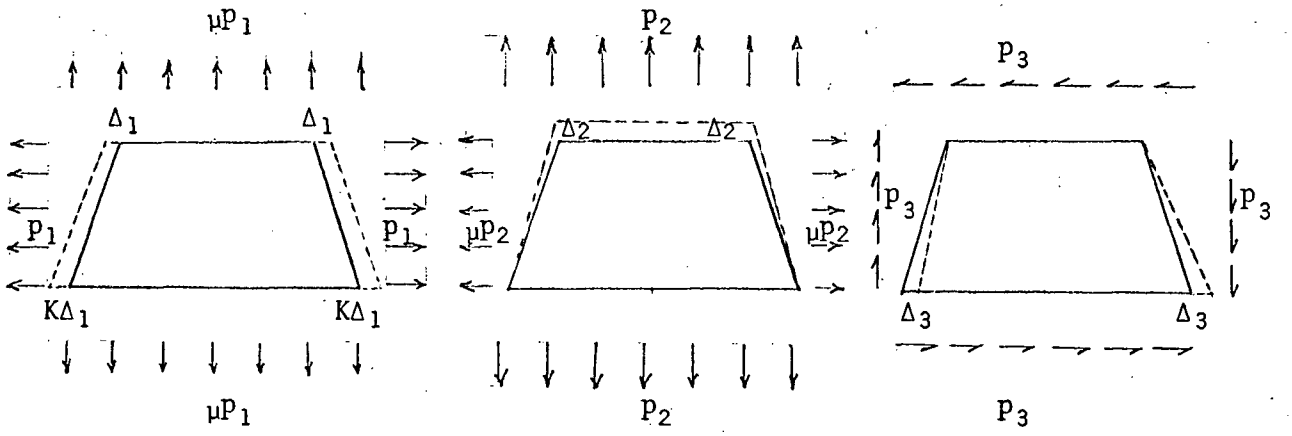

Under the uniform stress conditions, the edge displacements of the piece of plate become linear. Since it is the lack of the edge linearity that causes the difference between the Statics and the Energy stiffness coefficients[23] the nodal forces in the finite element corresponding to the Statics and the Energy stiffness matrices will coincide and the conditions of reciprocity will be restored as is always the case with the Energy matrix.

Table (II-7,C) Entries of the Statics Stiffness Matrix for a Trapezoid in Plane Stress. (Fig. (II-2))

Let, $D_1 = \frac{Et}{(1 - \mu^2)}$ = Extensional rigidity per unit length of the plate.

Here, t = thickness of the plate element.

Also, defining the dimensionless numbers

$K = \frac{2(a + c)}{2a} = \frac{\text{Bottom side}}{\text{Top side}}$

$K_1 = \frac{2h}{2a} = \frac{\text{Height}}{\text{Top side}}$

The entries of the statics stiffness matrix, defined by Eqn. (II-18), are:

Entries of the 1st Column ($\delta_1 = 1$; all other displacements are zero)

$$k_{1,1} = \frac{D_1}{4}\left[\frac{(4 - \mu^2)K_1}{3K} + \frac{(1 - \mu)(K + 1)}{4K_1} + \frac{\mu(K^2 - 1)}{4KK_1}\right]$$

$$K_{2,1} = \frac{-D_1}{8}\left[1 + \frac{\mu}{K} + \frac{(K^2 - 1)(K + 1)}{4KK_1^2}\right]$$

$$K_{3,1} = \frac{D_1}{4}\left[-\frac{(4 - \mu^2)K_1}{3K} + \frac{(1 - \mu)(K + 1)}{4K_1} - \frac{\mu(K^2 - 1)}{4KK_1}\right]$$

$$K_{4,1} = \frac{-D_1}{8}\left[-1 + \mu(2 + \frac{1}{K}) + \frac{(K^2 - 1)(K + 1)}{4KK_1^2}\right]$$

$$K_{5,1} = \frac{D_1}{4}\left[\frac{(2 + \mu^2)K_1}{3K} - \frac{(1 - \mu)(K + 1)}{4K_1} + \frac{\mu(K^2 - 1)}{4KK_1}\right]$$

$$K_{6,1} = \frac{-D_1}{8}\left[1 - \mu(2 + \frac{1}{K}) - \frac{(K^2 - 1)(K + 1)}{4KK_1^2}\right]$$

$$K_{7,1} = \frac{D_1}{4}\left[-\frac{(2 + \mu^2)K_1}{3K} - \frac{(1 - \mu)(K + 1)}{4K_1} - \frac{\mu(K^2 - 1)}{4KK_1}\right]$$

$$K_{8,1} = \frac{-D_1}{8}\left[-1 - \frac{\mu}{K} - \frac{(K^2 - 1)(K + 1)}{4KK_1^2}\right]$$

Continued Table (II-7,C)

Entries of the 2nd Column ($\delta_2 = 1$; all other displacements are zero)

$$K_{1,2} = \frac{-D_1}{4}\left[\frac{\mu}{4}\left(3 - \frac{1}{K}\right) + \frac{1+K}{4K} + \frac{\mu(1-\mu)(K^2-1)(K+1)}{16KK_1^2}\right]$$

$$K_{2,2} = \frac{D_1}{4}\left[\frac{(1-\mu^2+3K)(K+1)}{6KK_1} + \frac{(1-\mu)K_1}{2K} + \frac{\mu(1-\mu)(K^2-1)}{8KK_1}\right]$$

$$K_{3,2} = \frac{-D_1}{4}\left[-\frac{\mu}{4}\left(5 + \frac{1}{K}\right) + \frac{(1+K)}{4K} + \frac{\mu(1-\mu)(K^2-1)(K+1)}{16KK_1^2}\right]$$

$$K_{4,2} = \frac{D_1}{4}\left[\frac{(-1+\mu^2+3K)(K+1)}{6KK_1} - \frac{(1-\mu)K_1}{2K} - \frac{\mu(1-\mu)(K^2-1)}{8KK_1}\right]$$

$$K_{5,2} = \frac{-D_1}{4}\left[\frac{\mu}{4}\left(5 + \frac{1}{K}\right) - \frac{(1+K)}{4K} - \frac{\mu(1-\mu)(K^2-1)(K+1)}{16KK_1^2}\right]$$

$$K_{6,2} = \frac{D_1}{4}\left[-\frac{(4-\mu^2)(K+1)}{6K_1} + \frac{(1-\mu)K_1}{2K} + \frac{\mu(1-\mu)(K^2-1)}{8KK_1}\right]$$

$$K_{7,2} = \frac{-D_1}{4}\left[-\frac{\mu}{4}\left(3 - \frac{1}{K}\right) - \frac{1+K}{4K} - \frac{\mu(1-\mu)(K^2-1)(K+1)}{16KK_1^2}\right]$$

$$K_{8,2} = \frac{D_1}{4}\left[-\frac{(2+\mu^2)(K+1)}{6K_1} - \frac{(1-\mu)K_1}{2K} - \frac{\mu(1-\mu)(K^2-1)}{8KK_1}\right]$$

Entries of the 5th Column ($\delta_5 = 1$; all other displacements are zero)

$$K_{1,5} = \frac{D_1}{4}\left[\frac{(2+\mu^2)K_1}{3} - \frac{(1-\mu)(K+1)}{4K_1} - \frac{\mu(K^2-1)}{4K_1}\right]$$

$$K_{2,5} = \frac{-D_1}{8}\left[-1 + \mu(2+K) - \frac{(K^2-1)(K+1)}{4K_1^2}\right]$$

$$K_{3,5} = \frac{D_1}{4}\left[-\frac{(2+\mu^2)K_1}{3} - \frac{(1-\mu)(K+1)}{4K_1} + \frac{\mu(K^2-1)}{4K_1}\right]$$

Continued Table (II-7,C)

$$K_{4,5} = \frac{-D_1}{8}\left[1 + \mu K - \frac{(K^2 - 1)(K + 1)}{4K_1^2}\right]$$

$$K_{5,5} = \frac{D_1}{4}\left[\frac{(4 - \mu^2)K_1}{3} + \frac{(1 - \mu)(K + 1)}{4K_1} - \frac{\mu(K^2 - 1)}{4K_1}\right]$$

$$K_{6,5} = \frac{-D_1}{8}\left[-1 - \mu K + \frac{(K^2 - 1)(K + 1)}{4K_1^2}\right]$$

$$K_{7,5} = \frac{D_1}{4}\left[-\frac{(4 - \mu^2)K_1}{3} + \frac{(1 - \mu)(K + 1)}{4K_1} + \frac{\mu(K^2 - 1)}{4K_1}\right]$$

$$K_{8,5} = \frac{-D_1}{8}\left[1 - \mu(2 + K) + \frac{(K^2 - 1)(K + 1)}{4K_1^2}\right]$$

Entries of the 6th Column ($\delta_6 = 1$; all other displacements are zero)

$$K_{1,6} = \frac{-D_1}{4}\left[-\frac{\mu}{4}(5 + K) + \frac{(1 + K)}{4} - \frac{\mu(1 - \mu)(K^2 - 1)(K + 1)}{16K_1^2}\right]$$

$$K_{2,6} = \frac{D_1}{4}\left[-\frac{(4 - \mu^2)(K + 1)}{6K_1} + \frac{(1 - \mu)K_1}{2} - \frac{\mu(1 - \mu)(K^2 - 1)}{8K_1}\right]$$

$$K_{3,6} = \frac{-D_1}{4}\left[\frac{\mu}{4}(3 - K) + \frac{1 + K}{4} - \frac{\mu(1 - \mu)(K^2 - 1)(K + 1)}{16K_1^2}\right]$$

$$K_{4,6} = \frac{D_1}{4}\left[-\frac{(2 + \mu^2)(K + 1)}{6K_1} - \frac{(1 - \mu)K_1}{2} + \frac{\mu(1 - \mu)(K^2 - 1)}{8K_1}\right]$$

$$K_{5,6} = \frac{-D_1}{4}\left[-\frac{\mu}{4}(3 - K) - \frac{1 + K}{4} + \frac{\mu(1 - \mu)(K^2 - 1)(K + 1)}{16K_1^2}\right]$$

$$K_{6,6} = \frac{D_1}{4}\left[\frac{(K - K\mu^2 + 3)(K + 1)}{6K_1} + \frac{(1 - \mu)K_1}{2} - \frac{\mu(1 - \mu)(K^2 - 1)}{8K_1}\right]$$

Continued Table (II-7,C)

$$K_{7,6} = -\frac{D_1}{4}\left[\frac{\mu}{4}(5+K) - \frac{(1+K)}{4} + \frac{\mu(1-\mu)(K^2-1)(K+1)}{16K_1^2}\right]$$

$$K_{8,6} = \frac{D_1}{4}\left[\frac{(-K+K\mu^2+3)(K+1)}{6K_1} - \frac{(1-\mu)K_1}{2} + \frac{\mu(1-\mu)(K^2-1)}{8K_1}\right]$$

2.10 Derivation of Plane Stress Energy Stiffness Matrix for an Equilateral Trapezoid

This method uses the virtual work principle to define the equivalent nodal forces.

The finite element has been defined as a body, the nodes of which undergo the same deformations as the plate and are acted upon by forces statically equivalent to the distributed edge stresses of the plate. The condition imposed on the values of the equivalent nodal forces here is that during a virtual deformation the external work done by the equivalent nodal forces of the finite element is the same as the external work done by the edge forces of the plate element.

During a virtual deformation, the external work done by the edge forces of the plate is equal to the internal work done by the internal stresses in the plate. The equality of the external work of the plate and the finite element requires the equality of their internal work. Let these nodal forces in reverse directions be applied to the plate element. This action makes the plate element suffer additional deformations and stresses superimposed on the ones carried originally. However, the edge forces are not affected because the new forces have been applied at the nodes only. The plate element is now acted upon by two sets of forces external to the element; the edge forces and the nodal forces, each set being in a state of equilibrium by itself. In this state the plate element of course continues to carry some internal stresses. The error of present formulation lies in disregarding the work of these internal stresses within the plate element. This work is not likely to be great because the originally present interior stresses were largely cancelled by the action of reversed nodal forces, but

still this work is not zero. Thus, the supposition of the equality of external work of the finite element and of the plate element is hypothetical.

If the selected virtual displacement $\{\bar{\delta}\}_j$ is such that it is unity in the direction of a particular external force f_j and zero in the direction of all other forces, then the external work in the finite element We_j will be the same as the value of the nodal force, i.e.

$$We_j = \{\bar{\delta}\}_j^T \{f\} = f_j \qquad \text{(II-19)}$$

Here, $\{\bar{\delta}\}_j$ = 8 x 1 column vector of virtual displacements. Its jth entry is unity and all other entries are zero.

$\{f\}$ = 8 x 1 column vector of nodal forces.

Writing the external work expressions for all such virtual displacements $\{\bar{\delta}\}_j$ (j = 1,2,...,8)

due to $\{\bar{\delta}\}_1$; $We_1 = (\bar{\delta}_1 = 1,0,0,\ldots,0)\{f\} = f_1$

due to $\{\bar{\delta}\}_2$; $We_2 = (0,\bar{\delta}_2 = 1,0,\ldots,0)\{f\} = f_2$

. . . . .

. . . . .

. . . . .

due to $\{\bar{\delta}\}_j$; $We_j = (0,\ldots,\bar{\delta}_j = 1,0,\ldots,0)\{f\} = f_j$

. . . . .

. . . . .

Collectively, these virtual displacements $\{\bar{\delta}\}_j$ (j = 1,2,...,8) can be written as $[\bar{\delta}]$ which is the same as an 8 x 8 Identity matrix [I]. The corresponding external works for all virtual displacements can be expressed

in matrix form as

$$\underset{8x1}{\{We\}} = \underset{8x8}{[\bar{\delta}]^T}\underset{8x1}{\{f\}} = \underset{}{[I]\{f\}} = \underset{8x1}{\{f\}} \qquad \text{(II-20)}$$

During each of these virtual displacements $\{\bar{\delta}\}_j$, an internal work Wi_j is done by the internal stresses over the area of the plate which is the same as the external work We_j of the edge stresses. For a plate of constant thickness t , the internal work may be expressed as[24]

$$Wi_j = t\iint_{area} \{\bar{\varepsilon}\}_j^T\{\sigma\}dxdy \qquad \text{(II-21)}$$

Here $\{\bar{\varepsilon}\}_j$ = 3 x 1 column vector of strains due to virtual displacements $\{\bar{\delta}\}_j$

The integration is to be carried out over the entire area of the plate. Using Eqn. (II-11), the strains due to virtual displacements $\{\bar{\delta}\}_j$ may be expressed as

$$\{\bar{\varepsilon}\}_j = [G][A^{-1}]\{\bar{\delta}\}_j$$

Substituting for $\{\bar{\varepsilon}\}_j$ from above and for $\{\sigma\}$ from Eqn. (II-13) in the Eqn. (II-21) one obtains,

$$\underset{1x1}{Wi_j} = t\iint_{area} \underset{1x8}{\{\bar{\delta}\}_j^T}\underset{8x8}{[A^{-1}]^T}\underset{8x3}{[G]^T}\underset{3x3}{[D]}\underset{3x8}{[G]}\underset{8x8}{[A^{-1}]}\underset{8x1}{\{\delta\}}dxdy \qquad \text{(II-22)}$$

Writing the internal work expressions for all such virtual displacements $\{\bar{\delta}\}_j$, (j = 1,2,...,8),

due to $\{\bar{\delta}\}_1$; $Wi_1 = t \iint_{area} \{\bar{\delta}\}_1^T [A^{-1}]^T [G]^T [D][G][A^{-1}]\{\delta\} dxdy$

due to $\{\bar{\delta}\}_2$; $Wi_2 = t \iint_{area} \{\bar{\delta}\}_2^T [A^{-1}]^T [G]^T [D][G][A^{-1}]\{\delta\} dxdy$

. .
. .
. .

due to $\{\bar{\delta}\}_j$; $Wi_j = t \iint_{area} \{\bar{\delta}\}_j^T [A^{-1}]^T [G]^T [D][G][A^{-1}]\{\delta\} dxdy$

. .
. .
. .

Collectively, internal works $\{Wi\}$ due to all such virtual displacements $[\bar{\delta}]$ (i.e. $\{\bar{\delta}\}_j$, $j = 1,2,\ldots,8$) can be written in the matrix form as

$$\underset{8x1}{\{Wi\}} = t \iint_{area} \underset{8x8}{[\bar{\delta}]^T} \underset{8x8}{[A^{-1}]^T} \underset{8x3}{[G]^T} \underset{3x3}{[D]} \underset{3x8}{[G]} \underset{8x8}{[A^{-1}]} \underset{8x1}{\{\delta\}} dxdy \qquad \text{(II-23)}$$

$[A^{-1}]$ is a matrix in terms of constant corner coordinate and therefore can be taken out of the integration sign. Also, note that

$$[\bar{\delta}]^T [A^{-1}]^T = [I][A^{-1}]^T = [A^{-1}]^T$$

Only the [G] matrix contains variables x and y. Equation (II-23) can be rewritten as

$$\{Wi\} = [A^{-1}]^T \; t \iint_{area} [G]^T [D][G] dxdy \; [A^{-1}]\{\delta\} \qquad \text{(II-24)}$$

Equating the external work done by the nodal forces of the finite element during all virtual displacements (Eqn. (II-20)) to the corresponding internal work done by the internal stresses in the plate element (Eqn. (II-24)), one obtains;

$$\{f\} = [A^{-1}]^T \; t \iint_{area} [G]^T[D][G]dxdy \; [A^{-1}]\{\delta\} \qquad \text{(II-25)}$$

Comparing Eqn. (II-25) with the force-displacement relation of Eqn. (II-17), the Energy stiffness matrix may be written as

$$[K] = [A^{-1}]^T \; t \iint_{area} [G]^T[D][G]dxdy \; [A^{-1}] \qquad \text{(II-26)}$$

Letting, $[H] = t \iint_{area} [G]^T[D][G]dxdy$

The entries of the product matrix $[G]^T[D][G]$ are simple polynomials of x and y which are easily integrated over the area of the element. Due to the symmetry of the element about the Y-axis, integration of the polynomial terms containing odd powers of x result in zero value. The integrated [H] matrix is given in Table (II-8). Equation (II-26) is rewritten as

$$[K] = [A^{-1}]^T[H][A^{-1}] \qquad \text{(II-27,b)}$$

The congruent transformations of the symmetric matrix [D] in Eqn. (II-26) ensures the symmetry of the energy stiffness matrix[25].

Table (II-7,b) showing the equality of stiffness coefficients due to the geometrical symmetry of the element about the Y-axis is still valid.

Table (II-8) $[H] = t \iint_{\text{area}} [G]^T [D][G]\, dxdy$ Eqn. (II-27;a)

$$[H] = \frac{Et}{(1-\mu^2)} \begin{bmatrix} 0 & 0 & 0 & 0 & 0 & 0 & 0 & 0 \\ 0 & L_1 & 0 & 0 & 2(1-\mu^2)L_2 & \mu L_1 & 0 & 0 \\ 0 & 0 & \frac{(1-\mu)L_1}{2} & 0 & 0 & 0 & \frac{(1-\mu)L_1}{2} & 0 \\ 0 & 0 & 0 & 4(1-\mu^2)L_3 & 0 & 0 & 0 & 0 \\ 0 & 2(1-\mu^2)L_2 & 0 & 0 & 4(1-\mu^2)L_4 & 0 & 0 & 0 \\ 0 & \mu L_1 & 0 & 0 & 0 & L_1 & 0 & 0 \\ 0 & 0 & \frac{(1-\mu)L_1}{2} & 0 & 0 & 0 & \frac{(1-\mu)L_1}{2} & 0 \\ 0 & 0 & 0 & 0 & 0 & 0 & 0 & 0 \end{bmatrix}$$

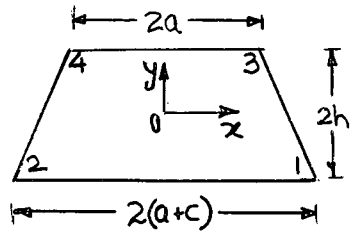

Here,

$$L_1 = 2(2a + c)h$$

$$L_2 = -\frac{2}{3} ch^2$$

$$L_3 = \frac{h(2a + c)}{6} \{c^2 + (2a + c)^2\}$$

$$L_4 = \frac{2}{3} (2a + c)h^3$$

Table (II-9) Entries of the Energy Stiffness Matrix for a Trapezoid in Plane Stress (Fig. (II-2))

$$[K]=\frac{Et}{(1-\mu^2)}\begin{bmatrix}
\eta_1+\beta_6 & & & & & & & & \\
\eta_2-\beta_2 & \eta_4+\beta_5 & & & & & & & \\
-\eta_1+\beta_6 & \eta_5+\beta_1 & \eta_1+\beta_6 & & & & & & \\
\eta_2+\beta_2 & -\eta_4+\beta_5 & -\eta_2+\beta_2 & \eta_4+\beta_5 & & & & & \\
\eta_3-\beta_6 & -\eta_5-\beta_3 & -\eta_3-\beta_6 & \eta_5-\beta_3 & \eta_7+\beta_6 & & & & \\
-\eta_2-\beta_4 & \eta_6-\beta_5 & \eta_2-\beta_4 & -\eta_6-\beta_5 & \eta_8+\beta_4 & \eta_9+\beta_5 & & & \\
-\eta_3-\beta_6 & -\eta_5+\beta_3 & \eta_3-\beta_6 & \eta_5+\beta_3 & -\eta_7+\beta_6 & -\eta_8+\beta_4 & \eta_7+\beta_6 & & \\
-\eta_2+\beta_4 & -\eta_6-\beta_5 & \eta_2+\beta_4 & \eta_6-\beta_5 & \eta_8-\beta_4 & -\eta_9+\beta_5 & -\eta_8-\beta_4 & \eta_9+\beta_5
\end{bmatrix}$$

symmetrical $(K_{ji}=K_{ij})$

Here,

$$\beta_1 = \frac{\{4\mu K_1^2 + (K^2-1)\}(K+1)}{32KK_1^2}$$

$$\beta_2 = \frac{\{4K_1^2 + \mu(K^2-1)\}(K+1)}{32KK_1^2}\ \frac{(1-\mu)}{2}$$

$$\beta_3 = \frac{\{4\mu K_1^2 - (K^2-1)\}(K+1)}{32K_1^2}$$

$$\beta_4 = \frac{\{4K_1^2 - \mu(K^2-1)\}(K+1)}{32K_1^2}\ \frac{(1-\mu)}{2}$$

$$\beta_5 = \frac{(K+1)}{8K_1}$$

$$\beta_6 = \frac{(K+1)}{8K_1}\ \frac{(1-\mu)}{2}$$

$$\eta_1 = \frac{1}{4K}\left[\frac{\{4K_1^2 + \mu(K^2-1)\}(K+1)}{8KK_1} + \frac{(1-\mu^2)(K-1)K_1}{6K}\right]$$

$$+ \frac{1}{8KK_1}\left[\frac{2}{3}(1-\mu^2)K_1^2 + \frac{\{4\mu K_1^2 + (K^2-1)\}(K+1)}{8KK_1}\ \frac{(K^2-1)}{2K_1}\right]$$

Continued Table (II-9)

$$\eta_2 = -\frac{(K+1)}{16KK_1}\left[\frac{(K^2-1)}{2K_1} + 2\mu K_1\right] = -\beta_1$$

$$\eta_3 = \frac{1}{4K}\left[\frac{\{4K_1^2 - \mu(K^2-1)\}}{8K_1}(K+1) - \frac{(1-\mu^2)(K-1)K_1}{6}\right]$$

$$- \frac{1}{8KK_1}\left[\frac{2}{3}(1-\mu^2)K_1^2 - \{\frac{4\mu K_1^2 - (K^2-1)}{8K_1}\}(K+1)\frac{(K^2-1)}{2K_1}\right]$$

$$\eta_4 = \left[\frac{4K_1^2 + \mu(K^2-1)}{8KK_1}\right]^2 \frac{(K+1)}{2K_1}\ \frac{(1-\mu)}{2}$$

$$+ \frac{1}{8KK_1}\ \frac{(1-\mu^2)}{12}\ \frac{(K+1)}{K}\{(K-1)^2 + (K+1)^2\}$$

$$\eta_5 = -\left[\frac{4K_1^2 + \mu(K^2-1)}{8KK_1}\right]\frac{(K+1)}{4K_1}\ \frac{(1-\mu)}{2} = -\beta_2$$

$$\eta_6 = \left[\frac{4K_1^2 + \mu(K^2-1)}{8KK_1}\right]\{4K_1^2 - \mu(K^2-1)\}\frac{(K+1)}{16K_1^2}\frac{(1-\mu)}{2}$$

$$- \frac{1}{8KK_1}\ \frac{(1-\mu^2)}{12}\ (K+1)\{(K-1)^2 + (K+1)^2\}$$

$$\eta_7 = \frac{1}{8K_1}\left[\{4K_1^2 - \mu(K^2-1)\}\frac{(K+1)}{4} - \frac{(1-\mu^2)}{3}(K-1)K_1^2\right.$$

$$\left. + \frac{2}{3}(1-\mu^2)K_1^2 - \frac{(K^2-1)(K+1)}{16K_1^2}\{4\mu K_1^2 - (K^2-1)\}\right]$$

$$\eta_8 = \{4\mu K_1^2 - (K^2-1)\}\ \frac{(K+1)}{32K_1^2} = \beta_3$$

$$\eta_9 = \{\frac{4K_1^2 - \mu(K^2-1)}{8K_1}\}^2\frac{(K+1)}{2K_1}\ \frac{(1-\mu)}{2}$$

$$+ \frac{1}{8K_1}\ \frac{(1-\mu^2)}{12}\ (K+1)\{(K-1)^2 + (K+1)^2\}$$

The stiffness coefficients belonging to the lower half of the symmetrical energy stiffness matrix are given in Table (II-9).

It is of interest to note that in conditions of uniform stress, the nodal forces obtained by using either Statics or Energy approach are identical.[23] Thus, in conditions of uniform stress, the Statics and Energy stiffness matrices will yield identical results.

When the trapezoid reduces to a rectangle, the Energy stiffness matrix coincides with the one derived by Clough.[20] It is of further interest to note that the Statics and Energy stiffness matrices for a rectangular element are identical.

2.11 Derivation of Plane Stress Stiffness Matrix for an Isosceles Triangle Fig. (II-6)

A triangle has six degrees of freedom. Three rigid body movements are possible without in any way affecting the state of stress. Thus, three independent stress conditions are required for the formation of the stiffness matrix. The three necessary stress conditions are, constant σ_x, constant σ_y and constant σ_{xy}.[38] These stress states are conveniently achieved by selecting a displacement function of the type.

$$u = b_1 + b_2x + b_3y$$
$$v = b_4 + b_5x + b_6y \qquad \text{(II-28)}$$

Nodal displacements in terms of the six constant parameters are expressed through an equation similar to Eqn. (II-7). The 6 x 6 matrix $[A_\Delta]$ of this

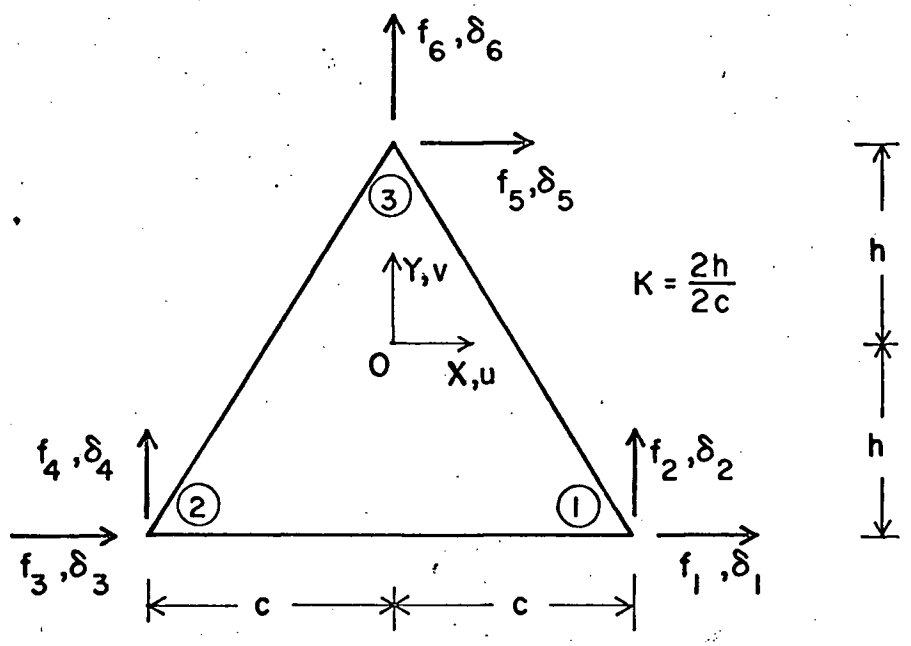

FIG. (II-6) ISOSCELES TRIANGULAR ELEMENT IN PLANE STRESS. (Positive directions of forces and displacements.)

case is shown in Table (II-10).

The parameters $b_1, b_2, \ldots, b_6$ are evaluated in terms of the nodal displacements as in Eqn. (II-8) and are shown in Table (II-11).

2.12 Derivation of Plane Stress - Statics Stiffness Matrix for an Isosceles Triangle

Equivalent nodal forces corresponding to each displacement mode are expressed as in Eqn. (II-15). The 6 x 6 matrix of equivalent corner forces, $[C_\Delta]$, is shown in Table (II-12). The stiffness matrix, $[K_\Delta]$, is obtained using Eqn. (II-18) and is shown in Table (II-13).

Note that the statics stiffness matrix for a triangle in plane stress is symmetrical.

2.13 Derivation of Plane Stress Energy Stiffness Matrix for an Isosceles Triangle

The plane stress energy stiffness matrix for an isosceles triangle element is expressed as in Eqn. (II-26) or Eqn. (II-27,b). The $[A^{-1}_\Delta]$ matrix is given in Table (II-11) and $[H_\Delta]$ matrix is shown in Table (II-14). Note that, for a triangle in plane stress, the energy stiffness matrix coincides with the statics stiffness matrix shown in Table (II-13). This matrix is identical to the matrix derived by Clough[20] and Turner et al.[38]

Table (II-10) Nodal Displacements of an Isosceles Triangle in Terms of Constant Parameters Fig. (II-6)

$$\begin{bmatrix} \delta_1 \\ \delta_2 \\ \delta_3 \\ \delta_4 \\ \delta_5 \\ \delta_6 \end{bmatrix} = \begin{bmatrix} 1 & c & -h & 0 & 0 & 0 \\ 0 & 0 & 0 & 1 & c & -h \\ 1 & -c & -h & 0 & 0 & 0 \\ 0 & 0 & 0 & 1 & -c & -h \\ 1 & 0 & h & 0 & 0 & 0 \\ 0 & 0 & 0 & 1 & 0 & h \end{bmatrix} \begin{bmatrix} b_1 \\ b_2 \\ b_3 \\ b_4 \\ b_5 \\ b_6 \end{bmatrix}$$

$$\{\delta_\Delta\} = [A_\Delta]\{B_\Delta\}$$

Table (II-11) Evaluation of Constant Parameters for an Isosceles Triangle in Terms of Nodal Displacements

$$\begin{bmatrix} b_1 \\ b_2 \\ b_3 \\ b_4 \\ b_5 \\ b_6 \end{bmatrix} = \begin{bmatrix} \frac{1}{4} & 0 & \frac{1}{4} & 0 & \frac{1}{2} & 0 \\ \frac{1}{2c} & 0 & \frac{-1}{2c} & 0 & 0 & 0 \\ \frac{-1}{4h} & 0 & \frac{-1}{4h} & 0 & \frac{1}{2h} & 0 \\ 0 & \frac{1}{4} & 0 & \frac{1}{4} & 0 & \frac{1}{2} \\ 0 & \frac{1}{2c} & 0 & \frac{-1}{2c} & 0 & 0 \\ 0 & \frac{-1}{4h} & 0 & \frac{-1}{4h} & 0 & \frac{1}{2h} \end{bmatrix} \begin{bmatrix} \delta_1 \\ \delta_2 \\ \delta_3 \\ \delta_4 \\ \delta_5 \\ \delta_6 \end{bmatrix}$$

$$\{B_\Delta\} = [A_\Delta^{-1}]\{\delta_\Delta\}$$

Table (II-12) Equivalent Nodal Forces in Terms of Constant Parameters for an Isosceles Triangle

$$\begin{bmatrix} f_1 \\ f_2 \\ f_3 \\ f_4 \\ f_5 \\ f_6 \end{bmatrix} = D_1 \begin{bmatrix} 0 & h & -\frac{(1-\mu)}{2}\frac{c}{2} & 0 & -\frac{(1-\mu)}{2}\frac{c}{2} & \mu h \\ 0 & -\frac{\mu c}{2} & \frac{(1-\mu)}{2}h & 0 & \frac{(1-\mu)}{2}h & -\frac{c}{2} \\ 0 & -h & -\frac{(1-\mu)}{2}\frac{c}{2} & 0 & -\frac{(1-\mu)}{2}\frac{c}{2} & -\mu h \\ 0 & -\frac{\mu c}{2} & -\frac{(1-\mu)}{2}h & 0 & -\frac{(1-\mu)}{2}h & -\frac{c}{2} \\ 0 & 0 & \frac{(1-\mu)}{2}c & 0 & \frac{(1-\mu)}{2}c & 0 \\ 0 & \mu c & 0 & 0 & 0 & c \end{bmatrix} \begin{bmatrix} b_1 \\ b_2 \\ b_3 \\ b_4 \\ b_5 \\ b_6 \end{bmatrix}$$

$$\{f_\Delta\} = [C_\Delta]\{B_\Delta\}$$

Table (II-13) Plane Stress Stiffness Matrix for an Isosceles Triangle (Fig. (II-6))

Let, $K = (\frac{2h}{2c}) = \frac{\text{height}}{\text{base}}$

$$[K_\Delta] = \frac{Et}{(1-\mu^2)} \begin{bmatrix} \frac{1}{2}\left[K + \frac{(1-\mu)}{8K}\right] & & & & & \\ -\frac{(1+\mu)}{8} & \frac{1}{8}\left[\frac{1}{K} + 2(1-\mu)K\right] & & & & \\ -\frac{1}{2}\left[K - \frac{(1-\mu)}{8K}\right] & \frac{(3\mu-1)}{8} & \frac{1}{2}\left[K + \frac{(1-\mu)}{8K}\right] & & \text{symmetrical} & \\ -\frac{(3\mu-1)}{8} & \frac{1}{8}\left[\frac{1}{K} - 2(1-\mu)K\right] & \frac{(1+\mu)}{8} & \frac{1}{8}\left[\frac{1}{K} + 2(1-\mu)K\right] & & \\ -\frac{(1-\mu)}{8K} & \frac{(1-\mu)}{4} & -\frac{(1-\mu)}{8K} & -\frac{(1-\mu)}{4} & \frac{(1-\mu)}{4K} & \\ \frac{\mu}{2} & -\frac{1}{4K} & -\frac{\mu}{2} & -\frac{1}{4K} & 0 & \frac{1}{2K} \end{bmatrix}$$

Table (II-14) Integrated $[H_\Delta]$ Matrix

$$[H_\Delta] = t \iint_{\text{area}} [G_\Delta]^T [D] [G_\Delta] \, dxdy = \frac{Et(2ch)}{(1-\mu^2)} \begin{bmatrix} 0 & 0 & 0 & 0 & 0 & 0 \\ 0 & 1 & 0 & 0 & 0 & \mu \\ 0 & 0 & \frac{(1-\mu)}{2} & 0 & \frac{(1-\mu)}{2} & 0 \\ 0 & 0 & 0 & 0 & 0 & 0 \\ 0 & 0 & \frac{(1-\mu)}{2} & 0 & \frac{(1-\mu)}{2} & 0 \\ 0 & \mu & 0 & 0 & 0 & 1 \end{bmatrix}$$

CHAPTER III

DERIVATION OF FLEXURE STIFFNESS MATRICES

3.1 General

In a plate bending problem, a point on the plate is allowed to displace in a direction normal to the plate and to rotate about two mutually perpendicular axes in the plane of the plate. Assuming that the deflections are small, stretching of the plate in its plane due to the deflections is neglected.

In the following discussions, the term "deformation" will include displacement or rotations, and the term "nodal force" will include transeverse force or moments.

The formulation of flexure stiffness matrices follows a similar systematic matrix procedure as is adopted in the derivation of plane stress stiffness matrices.

3.2 Equation of the Deflection Surface for a Quadrilateral Plate Element in Flexure

A flexural finite element having n nodes has (3n) degrees of freedom as these nodes move or rotate while the plate element deforms under the action of moments. However, there are three rigid body movements: a rigid body displacement in the Z direction, and rigid body rotation about X and Y directions respectively. Thus, three of the corner

displacements may be made zero by rigid body movements without interferring in any way with the shears and moments imposed on the plate element. This leaves (3n-3) independent deformation conditions for the formulation of the stiffness matrix, irrespective of the shape of the finite element. For a quadrilateral with four nodes, this number is (3)(4)-(3)=(9). Three of these conditions must be constant curvatures for bending in two perpendicular directions and a constant twist.

Lateral deflections are represented throughout the plate element by a polynomial in x and y as[27]

$$w = b_1 + b_2x + b_3y + b_4x^2 + b_5xy + b_6y^2 + b_7x^3 + b_8x^2y + b_9xy^2 + b_{10}y^3 + b_{11}x^3y + b_{12}xy^3 \qquad \text{(III-1)}$$

Here, w = displacement normal to the plane of the plate and is positive upwards

$b_1, b_2, \ldots, b_{12}$ = constant parameters

Rotations are defined as

$$\theta_x = \frac{\partial w}{\partial y} \; ; \quad \theta_y = -\frac{\partial w}{\partial x}$$

and are positive in the direction of right hand screw when viewed in the positive directions of x and y axes.

Note that each term of the displacement surface Eqn. (III-1) satisfies the biharmonic equation governing the deflection of an unloaded plate.

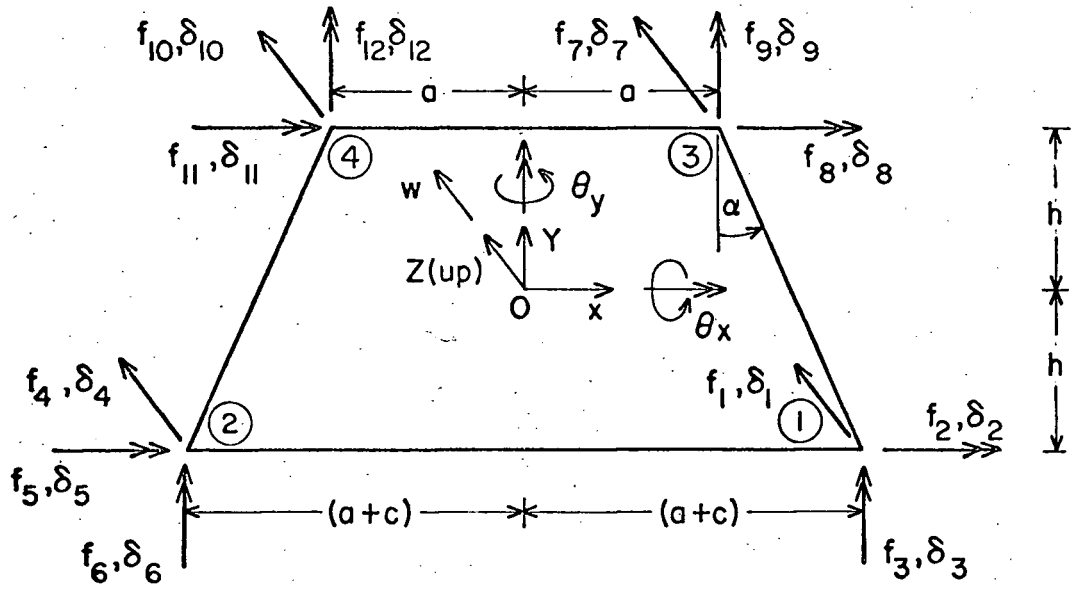

FIG (III-1) EQUILATERAL TRAPEZOID IN FLEXURE

(Positive directions of nodal forces and deformations)

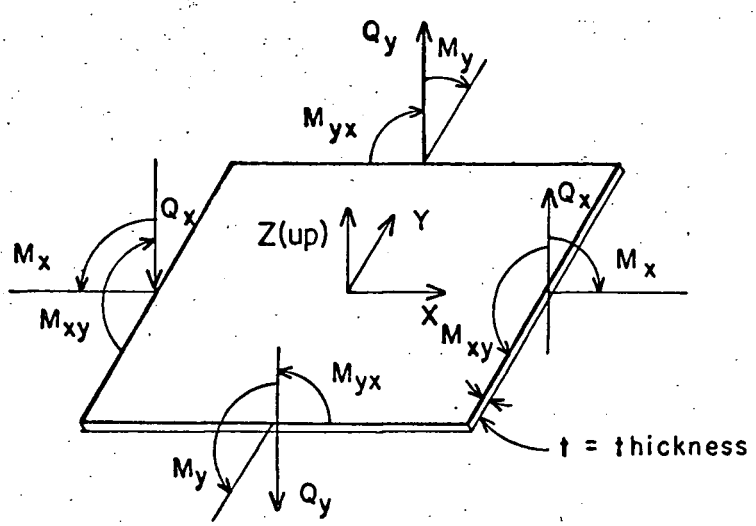

FIG (III-2) DIRECTIONS OF POSITIVE TRANSEVERSE SHEARS AND MOMENTS

3.3 Evaluation of the Constant Parameters for an Equilateral Trapezoid Element in Flexure

For an equilateral trapezoid plate element, the twelve nodal displacements and rotations are obtained in terms of the twelve parameters, $b_1, b_2, \ldots, b_{12}$. These displacements and rotations may be written in a matrix form:

$$\{\delta^*\} = [A^*]\{B^*\} \qquad \text{(III-2)}$$

Here, $\{\delta^*\}$ = 12 x 1 column vector of nodal deformations $\delta_1, \delta_2, \ldots, \delta_{12}$ Fig. (III-1)

$[A^*]$ = 12 x 12 matrix in terms of corner coordinates of the trapezoid.

$\{B^*\}$ = 12 x 1 column vector of constant parameters $b_1, b_2, \ldots, b_{12}$.

The matrix Eqn. (III-2) is shown in full in Table (III-1).

The parameters, $\{B^*\}$, are evaluated in terms of the corner deformations:

$$\{B^*\} = [A^{*-1}]\{\delta^*\} \qquad \text{(III-3)}$$

The matrix $[A^{*-1}]$ is given in Table (III-2).

Knowing the corner deformations, $\{\delta^*\}$, of a finite element, the displacement surface of the piece of plate having the same deformations as the finite element is completely known.

Table (III-1) Nodal Deformations for a Trapezoid Element in Terms of Constant Parameters

Fig. (III-1)

$$W = b_1 + b_2x + b_3y + b_4x^2 + b_5xy + b_6y^2 + b_7x^3 + b_8x^2y + b_9xy^2 + b_{10}y^3 + b_{11}x^3y + b_{12}xy^3$$

$$\theta_x = \frac{\partial w}{\partial y} \; ; \; \theta_y = -\frac{\partial w}{\partial x}$$

$$\begin{bmatrix} \delta_1 \\ \delta_2 \\ \delta_3 \\ \delta_4 \\ \delta_5 \\ \delta_6 \\ \delta_7 \\ \delta_8 \\ \delta_9 \\ \delta_{10} \\ \delta_{11} \\ \delta_{12} \end{bmatrix} = \begin{bmatrix} 1 & (a+c) & -h & (a+c)^2 & -(a+c)h & h^2 & (a+c)^3 & -(a+c)^2h & (a+c)h^2 & -h^3 & -(a+c)^3h & -(a+c)h^3 \\ 0 & 0 & 1 & 0 & (a+c) & -2h & 0 & (a+c)^2 & -2(a+c)h & 3h^2 & (a+c)^3 & 3(a+c)h^2 \\ 0 & -1 & 0 & -2(a+c) & h & 0 & -3(a+c)^2 & 2(a+c)h & -h^2 & 0 & 3(a+c)^2h & h^3 \\ 1 & -(a+c) & -h & (a+c)^2 & (a+c)h & h^2 & -(a+c)^3 & -(a+c)^2h & -(a+c)h^2 & -h^3 & (a+c)^3h & (a+c)h^3 \\ 0 & 0 & 1 & 0 & -(a+c) & -2h & 0 & (a+c)^2 & 2(a+c)h & 3h^2 & -(a+c)^3 & -3(a+c)h^2 \\ 0 & -1 & 0 & 2(a+c) & h & 0 & -3(a+c)^2 & -2(a+c)h & -h^2 & 0 & 3(a+c)^2h & h^3 \\ 1 & a & h & a^2 & ah & h^2 & a^3 & a^2h & ah^2 & h^3 & a^3h & ah^3 \\ 0 & 0 & 1 & 0 & a & 2h & 0 & a^2 & 2ah & 3h^2 & a^3 & 3ah^2 \\ 0 & -1 & 0 & -2a & -h & 0 & -3a^2 & -2ah & -h^2 & 0 & -3a^2h & -h^3 \\ 1 & -a & h & a^2 & -ah & h^2 & -a^3 & a^2h & -ah^2 & h^3 & -a^3h & -ah^3 \\ 0 & 0 & 1 & 0 & -a & 2h & 0 & a^2 & -2ah & 3h^2 & -a^3 & -3ah^2 \\ 0 & -1 & 0 & 2a & -h & 0 & -3a^2 & 2ah & -h^2 & 0 & -3a^2h & -h^3 \end{bmatrix} \begin{bmatrix} b_1 \\ b_2 \\ b_3 \\ b_4 \\ b_5 \\ b_6 \\ b_7 \\ b_8 \\ b_9 \\ b_{10} \\ b_{11} \\ b_{12} \end{bmatrix}$$

$$\{\delta^*\} = [A^*]\{B^*\} \qquad \text{Eqn. (III-2)}$$

Table (III-2) Evaluation of Constant Parameters in Terms of Nodal Displacements and Rotations for a Trapezoid in Flexure

$$
\begin{bmatrix} b_1 \\ b_2 \\ b_3 \\ b_4 \\ b_5 \\ b_6 \\ b_7 \\ b_8 \\ b_9 \\ b_{10} \\ b_{11} \\ b_{12} \end{bmatrix} =
\begin{bmatrix}
1/4 & h/8 & \alpha_1 & 1/4 & h/8 & -\alpha_1 & 1/4 & -h/8 & \alpha_2 & 1/4 & \frac{-h}{8} & -\alpha_2 \\
\alpha_3 & \frac{h}{8(a+c)} & \frac{\alpha_1}{(a+c)} & -\alpha_3 & \frac{-h}{8(a+c)} & \frac{\alpha_1}{(a+c)} & \alpha_4 & -h/8a & \frac{\alpha_2}{a} & -\alpha_4 & \frac{h}{8a} & \frac{\alpha_2}{a} \\
-\frac{3}{8h} & -1/8 & \alpha_5 & -3/8h & -1/8 & -\alpha_5 & 3/8h & -1/8 & \alpha_6 & 3/8h & -\frac{1}{8} & -\alpha_6 \\
0 & 0 & -\frac{1}{8(a+c)} & 0 & 0 & \frac{1}{8(a+c)} & 0 & 0 & \frac{-1}{8a} & 0 & 0 & \frac{1}{8a} \\
\alpha_7 & -\frac{1}{8(a+c)} & \frac{\alpha_5}{(a+c)} & -\alpha_7 & \frac{1}{8(a+c)} & \frac{\alpha_5}{(a+c)} & \alpha_8 & -1/8a & \frac{\alpha_6}{a} & -\alpha_8 & \frac{1}{8a} & \frac{\alpha_6}{a} \\
0 & -\frac{1}{8h} & \frac{\alpha_9}{8(a+c)h} & 0 & -1/8h & \frac{-\alpha_9}{8(a+c)h} & 0 & 1/8h & \frac{-\alpha_9}{8ah} & 0 & \frac{1}{8h} & \frac{\alpha_9}{8ah} \\
-\frac{1}{8(a+c)^3} & 0 & -\frac{1}{8(a+c)^2} & \frac{1}{8(a+c)^3} & 0 & \frac{-1}{8(a+c)^2} & \frac{-1}{8a^3} & 0 & \frac{-1}{8a^2} & \frac{1}{8a^3} & 0 & \frac{-1}{8a^2} \\
0 & 0 & \frac{1}{8(a+c)h} & 0 & 0 & \frac{-1}{8(a+c)h} & 0 & 0 & \frac{-1}{8ah} & 0 & 0 & \frac{1}{8ah} \\
\frac{\alpha_9}{8h(a+c)^3} & -\frac{1}{8h(a+c)} & \frac{\alpha_9}{8h(a+c)^2} & \frac{-\alpha_9}{8h(a+c)^3} & \frac{1}{8h(a+c)} & \frac{\alpha_9}{8h(a+c)^2} & \frac{-\alpha_9}{8ha^3} & \frac{1}{8ha} & \frac{-\alpha_9}{8ha^2} & \frac{\alpha_9}{8ha^3} & \frac{-1}{8ha} & \frac{-\alpha_9}{8ha^2} \\
\frac{1}{8h^3} & \frac{1}{8h^2} & \frac{\alpha_9}{8(a+c)h^2} & \frac{1}{8h^3} & \frac{1}{8h^2} & \frac{-\alpha_9}{8(a+c)h^2} & \frac{-1}{8h^3} & \frac{1}{8h^2} & \frac{\alpha_9}{8ah^2} & \frac{-1}{8h^3} & \frac{1}{8h^2} & \frac{-\alpha_9}{8ah^2} \\
\frac{1}{8h(a+c)^3} & 0 & \frac{1}{8h(a+c)^2} & \frac{-1}{8h(a+c)^3} & 0 & \frac{1}{8h(a+c)^2} & \frac{-1}{8ha^3} & 0 & \frac{-1}{8ha^2} & \frac{1}{8ha^3} & 0 & \frac{-1}{8ha^2} \\
-\frac{\alpha_5}{(a+c)^2h^2} & \frac{1}{8(a+c)h^2} & \frac{\alpha_9}{8h^2(a+c)^2} & \frac{\alpha_5}{(a+c)^2h^2} & \frac{-1}{8(a+c)h^2} & \frac{\alpha_9}{8(a+c)^2h^2} & \frac{-\alpha_6}{a^2h^2} & \frac{1}{8ah^2} & \frac{\alpha_9}{8h^2a^2} & \frac{\alpha_6}{a^2h^2} & -\frac{1}{8ah^2} & \frac{\alpha_9}{8h^2a^2}
\end{bmatrix}
\begin{bmatrix} \delta_1 \\ \delta_2 \\ \delta_3 \\ \delta_4 \\ \delta_5 \\ \delta_6 \\ \delta_7 \\ \delta_8 \\ \delta_9 \\ \delta_{10} \\ \delta_{11} \\ \delta_{12} \end{bmatrix}
$$

$$\{B^*\} = [A^{*-1}]\{\delta^*\} \qquad \text{Eqn. (III-3)}$$

Continued Table (III-2)

Here, $\alpha_1 = \frac{\{3(a+c)^2 + a^2\}}{32(a+c)}$

$\alpha_2 = \frac{\{(a+c)^2 + 3a^2\}}{32a}$

$\alpha_3 = \frac{\{11(a+c)^2 + a^2\}}{32(a+c)^3}$

$\alpha_4 = \frac{\{(a+c)^2 + 11a^2\}}{32a^3}$

$\alpha_5 = \frac{\{-5(a+c)^2 + a^2\}}{32h(a+c)}$

$\alpha_6 = \frac{\{-(a+c)^2 + 5a^2\}}{32ha}$

$\alpha_7 = \frac{\{-17(a+c)^2 + a^2\}}{32(a+c)^3h}$

$\alpha_8 = \frac{\{-(a+c)^2 + 17a^2\}}{32a^3h}$

$\alpha_9 = \frac{\{(a+c)^2 - a^2\}}{4h}$

3.4 Moments and Shears at a Point

Moments and transeverse shears at any point of the plate can be calculated using elasticity formulae.[26] The curvatures and twist at any point of the plate are written in terms of the twelve parameters;[27]

$$-\frac{\partial^2 w}{\partial x^2} = -(2b_4 + 6b_7 x + 2b_8 y + 6b_{11} xy)$$

$$-\frac{\partial^2 w}{\partial y^2} = -(2b_6 + 2b_9 x + 6b_{10} y + 6b_{12} xy)$$

$$2\frac{\partial^2 w}{\partial x \partial y} = (2b_5 + 4b_8 x + 4b_9 y + 6b_{11} x^2 + 6b_{12} y^2)$$

In the matrix form, these are written as,

$$\{\chi^*\} = [G^*]\{B^*\} \qquad \text{(III-4)}$$

Here, $\{\chi^*\}$ = 3 x 1 vector of curvatures and twist

$[G^*]$ = 3 x 12 matrix in terms of variables x and y

Expression (III-4) is shown in full in Table (III-3). Substituting in Eqn. (III-4) for $\{B^*\}$ from Eqn. (III-3), one obtains

$$\{\chi^*\} = [G^*][A^{*-1}]\{\delta^*\} \qquad \text{(III-5)}$$

Moments and shears per unit length of the plate are given by[26]

$$\text{Moments, } M_x = D_2\left[-\frac{\partial^2 w}{\partial x^2} - \mu\frac{\partial^2 w}{\partial y^2}\right]$$

$$M_y = D_2\left[-\frac{\partial^2 w}{\partial y^2} - \mu\frac{\partial^2 w}{\partial x^2}\right] \qquad \text{(III-6,a)}$$

$$M_{xy} = -M_{yx} = \frac{(1-\mu)}{2} D_2\left(2\frac{\partial^2 w}{\partial x \partial y}\right)$$

and Transeverse shears,

$$Q_x = -D_2 \frac{\partial}{\partial x} \left(\frac{\partial^2 w}{\partial x^2} + \frac{\partial^2 w}{\partial y^2} \right)$$

$$Q_y = -D_2 \frac{\partial}{\partial y} \left(\frac{\partial^2 w}{\partial x^2} + \frac{\partial^2 w}{\partial y^2} \right) \qquad \text{(III-6,b)}$$

Here, $D_2 = \frac{Et^3}{12(1-\mu^2)}$ = flexural rigidity per unit length of the plate

The positive directions of these moments and shears are shown in Fig. (III-2).

3.5 Moments at a point on the Trapezoid Element

Internal moments, given by Eqn. (III-6,a), can be expressed in the matrix form:

$$\{M^*\} = [D^*]\{\chi^*\} \qquad \text{(III-7)}$$

Here, $\{M^*\}$ = 3 x 1 matrix of internal moment

$[D^*]$ = 3 x 3 symmetrix matrix of elastic constants

The matrix equation (III-7) is shown in Table (III-4). Substituting for $\{\chi^*\}$ for a trapezoid from Eqn. (III-5) in Eqn. (III-7) one obtains

$$\{M^*\} = [D^*][G^*][A^{*-1}]\{\delta^*\} \qquad \text{(III-8)}$$

Letting $$[MT^*] = [D^*][G^*][A^{*-1}] \qquad \text{(III-9)}$$

Eqn. (III-8) can be rewritten:

$$\{M^*\} = [MT^*]\{\delta^*\} \qquad \text{(III-10)}$$

Here, $[MT^*]$ = 3 x 12 moment matrix in terms of the variables x and y

Table (III-3) Curvatures and Twist at Any Point (x,y) in Terms of Constant Parameters for a Trapezoid in Flexure

$$\begin{bmatrix} -\frac{\partial^2 w}{\partial x^2} \\ -\frac{\partial^2 w}{\partial y^2} \\ 2\frac{\partial^2 w}{\partial x \partial y} \end{bmatrix} = \begin{bmatrix} 0 & 0 & 0 & -2 & 0 & 0 & -6x & -2y & 0 & 0 & -6xy & 0 \\ 0 & 0 & 0 & 0 & 0 & -2 & 0 & 0 & -2x & -6y & 0 & -6xy \\ 0 & 0 & 0 & 0 & 2 & 0 & 0 & 4x & 4y & 0 & 6x^2 & 6y^2 \end{bmatrix} \begin{bmatrix} b_1 \\ b_2 \\ b_3 \\ b_4 \\ b_5 \\ b_6 \\ b_7 \\ b_8 \\ b_9 \\ b_{10} \\ b_{11} \\ b_{12} \end{bmatrix}$$

$$\{\chi^*\} = [G^*]\{B^*\} \qquad \text{Eqn. (III-4,b)}$$

Table (III-4) Relation Between Internal Moments and Curvatures and Twist

$$\begin{bmatrix} Mx \\ My \\ Mxy \end{bmatrix} = \begin{bmatrix} D_2 & \mu D_2 & 0 \\ \mu D_2 & D_2 & 0 \\ 0 & 0 & \frac{(1-\mu)D_2}{2} \end{bmatrix} \begin{bmatrix} -\frac{\partial^2 w}{\partial x^2} \\ -\frac{\partial^2 w}{\partial y^2} \\ 2\frac{\partial^2 w}{\partial x \partial y} \end{bmatrix}$$

$$\{M^*\} = [D^*]\{\chi^*\} \qquad \text{(III-7)}$$

Here, $D_2 = \frac{Et^3}{12(1-\mu^2)}$ flexural rigidity per unit length of the plate

Table (III-5) Moment Matrix for a Trapezoid Element in Flexure

All entries to be multiplied by $D_2 = Et^3/12(1-\mu^2)$

$$MT^*_{1,1} = [x(6h^3-2\mu\alpha_9h^2) - 6\mu(a+c)^3y - xy\{6h^2-48\mu\alpha_5h(a+c)\}]/8(a+c)^3h^3$$

$$MT^*_{2,1} = [x(6\mu h^3-2\alpha_9h^2) - 6y(a+c)^3 - xy\{6\mu h^2-48\alpha_5h(a+c)\}]/8h^3(a+c)^3$$

$$MT^*_{3,1} = \alpha_7(1-\mu) + \frac{\{3h(1-\mu)x^2 + 2(1-\mu)\alpha_9hy - 24(1-\mu)\alpha_5(a+c)y^2\}}{8h^2(a+c)^3}$$

$$MT^*_{1,2} = \{2\mu(a+c)h + 2\mu hx - 6\mu(a+c)y - 6\mu xy\}/8h^2(a+c)$$

$$MT^*_{2,2} = \{2h(a+c) + 2hx - 6(a+c)y - 6xy\}/8h^2(a+c)$$

$$MT^*_{3,2} = \{-(1-\mu)h^2 - 2(1-\mu)hy + 3(1-\mu)y^2\}/8h^2(a+c)$$

$$MT^*_{1,3} = [2(a+c)h(h-\mu\alpha_9) + x(6h^2-2\mu\alpha_9h) - y(a+c)(2h+6\mu\alpha_9) - 6xy(h+\mu\alpha_9)]/8h^2(a+c)^2$$

$$MT^*_{2,3} = [2(a+c)h(\mu h-\alpha_9) + x(6\mu h^2-2\alpha_9h) - y(a+c)(2\mu h+6\alpha_9) - 6xy(\mu h+\alpha_9)]/8h^2(a+c)^2$$

$$MT^*_{3,3} = [8h^2\alpha_5(a+c)(1-\mu) + 2xh(a+c)(1-\mu) + 3h(1-\mu)x^2 + 2h(1-\mu)y\alpha_9 + 3(1-\mu)\alpha_9y^2]/8(a+c)^2h^2$$

$$MT^*_{1,4} = [2xh^2(-3h+\mu\alpha_9) - 6\mu y(a+c)^3 + 6xyh\{h-8\mu\alpha_5(a+c)\}]/8h^3(a+c)^3$$

$$MT^*_{2,4} = [2xh^2(-3\mu h+\alpha_9) - 6y(a+c)^3 + 6xyh\{\mu h-8\alpha_5(a+c)\}]/8h^3(a+c)^3$$

$$MT^*_{3,4} = -\alpha_7(1-\mu) - \frac{\{3h(1-\mu)x^2 + 2(1-\mu)\alpha_9hy - 24(1-\mu)\alpha_5(a+c)y^2\}}{8h^2(a+c)^3}$$

$$MT^*_{1,5} = \{2\mu h(a+c) - 2\mu hx - 6\mu(a+c)y + 6\mu xy\}/8h^2(a+c)$$

$$MT^*_{2,5} = \{2h(a+c) - 2hx - 6(a+c)y + 6xy\}/8h^2(a+c)$$

$$MT^*_{3,5} = \{(1-\mu)h^2 + 2(1-\mu)hy - 3(1-\mu)y^2\}/8h^2(a+c)$$

$$MT^*_{1,6} = [-2h(a+c)(h-\mu\alpha_9) + 2hx(3h-\mu\alpha_9) + 2(a+c)y(h+3\mu\alpha_9) - 6xy(h+\mu\alpha_9)]/8h^2(a+c)^2$$

$$MT^*_{2,6} = [-2h(a+c)(\mu h-\alpha_9) + 2hx(3\mu h-\alpha_9) + 2(a+c)y(\mu h+3\alpha_9) - 6xy(\mu h+\alpha_9)]/8h^2(a+c)^2$$

Continued Table (III-5)

$$MT^*_{3,6} = [8\alpha_5(1-\mu)h^2(a+c) - 2h(1-\mu)(a+c)x + 2h(1-\mu)\alpha_9 y + 3h(1-\mu)x^2 + 3(1-\mu)\alpha_9 y^2]/8h^2(a+c)^2$$

$$MT^*_{1,7} = [2h^2x(3h+\mu\alpha_9) + 6\mu a^3 y + 6hxy(h+8\mu a\alpha_6)]/8h^3a^3$$

$$MT^*_{2,7} = [2h^2x(3\mu h+\alpha_9) + 6a^3 y + 6hxy(\mu h+8a\alpha_6)]/8h^3a^3$$

$$MT^*_{3,7} = (1-\mu)\alpha_8 - \frac{[3(1-\mu)hx^2 + 2(1-\mu)\alpha_9 hy + 24(1-\mu)a\alpha_6 y^2]}{8h^2a^3}$$

$$MT^*_{1,8} = -2\mu[ah + xh + 3ay + 3xy]/8ah^2$$

$$MT^*_{2,8} = -2[ah + xh + 3ay + 3xy]/8ah^2$$

$$MT^*_{3,8} = [-(1-\mu)h^2 + 2(1-\mu)hy + 3(1-\mu)y^2]/8ah^2$$

$$MT^*_{1,9} = [-2ah(h-\mu\alpha_9) + 2hx(3h+\mu\alpha_9) + 2ay(h-3\mu\alpha_9) + 6xy(h-\mu\alpha_9)]/8h^2a^2$$

$$MT^*_{2,9} = [-2ah(\mu h-\alpha_9) + 2hx(3\mu h+\alpha_9) + 2ay(\mu h-3\alpha_9) + 6xy(\mu h-\alpha_9)]/8h^2a^2$$

$$MT^*_{3,9} = [8\alpha_6(1-\mu)h^2a - 2(1-\mu)ahx - 2(1-\mu)h\alpha_9 y - 3(1-\mu)hx^2 + 3(1-\mu)\alpha_9 y^2]/8a^2h^2$$

$$MT^*_{1,10} = [-2h^2x(3h+\mu\alpha_9) + 6\mu a^3 y - 6hxy(h + 8\mu\alpha_6 a)]/8a^3h^3$$

$$MT^*_{2,10} = [-2h^2x(3\mu h+\alpha_9) + 6a^3 y - 6hxy(\mu h+8\alpha_6 a)]/8a^3h^3$$

$$MT^*_{3,10} = -(1-\mu)\alpha_8 + \frac{[2h(1-\mu)\alpha_9 y + 3h(1-\mu)x^2 + 24a(1-\mu)\alpha_6 y^2]}{8h^2a^3}$$

$$MT^*_{1,11} = 2\mu[-ah + hx - 3ay + 3xy]/8h^2a$$

$$MT^*_{2,11} = 2[-ah + hx - 3ay + 3xy]/8h^2a$$

$$MT^*_{3,11} = [(1-\mu)h^2 - 2(1-\mu)hy - 3(1-\mu)y^2]/8ah^2$$

$$MT^*_{1,12} = [-2ah(h+\mu\alpha_9) + 2hx(3h+\mu\alpha_9) - 2ay(h-3\mu\alpha_9) + 6xy(h-\mu\alpha_9)]/8a^2h^2$$

$$MT^*_{2,12} = [-2ah(\mu h+\alpha_9) + 2hx(3\mu h+\alpha_9) - 2ay(\mu h-3\alpha_9) + 6xy(\mu h-\alpha_9)]/8a^2h^2$$

$$MT^*_{3,12} = [8h^2(1-\mu)a\alpha_6 + 2(1-\mu)ahx - 2(1-\mu)\alpha_9 hx - 3(1-\mu)hx^2 + 3(1-\mu)\alpha_9 y^2]/8a^2h^2$$

Table (III-6) Transeverse Shear at a Point on the Trapezoid Element

$$\begin{bmatrix} Qx \\ Qy \end{bmatrix} = \begin{bmatrix} 0 & 0 & 0 & 0 & 0 & 0 & -6D_2 & 0 & -2D_2 & 0 & -6yD_2 & -6yD_2 \\ 0 & 0 & 0 & 0 & 0 & 0 & 0 & -2D_2 & 0 & -6D_2 & -6xD_2 & -6xD_2 \end{bmatrix} \begin{bmatrix} b_1 \\ b_2 \\ \vdots \\ b_{11} \\ b_{12} \end{bmatrix}$$

$$\{Q^*\} = [R^*]\{B^*\} \qquad \text{Eqn. (III-6,c)}$$

Once the deformation vector $\{\delta^*\}$ for an element is known, the moments at any point within the plate can be obtained from Eqn. (III-10) by simply substituting the coordinates of that point. Entries of the moment matrix [MT*] are shown in Table (III-5).

3.6 Transeverse Shears at any Point (x,y) on the Trapezoid Element

Substituting for w from Eqn. (III-1) in the expression for transeverse shears, Eqn. (III-6,b) can be written in the matrix form:

$$\{Q^*\} = [R^*]\{B^*\} \qquad \text{(III-6,c)}$$

Here, $\{Q^*\}$ = 2 x 1 vector of transeverse shears at a point (x,y) in the plate, and $[R^*]$ = 2 x 12 matrix in terms of variables x and y. See Table (III-6) Substituting in the above for $\{B^*\}$ from Eqn. (III-3), one obtains

$$\{Q^*\} = [R^*][A^{*-1}]\{\delta^*\} \qquad \text{(III-6,d)}$$

3.7 Equivalent Nodal Forces

The stiffness matrix depends upon the definition of equivalent nodal force. As in plane stress, the plate edge transeverse shears and moments may be transferred as equivalent nodal forces to the corners of the finite element in two different ways:

1. The edge shears and bending moments are transferred to the adjacent corners by the simple law of the lever - an operation completely consistent with statics. The stiffness matrix so obtained will be referred to as the Statics stiffness matrix

of the finite element in flexure,

2. The principle of virtual work is employed in a special way to determine the equivalent nodal forces from the plate edge shears and moments. The matrix so obtained will be referred to as the Energy stiffness matrix of the finite element in flexure.

3.8 Statics Stiffness Matrix for an Equilateral Trapezoid Element in Flexure

Each term of the displacement function given by Eqn. (III-1) represents an independent simple displacement mode (or an independent curvature and twist state). Its first three terms (b_1, $b_2 x$, and $b_3 y$) correspond to rigid body motions and, as such, do not cause any shear or moments. The remaining displacement terms are considered one at a time. The corresponding edge moments and shears are transferred to the adjacent nodes essentially in accordance with statics.

With regard to edge shears this obviously means that they are carried to the nodes at the ends of the edge by the law of the lever. The situation with bending and torsional moments is more complicated. The procedure for calculating equivalent nodal forces from edge bending and twisting moments is explained as follows.

Twisting Moment One might think that there is no unique way in which the twisting moments may be transferred to the nodes as moments since any proportion of the total edge twisting moment as node moment would satisfy statics.

Figure (III-3,a) shows the distribution of the torsional moment M_{yx} along the edge 1-2 of the element. The elementary torques, $M_{yx}dx$, are made up of couples of equal horizontal forces indicated in Fig. (III-3,b).

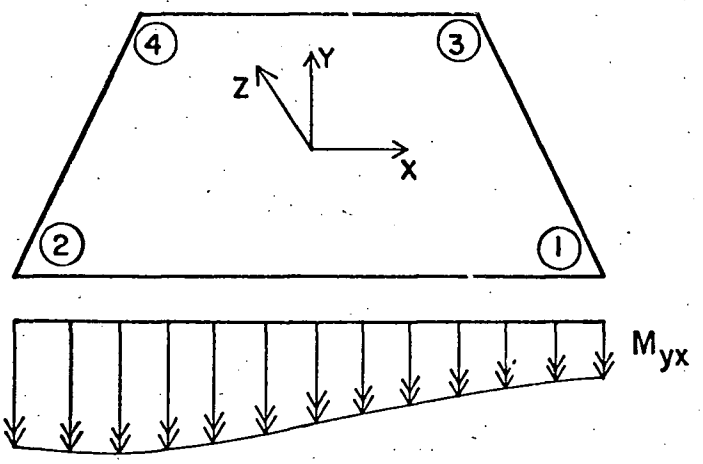

(a) Distribution of Torsional Moment, M_{yx} on Edge 1-2

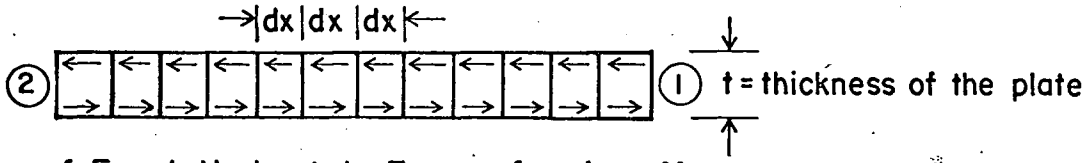

(b) Couples of Equal Horizontal Forces forming M_{yx}

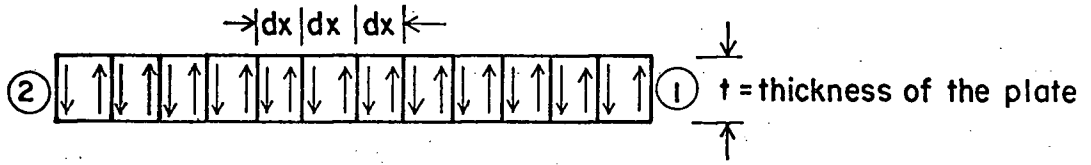

(c) Horizontal Couples replaced by Equivalent Couples of Vertical Forces

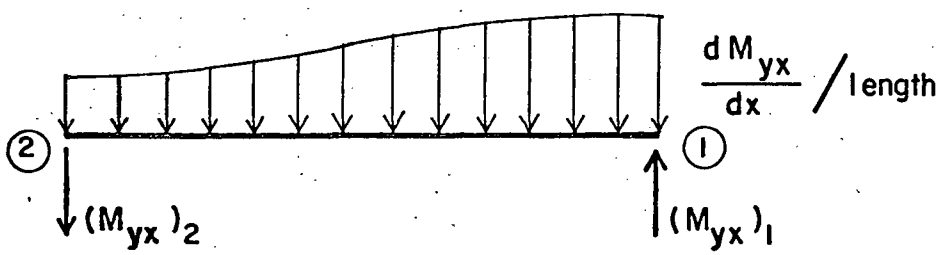

(d) Equivalent Shear and Corner Concentrated Shear

FIG. (III-3) CONVERSION OF TWISTING MOMENT INTO DISTRIBUTED TRANSVERSE SHEAR AND CORNER CONCENTRATED FORCE

These couples, however, may be replaced by the equivalent couples of vertical forces, Fig. (III-3,c). The neighbouring members of these couples in the two adjacent elements, dx, subtract from each other giving

$$\frac{(M_{yx} + \frac{\partial M_{yx}}{\partial x} dx)dx}{dx} - \frac{M_{yx} dx}{dx} = \frac{\partial M_{yx}}{\partial x} dx$$

on every length dx which is equivalent to the distributed shear $\frac{\partial M_{yx}}{\partial x}$ per unit length (Fig. (III-3,d)). The members of the torques at the corners of the edge have no partners to combine with and so they persist as the concentrated corner shears (M_{yx}). The distributed edge shear, $\frac{\partial M_{yx}}{\partial x}$, is carried uniquely to the corners by the law of the lever.

The combination of these two effects (i.e., distributed edge shear, $\frac{\partial M_{yx}}{\partial x}$, and concentrated corner shear, M_{yx}) amounts to equal and opposite vertical corner forces whose moment equals the sum of all torques on this particular edge.

Edge Bending Moment The bending moment on the edge of the plate (Fig. III-4,a) can be viewed as a result of distributed direct stresses (Fig. III-4,b). These direct stresses over the thickness may be replaced by two equal and opposite lines of forces (Fig. III-4,c). Thus, the edge moments are equivalent to two equal and opposite lines of forces. These forces may now be collected at the corners uniquely by the simple law of the lever. This results in two equal and opposite nodal forces at each corner which are equivalent to nodal moments. This procedure is obviously equivalent to the transfer of the bending moments to the nodes in accordance with the law of the lever in the same way as in the case of shears.

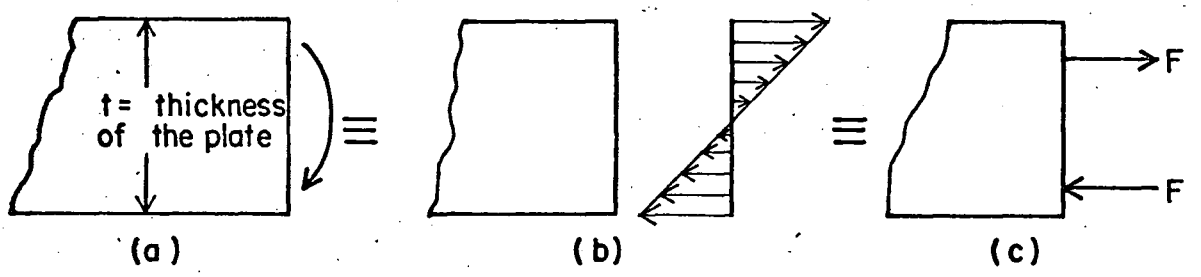

FIG. (III-4) CONVERSION OF EDGE BENDING MOMENT INTO EQUIVALENT DIRECT FORCES.

3.9 Forces on Inclined Edges

Equations (III-6,a and b) give expressions for the moments and shears on the x and y planes. Calculations of moments and shears for inclined edges must refer to the normal and parallel directions of the particular edge. The directions of normal and parallel axes, Fig. (III-5), are selected to be the same as the x and y directions (Fig. (III-2)) when the angle of inclination of the edge to the Y-axis would approach zero. By simple direction transformation,[26] the moments and shear in n and t directions of the inclined edge are given by

$$M_n = M_x \text{Cos}^2\alpha + M_y \text{Sin}^2\alpha - M_{xy} \text{Sin}2\alpha$$

$$M_{nt} = \frac{1}{2}(M_x - M_y)\text{Sin}2\alpha + M_{xy}\text{Cos}2\alpha \qquad \text{(III-6,d)}$$

and, $$Q_n = Q_x \text{Cos}\alpha + Q_y \text{Sin}\alpha$$

Here, α = the angle which the positive direction of n-axis makes with the positive direction of x-axis and is considered positive in the counter clockwise direction, looking from above. Fig. (III-5) The angle α is positive for edge 1-3 and negative for edge 2-4 of the trapezoid

The expressions for moments and shears on edge 2-4 are obtained from those given above by simply replacing the angle α with $-\alpha$. These are

$$M_{n_{2-4}} = M_x \text{Cos}^2\alpha + M_y \text{Sin}^2\alpha + M_{xy} \text{Sin}2\alpha$$

$$M_{nt_{2-4}} = \frac{1}{2}(M_y - M_x)\text{Sin}2\alpha + M_{xy}\text{Cos}2\alpha \qquad \text{(III-6,e)}$$

and, $$Q_{n_{2-4}} = Q_x \text{Cos}\alpha - Q_y \text{Sin}\alpha$$

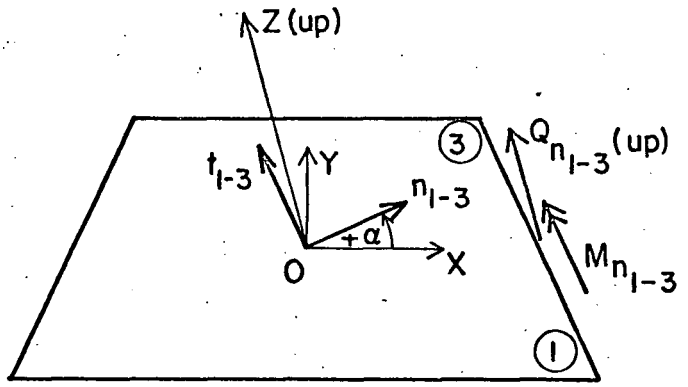

(a) n and t Directions for the Inclined Edge 1–3

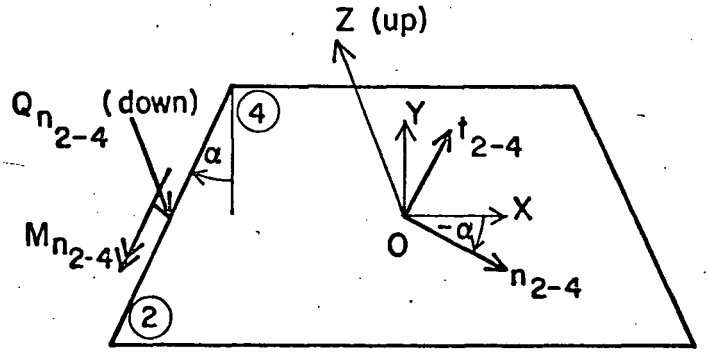

(b) n and t Directions for the Inclined Edge 2–4

FIG. (III-5) n AND t DIRECTIONS FOR THE INCLINED EDGES

The procedure for calculating nodal forces is illustrated for the displacement mode b_9xy^2.

3.10 Sample Procedure to Determine the Statically Equivalent Nodal Forces Due to the Displacement Mode, $w = b_9xy^2$

The distributions of moments and shears on the X and Y planes are obtained from Eqns. (III-6,a and b) by subsituting $w = b_9xy^2$. These are:

$$M_x = -2\ D_2b_9x$$

$$M_y = -2D_2b_9x$$

$$M_{xy} = -M_{yx} = 2(1-\mu)D_2b_9y$$

$$Q_x = -2D_2b_9$$

$$Q_y = 0$$

Nodal Force Contributions from Edges 1-2 and 3-4

Statically equivalent nodal force contributions are calculated from the distributed edge forces M_y, M_{yx} and Q_y and are shown in Fig. (III-6).

Edge 1-3

Angle α for this edge is positive. Fig. (III-5,a). The distributions of edge moments and shear are obtained from Eqn. (III-6,d). These are given by

$$M_n = -2D_2b_9\{x(\mathrm{Sin}^2\alpha + \mu\mathrm{Cos}^2\alpha) + (1-\mu)y\mathrm{Sin}2\alpha\}$$

$$M_{nt} = (1-\mu)D_2b_9\{x\mathrm{Sin}2\alpha + 2y\mathrm{Cos}2\alpha\}$$

$$Q_n = -2D_2b_9\mathrm{Cos}\alpha$$

and are shown in Fig. (III-7). The components of equivalent nodal forces are

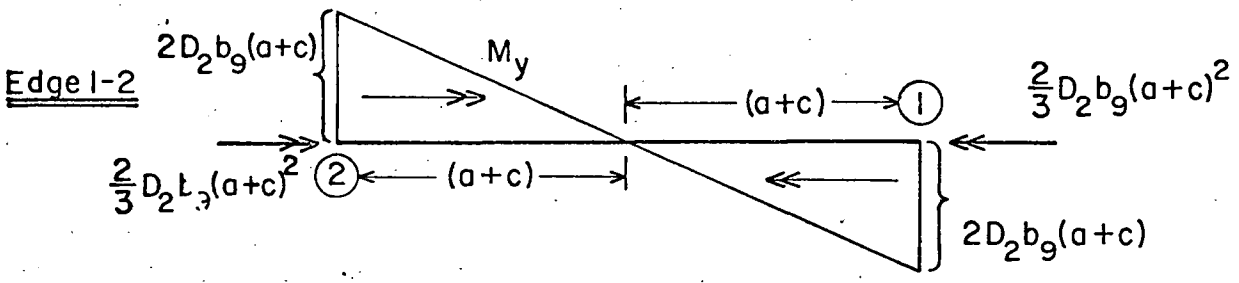

Nodal Moments due to M_y

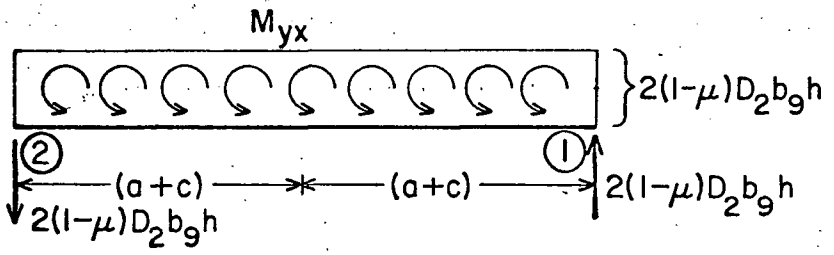

Nodal Reactions due to M_{yx}

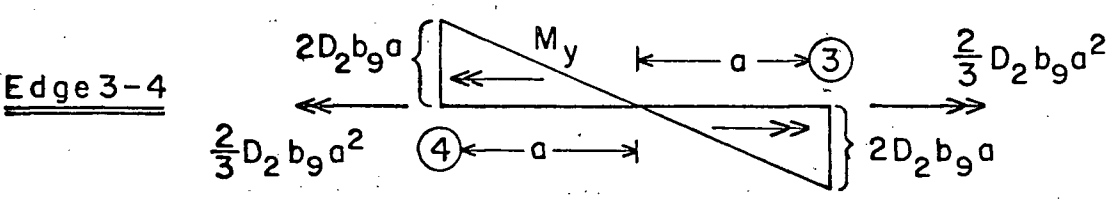

Nodal Moments due to M_y

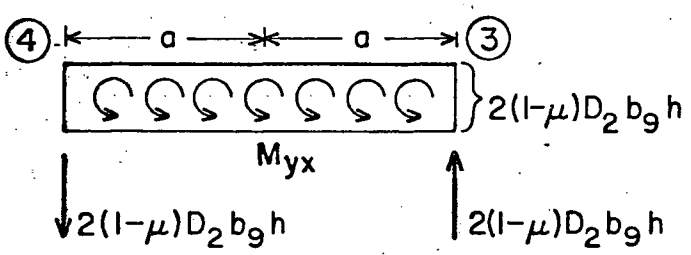

Nodal Reactions due to M_{yx}

FIG(III-6) CALCULATION OF EQUIVALENT NODAL FORCES FROM EDGES 1-2 AND 3-4 OF THE TRAPEZOID ELEMENT DUE TO DISPLACEMENT MODE $W=b_9xy^2$

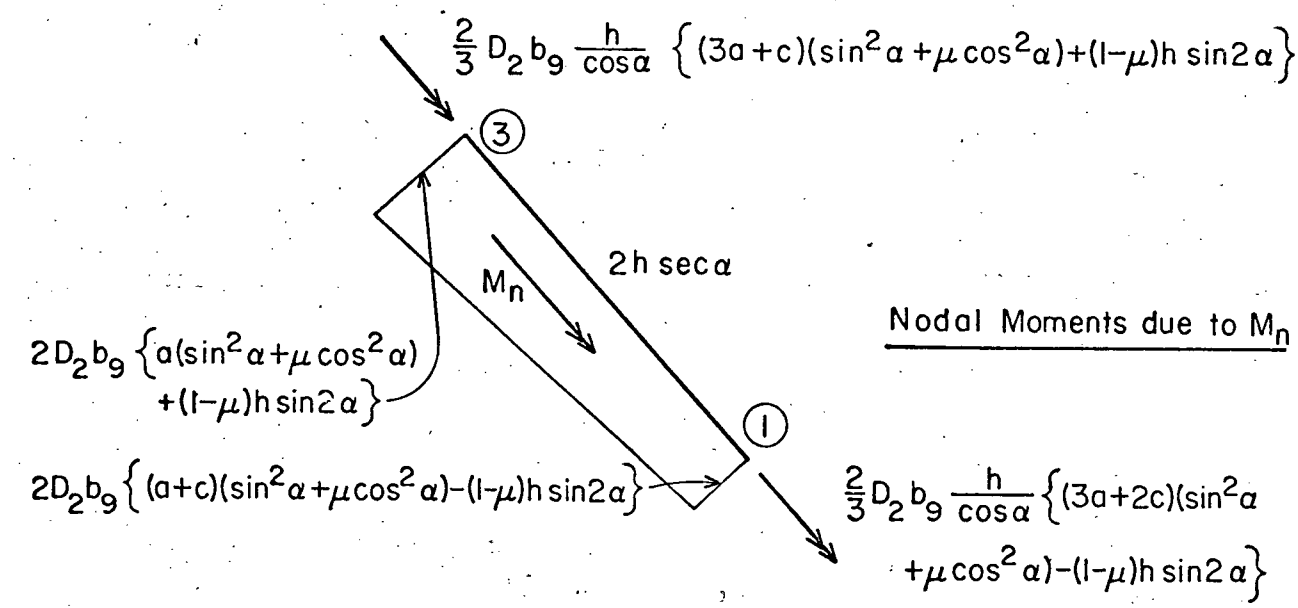

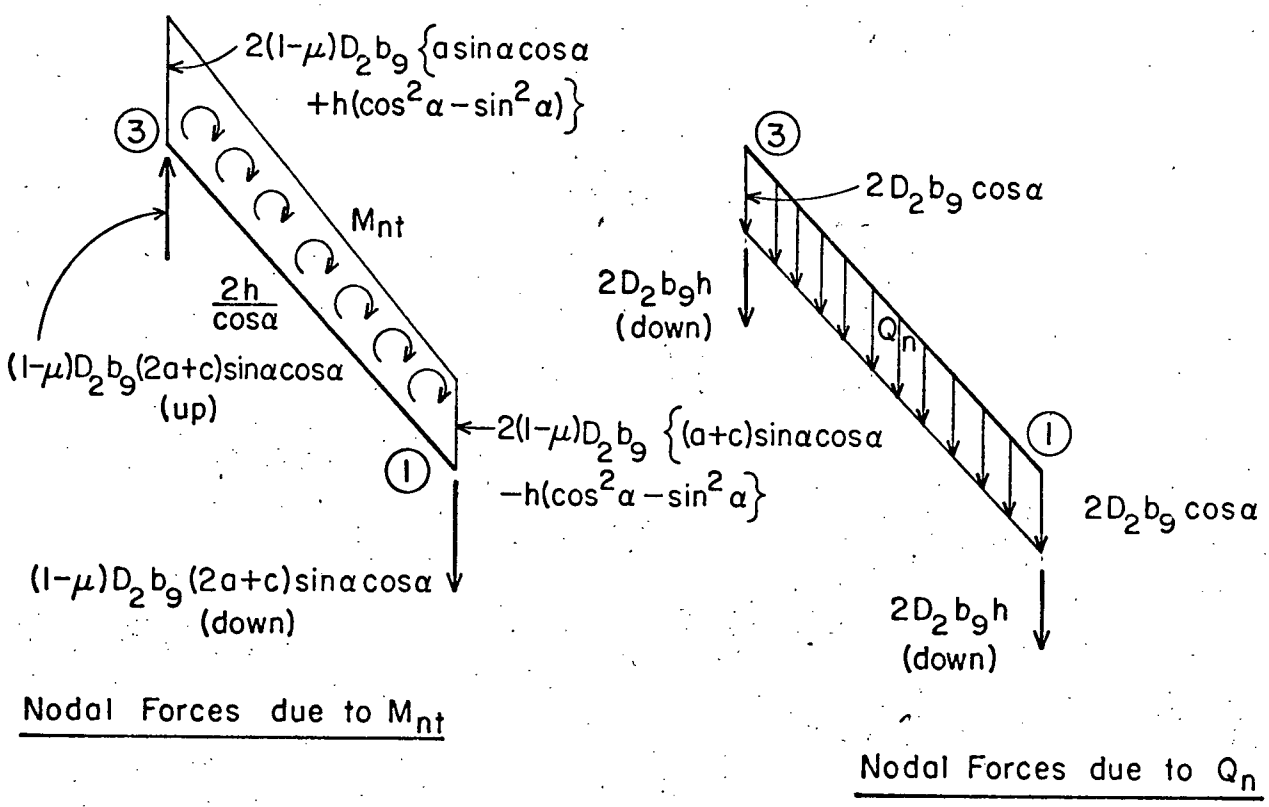

FIG(III-7) EQUIVALENT NODAL FORCES FROM EDGE 1-3 ($W=b_9xy^2$)

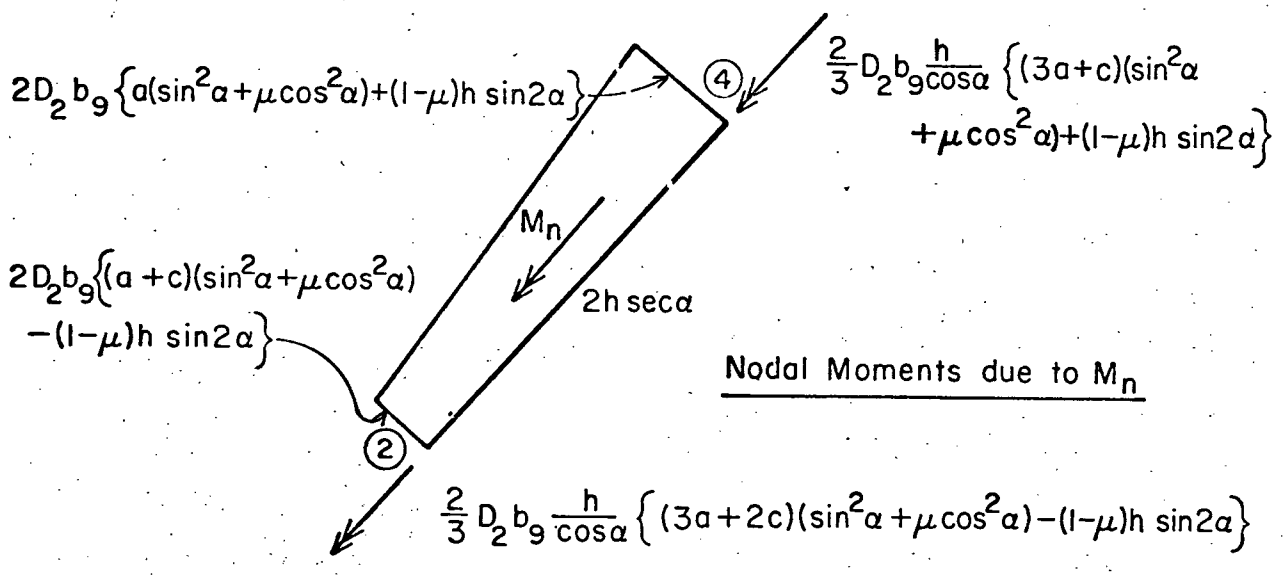

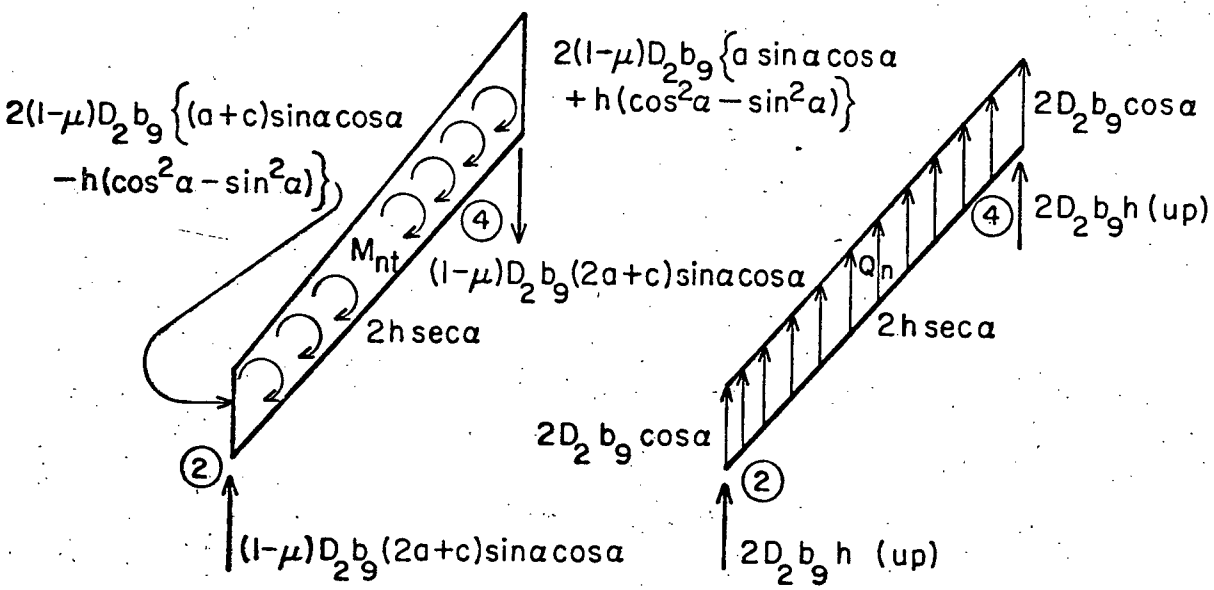

FIG.(III-8) EQUIVALENT NODAL FORCES FROM EDGE 2-4 ($W = b_9 x y^2$)

calculated using the law of the lever and are shown in the same figure.

Edge 2-4

Angle α, for this edge is negative Fig. (III-5,b). The distributions of edge moments and shear are obtained from Eqn. (III-6,e). These are

$$M_n = -2D_2 b_9 \{x(\mathrm{Sin}^2\alpha + \mu\mathrm{Cos}^2\alpha) - (1-\mu)y\mathrm{Sin}2\alpha\}$$

$$M_{nt} = (1-\mu)D_2 b_9 \{-x\mathrm{Sin}2\alpha + 2y\mathrm{Cos}2\alpha\}$$

and, $$Q_n = -2D_2 b_9 \mathrm{Cos}\alpha$$

The distribution and nodal force contributions are shown in Fig. (III-8). The nodal components of moments from the inclined edges, 1-3 and 2-4, are resolved into x and y directions. Finally, the contributions of nodal forces from all the edges are added. This results in the equivalent nodal forces due to the displacement mode, $w = b_9 xy^2$.

3.11 Equivalent Nodal Forces from all Displacement Modes

The equivalent nodal forces from all displacement modes b_j ($j = 1,2,\ldots,12$) can be written collectively in a matrix form

$$\{f^*\} = [C^*]\{B^*\} \qquad \text{(III-11)}$$

Here, $[C^*]$ = 12 x 12 matrix of equivalent nodal forces. The equivalent nodal forces corresponding to a displacement mode b_j constitute the jth column of this matrix,

and $\{f^*\}$ = 12 x 1 column vector of nodal forces due to a general state of deformation of the finite element.

Entries of $[C^*]$ matrix are shown in Table (III-7).

Table (III-7) Entries of [C*] Matrix (Trapezoid Element)

Entries of the first three columns of [C*] matrix are zero as displacement surfaces b_1, b_2x and b_3y correspond to rigid body displacement and rotations and therefore do not produce any shears or moments in the plate.

Entries of the 4th Column (due to $w = b_4x^2$)

$C^*_{1,4} = 2D_2(1-\mu)\ \text{Sin}\alpha\ \text{Cos}\alpha$

$C^*_{2,4} = D_2\{(\text{Cos}^2\alpha + \mu\text{Sin}^2\alpha)c - 2\mu(a+c)\}$

$C^*_{3,4} = -2D_2(\text{Cos}^2\alpha + \mu\text{Sin}^2\alpha)h$

$C^*_{4,4} = 2D_2(1-\mu)\text{Sin}\alpha\ \text{Cos}\alpha$

$C^*_{5,4} = D_2\{(\text{Cos}^2\alpha + \mu\text{Sin}^2\alpha)c - 2\mu(a+c)\}$

$C^*_{6,4} = 2D_2(\text{Cos}^2\alpha + \mu\text{Sin}^2\alpha)h$

$C^*_{7,4} = -2D_2(1-\mu)\text{Sin}\alpha\ \text{Cos}\alpha$

$C^*_{8,4} = D_2\{(\text{Cos}^2\alpha + \mu\text{Sin}^2\alpha)c + 2\mu a\}$

$C^*_{9,4} = -2D_2(\text{Cos}^2\alpha + \mu\text{Sin}^2\alpha)h$

$C^*_{10,4} = -2D_2(1-\mu)\text{Sin}\alpha\ \text{Cos}\alpha$

$C^*_{11,4} = D_2\{(\text{Cos}^2\alpha + \mu\text{Sin}^2\alpha)c + 2\mu a\}$

$C^*_{12,4} = 2D_2(\text{Cos}^2\alpha + \mu\text{Sin}^2\alpha)h$

Entries of the 5th Column (due to $w = b_5xy$)

$C^*_{1,5} = -2D_2(1-\mu)\text{Cos}^2\alpha$

$C^*_{2,5} = 2D_2(1-\mu)h\ \text{Sin}^2\alpha$

$C^*_{3,5} = -2D_2(1-\mu)h\ \text{Sin}\alpha\ \text{Cos}\alpha$

$C^*_{4,5} = 2D_2(1-\mu)\text{Cos}^2\alpha$

$C^*_{5,5} = -2D_2(1-\mu)h\ \text{Sin}^2\alpha$

$C^*_{6,5} = -2D_2(1-\mu)h\ \text{Sin}\alpha\ \text{Cos}\alpha$

$C^*_{7,5} = 2D_2(1-\mu)\text{Cos}^2\alpha$

$C^*_{8,5} = 2D_2(1-\mu)h\ \text{Sin}^2\alpha$

$C^*_{9,5} = -2D_2(1-\mu)h\ \text{Sin}\alpha\ \text{Cos}\alpha$

Continued Table (III-7)

$C^*_{10,5} = -2D_2(1-\mu)\cos^2\alpha$

$C^*_{11,5} = -2D_2(1-\mu)h\sin^2\alpha$

$C^*_{12,5} = -2D_2(1-\mu)h\sin\alpha\cos\alpha$

Entries of the 6th Column (due to $w = b_6y^2$)

$C^*_{1,6} = -2D_2(1-\mu)\sin\alpha\cos\alpha$

$C^*_{2,6} = D_2[(\sin^2\alpha + \mu\cos^2\alpha)c - 2(a+c)]$

$C^*_{3,6} = -2D_2h(\sin^2\alpha + \mu\cos^2\alpha)$

$C^*_{4,6} = -2D_2(1-\mu)\sin\alpha\cos\alpha$

$C^*_{5,6} = D_2\{(\sin^2\alpha + \mu\cos^2\alpha)c - 2(a+c)\}$

$C^*_{6,6} = 2D_2h(\sin^2\alpha + \mu\cos^2\alpha)$

$C^*_{7,6} = 2D_2(1-\mu)\sin\alpha\cos\alpha$

$C^*_{8,6} = D_2\{(\sin^2\alpha + \mu\cos^2\alpha)c + 2a\}$

$C^*_{9,6} = -2D_2h(\sin^2\alpha + \mu\cos^2\alpha)$

$C^*_{10,6} = 2D_2(1-\mu)\sin\alpha\cos\alpha$

$C^*_{11,6} = D_2\{(\sin^2\alpha + \mu\cos^2\alpha)c + 2a\}$

$C^*_{12,6} = 2D_2h(\sin^2\alpha + \mu\cos^2\alpha)$

Entries of the 7th Column (due to $w = b_7x^3$)

$C^*_{1,7} = -6D_2[h\{1 + (1-\mu)\sin^2\alpha\} - (1-\mu)(a+c)\sin\alpha\cos\alpha]$

$C^*_{2,7} = D_2[c(3a+2c)\{1 - (1-\mu)\sin^2\alpha\} - 2\mu(a+c)^2]$

$C^*_{3,7} = -2D_2h(3a+2c)\{1 - (1-\mu)\sin^2\alpha\}$

$C^*_{4,7} = 6D_2[h\{1 + (1-\mu)\sin^2\alpha\} - (1-\mu)(a+c)\sin\alpha\cos\alpha]$

$C^*_{5,7} = -D_2[c(3a+2c)\{1 - (1-\mu)\sin^2\alpha\} - 2\mu(a+c)^2]$

$C^*_{6,7} = -2D_2h(3a+2c)\{1 - (1-\mu)\sin^2\alpha\}$

$C^*_{7,7} = -6D_2[h\{1 + (1-\mu)\sin^2\alpha\} + (1-\mu)a\sin\alpha\cos\alpha]$

$C^*_{8,7} = D_2[c(3a+c)\{1 - (1-\mu)\sin^2\alpha\} + 2\mu a^2]$

Continued Table (III-7)

$C^*_{9,7} = -2D_2h(3a+c)\{1 - (1-\mu)\sin^2\alpha\}$

$C^*_{10,7} = 6D_2[h\{1 + (1-\mu)\sin^2\alpha\} + (1-\mu)a\sin\alpha\cos\alpha]$

$C^*_{11,7} = -D_2[c(3a+c)\{1 - (1-\mu)\sin^2\alpha\} + 2\mu a^2]$

$C^*_{12,7} = -2D_2h(3a+c)\{1 - (1-\mu)\sin^2\alpha\}$

Entries of the 8th Column (due to $w = b_8x^2y$)

$C^*_{1,8} = D_2\{\mu + 2(1-\mu)\sin^2\alpha\}(2a+c)$

$C^*_{2,8} = D_2[2\mu h(a+c) + \frac{h}{3}\{3(1-\mu)(4a+3c)\sin^2\alpha - c\}]$

$C^*_{3,8} = -\frac{2}{3}D_2h\{2(1-\mu)(3a+2c)\sin\alpha\cos\alpha - h(\cos^2\alpha + \mu\sin^2\alpha)\}$

$C^*_{4,8} = D_2\{\mu + 2(1-\mu)\sin^2\alpha\}(2a+c)$

$C^*_{5,8} = D_2[2\mu h(a+c) + \frac{h}{3}\{3(1-\mu)(4a+3c)\sin^2\alpha - c\}]$

$C^*_{6,8} = \frac{2}{3}D_2h[2(1-\mu)(3a+2c)\sin\alpha\cos\alpha - h(\cos^2\alpha + \mu\sin^2\alpha)]$

$C^*_{7,8} = -D_2\{\mu + 2(1-\mu)\sin^2\alpha\}(2a+c)$

$C^*_{8,8} = D_2[2\mu ha + \frac{h}{3}\{3(1-\mu)(4a+c)\sin^2\alpha + c\}]$

$C^*_{9,8} = -\frac{2}{3}D_2h[2(1-\mu)(3a+c)\sin\alpha\cos\alpha + h(\cos^2\alpha + \mu\sin^2\alpha)]$

$C^*_{10,8} = -D_2[\mu + 2(1-\mu)\sin^2\alpha](2a+c)$

$C^*_{11,8} = D_2[2\mu ha + \frac{h}{3}\{3(1-\mu)(4a+c)\sin^2\alpha + c\}]$

$C^*_{12,8} = \frac{2}{3}D_2h[2(1-\mu)(3a+c)\sin\alpha\cos\alpha + h(\cos^2\alpha + \mu\sin^2\alpha)]$

Entries of the 9th Column (due to $w = b_9xy^2$)

$C^*_{1,9} = -D_2[2\mu h + (1-\mu)(2a+c)\sin\alpha\cos\alpha]$

$C^*_{2,9} = -\frac{D_2}{3}[a(2a+c) + 3(1-\mu)c(a+c)\cos^2\alpha]$

$C^*_{3,9} = -\frac{2}{3}D_2h[(3a+2c) - 3(1-\mu)(a+c)\cos^2\alpha]$

$C^*_{4,9} = D_2[2\mu h + (1-\mu)(2a+c)\sin\alpha\cos\alpha]$

$C^*_{5,9} = \frac{D_2}{3}[a(2a+c) + 3(1-\mu)c(a+c)\cos^2\alpha]$

$C^*_{6,9} = -\frac{2}{3}D_2h[(3a+2c) - 3(1-\mu)(a+c)\cos^2\alpha]$

$C^*_{7,9} = -D_2[2\mu h - (1-\mu)(2a+c)\sin\alpha\cos\alpha]$

Continued Table (III-7)

$C^*_{8,9} = \frac{D_2}{3}[(a+c)(2a+c) - 3(1-\mu)ac\,Cos^2\alpha]$

$C^*_{9,9} = -\frac{2}{3}D_2h[(3a+c) - 3(1-\mu)a\,Cos^2\alpha]$

$C^*_{10,9} = D_2[2\mu h - (1-\mu)(2a+c)Sin\alpha\,Cos\alpha]$

$C^*_{11,9} = -\frac{D_2}{3}[(a+c)(2a+c) - 3(1-\mu)a.c\,Cos^2\alpha]$

$C^*_{12,9} = -\frac{2}{3}D_2h[(3a+c) - 3(1-\mu)a\,Cos^2\alpha]$

Entries of the 10th Column (due to $w = b_{10}y^3$)

$C^*_{1,10} = 3D_2(2a+c)$

$C^*_{2,10} = D_2h[6(a+c) - c(Sin^2\alpha + \mu Cos^2\alpha)]$

$C^*_{3,10} = 2D_2h^2(Sin^2\alpha + \mu Cos^2\alpha)$

$C^*_{4,10} = 3D_2(2a+c)$

$C^*_{5,10} = D_2h[6(a+c) - c(Sin^2\alpha + \mu Cos^2\alpha)]$

$C^*_{6,10} = -2D_2h^2(Sin^2\alpha + \mu Cos^2\alpha)$

$C^*_{7,10} = -3D_2(2a+c)$

$C^*_{8,10} = D_2h[6a + c(Sin^2\alpha + \mu Cos^2\alpha)]$

$C^*_{9,10} = -2D_2h^2(Sin^2\alpha + \mu Cos^2\alpha)$

$C^*_{10,10} = -3D_2(2a+c)$

$C^*_{11,10} = D_2h[6a + c(Sin^2\alpha + \mu Cos^2\alpha)]$

$C^*_{12,10} = 2D_2h^2(Sin^2\alpha + \mu Cos^2\alpha)$

Entries of the 11th Column (due to $w = b_{11}x^3y$)

$C^*_{1,11} = D_2[-(1-\mu)(4a^2+5ac+3c^2) + a(2a+c) + 2h^2 + (1-\mu)(6a^2+6ac+3c^2+2h^2)Sin^2\alpha]$

$C^*_{2,11} = D_2h[2\mu(a+c)^2 + (1-\mu)(6a^2+9ac+4c^2)Sin^2\alpha - c(a+c)]$

$C^*_{3,11} = -D_2h[(1-\mu)(6a^2+9ac+4c^2)Sin\alpha\,Cos\alpha - 2h(a+c)]$

$C^*_{4,11} = -D_2[-(1-\mu)(4a^2+5ac+3c^2) + a(2a+c) + 2h^2 + (1-\mu)(6a^2+6ac+3c^2+2h^2)Sin^2\alpha]$

$C^*_{5,11} = -D_2h[2\mu(a+c)^2 + (1-\mu)(6a^2+9ac+4c^2)Sin^2\alpha - c(a+c)]$

$C^*_{6,11} = -D_2h[(1-\mu)(6a^2+9ac+4c^2)Sin\alpha\,Cos\alpha - 2h(a+c)]$

Continued Table (III-7)

$$C^*_{7,11} = -D_2[-(1-\mu)(4a^2+3ac+2c^2) + (a+c)(2a+c) + 2h^2 + (1-\mu)(6a^2+6ac+3c^2+2h^2)\sin^2\alpha]$$

$$C^*_{8,11} = D_2h[2\mu a^2 + (1-\mu)(6a^2+3ac+c^2)\sin^2\alpha + ac]$$

$$C^*_{9,11} = -D_2h[(1-\mu)(6a^2+3ac+c^2)\sin\alpha\cos\alpha + 2ah]$$

$$C^*_{10,11} = D_2[-(1-\mu)(4a^2+3ac+2c^2) + (a+c)(2a+c) + 2h^2 + (1-\mu)(6a^2+6ac+3c^2+2h^2)\sin^2\alpha]$$

$$C^*_{11,11} = -D_2h[2\mu a^2 + (1-\mu)(6a^2+3ac+c^2)\sin^2\alpha + ac]$$

$$C^*_{12,11} = -D_2h[(1-\mu)(6a^2+3ac+c^2)\sin\alpha\cos\alpha + 2ah]$$

Entries of the 12th Column (due to $w = b_{12}xy^3$)

$$C^*_{1,12} = D_2[a(2a+c) + (1-\mu)c^2\cos^2\alpha - 2(1-2\mu)h^2]$$

$$C^*_{2,12} = \frac{D_2h}{2}[4(a+c)^2 + c^2 - c(2a+3c)(\sin^2\alpha + \mu\cos^2\alpha)]$$

$$C^*_{3,12} = -D_2h^2[c - (2a+3c)(\sin^2\alpha + \mu\cos^2\alpha)]$$

$$C^*_{4,12} = -D_2[a(2a+c) + (1-\mu)c^2\cos^2\alpha - 2(1-2\mu)h^2]$$

$$C^*_{5,12} = \frac{-D_2h}{2}[4(a+c)^2 + c^2 - c(2a+3c)(\sin^2\alpha + \mu\cos^2\alpha)]$$

$$C^*_{6,12} = -D_2h^2[c - (2a+3c)(\sin^2\alpha + \mu\cos^2\alpha)]$$

$$C^*_{7,12} = -D_2[(a+c)(2a+c) + (1-\mu)c^2\cos^2\alpha - 2(1-2\mu)h^2]$$

$$C^*_{8,12} = \frac{D_2h}{2}[4a^2 + c^2 + c(2a-c)(\sin^2\alpha + \mu\cos^2\alpha)]$$

$$C^*_{9,12} = -D_2h^2[c + (2a-c)(\sin^2\alpha + \mu\cos^2\alpha)]$$

$$C^*_{10,12} = D_2[(a+c)(2a+c) + (1-\mu)c^2\cos^2\alpha - 2(1-2\mu)h^2]$$

$$C^*_{11,12} = \frac{-D_2h}{2}[4a^2 + c^2 + c(2a-c)(\sin^2\alpha + \mu\cos^2\alpha)]$$

$$C^*_{12,12} = -D_2h^2[c + (2a-c)(\sin^2\alpha + \mu\cos^2\alpha)]$$

Using Eqn. (III-3) to replace $\{B^*\}$ in Eqn. (III-11) one obtains

$$\{f^*\} = [C^*][A^{*-1}]\{\delta^*\} \qquad \text{(III-12)}$$

Equation (III-12) relates the nodal forces with the nodal deformations. The force-deformation relation for a finite element is commonly expressed in the matrix form as

$$\{f^*\} = [K^*]\{\delta^*\} \qquad \text{(III-13)}$$

Here, $[K^*]$ = 12 x 12 stiffness matrix for a trapezoid element in flexure. Comparing matrix equations (III-12) and (III-13), one obtains

$$[K^*] = [C^*][A^{*-1}] \qquad \text{(III-14)}$$

The entries of $[K^*]$, being very long expressions, are not listed.
Note that the flexure stiffness matrix of the trapezoid element obtained by using the statics approach is asymmetrix (i.e. $K^*_{i,j} \neq K^*_{j,i}$). Note also that if the trapezoid reduces to a rectangle (top side = bottom side), the asymmetry of the statics stiffness matrix disappears and the resulting matrix coincides with the one derived by the author earlier.[37] Apparently its lack of symmetry reflects the asymmetry of the trapezoid element itself about the x-axis. However, it is more important to note that in conditions of uniform curvatures or twist the nodal forces satisfy the reciprocal relations with the element remaining trapezoid.[23] When the element size is decreased in the limit, uniform curvature conditions will in fact prevail in the vicinity of the element and the reciprocal relations will be automatically satisfied.

3.12 Energy Stiffness Matrix for a Trapezoid Element in Flexure

As in plane stress, this method uses the virtual work principle to define the equivalent nodal forces.

"Finite element" has been defined as a body whose nodes undergo the same deformations as the plate whose nodes are acted upon by concentrated forces statically equivalent to the edge forces. Since during a virtual deformation in a plate the same nodal deformations occur in the finite element, the condition imposed on the values of the equivalent nodal forces then is, that during virtual deformation, the external work done by the equivalent nodal forces of the finite element be the same as the external work done by the edge forces of the plate

Note that during virtual deformation of a plate loaded along the edges only, the external work done by the edge forces of the plate is equal to the internal work done by the internal moments in the plate. However, as explained in the case of plane stress, the supposition of equality of external work in the finite element and in the plate element is hypothetical.

In particular, if the virtual deformation $\{\bar{\delta}^*\}_j$ is such that it is unity in the direction of a selected nodal force f_j^* and zero in the direction of all other forces, then the external work in the finite element We_j^* will be the same as the value of this selected nodal force f_j^*, i.e.

$$We_j^* = \{\bar{\delta}^*\}_j^T \{f^*\} = f_j^* \qquad \text{(III-15)}$$

Here, $\{\bar{\delta}^*\}_j$ = 12 x 1 column vector of virtual deformations. Its jth entry is unity and all other entries are zero.

All such virtual deformations $\{\bar{\delta}^*\}_j$ (j = 1,2,...,12) can be collectively written as $[\bar{\delta}^*]$ which is the same as a 12 x 12 Identity matrix [I].

The corresponding external works for all such virtual deformations can be expressed in the matrix form

$$\underset{12x1}{\{We^*\}} = \underset{12x12}{[\bar{\delta}^*]}\underset{12x1}{\{f^*\}} = [I]\{f^*\} = \underset{12x1}{\{f^*\}} \qquad \text{(III-16)}$$

Here, $\{We^*\}$ = 12 x 1 column matrix of external work done by the nodal forces for all virtual deformations $\{\bar{\delta}^*\}_j$ $(j = 1,2,\ldots,12)$

Work is done corresponding to each of these virtual deformations $\{\bar{\delta}^*\}_j$, by the edge moments and shears of the plate element which is the same as the internal work Wi^*_j done by the internal moments over the area of the plate. For a plate of constant thickness, the internal work may be expressed as,[26]

$$Wi^*_j = \iint_{area} \{\bar{\chi}^*\}_j^T \{M^*\} dxdy \qquad \text{(III-17)}$$

Here, $\{\bar{\chi}^*\}_j$ = curvatures due to a virtual deformations $\{\bar{\delta}^*\}_j$. The integration is carried out over the entire area of the plate.

Using Eqn. (III-5), the curvatures due to virtual deformations can be expressed as,

$$\{\bar{\chi}^*\}_j = [G^*][A^{*-1}]\{\bar{\delta}^*\}_j \qquad \text{(III-18)}$$

Substituting for $\{\bar{\chi}^*\}_j$ from Eqn. (III-18) and for $\{M^*\}$ from Eqn. (III-8) into Eqn. (III-17) for internal work, one obtains

$$\underset{1x1}{Wi^*_j} = \iint_{area} \underset{1x12}{\{\bar{\delta}^*\}_j^T}\underset{12x12}{[A^{*-1}]^T}\underset{12x3}{[G^*]^T}\underset{3x3}{[D^*]}\underset{3x12}{[G^*]}\underset{12x12}{[A^{*-1}]}\underset{12x1}{\{\delta^*\}} dxdy \qquad \text{(III-19)}$$

Collectively, internal works for all such virtual deformations $\{\bar{\delta}^*\}_j$, j = 1,2,...,12 (i.e. $[\bar{\delta}^*]$), can be written in matrix form

$$\underset{12x1}{\{W\bar{i}^*\}} = \iint_{area} \underset{12x12}{[\bar{\delta}^*]^T} \underset{12x12}{[A^{*-1}]^T} \underset{12x3}{[G^*]^T} \underset{3x3}{[D^*]} \underset{3x12}{[G^*]} \underset{12x12}{[A^{*-1}]} \underset{12x1}{\{\delta^*\}} dxdy \qquad \text{(III-20)}$$

Here, $\{W\bar{i}^*\}$ = 12 x 1 column matrix of internal work done by the internal forces in the plate during all virtual deformations $\{\bar{\delta}^*\}_j$, j = 1,2,...,12

and $[\bar{\delta}^*]$ = [I], 12 x 12 Identity matrix.

The matrix $[A^{*-1}]$ is expressed in terms of constant nodal coordinates and, as such, can be taken out of the integral sign. Eqn. (III-20) can be rewritten as

$$\{W\bar{i}^*\} = [A^{*-1}]^T \iint_{area} [G^*]^T [D^*] [G^*] dxdy [A^{*-1}] \{\delta^*\} \qquad \text{(III-21)}$$

Equating the external work done by the nodal forces of the finite element, Eqn. (III-16), to the corresponding internal work done by the internal moments in the plate element, Eqn. (III-21), one obtains

$$\{f^*\} = [A^{*-1}]^T \iint_{area} [G^*]^T [D^*] [G^*] dxdy [A^{*-1}] \{\delta^*\} \qquad \text{(III-22)}$$

$$\text{let, } [H^*] = \iint_{area} [G^*]^T [D^*] [G^*] dxdy \qquad \text{(III-23)}$$

The integrated 12 x 12 [H*] matrix is given in Table (III-8). Equation (III-22) can be rewritten as,

$$\{f^*\} = [A^{*-1}]^T [H^*] [A^{*-1}] \{\delta^*\} \qquad \text{(III-24)}$$

Table (III-8) Integrated $[H^*]$ Matrix for a Trapezoid

Here, $[H^*] = \iint_{\text{area}} [G^*]^T [D^*] [G^*] \, dxdy$ Eqn. (III-23)

$$[H^*] = \frac{Et^3}{12(1-\mu^2)} \begin{bmatrix}
0 & & & & & & & & & \\
0 & 0 & & & & & & & & \\
0 & 0 & 0 & & & & & & & \\
0 & 0 & 0 & 4L_1 & & & & & & \\
0 & 0 & 0 & 0 & 2(1-\mu)L_1 & & & & & \\
0 & 0 & 0 & 4\mu L_1 & 0 & 4L_1 & \text{Symmetrical} & & & \\
0 & 0 & 0 & 0 & 0 & 0 & 36L_3 & & & \\
0 & 0 & 0 & 4L_2 & 0 & 4\mu L_2 & 0 & 4L_4 + 8(1-\mu)L_3 & & \\
0 & 0 & 0 & 0 & 4(1-\mu)L_2 & 0 & 12\mu L_3 & 0 & 4L_3 + 8(1-\mu)L_4 & \\
0 & 0 & 0 & 12\mu L_2 & 0 & 12L_2 & 0 & 12\mu L_4 & 0 & 36L_4 \\
0 & 0 & 0 & 0 & 6(1-\mu)L_3 & 0 & 36L_5 & 0 & 12L_5 & 0 & 36L_8 + 18(1-\mu)L_7 \\
0 & 0 & 0 & 0 & 6(1-\mu)L_4 & 0 & 36\mu L_5 & 0 & 12L_5 + 12(1-\mu)L_6 & 0 & 18(1+\mu)L_8 & 36L_8 + 18(1-\mu)L_9
\end{bmatrix}$$

$$L_1 = 2(2a+c)h$$

$$L_2 = -\frac{2}{3} ch^2$$

$$L_3 = \frac{h(2a+c)}{6} \{c^2 + (2a+c)^2\}$$

$$L_4 = \frac{2}{3}(2a+c)h^3$$

$$L_5 = -\frac{ch^2}{30}[c^2 + 5(2a+c)^2]$$

$$L_6 = -\frac{2}{5} ch^4$$

$$L_7 = \frac{(2a+c)h}{40}[c^4 + \frac{10}{3}c^2(2a+c)^2 + (2a+c)^4]$$

$$L_8 = (2a+c)h^3[\frac{c^2}{10} + \frac{(2a+c)^2}{18}]$$

$$L_9 = \frac{2}{5}(2a+c)h^5$$

Equation (III-24) provides the force-deformation relationship for an equilateral trapezoid in flexure. Comparing Eqn. (III-13) with Eqn. (III-24), the Energy stiffness matrix for a trapezoid in flexure is

$$[K^*] = [A^{*-1}]^T [H^*] [A^{*-1}] \qquad \text{(III-25)}$$

Note that [D*] is a symmetric matrix. Equation (III-22) represents a congruent transformation[25] of the symmetric matrix. Thus, the energy stiffness matrix [K*] is symmetrical.

The matrix multiplication of Eqn. (III-25) being very involved, is performed preferably by computer.

Due to the geometrical symmetry of the finite element about Y-axis, certain equalities in the stiffness coefficients exist irrespective of the manner in which these are calculated. These equalities in stiffness coefficients, shown in Table (III-9), provide an additional check on the computation of stiffness matrices.

When a trapezoid is reduced to a rectangle, the Energy stiffness matrix becomes identical to the one derived by Zienkiewicz and Cheung[27] for an isotropic plate.

Table (III-9) Equalities in the Stiffness Coefficients due to the Geometrical Symmetry of the Equilateral Trapezoid in Flexure Fig. (III-1)

$$[K^*] = \begin{bmatrix}
K^*_{1,1} & K^*_{1,2} & K^*_{1,3} & K^*_{4,1} & K^*_{4,2} & -K^*_{4,3} & K^*_{1,7} & K^*_{1,8} & K^*_{1,9} & K^*_{4,7} & K^*_{4,8} & -K^*_{4,9} \\
K^*_{2,1} & K^*_{2,2} & K^*_{2,3} & K^*_{5,1} & K^*_{5,2} & -K^*_{5,3} & K^*_{2,7} & K^*_{2,8} & K^*_{2,9} & K^*_{5,7} & K^*_{5,8} & -K^*_{5,9} \\
K^*_{3,1} & K^*_{3,2} & K^*_{3,3} & -K^*_{6,1} & -K^*_{6,2} & K^*_{6,3} & K^*_{3,7} & K^*_{3,8} & K^*_{3,9} & -K^*_{6,7} & -K^*_{6,8} & K^*_{6,9} \\
K^*_{4,1} & K^*_{4,2} & K^*_{4,3} & K^*_{1,1} & K^*_{1,2} & -K^*_{1,3} & K^*_{4,7} & K^*_{4,8} & K^*_{4,9} & K^*_{1,7} & K^*_{1,8} & -K^*_{1,9} \\
K^*_{5,1} & K^*_{5,2} & K^*_{5,3} & K^*_{2,1} & K^*_{2,2} & -K^*_{2,3} & K^*_{5,7} & K^*_{5,8} & K^*_{5,9} & K^*_{2,7} & K^*_{2,8} & -K^*_{2,9} \\
K^*_{6,1} & K^*_{6,2} & K^*_{6,3} & -K^*_{3,1} & -K^*_{3,2} & K^*_{3,3} & K^*_{6,7} & K^*_{6,8} & K^*_{6,9} & -K^*_{3,7} & -K^*_{3,8} & K^*_{3,9} \\
K^*_{7,1} & K^*_{7,2} & K^*_{7,3} & K^*_{10,1} & K^*_{10,2} & -K^*_{10,3} & K^*_{7,7} & K^*_{7,8} & K^*_{7,9} & K^*_{10,7} & K^*_{10,8} & -K^*_{10,9} \\
K^*_{8,1} & K^*_{8,2} & K^*_{8,3} & K^*_{11,1} & K^*_{11,2} & -K^*_{11,3} & K^*_{8,7} & K^*_{8,8} & K^*_{8,9} & K^*_{11,7} & K^*_{11,8} & -K^*_{11,9} \\
K^*_{9,1} & K^*_{9,2} & K^*_{9,3} & -K^*_{12,1} & -K^*_{12,2} & K^*_{12,3} & K^*_{9,7} & K^*_{9,8} & K^*_{9,9} & -K^*_{12,7} & -K^*_{12,8} & K^*_{12,9} \\
K^*_{10,1} & K^*_{10,2} & K^*_{10,3} & K^*_{7,1} & K^*_{7,2} & -K^*_{7,3} & K^*_{10,7} & K^*_{10,8} & K^*_{10,9} & K^*_{7,7} & K^*_{7,8} & -K^*_{7,9} \\
K^*_{11,1} & K^*_{11,2} & K^*_{11,3} & K^*_{8,1} & K^*_{8,2} & -K^*_{8,3} & K^*_{11,7} & K^*_{11,8} & K^*_{11,9} & K^*_{8,7} & K^*_{8,8} & -K^*_{8,9} \\
K^*_{12,1} & K^*_{12,2} & K^*_{12,3} & -K^*_{9,1} & -K^*_{9,2} & K^*_{9,3} & K^*_{12,7} & K^*_{12,8} & K^*_{12,9} & -K^*_{9,7} & -K^*_{9,8} & K^*_{9,9}
\end{bmatrix}$$

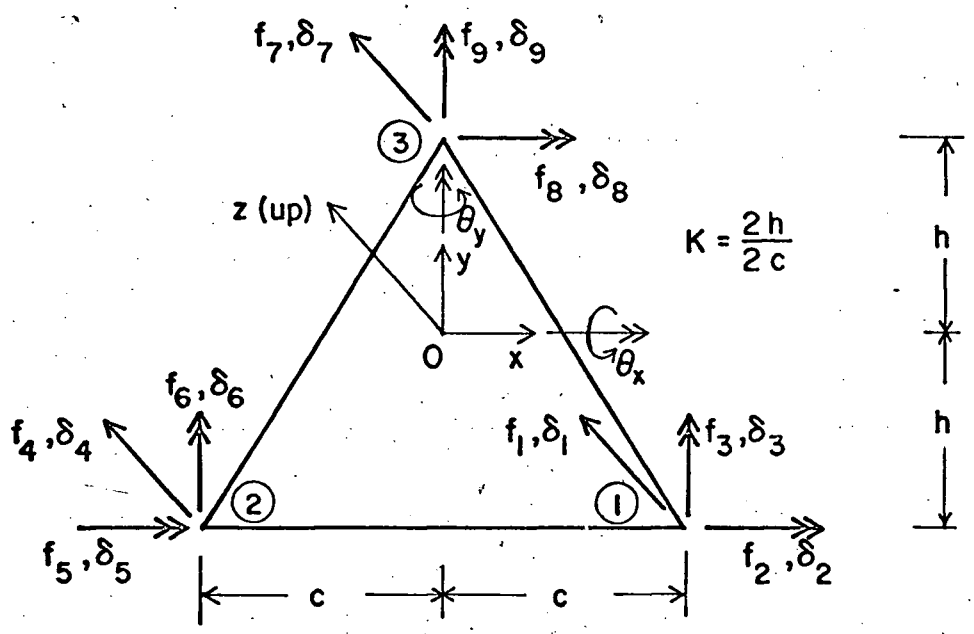

FIG. (III-9) ISOSCELES TRIANGULAR ELEMENT IN FLEXURE. (Positive directions of nodal forces and deformations.)

3.13 Flexure Stiffness Matrix for a Finite Element in the Shape of an Isosceles Triangle. Fig. (III-9)

Selection of Displacement Field

An isosceles triangular element in flexure has nine degrees of freedom of displacements and rotations at its joints. Thus a displacement field containing nine independent displacement modes is required for the complete determination of the element stiffness matrix. A polynomial expression in x and y is selected to represent various displacement modes of the element. The expression must include three displacement modes corresponding to rigid body movements of the element which do not affect the stresses in any way. It must also contain three independent displacement modes corresponding to constant curvatures in x and y directions and constant twist. Thus, the assumed general expression for w must necessarily contain the linear and quadretic terms, b_1, b_2x, b_3y, b_4x^2, b_5xy, and b_6y^2. Restricting the choice of the remaining three terms to the cubic, the following four terms are available for selection; b_7x^3, $b_8'x^2y$, b_8xy^2 and b_9y^3.

In the present study, only isosceles triangles symmetrical about Y-axis are encountered (Fig. (III-9). The symmetry of the element about Y-axis is used to select the displacement modes. In the cubic polynomial containing ten terms, six terms marked S produce symmetric and four terms marked A produce antisymmetric deflections with respect to Y-axis.

b_1,	b_2x,	b_3y,	b_4x^2,	b_5xy,	b_6y^2,	b_7x^3,	$b_8'x^2y$,	b_8xy^2,	b_9y^3
S	A	S	S	A	S	A	S	A	S

An arbitrary deflection field represented by a particular polynomial may be considered as made up of a symmetrical part composed only of the symmetrical

terms and an antisymmetrical part composed only of the antisymmetrical terms. Nine deflection fields are needed for determination of the stiffness coefficients: δ_1^*, δ_2^* and δ_3^* for node 1; δ_4^*, δ_5^* and δ_6^* for node 2, and δ_7^*, δ_8^* and δ_9^* for node 3 Fig. (III-9). The six displacement fields δ_1^* to δ_6^*, related to nodes 1 and 2, may evidently be made up of three symmetric and three antisymmetric terms. As to the deflection fields of the node 3, two, δ_7^* and δ_8^*, are symmetrical, and one, δ_9^*, is antisymmetrical.[23] Thus, five symmetrical and four-antisymmetrical terms are needed in the polynomial capable of describing the nine independent displacement fields required for the derivation of the stiffness matrix of an element in the shape of an isosceles triangle. Thus, all four antisymmetric terms must be used. Out of the six symmetric terms, only five are required leaving the option of discarding either $b_8'x^2y$ or b_9y^3 symmetric term. In the present case, $b_8'x^2y$ term has been omitted. Retaining $b_8'x^2y$ symmetric term in place of the b_9y^3 term is expected to yield an equally good stiffness matrix.

Note: Various choices have been suggested in the past for selecting nine independent displacement modes for a general triangle[11,14,28,29]. The suitability of the resulting polynomials is examined for the special case when the general triangle reduces to an isosceles triangle of the present study.

3.14 Choice 1. Omission of $b_5 xy$ term.[11] This is an antisymmetric term. All antisymmetric terms are required for the evaluation of the parameters $b_1,\ldots,b_9$. Omission of this term makes it impossible to evaluate these parameters as the resulting [A*] matrix will be singular. Moreover, $b_5 xy$ term corresponds to constant twist in the X and Y planes. Omission of this term will violate the necessary condition for convergence.[21,22]

3.15 Choice 2. Omission of $b_8 xy^2$ term. This is an antisymmetric term and, as explained before, can not be omitted.

3.16 Choice 3. Combination term $b_8(x^2y + xy^2)$.[28] Here the symmetric term x^2y is combined with the antisymmetric term xy^2 under a common parameter b_8. Using this combination term, the statics and energy stiffness matrices for an isosceles triangle were evaluated. Due to the geometrical symmetry of the element about Y-axis, certain equality relations among the stiffness coefficients must hold. Table (III-10). These equality relations are independent of the size of the element and the manner in which the stiffness coefficients are derived. The stiffness coefficients of the evaluated stiffness matrices failed to satisfy these equality relations suggesting the use of the above combination term unsuitable for an isosceles triangle. For clarification of this point,[23] assume that it is necessary to determine the values of the parameters $\{B^*_\Delta\}$ in several independent antisymmetrical fields. 1, θ_{y_3}; 2, W_1 and $-W_2$ meaning by this simultaneous equal and opposite deflections at the nodes 1 and 2 (all other nodal deflections or rotations being zero); 3, simultaneous θ_{x_1} and $-\theta_{x_2}$, and 4, simultaneous θ_{y_1} and θ_{y_2}. These four independent antisymmetric displacement fields require definite values of the four antisymmetrical parameters. Among these

Table (III-10) Equalities in the Stiffness Coefficients due to the Geometrical Symmetry of the Isosceles Triangle

$$[K^*_{\Delta}] = \begin{bmatrix} K^*_{11} & K^*_{12} & K^*_{13} & K^*_{41} & K^*_{42} & -K^*_{43} & K^*_{17} & K^*_{18} & K^*_{19} \\ K^*_{21} & K^*_{22} & K^*_{23} & K^*_{51} & K^*_{52} & -K^*_{53} & K^*_{27} & K^*_{28} & K^*_{29} \\ K^*_{31} & K^*_{32} & K^*_{33} & -K^*_{61} & -K^*_{62} & K^*_{63} & K^*_{37} & K^*_{38} & K^*_{39} \\ K^*_{41} & K^*_{42} & K^*_{43} & K^*_{11} & K^*_{12} & -K^*_{13} & K^*_{17} & K^*_{18} & -K^*_{19} \\ K^*_{51} & K^*_{52} & K^*_{53} & K^*_{21} & K^*_{22} & -K^*_{23} & K^*_{27} & K^*_{28} & -K^*_{29} \\ K^*_{61} & K^*_{62} & K^*_{63} & -K^*_{31} & -K^*_{32} & K^*_{33} & -K^*_{37} & -K^*_{38} & K^*_{39} \\ K^*_{71} & K^*_{72} & K^*_{73} & K^*_{71} & K^*_{72} & -K^*_{73} & K^*_{77} & K^*_{78} & 0 \\ K^*_{81} & K^*_{82} & K^*_{83} & K^*_{81} & K^*_{82} & -K^*_{83} & K^*_{87} & K^*_{88} & 0 \\ K^*_{91} & K^*_{92} & K^*_{93} & -K^*_{91} & -K^*_{92} & K^*_{93} & 0 & 0 & K^*_{99} \end{bmatrix}$$

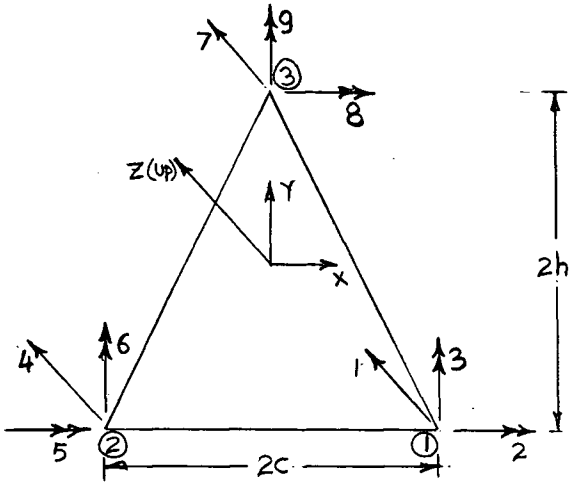

is the combination term parameter b_8, whose value cannot be zero in all four fields. The existence of b_8 introduces a symmetrical component of W associated with its antisymmetrical term. Other symmetrical terms will also be found necessary to satisfy the equations. This means that although the corner conditions in the assumed fields are antisymmetrical the displacement W is not, because it contains also some symmetrical terms which contradicts structural theory. Thus, the symmetrical and antisymmetrical terms must not be combined under the same parameter.

3.17 Evaluation of the Constant Parameters

On the basis of the foregoing arguements, the following displacement function containing nine independent displacement modes is selected:

$$W = b_1 + b_2x + b_3y + b_4x^2 + b_5xy + b_6y^2 + b_7x^3 + b_8xy^2 + b_9y^3 \qquad \text{(III-26)}$$

The displacements and rotations, $\{\delta^*_\Delta\}$, at the nodes of the isosceles triangle are expressed in terms of the nine constant parameters, $\{B^*_\Delta\}$, as in Eqn. (III-2) and are shown in Table (III-11).

The parameters $\{B^*_\Delta\}$ are evaluated in terms of the nodal deformations as in Eqn. (III-3) and are shown in Table (III-12).

Table (III-11) Nodal Deformations in Terms of Constant Parameters

(Isosceles Triangle in Flexure) (Fig. (III-9))

$$\begin{bmatrix} \delta_1 \\ \delta_2 \\ \delta_3 \\ \delta_4 \\ \delta_5 \\ \delta_6 \\ \delta_7 \\ \delta_8 \\ \delta_9 \end{bmatrix} = \begin{bmatrix} 1 & c & -h & c^2 & -ch & h^2 & c^3 & ch^2 & -h^3 \\ 0 & 0 & 1 & 0 & c & -2h & 0 & -2ch & 3h^2 \\ 0 & -1 & 0 & -2c & h & 0 & -3c^2 & -h^2 & 0 \\ 1 & -c & -h & c^2 & ch & h^2 & -c^3 & -ch^2 & -h^3 \\ 0 & 0 & 1 & 0 & -c & -2h & 0 & 2ch & 3h^2 \\ 0 & -1 & 0 & 2c & h & 0 & -3c^2 & -h^2 & 0 \\ 1 & 0 & h & 0 & 0 & h^2 & 0 & 0 & h^3 \\ 0 & 0 & 1 & 0 & 0 & 2h & 0 & 0 & 3h^2 \\ 0 & -1 & 0 & 0 & -h & 0 & 0 & -h^2 & 0 \end{bmatrix} \begin{bmatrix} b_1 \\ b_2 \\ b_3 \\ b_4 \\ b_5 \\ b_6 \\ b_7 \\ b_8 \\ b_9 \end{bmatrix}$$

$$\{\delta^*_\Delta\} = [A^*_\Delta]\{B^*_\Delta\}$$

Table (III-12) Evaluation of Parameters in Terms of Nodal Deformations (Isosceles Triangle in Flexure)

$$
\begin{bmatrix} b_1 \\ b_2 \\ b_3 \\ b_4 \\ b_5 \\ b_6 \\ b_7 \\ b_8 \\ b_9 \end{bmatrix} =
\begin{bmatrix}
\frac{1}{4} & \frac{h}{8} & \frac{c}{8} & \frac{1}{4} & \frac{h}{8} & \frac{-c}{8} & \frac{1}{2} & \frac{-h}{4} & 0 \\
\frac{9}{16c} & \frac{h}{4c} & \frac{3}{16} & \frac{-9}{16c} & \frac{-h}{4c} & \frac{3}{16} & 0 & 0 & \frac{-1}{4} \\
-\frac{3}{8h} & \frac{-1}{8} & \frac{-3c}{16h} & \frac{-3}{8h} & -\frac{1}{8} & \frac{3c}{16h} & \frac{3}{4h} & \frac{-1}{4} & 0 \\
0 & 0 & \frac{-1}{4c} & 0 & 0 & \frac{1}{4c} & 0 & 0 & 0 \\
\frac{-3}{8ch} & 0 & \frac{-1}{8h} & \frac{3}{8ch} & 0 & \frac{-1}{8h} & 0 & 0 & \frac{-1}{2h} \\
0 & \frac{-1}{8h} & 0 & 0 & \frac{-1}{8h} & 0 & 0 & \frac{1}{4h} & 0 \\
\frac{-1}{4c^3} & 0 & \frac{-1}{4c^2} & \frac{1}{4c^3} & 0 & \frac{-1}{4c^2} & 0 & 0 & 0 \\
\frac{-3}{16ch^2} & \frac{-1}{4ch} & \frac{-1}{16h^2} & \frac{3}{16ch^2} & \frac{1}{4ch} & \frac{-1}{16h^2} & 0 & 0 & \frac{-1}{4h^2} \\
\frac{1}{8h^3} & \frac{1}{8h^2} & \frac{c}{16h^3} & \frac{1}{8h^3} & \frac{1}{8h^2} & \frac{-c}{16h^3} & \frac{-1}{4h^3} & \frac{1}{4h^2} & 0
\end{bmatrix}
\begin{bmatrix} \delta_1 \\ \delta_2 \\ \delta_3 \\ \delta_4 \\ \delta_5 \\ \delta_6 \\ \delta_7 \\ \delta_8 \\ \delta_9 \end{bmatrix}
$$

$$\{B_\Delta^*\} = [A_\Delta^{*-1}]\{\delta_\Delta^*\}$$

3.18 Curvatures and Moments at a Point

Curvatures and twist are expressed through a matrix equation similar to Eqn. (III-4) and are shown in Table (III-13).

Moments at any point in the element are expressed through a matrix equation similar to Eqn. (III-8) and are obtained by substituting proper values of the component matrices $[D^*]$, $[G^*_\Delta]$, and $[A^{*-1}_\Delta]$ for an isosceles triangle given in Tables (III-4, 13, and 12).

3.19 Statics Stiffness Matrix for an Isosceles Triangular Element in Flexure

Equivalent corner forces for each displacement mode b_i are obtained in a manner similar to a trapezoid. Collectively, these forces can be expressed in terms of constant parameters as in Eqn. (III-11). The equivalent corner forces for individual displacement mode are shown in Table (III-14). Finally, the Statics stiffness matrix for flexure is obtained using Eqn. (III-14). The component matrices of this equation, i.e. $[A^{*-1}_\Delta]$ and $[C^*_\Delta]$ are given in Tables (III-12) and (III-14). The entries of the Statics stiffness matrix are shown in Table (III-15). The Statics stiffness matrix for a triangle in flexure is found to be asymmetric.

3.20 Energy Stiffness Matrix for an Isosceles Triangular Element in Flexure

The derivation of the flexure stiffness matrix for an isosceles triangle by the Energy approach is carried out in a manner similar to that for a trapezoid and is given by a matrix equation similar to Eqn. (III-25). The component matrices of Eqn. (III-25) for an isosceles triangle, i.e., $[A^{*-1}_\Delta]$ and the central integrated matrix $[H^*_\Delta]$ are given in Tables (III-12) and (III-16). The entries of the Energy stiffness matrix are given in Table (III-17).

Table (III-13) Curvantures and Twist at a Point on a Triangular Element

$$\begin{Vmatrix} -\frac{\partial^2 w}{\partial x^2} \\ -\frac{\partial^2 w}{\partial y^2} \\ 2\frac{\partial^2 w}{\partial x \partial y} \end{Vmatrix} = \begin{vmatrix} 0 & 0 & 0 & -2 & 0 & 0 & -6x & 0 & 0 \\ 0 & 0 & 0 & 0 & 0 & -2 & 0 & -2x & -6y \\ 0 & 0 & 0 & 0 & 2 & 0 & 0 & 4y & 0 \end{vmatrix} \begin{Vmatrix} b_1 \\ b_2 \\ b_3 \\ b_4 \\ b_5 \\ b_6 \\ b_7 \\ b_8 \\ b_9 \end{Vmatrix}$$

$$\{\chi^*_\Delta\} = [G^*_\Delta]\{B^*_\Delta\}$$

Table (III-14) Entries of $[C^*_\Delta]$ Matrix (Isosceles Triangular Element in Flexure).

First three terms of the displacement function, $(b_1, b_2 x, b_3 y)$, correspond to rigid body displacement and rotations thus they do not produce any forces or moments.

Entries of 4th Column (due to $w = b_4 x^2$)

$C^*_{\Delta 1,4} = 2D_2(1-\mu)\text{Sin}\alpha\ \text{Cos}\alpha$

$C^*_{\Delta 2,4} = D_2 c\{-2\mu + \text{Cos}^2\alpha + \mu\text{Sin}^2\alpha\}$

$C^*_{\Delta 3,4} = -2D_2 h\{\text{Cos}^2\alpha + \mu\text{Sin}^2\alpha\}$

$C^*_{\Delta 4,4} = 2D_2(1-\mu)\text{Sin}\alpha\ \text{Cos}\alpha$

$C^*_{\Delta 5,4} = D_2 c\{-2\mu + \text{Cos}^2\alpha + \mu\text{Sin}^2\alpha\}$

$C^*_{\Delta 6,4} = 2D_2 h\{\text{Cos}^2\alpha + \mu\text{Sin}^2\alpha\}$

$C^*_{\Delta 7,4} = -4D_2(1-\mu)\text{Sin}\alpha\ \text{Cos}\alpha$

$C^*_{\Delta 8,4} = 2D_2 c(\text{Cos}^2\alpha + \mu\text{Sin}^2\alpha)$

$C^*_{\Delta 9,4} = 0$

Entries of 5th Column (due to $w = b_5 xy$)

$C^*_{\Delta 1,5} = -2(1-\mu)D_2\text{Cos}^2\alpha$

$C^*_{\Delta 2,5} = 2D_2 h(1-\mu)\text{Sin}^2\alpha$

$C^*_{\Delta 3,5} = -2D_2 h(1-\mu)\text{Sin}\alpha\ \text{Cos}\alpha$

$C^*_{\Delta 4,5} = 2(1-\mu)D_2\text{Cos}^2\alpha$

$C^*_{\Delta 5,5} = -2D_2 h(1-\mu)\text{Sin}^2\alpha$

$C^*_{\Delta 6,5} = -2D_2 h(1-\mu)\text{Sin}\alpha\ \text{Cos}\alpha$

$C^*_{\Delta 7,5} = 0$

$C^*_{\Delta 8,5} = 0$

$C^*_{\Delta 9,5} = -4D_2 h(1-\mu)\text{Sin}\alpha\ \text{Cos}\alpha$

Continued Table (III-14)

Entries of 6th Column (due to $w = b_6 y^2$)

$C^*_{\Delta 1,6} = -2(1-\mu)D_2 \sin\alpha \cos\alpha$

$C^*_{\Delta 2,6} = D_2 c[-2 + \{\mu + (1-\mu)\sin^2\alpha\}]$

$C^*_{\Delta 3,6} = -2D_2 h\{\mu + (1-\mu)\sin^2\alpha\}$

$C^*_{\Delta 4,6} = -2(1-\mu)D_2 \sin\alpha \cos\alpha$

$C^*_{\Delta 5,6} = D_2 c[-2 + \{\mu + (1-\mu)\sin^2\alpha\}]$

$C^*_{\Delta 6,6} = 2D_2 h\{\mu + (1-\mu)\sin^2\alpha\}$

$C^*_{\Delta 7,6} = 4(1-\mu)D_2 \sin\alpha \cos\alpha$

$C^*_{\Delta 8,6} = 2D_2 c\{\mu + (1-\mu)\sin^2\alpha\}$

$C^*_{\Delta 9,6} = 0$

Entries of 7th Column (due to $w = b_7 x^3$)

$C^*_{\Delta 1,7} = -6D_2[h\{1 + (1-\mu)\sin^2\alpha\} - c(1-\mu)\sin\alpha \cos\alpha]$

$C^*_{\Delta 2,7} = 2D_2 c^2[(1-\mu)\cos^2\alpha]$

$C^*_{\Delta 3,7} = -4D_2 hc\{1-(1-\mu)\sin^2\alpha\}$

$C^*_{\Delta 4,7} = 6D_2[h\{1 + (1-\mu)\sin^2\alpha\} - c(1-\mu)\sin\alpha \cos\alpha]$

$C^*_{\Delta 5,7} = -2D_2 c^2(1-\mu)\cos^2\alpha$

$C^*_{\Delta 6,7} = -4D_2 hc\{1 - (1-\mu)\sin^2\alpha\}$

$C^*_{\Delta 7,7} = 0$

$C^*_{\Delta 8,7} = 0$

$C^*_{\Delta 9,7} = -4D_2 hc\{1 - (1-\mu)\sin^2\alpha\}$

Entries of 8th Column (due to $w = b_8 xy^2$)

$C^*_{\Delta 1,8} = -D_2\{2\mu h + (1-\mu)c \sin\alpha \cos\alpha\}$

$C^*_{\Delta 2,8} = -D_2 c^2(1-\mu)\cos^2\alpha$

$C^*_{\Delta 3,8} = -\frac{2}{3} D_2 hc\{2 - 3(1-\mu)\cos^2\alpha\}$

$C^*_{\Delta 4,8} = D_2\{2\mu h + (1-\mu)c \sin\alpha \cos\alpha\}$

Continued Table (III-14)

$$C^*_{\Delta 5,8} = D_2 c^2 (1-\mu)\cos^2\alpha$$

$$C^*_{\Delta 6,8} = -\frac{2}{3} D_2 hc\{2 - 3(1-\mu)\cos^2\alpha\}$$

$$C^*_{\Delta 7,8} = 0$$

$$C^*_{\Delta 8,8} = 0$$

$$C^*_{\Delta 9,8} = -\frac{4}{3} D_2 hc$$

Entries of 9th Column (due to $w = b_9 y^3$)

$$C^*_{\Delta 1,9} = 3D_2 c$$

$$C^*_{\Delta 2,9} = D_2 hc\{6 - (\sin^2\alpha + \mu\cos^2\alpha)\}$$

$$C^*_{\Delta 3,9} = 2D_2 h^2 (\sin^2\alpha + \mu\cos^2\alpha)$$

$$C^*_{\Delta 4,9} = 3D_2 c$$

$$C^*_{\Delta 5,9} = D_2 hc\{6 - (\sin^2\alpha + \mu\cos^2\alpha)\}$$

$$C^*_{\Delta 6,9} = -2D_2 h^2 (\sin^2\alpha + \mu\cos^2\alpha)$$

$$C^*_{\Delta 7,9} = -6D_2 c$$

$$C^*_{\Delta 8,9} = 2D_2 hc (\sin^2\alpha + \mu\cos^2\alpha)$$

$$C^*_{\Delta 9,9} = 0$$

Table (III-15) Statics Stiffness Matrix for an Isosceles Triangular Element in Flexure. (Fig. (III-9))

Let, $K = \frac{2h}{2c} = \frac{\text{height}}{\text{base}}$

and $D_2 = \frac{Et^3}{12(1-\mu^2)}$ = flexural rigidity per unit length of the plate.

$$K^*_{\Delta 1,1} = \left(\frac{3}{2K^3} + \frac{3}{2K} + 6K\right) \frac{D_2}{4c^2}$$

$$K^*_{\Delta 2,1} = \frac{-16K^4 + 24K^2 + 5 + 4\mu K^2(4K^2-1)}{4K^2(4K^2+1)} \frac{D_2}{2c}$$

$$K^*_{\Delta 3,1} = \left[2K + \frac{1 + 4\mu K^2}{K(4K^2+1)}\right] \frac{D_2}{2c}$$

$$K^*_{\Delta 4,1} = \left(\frac{3}{2K^3} - \frac{3}{2K} - 6K\right) \frac{D_2}{4c^2}$$

$$K^*_{\Delta 5,1} = \left(\frac{5}{4K^2} + 1 - \mu\right) \frac{D_2}{2c}$$

$$K^*_{\Delta 6,1} = 2K \frac{D_2}{2c}$$

$$K^*_{\Delta 7,1} = -\frac{3}{K^3} \frac{D_2}{4c^2}$$

$$K^*_{\Delta 8,1} = \frac{1 + 4\mu K^2}{2K^2(4K^2+1)} \frac{D_2}{2c}$$

$$K^*_{\Delta 9,1} = \frac{16K^4 + 16K^2 + 1 - 8\mu K^2}{2K(4K^2+1)} \frac{D_2}{2c}$$

$$K^*_{\Delta 1,2} = \left[\frac{3}{4K^2} + \mu + \frac{2(1-\mu)}{4K^2+1}\right] \frac{D_2}{2c}$$

$$K^*_{\Delta 2,2} = \left[\frac{3}{4K} + 5K - 2\mu K\right] \frac{D_2}{4K^2+1}$$

$$K^*_{\Delta 3,2} = \left[\frac{5}{6} - \frac{2}{3}K^2 + 4\mu K^2\right] \frac{D_2}{4K^2+1}$$

$$K^*_{\Delta 4,2} = \left[\frac{3}{4K^2} - \mu\right] \frac{D_2}{2c}$$

Continued Table (III-15)

$$K^*_{\Delta 5,2} = \left[\frac{3}{4K} + 3K\right] \frac{D_2}{4K^2+1}$$

$$K^*_{\Delta 6,2} = -\left[\frac{1}{6} + \frac{2}{3}K^2\right] \frac{D_2}{4K^2+1}$$

$$K^*_{\Delta 7,2} = \left[-\frac{3}{2K^2} - \frac{2(1-\mu)}{4K^2+1}\right] \frac{D_2}{2C}$$

$$K^*_{\Delta 8,2} = 0$$

$$K^*_{\Delta 9,2} = \frac{1}{3} D_2$$

$$K^*_{\Delta 1,3} = \left[\frac{3}{8K^3} + \frac{1}{4K} + 3K - \frac{4K(1-\mu)}{4K^2+1}\right] \frac{D_2}{2C}$$

$$K^*_{\Delta 2,3} = \left[\frac{5}{16K^2} + \frac{3}{2} - 3K^2 + 4\mu K^2\right] \frac{D_2}{4K^2+1}$$

$$K^*_{\Delta 3,3} = \left[\frac{5}{24K} + \frac{K}{3} + 6K^3 + 2\mu K\right] \frac{D_2}{4K^2+1}$$

$$K^*_{\Delta 4,3} = \left[\frac{3}{8K^3} - \frac{1}{4K} - 3K\right] \frac{D_2}{2C}$$

$$K^*_{\Delta 5,3} = \left[\frac{5}{16K^2} + \frac{3}{2} + K^2\right] \frac{D_2}{4K^2+1}$$

$$K^*_{\Delta 6,3} = \left[-\frac{1}{24K} + \frac{K}{3} + 2K^3\right] \frac{D_2}{4K^2+1}$$

$$K^*_{\Delta 7,3} = \left[-\frac{3}{4K^3} + \frac{4K(1-\mu)}{4K^2+1}\right] \frac{D_2}{2C}$$

$$K^*_{\Delta 8,3} = \left[\frac{1}{8K^2} - 2K^2\right] \frac{D_2}{4K^2+1}$$

$$K^*_{\Delta 9,3} = \left[\frac{1}{12K} + \frac{4K}{3} + 4K^3\right] \frac{D_2}{4K^2+1}$$

$$K^*_{\Delta 1,7} = -\frac{3}{K^3} \frac{D_2}{4C^2}$$

Continued Table (III-15)

$$K^*_{\Delta 2,7} = \left[-\frac{3}{K^2} + \frac{1+4\mu K^2}{2K^2(4K^2+1)}\right]\frac{D_2}{2C}$$

$$K^*_{\Delta 3,7} = -\left[\frac{1+4\mu K^2}{K(4K^2+1)}\right]\frac{D_2}{2C}$$

$$K^*_{\Delta 4,7} = -\frac{3}{K^3}\frac{D_2}{4C^2}$$

$$K^*_{\Delta 5,7} = \left[-\frac{3}{K^2} + \frac{1+4\mu K^2}{2K^2(4K^2+1)}\right]\frac{D_2}{2C}$$

$$K^*_{\Delta 6,7} = \left[\frac{1+4\mu K^2}{K(4K^2+1)}\right]\frac{D_2}{2C}$$

$$K^*_{\Delta 7,7} = \frac{6}{K^3}\frac{D_2}{4C^2}$$

$$K^*_{\Delta 8,7} = -\left[\frac{1+4\mu K^2}{K^2(4K^2+1)}\right]\frac{D_2}{2C}$$

$$K^*_{\Delta 9,7} = 0$$

$$K^*_{\Delta 1,8} = \left[\frac{3}{2K^2} - \frac{2(1-\mu)}{4K^2+1}\right]\frac{D_2}{2C}$$

$$K^*_{\Delta 2,8} = \frac{1}{K}D_2$$

$$K^*_{\Delta 3,8} = 0$$

$$K^*_{\Delta 4,8} = \left[\frac{3}{2K^2} - \frac{2(1-\mu)}{4K^2+1}\right]\frac{D_2}{2C}$$

$$K^*_{\Delta 5,8} = \frac{1}{K}D_2$$

$$K^*_{\Delta 6,8} = 0$$

$$K^*_{\Delta 7,8} = \left[-\frac{3}{K^2} + \frac{4(1-\mu)}{4K^2+1}\right]\frac{D_2}{2C}$$

$$K^*_{\Delta 8,8} = \frac{1+4\mu K^2}{K(4K^2+1)}D_2$$

$$K^*_{\Delta 9,8} = 0$$

$$K^*_{\Delta 1,9} = \left[\frac{1}{K} + \frac{4K(1-\mu)}{4K^2+1}\right]\frac{D_2}{2C}$$

$$K^*_{\Delta 2,9} = 0$$

$$K^*_{\Delta 3,9} = \frac{1}{3K}D_2$$

$$K^*_{\Delta 4,9} = -\left[\frac{1}{K} + \frac{4K(1-\mu)}{4K^2+1}\right]\frac{D_2}{2C}$$

$$K^*_{\Delta 5,9} = 0$$

$$K^*_{\Delta 6,9} = \frac{1}{3K}D_2$$

$$K^*_{\Delta 7,9} = 0$$

$$K^*_{\Delta 8,9} = 0$$

$$K^*_{\Delta 9,9} = \left[\frac{1+16K^2-12\mu K^2}{3K(4K^2+1)}\right]D_2$$

Table (III-16) Integrated $[H_\Delta^*]$ Matrix for an Isosceles Triangle in Flexure

$$[H_\Delta^*] = \iint_{\text{area}} [G_\Delta^*]^T [D^*] [G_\Delta^*] \, dxdy$$

$$[H_\Delta^*] = D_2 \begin{bmatrix}
0 & 0 & 0 & 0 & 0 & 0 & 0 & 0 & 0 \\
0 & 0 & 0 & 0 & 0 & 0 & 0 & 0 & 0 \\
0 & 0 & 0 & 0 & 0 & 0 & 0 & 0 & 0 \\
0 & 0 & 0 & 8ch & 0 & 8\mu ch & 0 & 0 & -8\mu ch^2 \\
0 & 0 & 0 & 0 & 4(1-\mu)ch & 0 & 0 & -\frac{8}{3}(1-\mu)ch^2 & 0 \\
0 & 0 & 0 & 8\mu ch & 0 & 8ch & 0 & 0 & -8ch^2 \\
0 & 0 & 0 & 0 & 0 & 0 & 12c^3h & 4\mu c^3h & 0 \\
0 & 0 & 0 & 0 & -\frac{8}{3}(1-\mu)ch^2 & 0 & 4\mu c^3h & \frac{4}{3}c^3h + \frac{16}{3}(1-\mu)ch^3 & 0 \\
0 & 0 & 0 & -8\mu ch^2 & 0 & -8ch^2 & 0 & 0 & 24ch^3
\end{bmatrix}$$

Table (III-17) Energy Stiffness Matrix for an Isosceles Triangular Element in Flexure. (Fig. (III-9))

$$K^*_{\Delta 1,1} = \left[\frac{27}{16K^3} + \frac{3}{2K} + 3K\right] \frac{D_2}{4C^2}$$

$$K^*_{\Delta 2,1} = \left[\frac{9}{8K^2} + \frac{\mu}{2}\right] \frac{D_2}{2C}$$

$$K^*_{\Delta 3,1} = \left[\frac{13}{32K^3} + \frac{1}{4K} + \frac{3K}{2} + \frac{3}{4}\frac{\mu}{K}\right] \frac{D_2}{2C}$$

$$K^*_{\Delta 4,1} = \left[\frac{21}{16K^3} - \frac{3}{2K} - 3K\right] \frac{D_2}{4C^2}$$

$$K^*_{\Delta 5,1} = \left[\frac{7}{8K^2} - \frac{\mu}{2}\right] \frac{D_2}{2C}$$

$$K^*_{\Delta 6,1} = \left[-\frac{11}{32K^3} + \frac{1}{4K} + \frac{3K}{2} - \frac{\mu}{4K}\right] \frac{D_2}{2C}$$

$$K^*_{\Delta 7,1} = \left[-\frac{3}{K^3}\right] \frac{D_2}{4C^2}$$

$$K^*_{\Delta 8,1} = \frac{1}{K^2} \frac{D_2}{2C}$$

$$K^*_{\Delta 9,1} = \left[\frac{1}{8K^3} + \frac{1}{K} - \frac{\mu}{2K}\right] \frac{D_2}{2C}$$

$$K^*_{\Delta 1,2} = \left[\frac{9}{8K^2} + \frac{\mu}{2}\right] \frac{D_2}{2C}$$

$$K^*_{\Delta 2,2} = \left[\frac{5}{6K} + \frac{K}{3} - \frac{\mu K}{3}\right] D_2$$

$$K^*_{\Delta 3,2} = \left[\frac{13}{48K^2} + \frac{3\mu}{4}\right] D_2$$

$$K^*_{\Delta 4,2} = \left[\frac{7}{8K^2} - \frac{\mu}{2}\right] \frac{D_2}{2C}$$

$$K^*_{\Delta 5,2} = \left[\frac{2}{3K} - \frac{K}{3} + \frac{\mu K}{3}\right] D_2$$

$$K^*_{\Delta 6,2} = -\left[\frac{11}{48K^2} + \frac{\mu}{4}\right] D_2$$

Continued Table (III-17)

$$K^*_{\Delta 7,2} = -\frac{2}{K^2}\cdot\frac{D_2}{2C}$$

$$K^*_{\Delta 8,2} = \frac{1}{2K}\ D_2$$

$$K^*_{\Delta 9,2} = \frac{1}{12K^2}\ D_2$$

$$K^*_{\Delta 1,3} = \left[\frac{13}{32K^3} + \frac{1}{4K} + \frac{3}{2}K + \frac{3}{4}\frac{\mu}{K}\right]\frac{D_2}{2C}$$

$$K^*_{\Delta 2,3} = \left[\frac{13}{48K^2} + \frac{3\mu}{4}\right] D_2$$

$$K^*_{\Delta 3,3} = \left[\frac{19}{192K^3} + \frac{1}{24K} + \frac{5}{4}K + \frac{\mu}{3K}\right] D_2$$

$$K^*_{\Delta 4,3} = -\left[\frac{3}{4K^3} + \frac{\mu}{K}\right]\frac{D_2}{2C}$$

$$K^*_{\Delta 5,3} = \left[\frac{11}{48K^2} + \frac{\mu}{4}\right] D_2$$

$$K^*_{\Delta 6,3} = \left[-\frac{17}{192K^3} + \frac{1}{24K} + \frac{K}{4} - \frac{\mu}{6K}\right] D_2$$

$$K^*_{\Delta 7,3} = -\left[\frac{3}{4K^3} + \frac{\mu}{K}\right]\frac{D_2}{2C}$$

$$K^*_{\Delta 8,3} = \frac{1}{4K^2}\ D_2$$

$$K^*_{\Delta 9,3} = \left[\frac{1}{48K^3} + \frac{1}{6K} + \frac{\mu}{12K}\right] D_2$$

$$K^*_{\Delta 1,7} = -\frac{3}{K^3}\ \frac{D_2}{4C^2}$$

$$K^*_{\Delta 2,7} = -\frac{2}{K^2}\ \frac{D_2}{2C}$$

$$K^*_{\Delta 3,7} = -\left[\frac{3}{4K^3} + \frac{\mu}{K}\right]\frac{D_2}{2C}$$

$$K^*_{\Delta 4,7} = -\frac{3}{K^3}\ \frac{D_2}{4C^2}$$

Continued Table (III-17)

$$K^*_{\Delta 5,7} = -\frac{2}{K^2}\ \frac{D_2}{2C}$$

$$K^*_{\Delta 6,7} = \left[\frac{3}{4K^3} + \frac{\mu}{K}\right]\frac{D_2}{2C}$$

$$K^*_{\Delta 7,7} = \frac{6}{K^3}\ \frac{D_2}{4C^2}$$

$$K^*_{\Delta 8,7} = -\frac{2}{K^2}\ \frac{D_2}{2C}$$

$$K^*_{\Delta 9,7} = 0$$

$$K^*_{\Delta 1,8} = \frac{1}{K^2}\ \frac{D_2}{2C}$$

$$K^*_{\Delta 2,8} = \frac{1}{2K}\ D_2$$

$$K^*_{\Delta 3,8} = \frac{1}{4K^2}\ D_2$$

$$K^*_{\Delta 4,8} = \frac{1}{K^2}\ \frac{D_2}{2C}$$

$$K^*_{\Delta 5,8} = \frac{1}{2K}\ D_2$$

$$K^*_{\Delta 6,8} = -\frac{1}{4K^2}\ D_2$$

$$K^*_{\Delta 7,8} = -\frac{2}{K^2}\ \frac{D_2}{2C}$$

$$K^*_{\Delta 8,8} = \frac{1}{K}\ D_2$$

$$K^*_{\Delta 9,8} = 0$$

$$K^*_{\Delta 1,9} = \left[\frac{1}{8K^3} + \frac{1}{K} - \frac{\mu}{2K}\right]\frac{D_2}{2C}$$

$$K^*_{\Delta 2,9} = \frac{1}{12K^2}\ D_2$$

$$K^*_{\Delta 3,9} = \left[\frac{1}{48K^3} + \frac{1}{6K} + \frac{\mu}{12K}\right] D_2$$

$$K^*_{\Delta 4,9} = -\left[\frac{1}{8K^3} + \frac{1}{K} - \frac{\mu}{2K}\right]\frac{D_2}{2C}$$

$$K^*_{\Delta 5,9} = -\frac{1}{12K^2}\ D_2$$

$$K^*_{\Delta 6,9} = \left[\frac{1}{48K^3} + \frac{1}{6K} + \frac{\mu}{12K}\right] D_2$$

$$K^*_{\Delta 7,9} = 0$$

$$K^*_{\Delta 8,9} = 0$$

$$K^*_{\Delta 9,9} = \left[\frac{1}{12K^3} + \frac{2}{3K} - \frac{2}{3}\frac{\mu}{K}\right] D_2$$

CHAPTER IV

TRANSFORMATION OF STIFFNESS MATRICES FROM ELEMENT COORDINATES TO SHELL COORDINATES

4.1 General

In the finite element model of a shell of revolution, the adjacent flat elements meet at an angle. The stiffness matrices for these elements, derived in chapters II and III, are in the local element coordinate directions. Thus, deformations and forces of all the elements meeting at a node have different directions. In order to be able to directly superimpose the stiffness coefficients from the adjoining elements to obtain the force-displacement relations at any node of the assemblage, it is necessary to transform the deformations and forces from the element coordinate directions into the common shell directions.

For the present analysis, it is most suitable to select at any point of the shell surface directions defined by; (see Fig. (IV-1))

(i) P - along tangent to the parallel circle, positive to the right looking from outside of the shell

(ii) M - along tangent to the meridian, positive towards the apex

and (iii) R - along the direction of the normal to the surface, positive outwards.

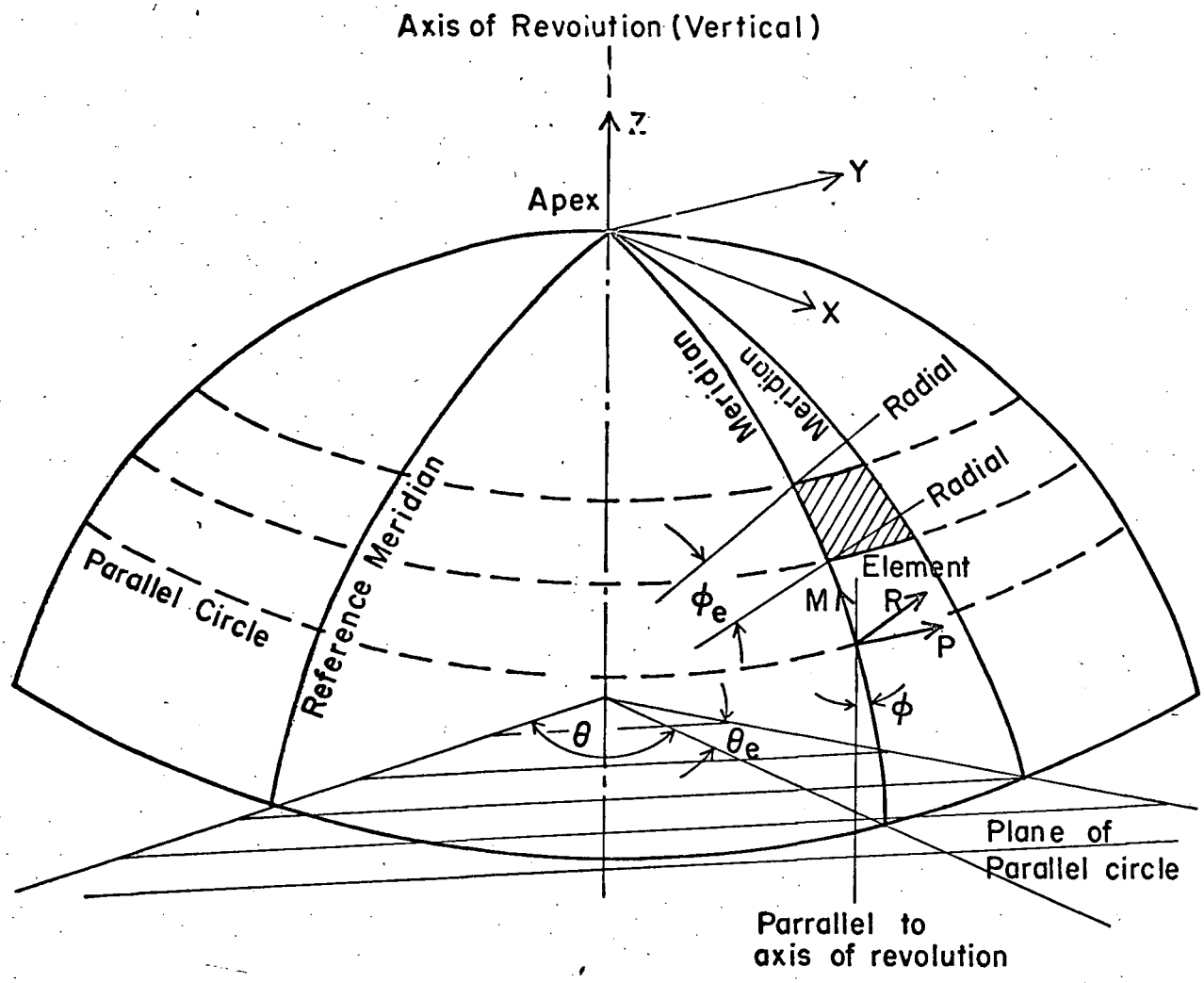

P — Tangent to the parallel circle in the plane of the parallel, positive to the right-looking from outside.

M — Tangent to the meridian in the plane of the meridian, positive towards the apex.

R — Normal to the surface, positive outwards.

ϕ = Angle between M-direction and the axis of revolution.

θ = Angle between the planes of the meridian and the reference meridian.

FIG. (IV-1) SHELL CO-ORDINATE DIRECTIONS: P, M and R.

Nodal displacements of a shell element are defined as; (i) P-displacement, (ii) M-displacement, (iii) R-displacement, (iv) P-rotation (i.e., rotation about P-axis, positive if clockwise looking in the positive direction of the axis), and (v) M-rotation. No rotation about R-axis need be considered since it is already covered by the displacements in P and M directions.

Similarly, nodal forces of a shell-element are defined as; (i) P-force, (ii) M-force, (iii) R-force, (iv) P-moment (i.e., moment about P-axis, considered positive if clockwise looking in the positive direction of the axis), and (v) M-moment.

No rotation or moment about the R-axis may be present in an infinitesimal element of the shell itself and for this reason no R-rotation need be contemplated at any node of the finite element of the shell model, even though some unbalanced R-moment will remain at the nodes.

4.2 Transformation of Deformations and Forces

Let $\{\delta^i\}_{XYZ}$ and $\{f^i\}_{XYZ}$ be the three displacements and three forces in the XYZ (element) directions at a node i of the element. Also, let $\{\delta^i\}_{PMR}$ and $\{f^i\}_{PMR}$ be the corresponding displacements and forces in the PMR (shell) directions at the same node. The displacements and forces of the two coordinate systems may be related to each other through an orthogonal transformation matrix $[T^i]$ as follows:

$$\{\delta^i\}_{XYZ} = [T^i]\{\delta^i\}_{PMR}$$

and similarly, $$\{f^i\}_{XYZ} = [T^i]\{f^i\}_{PMR}$$

Here, $[T^i]$ = 3 x 3 matrix containing the direction cosines of the element axes XYZ with respect to the shell axes PMR at node i.

Writing the above relations collectively for an n cornered element,

$$\begin{bmatrix} \{\delta^1\} \\ \{\delta^2\} \\ \\ \\ \{\delta^n\} \end{bmatrix}_{XYZ} = \begin{bmatrix} [T^1]_{3x3} & & 0 \\ & [T^2]_{3x3} & \\ & 0 & \\ 0 & & [T^n]_{3x3} \end{bmatrix} \begin{bmatrix} \{\delta^1\} \\ \{\delta^2\} \\ \\ \\ \{\delta^n\} \end{bmatrix}_{PMR}$$

or, $$\{\delta\}_{XYZ} = [T]\{\delta\}_{PMR} \qquad \text{(IV-1)}$$

similarly, $$\{f\}_{XYZ} = [T]\{f\}_{PMR} \qquad \text{(IV-2)}$$

Here, $\{\delta\}_{XYZ}$ and $\{f\}_{XYZ}$ = displacements and forces at all nodes of the element in XYZ (element)directions

$\{\delta\}_{PMR}$ and $\{f\}_{PMR}$ = displacements and forces at all nodes of the element in PMR (shell) directions.

$[T]$ = transformation matrix containing diagonally the direction cosine matrices of all corners

The (3x3) direction cosine matrices $[T^1]$, $[T^2]$, $[T^3]$ and $[T^4]$ belonging to nodes 1, 2, 3, and 4 respectively of a trapezoid element are shown in Table (IV-1). The various angles used in this table are defined as follows; (see Fig. (IV-2))

θ_e = angle between the meridian planes enclosing the element

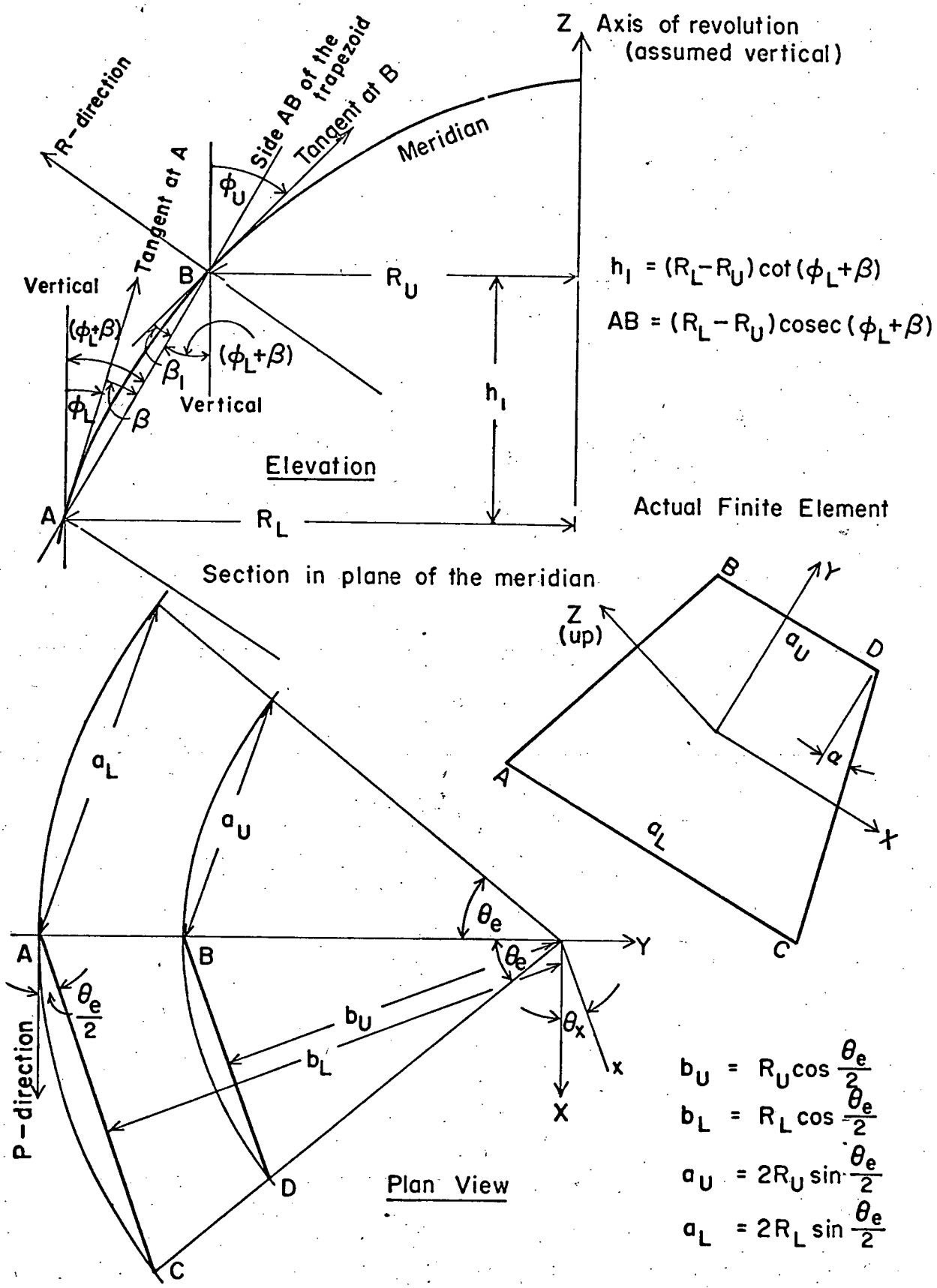

FIG. (IV-2) LOCATION OF A FINITE ELEMENT ON THE SHELL.

Table (IV-1) Transformation Submatrices for Various Nodes of a Trapezoid

$$[T^1] = \begin{bmatrix} \cos\frac{\theta_e}{2} & (\sin\beta \sin\varepsilon \cos\alpha - \cos\beta \sin\alpha) & (\cos\beta \sin\varepsilon \cos\alpha + \sin\beta \sin\alpha) \\ \sin\frac{\theta_e}{2} \cos\gamma & (\sin\beta \sin\varepsilon \sin\alpha + \cos\beta \cos\alpha) & (\cos\beta \sin\varepsilon \sin\alpha - \sin\beta \cos\alpha) \\ -\sin\frac{\theta_e}{2} \sin\gamma & \sin\beta \cos\varepsilon & \cos\beta \cos\varepsilon \end{bmatrix}$$ for node 1

$$[T^2] = \begin{bmatrix} \cos\frac{\theta_e}{2} & -(\sin\beta \sin\varepsilon \cos\alpha - \cos\beta \sin\alpha) & -(\cos\beta \sin\varepsilon \cos\alpha + \sin\beta \sin\alpha) \\ -\sin\frac{\theta_e}{2} \cos\gamma & (\sin\beta \sin\varepsilon \sin\alpha + \cos\beta \cos\alpha) & (\cos\beta \sin\varepsilon \sin\alpha - \sin\beta \cos\alpha) \\ \sin\frac{\theta_e}{2} \sin\gamma & \sin\beta \cos\varepsilon & \cos\beta \cos\varepsilon \end{bmatrix}$$ for node 2

$$[T^3] = \begin{bmatrix} \cos\frac{\theta_e}{2} & -(\sin\beta_1 \sin\varepsilon \cos\alpha + \cos\beta_1 \sin\alpha) & (\cos\beta_1 \sin\varepsilon \cos\alpha - \sin\beta_1 \sin\alpha) \\ \sin\frac{\theta_e}{2} \cos\gamma & -(\sin\beta_1 \sin\varepsilon \sin\alpha - \cos\beta_1 \cos\alpha) & (\cos\beta_1 \sin\varepsilon \sin\alpha + \sin\beta_1 \cos\alpha) \\ -\sin\frac{\theta_e}{2} \sin\gamma & -\sin\beta_1 \cos\varepsilon & \cos\beta_1 \cos\varepsilon \end{bmatrix}$$ for node 3

$$[T^4] = \begin{bmatrix} \cos\frac{\theta_e}{2} & (\sin\beta_1 \sin\varepsilon \cos\alpha + \cos\beta_1 \sin\alpha) & -(\cos\beta_1 \sin\varepsilon \cos\alpha - \sin\beta_1 \sin\alpha) \\ -\sin\frac{\theta_e}{2} \cos\gamma & -(\sin\beta_1 \sin\varepsilon \sin\alpha - \cos\beta_1 \cos\alpha) & (\cos\beta_1 \sin\varepsilon \sin\alpha + \sin\beta_1 \cos\alpha) \\ \sin\frac{\theta_e}{2} \sin\gamma & -\sin\beta_1 \cos\varepsilon & \cos\beta_1 \cos\varepsilon \end{bmatrix}$$ for node 4

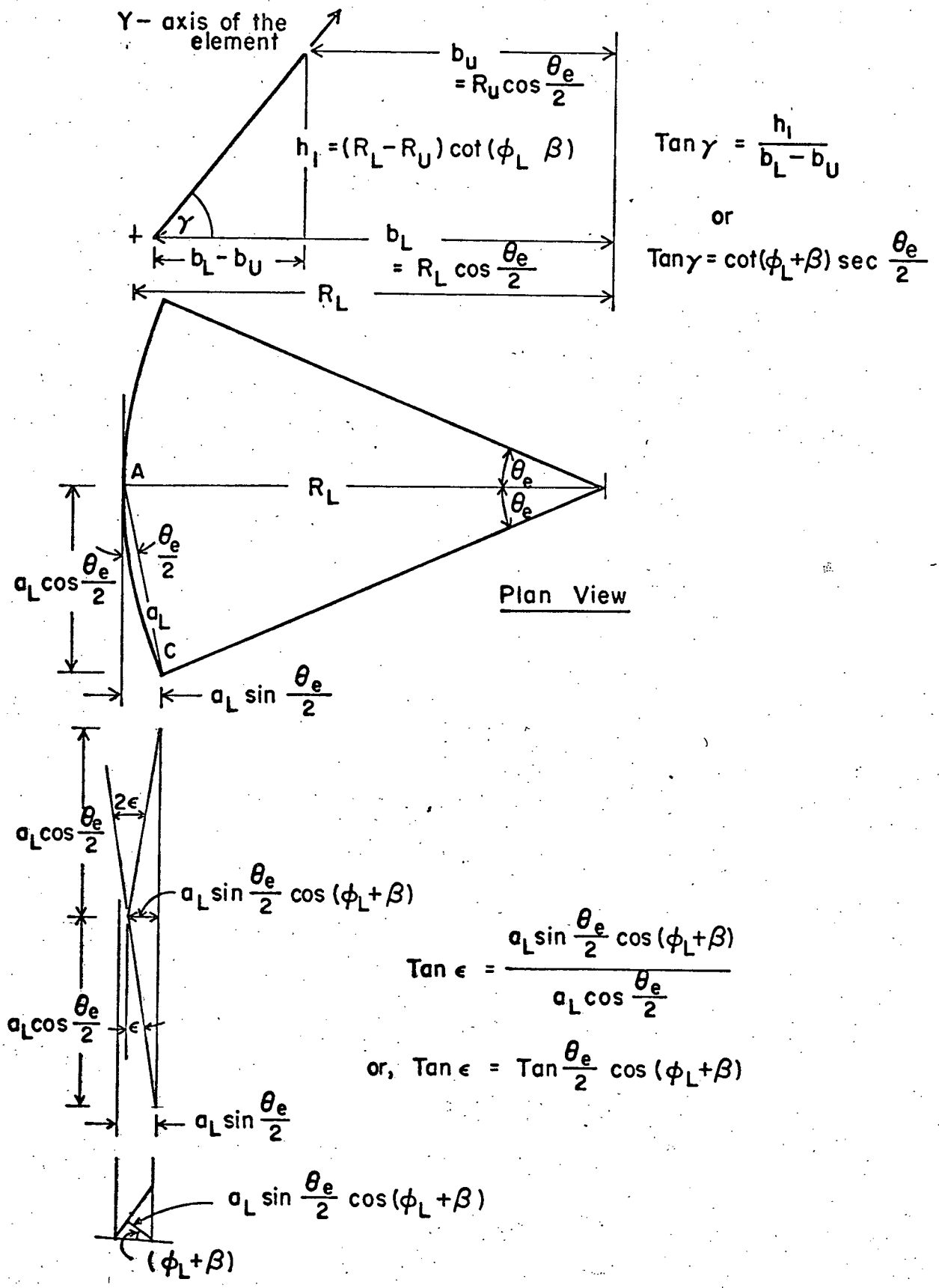

FIG. (IV-3) RELATING γ and ϵ ANGLES TO ϕ_L, β and θ_e ANGLES

ϕ_L = angle between tangent to the meridian at the lower nodes of the element and the axis of revolution

ϕ_U = angle between tangent to the meridian at the upper nodes of the element and the axis of revolution

β = angle between the tangent to the meridian at the lower node of the element and the chord line joining the lower and the upper nodes of the element

β_1 = angle between the tangent to the meridian at upper node and the chord joining the lower and the upper nodes [$\beta_1 = \phi_U - (\phi_L + \beta)$]

α = angle in the plane of the element which the inclined side makes with the Y-axis of the element

γ = angle of inclination of the element with the plane of a parallel circle

ε = half the angle between two equal elements intersecting along a common inclined edge (e.g. AB)

Angles γ and ε are related to the other angles as follows:

$$\text{Tan}\gamma = \text{Cot}(\phi_L + \beta)\sec\frac{\theta_e}{2}$$

$$\text{Tan}\varepsilon = \text{Tan}\frac{\theta_e}{2}\,\text{Cos}(\phi_L + \beta)$$

For derivation of these relations, refer to Figs. (IV-2 and 3).

The apex node of a triangle must be treated in a special manner. A new set of coordinate system $\mathcal{X}$, $\mathcal{Y}$, $\mathcal{Z}$ is defined at the apex. (see Figs. (IV-1 and 2)). $\mathcal{X}$ and $\mathcal{Y}$ axes lie in a plane tangent to the shell at the apex and $\mathcal{Z}$ axis is normal to the shell surface, positive outwards. The Direction of $\mathcal{X}$-axis may be selected arbitrarily. The direction of $\mathcal{Y}$-axis is selected so as to form a righthand system of coordinates. An independent

transformation submatrix $[T_{\Delta}^{3}]$ is defined for the apex node of a triangular element and is given in Table (IV-2).

Here, θ_x = angle in the horizontal plane (assuming the axis of revolution to be vertical) between the X-direction at the apex and X-axis of the triangle element. See Fig. (IV-2).

Derivation of the direction cosine matrix $[T^1]$ at node 1 of an equilateral trapezoid element is explained as below; vectors (δP), (δM), and (δR) along P, M and R directions are individually resolved into components along X, Y and Z direction (see Fig. (IV-4)).

(a) Components of (δP) along X, Y and Z directions

$$(\delta X) = \text{Cos}(\frac{\theta_e}{2})\ (\delta P)$$

$$(\delta Y) = \text{Sin}(\frac{\theta_e}{2})\text{Cos}\gamma\ (\delta P) \qquad \text{See Fig. (IV-4,a,b,d)}$$

$$(\delta Z) = -\ \text{Sin}(\frac{\theta_e}{2})\text{Sin}\gamma\ (\delta P)$$

(b) Components of (δM) along X, Y and Z directions

$$(\delta X) = (\text{Sin}\beta\text{Sin}\varepsilon\text{Cos}\alpha - \text{Cos}\beta\text{Sin}\alpha)(\delta M)$$

$$(\delta Y) = (\text{Sin}\beta\text{Sin}\varepsilon\text{Sin}\alpha + \text{Cos}\beta\text{Cos}\alpha)(\delta M) \qquad \text{Refer to Fig. (IV-4, c,d,e)}$$

$$(\delta Z) = (\text{Sin}\beta\text{Cos}\varepsilon)(\delta M)$$

(c) Components of (δR) along X, Y and Z directions

$$(\delta X) = (\text{Cos}\beta\text{Sin}\varepsilon\text{Cos}\alpha + \text{Sin}\beta\text{Sin}\alpha)(\delta R)$$

$$(\delta Y) = (\text{Cos}\beta\text{Sin}\varepsilon\text{Sin}\alpha - \text{Sin}\beta\text{Cos}\alpha)(\delta R) \qquad \text{Refer to Fig. (IV-4, c,d,e)}$$

$$(\delta Z) = (\text{Cos}\beta\text{Cos}\varepsilon)(\delta R)$$

The force-displacement relation in the XYZ (element) direction is given by

$$\{f\}_{XYZ} = [K]_{XYZ}\{\delta\}_{XYZ} \qquad \text{(IV-3)}$$

Table (IV-2) Transformation Submatrix for the Apex Node of a Triangular Element.

$$[T_{\Delta}^{3}] = \begin{bmatrix} \cos(\theta_x) & \sin(\theta_x) & 0 \\ -\sin(\theta_x)\cos\gamma & \cos(\theta_x)\cos\gamma & \sin\gamma \\ \sin(\theta_x)\sin\gamma & -\cos(\theta_x)\sin\gamma & \cos\gamma \end{bmatrix}$$

Table (IV-3) Transformation Matrices for Shell Elements Having Plane-Stress Properties

(a) Transformation Matrix for an Equilateral Trapezoid in Plane Stress (membrane shell)

$$[T]_{12x12} = \begin{bmatrix} [T^1] & & & 0 \\ & [T^2] & & \\ & & [T^3] & \\ 0 & & & [T^4] \end{bmatrix}$$

Each block $[T^i]$ is a 3 x 3 submatrix, it contains direction cosines at i^{th} corner. See Table (IV-1)

(b) Transformation Matrix for an Isosceles Triangle in Plane Stress (membrane shell)

$$[T]_{9x9} = \begin{bmatrix} [T^1] & & 0 \\ & [T^2] & \\ 0 & & [T_{\Delta}^3] \end{bmatrix}$$

Here $[T^1]$ and $[T^2]$ are the same as for a trapezoid and are given in Table (IV-1). $[T_{\Delta}^3]$ is a 3 x 3 submatrix containing the direction cosines at the apex; it is given in Table (IV-2)

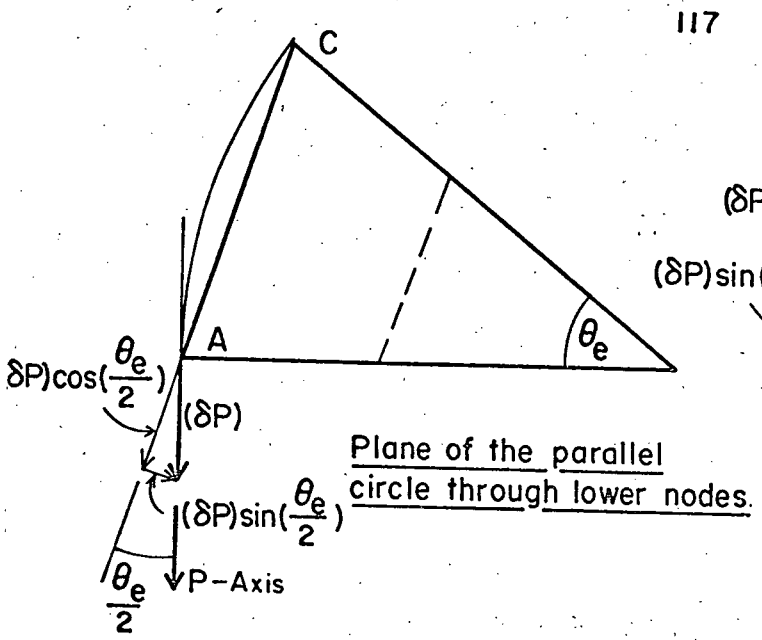

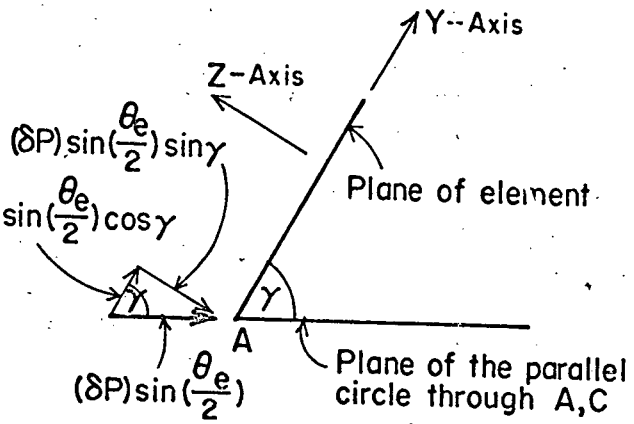

Section through Y–Z plane of the element.

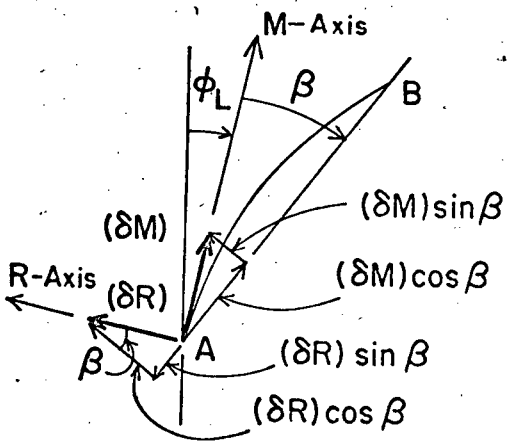

(c) Components of (δM) and (δR) along and normal to AB in the plane of the meridian AB.

Axis of Revolution

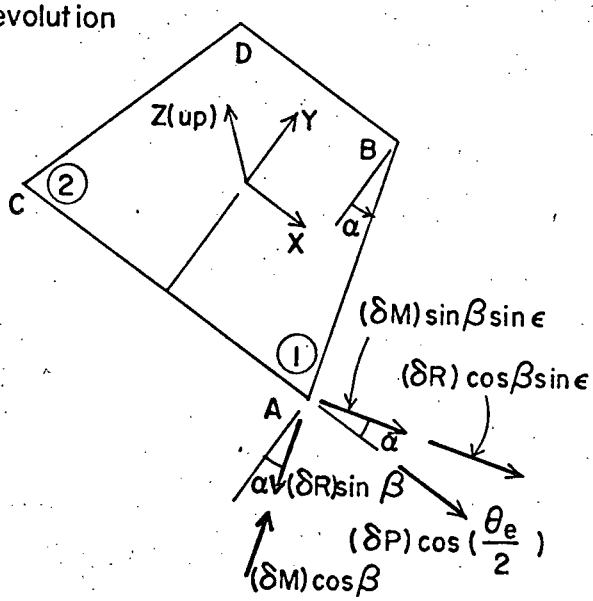

(d) Plane of the element

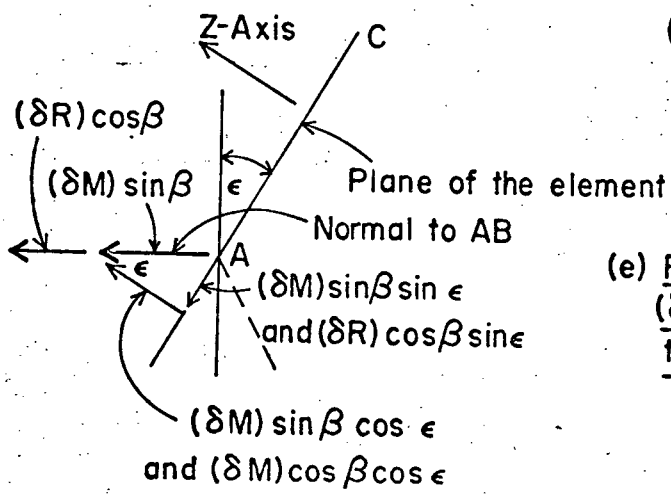

(e) Resolving components of (δM) and (δR) normal to AB in the plane of the element and in Z direction.

FIG. (Ⅳ-4) DERIVATION OF DIRECTION COSINE MATRIX AT NODE I.

Here, $[K]_{XYZ}$ is the stiffness matrix of the element in XYZ (element) coordinates.

Substituting Eqn. (IV-1) for $\{\delta\}_{XYZ}$ and Eqn. (IV-2) for $\{f\}_{XYZ}$ in Eqn. (IV-3), one obtains

$$[T]\{f\}_{PMR} = [K]_{XYZ}[T]\{\delta\}_{PMR} \tag{IV-4}$$

Premultiplying each side of the Eqn. (IV-4) by $[T]^{-1}$

$$\{f\}_{PMR} = [T]^{-1}[K]_{XYZ}[T]\{\delta\}_{PMR} \tag{IV-5}$$

Since, the matrix [T] transforms the deformations and forces from one set of orthogonal directions to the other, it is an orthogonal matrix. Thus,

$$[T]^{-1} = [T]^{T} \tag{IV-6}$$

Thus, Eqn. (IV-5) may be rewritten as

$$\{f\}_{PMR} = [T]^{T}[K]_{XYZ}[T]\{\delta\}_{PMR} \tag{IV-7}$$

Equation (IV-7) provides the force-deformation relation of the element in the PMR (shell) coordinate system. The transformed stiffness matrix $[K]_{PMR}$ of the element in the shell coordinate system is given by

$$[K]_{PMR} = [T]^{T}[K]_{XYZ}[T] \tag{IV-8}$$

It should be noted that rotations and moments at any node may be transformed from XYZ coordinate system to PMR coordinate system by means of the same direction cosine matrix as used for the transformations of displacements and forces.

4.3 Transformation Matrix for a Plane Stress Shell Element

When analysing a shell devoid of flexure stresses, the finite elements used are the ones possessing only plane stress properties. A node of a shell element is free to displace along P, M and R directions while stresses are induced in the shell. Thus, the transformation matrix is (12 x 12) for a trapezoid and (9 x 9) for a triangular element. These matrices are shown in Table (IV-3).

The element stiffness matrices in their local coordinates for a trapezoid and a triangle are (8 x 8) and (6 x 6) respectively. To make these matrices compatible for matrix multiplication of Eqn. (IV-8), rows and columns containing zero are introduced to correspond to the non-existing Z-direction stiffnesses. The resulting stiffness matrix in the local XYZ coordinate system is (12 x 12) for a trapezoid and (9 x 9) for a triangle element. The 3rd, 6th, 9th and 12th rows and columns containing zero, correspond to zero force due to the Z-direction displacements.

4.4 Transformation Matrix for a Shell Element having Membrane and Flexure Properties

In the analysis of a shell having membrane and flexure stresses, finite elements possessing both plane stress and flexure properties have to be used. The combined plane-stress and flexure stiffness matrices are (20 x 20) for a trapezoid and (15 x 15) for a triangular element.

A node of a shell element is free to displace in P, M and R directions and rotate about P and M axes while stresses and moments are induced in the shell. No rotation about R axis need be considered since it is covered by the displacements in P and M directions. The transformation matrices are (24 x 24) for a trapezoid and (18 x 18) for a triangle and are given in Table (IV-4). The element stiffness matrices in their local element-coordinates are made compatible for matrix multiplication of Eqn. (IV-8) by introducing rows and columns containing zero to correspond to the rotation about Z axis. The resulting stiffness matrix in the local XYZ coordinate system is (24 x 24) for a trapezoid and (18 x 18) for a triangle element. The 6th, 12th, 18th and 24th rows and columns containing zero forces due to rotation about Z-axis.

The nodes of the finite elements are not permitted to rotate about the R-axis because no such rotation takes place in the shell itself as its points find their deformed positions by undergoing two components of displacements in the plane of the shell. However, in the shell-model, prevention of rotation about R-axis results in some moment unbalance about the same axis brought about by the conversion of X and Y finite element moments into P, M, R shell moments. The R-moments so produced contain as factors sines of very small angles β and ε, which cause the R-moments to

Table (IV-4) Transformation Matrices for Shell Elements Having Plane Stress and Flexure Properties

(a) Transformation Matrix for an Equilateral Trapezoid in Plane Stress and Flexure.

$$[T]_{24x24} = \begin{bmatrix} [T^1] & & & & & & \\ & [T^1] & & & & & \\ & & [T^2] & & 0 & & \\ & & & [T^2] & & & \\ & & & & [T^3] & & \\ & & 0 & & & [T^3] & \\ & & & & & & [T^4] \\ & & & & & & & [T^4] \end{bmatrix}$$

Each $[T^i]$ is a (3 x 3) sub-matrix of direction cosines at the i^{th} corner. Entries of $[T^i]$ matrix are shown in Table (IV-1)

(b) Transformation Matrix for an Isosceles Triangle in Plane Stress and Flexure

$$[T]_{18x18} = \begin{bmatrix} [T^1] & & & & \\ & [T^1] & & 0 & \\ & & [T^2] & & \\ & & & [T^2] & \\ & 0 & & & [T^3_\Delta] \\ & & & & & [T^3_\Delta] \end{bmatrix}$$

Entries of $[T^3_\Delta]$ are shown in Table (IV-2)

disappear in the limit. With finite size elements, the R-moments are left unbalanced because they are purely fictitious from the viewpoint of the shell itself. With this in mind, R-rotations are made zero and the unbalanced R-moments are neglected in the analysis.

CHAPTER V

APPLICATION OF THE FINITE ELEMENT METHOD TO VARIOUS SHELL OF REVOLUTION PROBLEMS

5.1 General

In the following study, suitability of the formulation is established by comparing the finite element solution with the theoretical solution of several problems. Convergence trends are also demonstrated by reducing the element size.

The statics stiffness matrices derived in chapters II and III for trapezoidal and triangular elements in plane stress and flexure are asymmetric with the exception of a triangular element in plane stress. Asymmetry of the stiffness matrix means violation of Betti's reciprocal theorem. Although the evaluation of equivalent nodal forces from distributed edge forces is consistent with the laws of statics, yet, the asymmetry of the stiffness matrix raises some doubts with regard to the method. The asymmetry of the stiffness matrices of a trapezoid element in plane stress and in flexure disappears when the element reduces to a rectangle. It is even more important that as the states of stress reduce to uniform, the reciprocal theorem is satisfied in the limit even with the trapezoidal element. The asymmetric stiffness matrices were used and accuracy comparable to that of symmetrical energy stiffness matrices was obtained. However, the asymmetry of matrices is a disadvantage in the computer work in view of

the need for a double storage capacity. Asymmetric stiffness matrices, arising from the statics approach, have been derived and used successfully by Antebi et al.,[12] Gallagher[13] and Shah.[30]

In the present study, the asymmetric stiffness matrices are made symmetric by averaging the terms of the matrix and its transpose. The stiffness coefficients belonging in each column of an asymmetric matrix satisfy the equilibrium requirements. It is observed that the terms belonging to each column of the average matrix also satisfy the equilibrium requirements. Thus, the process of averaging corresponds to introduction of additional self equilibrating nodal forces making the asymmetric stiffness matrix symmetric. A similar procedure was independently adopted by Antebi et al.[12] They observed that the errors introduced by the averaging process are minor and that they are more pronounced in stresses than in displacements.

5.2 A General Solution Procedure

A computer program for use with the I.B.M. 7044 electronic computer, based on the general matrix algebra method of structural analysis, has been developed and is given in the Appendix. The basic steps in the solution procedure are:

(i) The shell surface is subdivided by meridian lines and parallel circles. The surfaces enclosed between meridian lines and parallel circles are approximated by flat elements connected to each other at the corners only. These elements are in the shape of equilateral trapezoids with the exception of the ones at the apex which are isosceles triangles. Different shape elements are normally not needed. If the meridians are spaced at a fixed horizontal angle,

then the elements inscribed between any two adjacent parallel circles are identical. These elements will have the same stiffness and transformation matrices which, thus, need to be generated only once. This is a big advantage as it results in a large saving of computer time and storage space. The transformation matrix for each triangular element is different and has to be generated for every element independently.

(ii) The loads acting on the shell are applied to the model in the same relative locations - at the nodes only. These loads are specified in the P, M, and R directions.

In most cases the loads acting on the shell are distributed over certain areas of the shell and so nodal concentrations are simply parts of the distributed load tributary to the nodes and computed, with some exercise of judgement, in conformity with the requirement of static equivalence. An alternative procedure is to assign the nodal loads consistent with the virtual work formulation. The distribution of the load applied within each element becomes dependent on the movements of its nodes. Both procedures suggested are in agreement with statics. The second one is unique, the first one is not. However, due to complexity of the second procedure, the first procedure is adopted in the present study.

(iii) The model is endowed with the same boundary conditions as the prototype. These are specified in the shell directions.

Boundary conditions for displacements do not present any problem. However, rotation boundary conditions involve some special considerations. The rotation boundary conditions for a shell are

provided similar to those of a plate. For a plate model, these are as follows;[23]

(a) Simply Supported Edge Suppose this is an edge y=c perpendicular to the Y-axis. The two obvious boundary conditions are w=0 and M_y=0. This means that the edge nodes have no deflection and are free to rotate about the edge.

In the plate prototype the edge y=c may develop no torsional moment M_{yx}. Since $M_{yx} = -(1-\mu)D\frac{\partial^2 w}{\partial x \partial y}$, this may appear to mean that,

$$\frac{\partial^2 w}{\partial x \partial y} = \frac{\partial}{\partial x}\left(\frac{\partial w}{\partial y}\right) = 0$$

On integration with regard to x, this relation gives $\partial w/\partial y$ = constant. This conclusion is obviously incorrect, since the slope of the deflection surface does vary along the simply supported edge.

The explanation of the seeming contradiction lies in the fact that the torsional moment along the simply supported edge is transformed into the edge shear $\partial M_{yx}/\partial x$ which is resisted by the additional vertical reactions rather than the reactive torques. Thus, although M_{yx}=0, $\partial^2 w/\partial x \partial y \neq 0$, and in order to comply with these two, the edge joints must be allowed to rotate about the Y-axis to bring into balance the moments acting about this axis.

(b) Built-in Edge Assume again this edge to be y=c. Along this edge w=0 and $\partial w/\partial y$=0. From these two relations, it follows that

$$\frac{\partial^2 w}{\partial x \partial y} = \frac{\partial}{\partial x}\left(\frac{\partial w}{\partial y}\right) = 0$$

and at the same time $\partial w/\partial x=0$ along the edge. This means that in the prototype, the edge develops no M_{yx} and the edge points do not rotate about the axis Y, perpendicular to the edge.

An absence of the edge torque accompanied by an absence of rotation about the Y-axis is however, impossible in the model since if the edge nodes do not rotate about the Y-axis some torsional moments will be present there being brought about by the rotations and displacements of the nodes one element away from the edge. To eliminate these the edge joints must be allowed to rotate about the Y-axis, but their displacements must satisfy the relation $w=0$ and $\partial w/\partial y=0$.

(c) Free Edge Nodes are permitted to deflect and rotate freely about both axes.

Similar, force considerations are used to decide the rotation boundary conditons of a corner of the plate model at a right angle intersection of its two edges.

(iv) From the supplied geometry, the element stiffness matrix $[K]_{XYZ}$ and the transformation matrix [T] are calculated. The stiffness matrix $[K]_{PMR}$ in the shell coordinates is obtained from the matrix equation

$$[K]_{PMR} = [T]^T [K]_{XYZ} [T]$$

(v) Stiffness matrix [S] for the entire model of the shell is generated from the transformed element stiffness matrices $[K]_{PMR}$ using the code number technique.[31] This technique automatically eliminates the rows and columns of the structure stiffness matrix [S] corresponding to the restraint directions.

(vi) Load vector $\{F\}$ is generated from the supplied joint loads.

(vii) Choleski's method of solution[32] (also called the square root method) is employed to solve the system of simultaneous linear equations,

$$\{F\} = [S]\{\Delta\}$$

Here, $\{\Delta\}$ is a column matrix of unknown nodal deformations of the structure.

(viii) Knowing the structure deformations $\{\Delta\}$, the shell element deformation vectors $\{\delta\}_{PMR}$ are found by using code numbers.

(ix) Following the calculation of nodal displacements and rotations, the shell stresses may be found by one of the two methods; the method of nodal displacements or the method of nodal force concentrations.

In the former method, once all nodal displacements and rotations of a trapezoid element are known in the element coordinates, the in-plane and flexure stresses may be found using Eqns. (II-14,b) and (III-10). Similar expressions may be written for a triangular element. The in-plane and flexure stresses, calculated at the nodes, are in the X-Y-Z (element coordinate) directions and need to be further transformed into PMR (shell) directions. At an interior node where four elements meet, it is necessary to compute and average the stress values at the node in question in all four elements. At the edge node there are only two elements involved and at the corner-only one. On account of the involved conversion of stresses from X-Y-Z directions into PMR directions, the method of determining stresses from nodal displacements is inconvenient to use when applied to shells.

In the present study, the method of nodal force concentration is used to calculate stresses at various node points. For each element, the nodal forces in shell directions, $\{f\}_{PMR}$, are calculated from the equation

$$\{f\}_{PMR} = [K]_{PMR}\{\delta\}_{PMR}$$

The average stresses and moments (Fig. (V-0-1) are found by spreading the nodal forces over the appropriate areas of the section.[23,33] The procedure is illustrated by reference to Fig. (V-0-2) representing four elements surrounding the common node 1 of the model. In the absence of an external load at the node 1, the internal forces acting on the four elements are mutually balanced. Should an external load be present, the nodal forces will balance it. The following membrane and flexure forces per unit length may be assumed to exist in the shell in P, M and R-directions at the node 1 in the absence of the external load. The positive directions of stresses and moments are shown in Fig. (V-0-1).

$$\text{P-force/length, } (N_\theta) = \frac{2(N_{P4} + N_{P2})}{(a_2 + a_3)} = -\frac{2(N_{P3} + N_{P1})}{(a_2 + a_3)}$$

$$\text{M-force/length, } (N_\phi) = \frac{(N_{M2} + N_{M1})}{a_1} = -\frac{(N_{M4} + N_{M3})}{a_1}$$

Membrane shear force/length

$$(N_{\theta\phi}) = \frac{2(N_{M2} + N_{M4})}{(a_2 + a_3)} = -\frac{2(N_{M1} + N_{M3})}{(a_2 + a_3)}$$

$$\text{also, } (N_{\phi\theta}) = \frac{(N_{P2} + N_{P1})}{a_1} = -\frac{(N_{P4} + N_{P3})}{a_1}$$

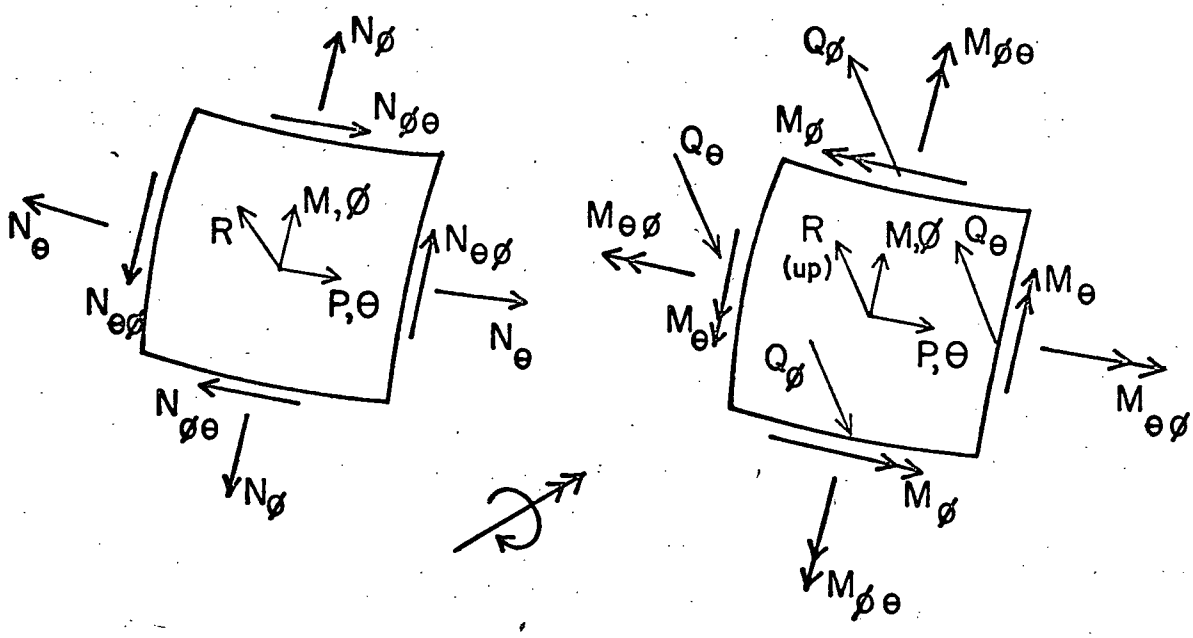

FIGURE V-0-1. POSITIVE DIRECTIONS OF STRESSES AND MOMENTS IN A SHELL ELEMENT

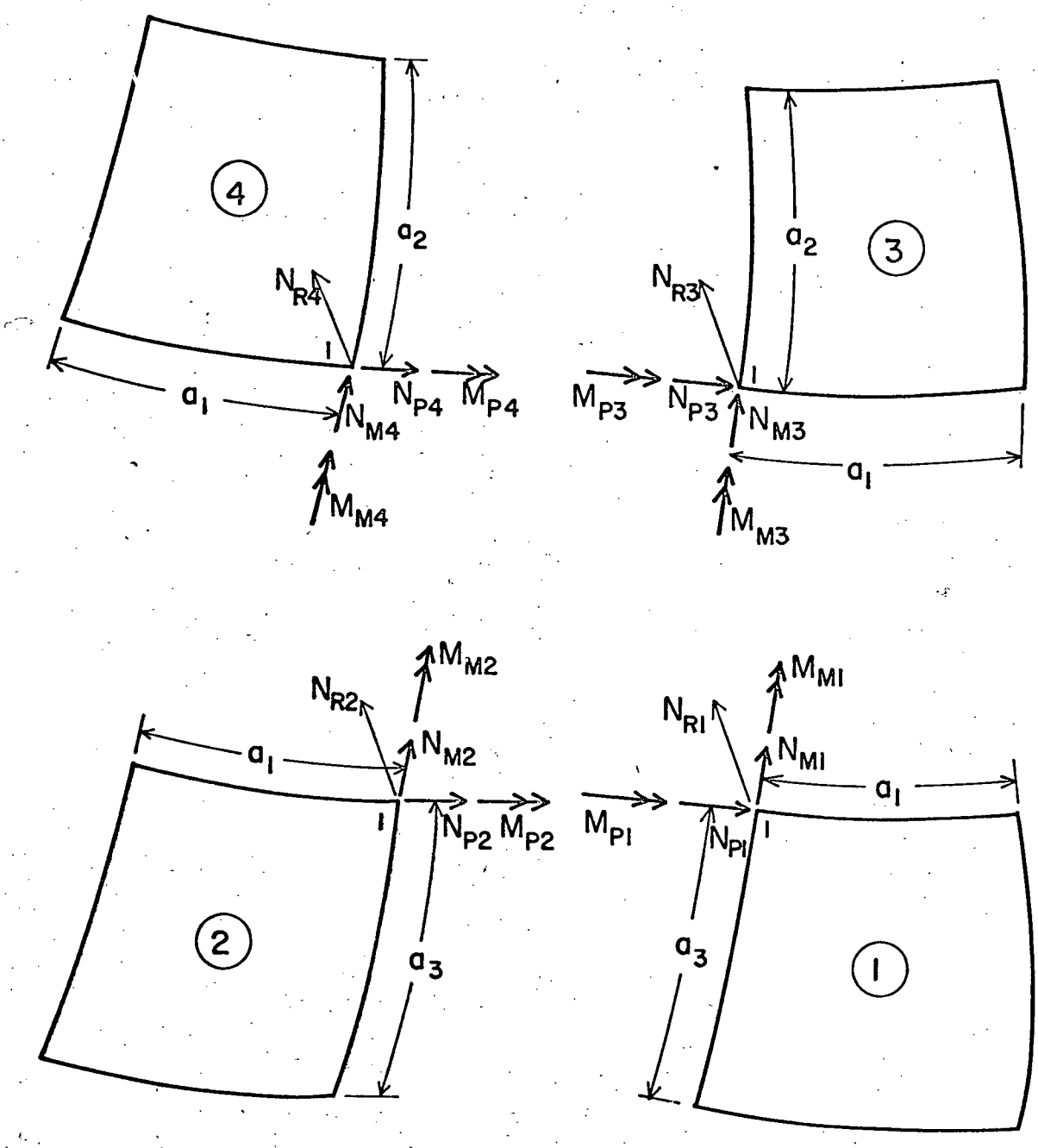

FIGURE V-0-2. CALCULATION OF STRESSES AT AN INTERNAL NODE

$N_{\theta\phi}$ and $N_{\phi\theta}$ should theoretically be equal and since their calculated values nearly always disagree somewhat, they should be averaged.

$$\text{P-moment/length, } (M_\phi) = \frac{(M_{P4} + M_{P3})}{a_1} = -\frac{(M_{P2} + M_{P1})}{a_1}$$

$$\text{M-moment/length, } (M_\theta) = \frac{2(M_{M4} + M_{M2})}{(a_2 + a_3)} = \frac{-2(M_{M3} + M_{M1})}{(a_2 + a_3)}$$

Transeverse shear/length,

$$(Q_\theta) = \frac{2(N_{R4} + N_{R2})}{(a_2 + a_3)} = \frac{-2(N_{R3} + N_{R1})}{(a_2 + a_3)}$$

Transeverse shear/length,

$$(Q_\phi) = \frac{(N_{R2} + N_{R1})}{a_1} = -\frac{(N_{R4} + N_{R3})}{a_1}$$

Twisting moment/length,

$$(M_{\theta\phi}) = \frac{2(M_{P4} + M_{P2})}{(a_2 + a_3)} = -\frac{2(M_{P3} + M_{P1})}{(a_2 + a_3)}$$

$$\text{and, } (M_{\phi\theta}) = \frac{(M_{M2} + M_{M1})}{a_1} = -\frac{(M_{M4} + M_{M3})}{a_1}$$

Twisting moments $M_{\theta\phi}$ and $M_{\phi\theta}$ should be numerically equal and opposite in sign. If they are not, the two values should be averaged.

If concentrated forces P_P, P_M and P_R are present at the node 1, they should be properly apportioned between the four elements into the parts P_{P1}, P_{M1}, P_{R1}; P_{P2}, P_{M2}, P_{R2}; P_{P3}, P_{M3}, P_{R3}; and P_{P4}, P_{M4}, P_{R4}. The nodal forces satisfy the relations,

$$(N_{P1} - P_{P1}) + (N_{P2} - P_{P2}) + (N_{P3} - P_{P3}) + (N_{P4} - P_{P4}) = 0$$

$$(N_{M1} - P_{M1}) + (N_{M2} - P_{M2}) + (N_{M3} - P_{M3}) + (N_{M4} - P_{M4}) = 0$$

$$\text{and, } (N_{R1} - P_{R1}) + (N_{R2} - P_{R2}) + (N_{R3} - P_{R3}) + (N_{R4} - P_{R4}) = 0$$

Thus, the stresses are obtained from the previous equations by simply replacing N_{P1}, N_{P2}, ... by $(N_{P1} - P_{P1})$, $(N_{P2} - P_{P2})$, ... respectively.

Additional explanation is needed with regard to the stresses at the edges of the shell. Some decisions regarding these stresses must be based on judgement partly in view of the difficulty of deciding to which of the two planes some of the nodal forces should be attributed.

(a) Free Edge

Nodal forces acting on elements having a common edge node are shown in Fig. (V-0-3). If the distribution of P-stress (N_θ) is nonuniform on the meridian 1-2 (Fig. (V-0-4)) then its calculation on the basis of the edge nodal concentration alone results in high error. In such a case, the following modification is suggested for calculation of P-stress at the edge: P-force/length ($N_{\theta 2}$) at the interior node 2 is first calculated. Assuming the distribution of P-stress to be linear on the meridian 1-2, the equivalent P-force at node 1 due to P-stress alone (Fig. (V-0-4)) is

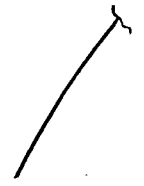

$$N_P^1 = \frac{a_2}{6} (2N_{\theta 1} + N_{\theta 2})$$

Thus, P-force/length at node 1 ($N_{\theta 1}$) may be expressed as

$$N_{\theta 1} = \frac{1}{2} \left(\frac{6N_P^1}{a_2} - N_{\theta 2}\right)$$

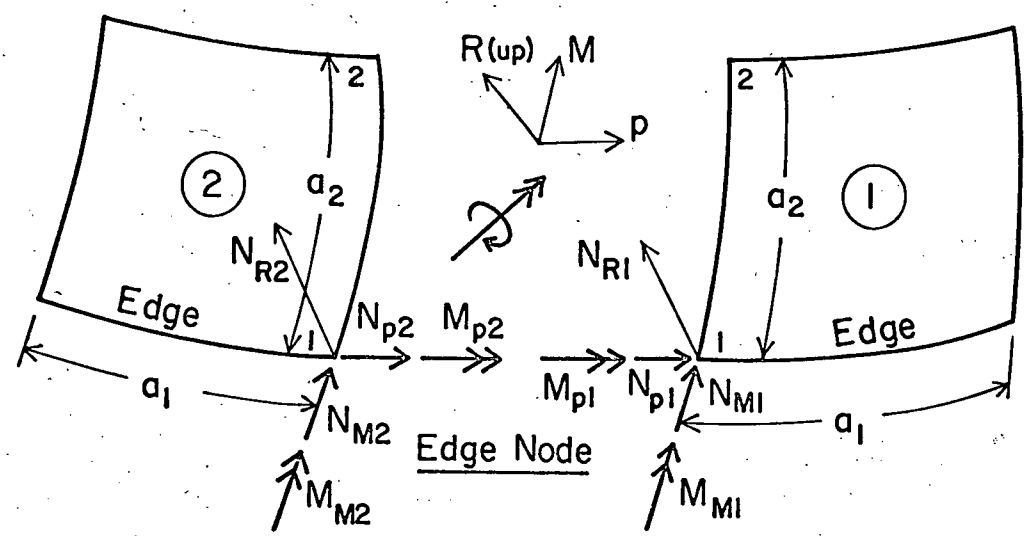

FIGURE V-0-3. CALCULATION OF STRESSES AT AN EDGE NODE

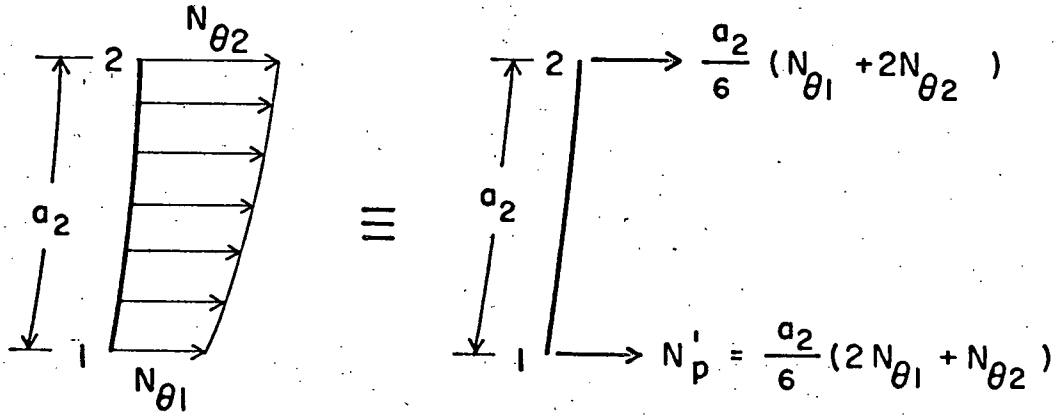

FIGURE(V-0-4) DISTRIBUTION OF P-STRESS (N_θ) ON MERIDIAN 1-2

Absence of $N_{\phi\theta}$ on the free edge results in

$$N_P^1 = N_{P1}$$

Thus,
$$N_{\theta 1} = \frac{1}{2}\left(\frac{6N_{P1}}{a_2} - N_{\theta 2}\right)$$

$$Q_\theta = \frac{2N_{R2}}{a_2} = -\frac{2N_{R1}}{a_2}$$

and
$$M_\theta = \frac{2M_{M2}}{a_2} = -\frac{2M_{M1}}{a_2}$$

Stresses N_ϕ, $N_{\phi\theta}$, M_ϕ, $M_{\phi\theta}$ and Q_ϕ may be assumed zero.

(b) Fixed Edge - Supported in P, M and R Directions

(Figs. (V-0-3 and 4))

The forces/length are;

$$N_{\theta 1} = \frac{1}{2}\left(\frac{6N_P^1}{a_2} - N_{\theta 2}\right)$$

Here, the equivalent force at node 1 due to P-stresses alone is

$$N_P^1 = N_{P2} + N_{\phi\theta}\left(\frac{a_1}{2}\right) = N_{P2} - \frac{(N_{P1} + N_{P2})}{2}$$

or, $$N_P^1 = (N_{P2} - N_{P1})/2$$

Thus, from above,

$$N_{\theta_1} = \frac{1}{2}\left\{\frac{3(N_{P2} - N_{P1})}{a_2} - N_{\theta 2}\right\}$$

$$N_\phi = -(N_{M1} + N_{M2})/a_1$$

$$N_{\phi\theta} = -(N_{P1} + N_{P2})/a_1$$

In view of the edge node being allowed to rotate about M-axis, $M_{M1} + M_{M2} = 0$.

$$M_\theta = 2M_{M2}/a_2 = -2M_{M1}/a_2$$

$$M_\phi = (M_{P1} + M_{P2})/a_1$$

$$M_{\theta\phi} = M_{\phi\theta} = 0 \quad \text{(from considerations of plate theory)}$$

$$Q_\theta = 2\{N_{R2} + Q_\phi(a_1/2)\}/a_2 = (N_{R2} - N_{R1})/a_2$$

and $$Q_\phi = -(N_{R1} + N_{R2})/a_1$$

(c) Simply Supported Edge - Displacements Restricted in P, M and R Directions (Figs. (V-0-3 and 4))

Here, $N_{\theta 1}$, N_ϕ, $N_{\phi\theta}$, Q_θ and Q_ϕ are the same as calculated for a fixed edge. (case b)

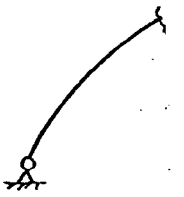

In view of the edge nodes being allowed to rotate about both axes, $M_{P1} + M_{P2} = 0$ and $M_{M1} + M_{M2} = 0$. M_ϕ is zero and M_θ may be assumed zero from general considerations of plate theory. M_{P2} may be assumed to correspond to the torsion moment in θ-plane, $M_{\theta\phi} = \frac{2M_{P2}}{a_2}$. The torsion moment $M_{\phi\theta}$ has been transformed into transeverse edge shear Q_ϕ.

(d) Edge with Displacements Restricted in the Parallel and Vertical Directions. (Fig. (V-0-3))

Vertical component of the reaction at node 1 is resolved in M and R directions; M = V Cos ϕ; R = V Sin ϕ.

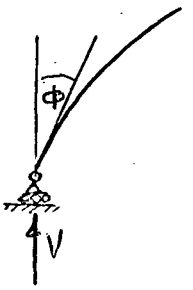

The components of nodal forces in P, M and R directions are shown in Fig. (V-0-3). Here, calculations for $N_{\theta 1}$, N_{ϕ}, $N_{\phi\theta}$, Q_{θ} and Q_{ϕ} are the same as for a fixed edge (case b).

In view of the edge nodes being allowed to rotate about both P and M axes, $M_{P1} + M_{P2} = 0$ and $M_{M1} + M_{M2} = 0$. Thus, M_{ϕ} is zero and $M_{\theta} = 2M_{M2}/a_2 = -2M_{M1}/a_2$.

M_{P2} may be assumed to correspond to the torsion moment in θ plane, $M_{\theta\phi} = 2M_{P2}/a_2$. The torsion moment $M_{\phi\theta}$ has been transformed into transeverse edge shear Q_{ϕ}.

Calculation of stresses by the above suggested formulae is not exact but for small sized elements it provides a good approximation. Large errors are expected in areas where the stress gradients change suddenly. These errors are expected to reduce on reduction of the element size.

(xi) Percentage errors in displacements and stresses are calculated using the following relation based on absolute values of displacements and stresses

$$\% \text{ Error} = \left(\frac{|\text{calculated value}| - |\text{elasticity value}|}{|\text{elasticity value}|}\right)(100)$$

Several shell of revolution problems for which elasticity solutions are known, are solved to demonstrate the suitability of the finite element method employing both statics and energy stiffness matrices of the trapezoid and isosceles triangle elements. Several values of Poisson's ratio ($\mu = 1/3$ for circular plate problem and $\mu = 0.0$ and 0.2 for spherical shell problems) are used. Convergence of the calculated results to the true solution is demonstrated by reducing the element size.

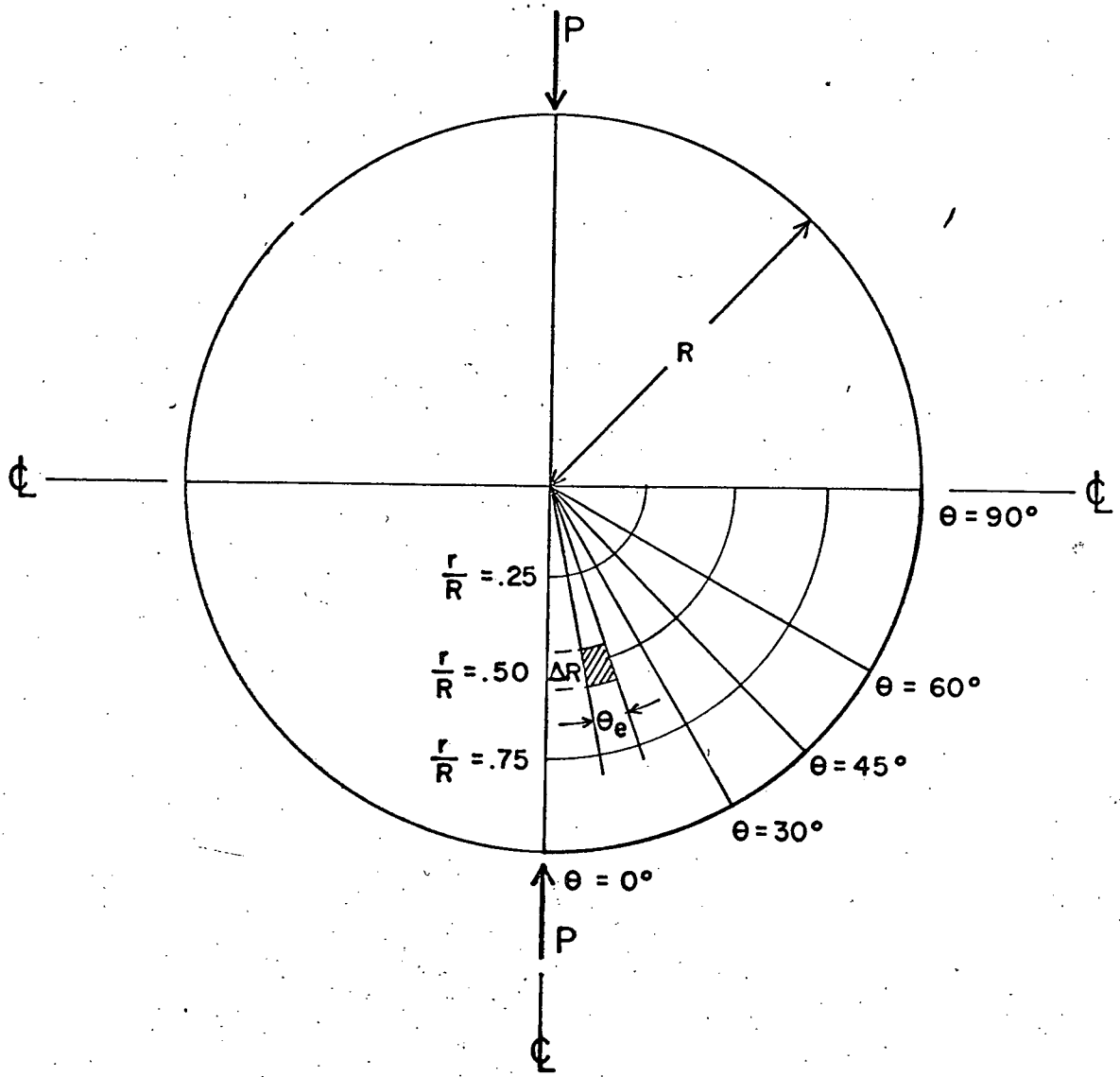

FIGURE V-I-1. CIRCULAR PLATE SUBJECTED TO THE ACTION OF A PAIR OF DIAMETRICALLY OPPOSITE POINT LOADS

5.3 Example-I Circular Plate Subjected to the Action of a Pair of Diametrically Opposite Point Loads. Fig. (V-I-1)

A circular plate may be considered as a shell of revolution having zero curvatures. Here, the generating curve is a straight line, perpendicular to the axis of rotation. The finite element method using equilateral trapezoids and isosceles triangles is well suited for the analysis.

The result of elasticity solution[34] for displacements ($\mu = 1/3$) and stresses (independent of μ) at various sections is shown in Figs. (V-I-2 to 6). The elasticity solution is compared with the finite element solution using Statics and Energy stiffness matrices. Due to the symmetry of the problem about two axes, only one quarter of the plate needs to be analysed. The application of point load produces very steep displacement and stress gradients requiring use of small elements to give a reasonable representation of displacement and stress distribution in the vicinity of the load.

The convergence trends are obtained by reducing the element size which is defined by θ_e and ΔR. Here, θ_e is the angle between two adjacent meridian lines and ΔR is the difference of radii of the two parallel circles enclosing the element. The percentage errors are calculated at various points and are shown in Tables (V-I-1 to 5).

Greater error in calculation of stresses than in displacements is noted. Calculation of stress by evenly distributing the nodal force on the appropriate cross section is reasonable where stress-gradients are small. At points where the absolute value of the function is small compared to its maximum value elsewhere, higher percentage error is noted. Such points may be disregarded as they are of little significance.

Stresses produced in the plate by a concentrated force are infinite at the point of application of the force according to the theory of elasticity. The finite element solution results in finite value of stresses. Thus, it is not realistic to expect the finite element results to agree with the elasticity at the point of application of the concentrated force. Also, due to the presence of high displacement and stress gradients in the vicinity of the concentrated force, large errors in the finite element solution near the load are inevitable.

Reduction of the size of elements improves the precision of the results in the neighbourhood of the load. Coarser mesh may be used away from the load with no ill effects on precision.

The results presented in Tables (V-I-1 to 5) reveal that for θ_e = 7.5°, ΔR = 0.0625 R element size and μ= 1/3, the finite element solution differs from the elasticity solution in displacements by 2% and in stresses by 4%. The error analysis clearly shows the rapid convergence of displacements and stresses to their elasticity values[34] on reduction of the element size.

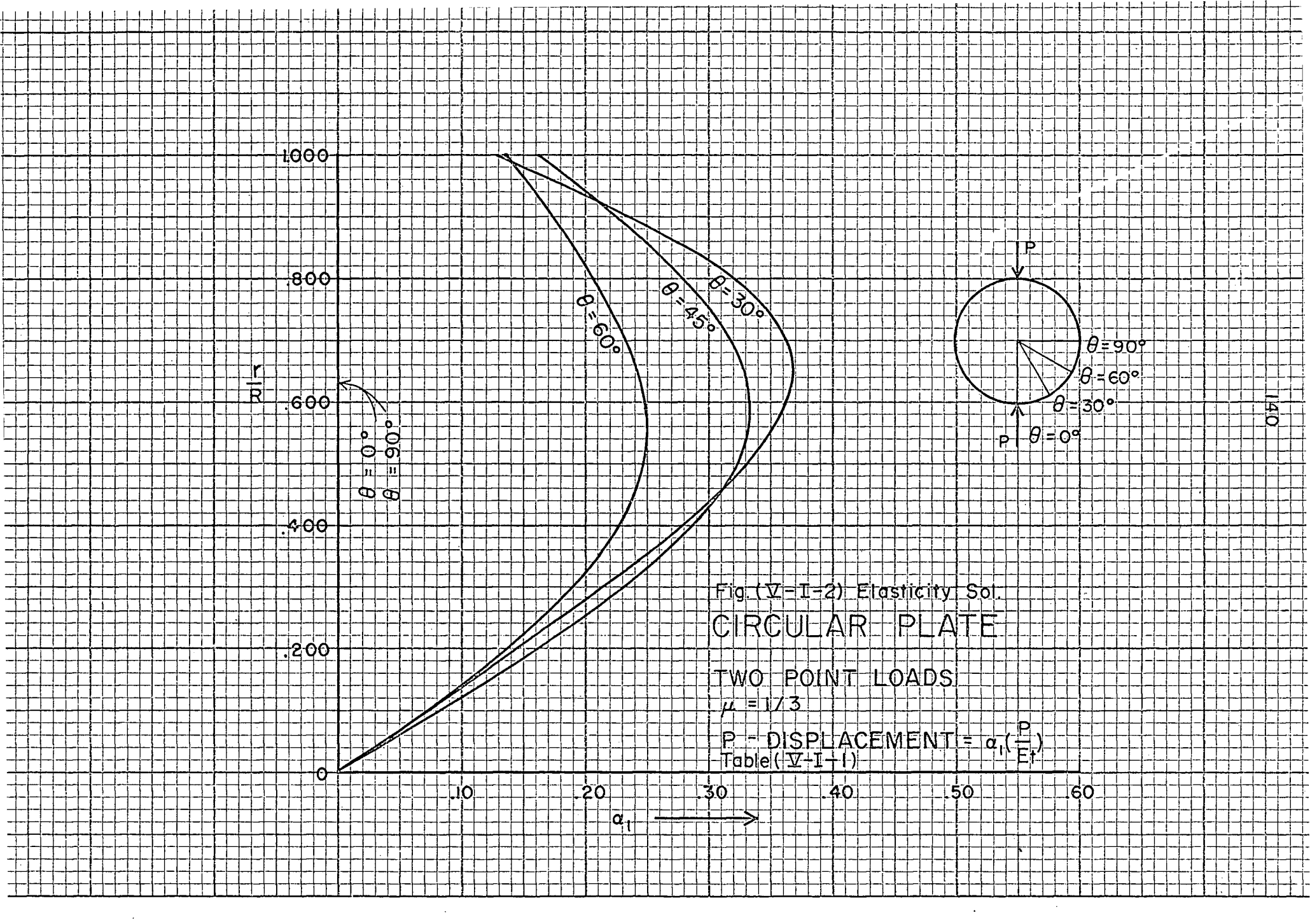

Fig. (V-I-2) Elasticity Sol.

CIRCULAR PLATE

TWO POINT LOADS

$\mu = 1/3$

P - DISPLACEMENT = $\alpha_1 \left(\frac{P}{Et}\right)$

Table (V-I-1)

Table (V-I-1) Circular Plate - Two Point Loads

P-Displacement = α_1 (P/Et) Fig. (V-I-2)

Poisson's Ratio = 1/3

At θ;r/R	Elasticity Solution α_1	Percentage Error — Statics Matrix θe=15° ΔR=.125R	Statics Matrix θe=10° ΔR=.0833R	Statics Matrix θe=7.5° ΔR=0.0625R	Energy Matrix θe=15° ΔR=.125R	Energy Matrix θe=10° ΔR=.0833R	Energy Matrix θe=7.5° ΔR=.0625R
.25	.1813	0.66	0.33	0.22	- 0.72	-0.28	-0.11
.50	.3332	2.49	1.14	0.66	0.93	0.45	0.30
30° .75	.3480	6.23	1.06	0.29	4.71	0.60	0.03
1.00	.1305	21.23	-10.50	-0.08	13.10	-8.05	-0.23
.25	.2007	1.44		0.40	0.05		0.05
.50	.3250	2.37		0.52	1.02		0.22
45° .75	.3010	- 5.12		-0.40	- 5.32		-0.60
1.00	.1611	-10.55		-0.99	- 8.26		-0.99
.25	.1671	1.91	0.84	0.47	0.48	0.24	0.18
.50	.2476	1.33	0.52	0.28	0.12	-0.04	0.00
60° .75	.2203	- 1.18	-1.04	-0.50	- 2.09	-1.36	-0.68
1.0	.1362	- 1.17	-1.32	-0.81	- 2.28	-1.54	-0.88

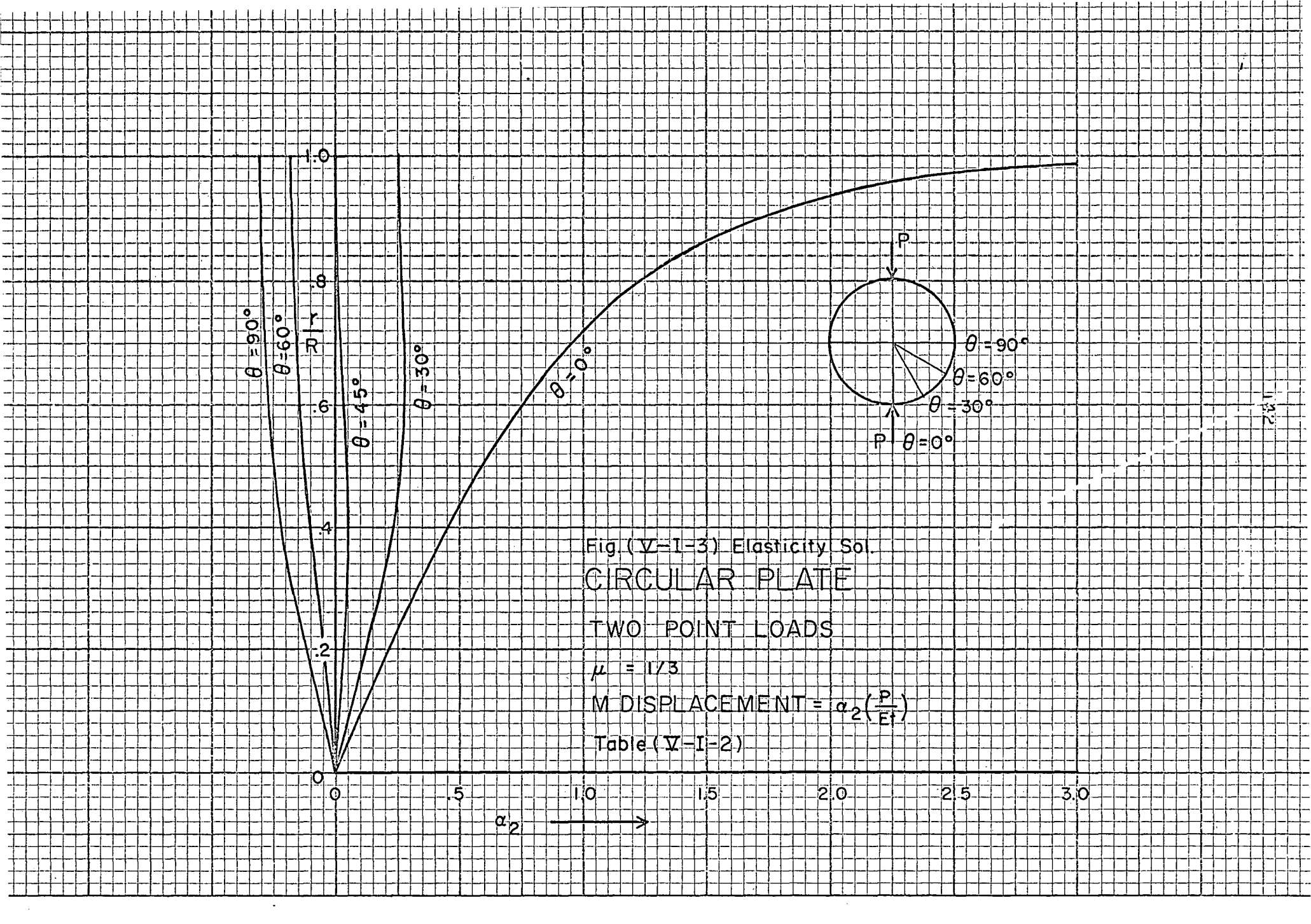

Fig. (V-I-3) Elasticity Sol.

CIRCULAR PLATE

TWO POINT LOADS

$\mu = 1/3$

M DISPLACEMENT = $\alpha_2\left(\frac{P}{Et}\right)$

Table (V-I-2)

Table (V-I-2) Circular Plate - Two Point Loads

M-Displacement = α_2 (P/Et) Fig. (V-I-3)

Poisson's Ratio = 1/3

			Percentage Error					
			Statics Matrix			Energy Matrix		
θ	At r/R	Elasticity Solution α_2	θe=15° ΔR=.125R	θe=10° ΔR=.0833R	θe=7.5° ΔR=.0625R	θe=15° ΔR=.125R	θe=10° ΔR=.0833R	θe=7.5° ΔR=.0625R
0°	.25	.2721	-0.44	-0.18	- 0.07	- 1.58	-0.70	- 0.37
	.50	.5933	1.15	0.49	0.27	0.79	0.30	0.19
	.75	1.0797	2.94	1.69	0.93	2.18	1.31	0.72
	1.00	--						
30°	.25	.1533	1.37	0.59	0.33	0.52	0.20	0.13
	.50	.2635	2.20	0.91	0.49	1.86	0.80	0.46
	.75	.2791	-5.34	-2.72	- 1.47	- 5.37	-2.72	- 1.47
	1.00	.2561	-9.88	-2.22	- 2.05	- 5.27	-2.62	- 2.03
45°	.25	.0445	5.17		1.12	5.62		1.35
	.50	.0463	-2.81		- 0.86	- 1.73		- 0.65
	.75	.0123	-98.50		-18.70	-84.5		-14.63
	1.00	-.0042	93.0		59.0	93.0		33.4
60°	.25	-.0558	-1.79	-0.72	- 0.36	- 4.84	-2.15	- 1.08
	.50	-.1169	2.91	1.20	0.68	1.20	0.43	0.26
	.75	-.1608	1.80	1.18	0.62	- 0.44	0.19	0.12
	1.00	-.1731	3.58	1.16	0.58	- 0.12	-0.17	0.12
90°	.25	-.1488	0.47	0.13	0.07	- 1.68	-0.87	- 0.34
	.50	-.2489	0.68	0.32	0.16	- 0.72	-0.32	- 0.16
	.75	-.2935	0.07	0.07	0.03	- 1.57	-0.68	- 0.34
	1.00	-.3033	0.33	0.06	0.03	- 1.68	-0.79	- 0.43

Fig. (V-I-4) Elasticity Sol.

CIRCULAR PLATE

TWO POINT-LOADS

$\mu = 1/3$

P STRESS $(N_\theta) = \alpha_3 \left(\frac{P}{R}\right)$

Table (V-I-3.)

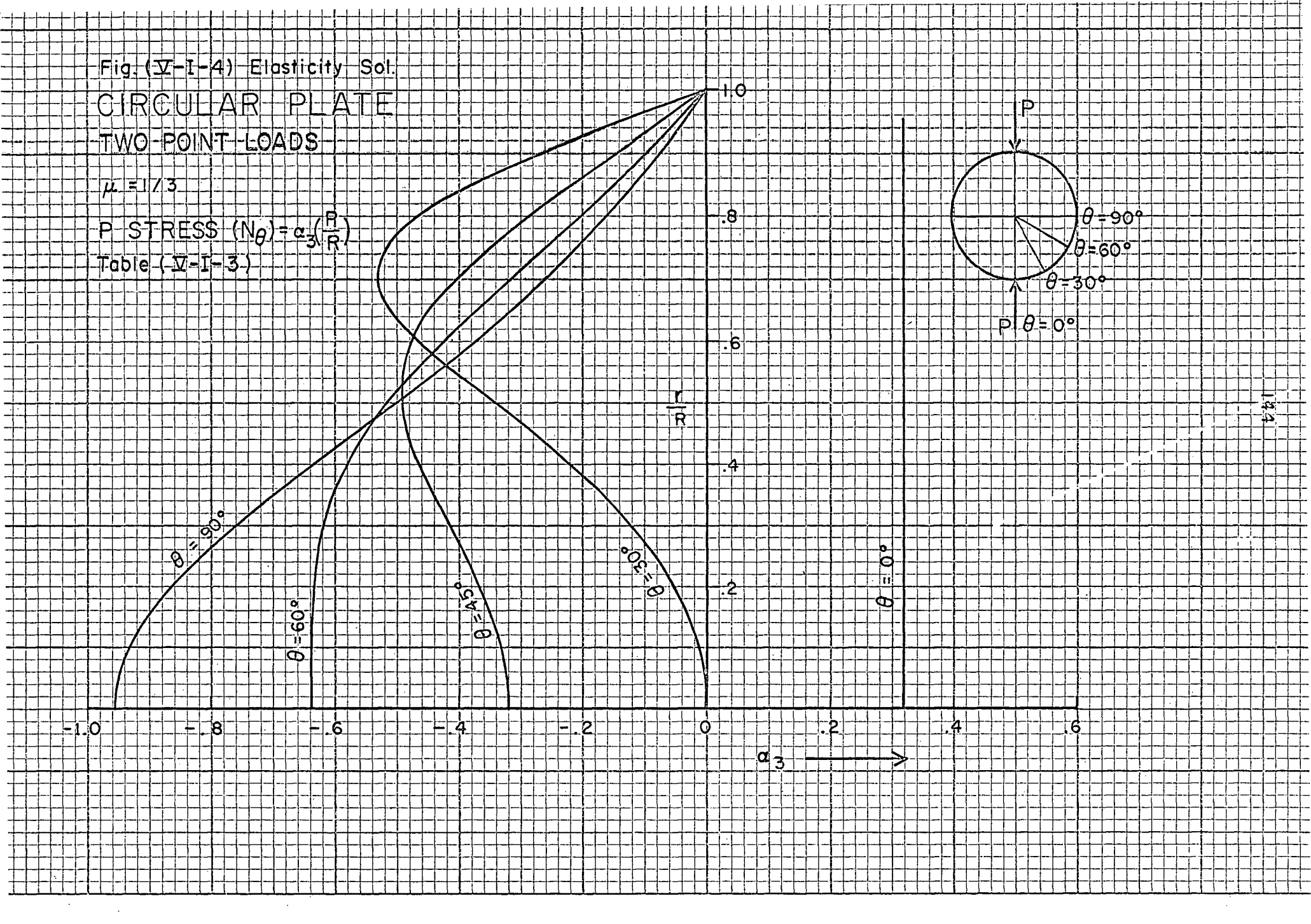

Table (V-I-3) Circular Plate - Two Point Loads

P-Force/Length, $(N_\theta) = \alpha_3(P/R)$ Fig. (V-I-4)

At θ ; r/R	Elasticity Solution α_3	Percentage Error: Statics Matrix Δθ=15° ΔR=1.25R	Statics Matrix Δθ=10° ΔR=.0833R	Statics Matrix Δθ=7.5° ΔR=.0625R	Energy Matrix Δθ=15° ΔR=.125R	Energy Matrix Δθ=10° ΔR=.0833R	Energy Matrix Δθ=7.5° ΔR=.0625R
.25	.3183	1.51	1.22	0.69	0.16	1.04	0.60
0° .50	.3183	8.58	3.23	1.70	7.79	2.80	1.45
.75	.3183	26.86	19.76	16.18	28.68	20.58	16.24
.25	-.0829	- 3.02	- 2.05	- 1.21	- 4.22	- 3.26	- 1.81
30° .50	-.3447	4.12	2.41	1.45	2.23	1.59	0.99
.75	-.5174	22.24	4.93	1.12	19.87	4.56	0.93
.25	-.3899	0.62		0.00	- 0.62		0.00
45° .50	-.4923	4.87		1.06	3.60		0.77
.75	-.3461	-23.98		- 1.73	-21.76		- 1.76
.25	-.6264	0.59	0.45	0.25	- 0.70	0.08	0.05
60° .50	-.5132	0.74	0.15	0.08	- 0.23	- 0.23	- 0.16
.75	-.2565	- 2.61	- 4.01	- 1.87	- 3.08	- 3.82	- 1.87
.25	-.8095	- 0.02	0.22	0.13	- 1.46	- 0.16	- 0.07
90° .50	-.4966	- 1.95	- 0.86	- 0.48	- 2.90	- 1.27	- 0.72
.75	-.2032	- 5.46	- 2.66	- 1.52	- 5.12	- 2.51	- 1.48

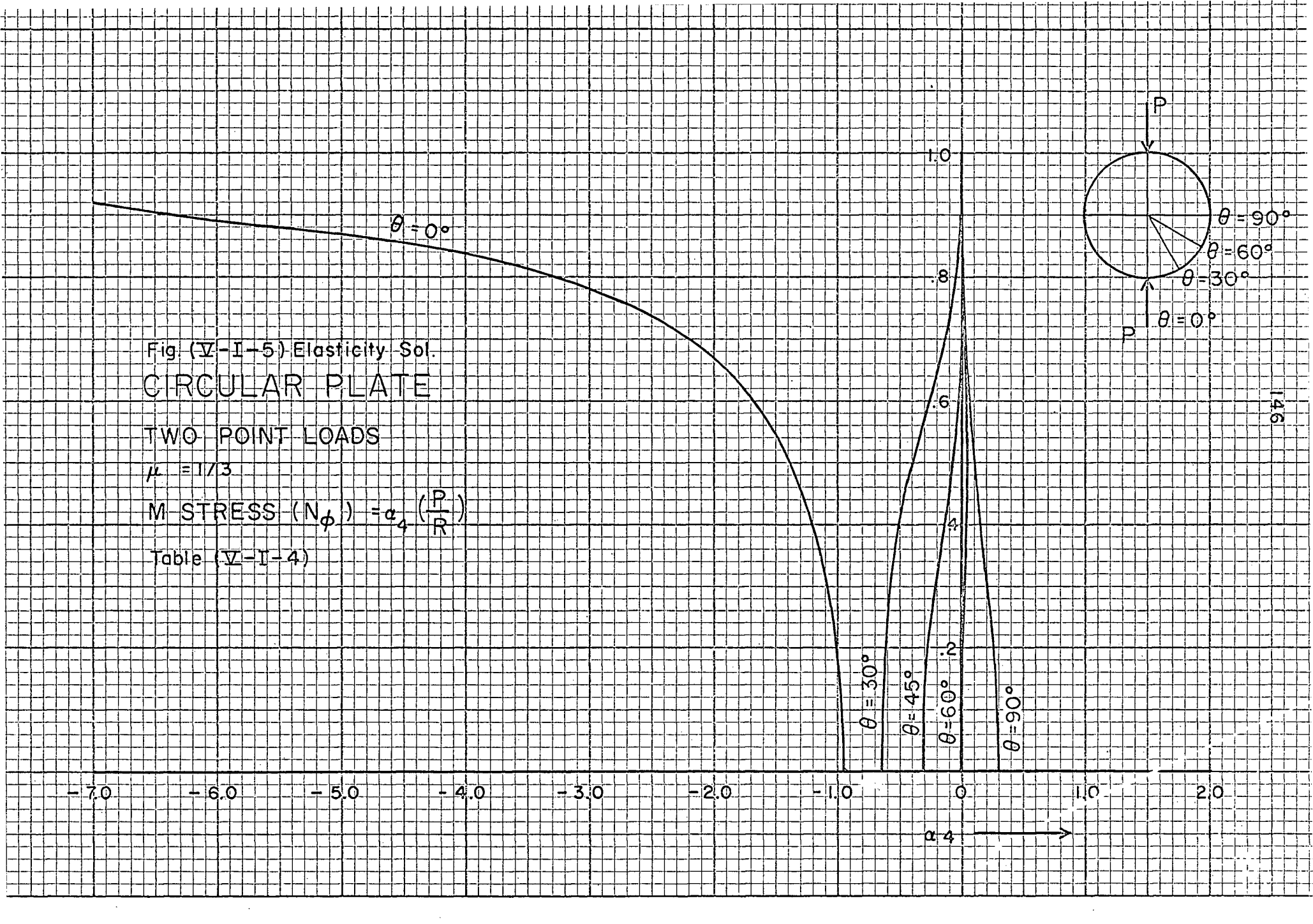
P
θ = 90°
θ = 60°
θ = 30°
θ = 0°
P
1.0
.8
.6
.4
.2
θ = 30°
θ = 45°
θ = 60°
θ = 90°
- 7.0
- 6.0
- 5.0
- 4.0
- 3.0
- 2.0
- 1.0
0
1.0
2.0
α 4
θ = 0°
Fig. (V-I-5) Elasticity Sol.
CIRCULAR PLATE
TWO POINT LOADS
μ = 1/3
M STRESS (N_ϕ) = $\alpha_4 \left(\frac{P}{R}\right)$
Table (V-I-4)

Table (V-I-4) Circular Plate - Two Point Loads

M-Force/Length, $(N_\phi) = \alpha_4(P/R)$ Fig. (V-I-5)

At θ ; r/R	Elasticity Solution α_4	Percentage Error: Statics Matrix Δθ=15° ΔR=.125R	Statics Matrix Δθ=10° ΔR=.0833R	Statics Matrix Δθ=7.5° ΔR=.0625R	Energy Matrix Δθ=15° ΔR=.125R	Energy Matrix Δθ=10° ΔR=.0833R	Energy Matrix Δθ=7.5° ΔR=.0625R
.25	-1.0398	- 2.86	- 1.43	- 0.85	- 3.05	- 1.62	- 0.97
0° .50	-1.3793	- 6.02	- 3.21	- 1.95	- 5.94	- 3.23	- 1.97
.75	-2.5920	-19.79	-11.60	- 7.85	-20.08	-11.89	- 8.07
.25	- .5907	4.28	2.10	1.22	4.72	2.34	1.34
30° .50	- .3899	14.21	6.33	3.46	15.72	7.10	3.87
.75	- .0599	35.56	47.91	26.04	18.53	42.40	23.87
.25	- .2418	11.37		2.85	12.90		3.31
45° .50	- .0684	8.50		- 0.14	13.83		1.01
.75	.0155			13.55			14.19
.25	.0317	-12.93	- 3.78	- 1.89	-16.40	- 5.99	- 2.84
60° .50	.0585	22.39	8.89	4.79	22.56	9.23	4.96
.75	.0249	-28.51	6.42	1.61	-20.08	8.03	2.41
.25	.2478	10.77	4.80	2.70	12.63	5.57	3.11
90° .50	.1146	6.54	3.23	1.74	9.24	4.36	2.44
.75	.0250	- 4.80	- 0.40	- 0.40	1.20	2.00	1.20

Fig. (V-I-6) Elasticity Sol.

CIRCULAR PLATE

TWO POINT LOADS

$\mu = 1/3$

SHEAR STRESS $(N_{\theta\phi}) = \alpha_5 \left(\frac{P}{R}\right)$

Table (V-I-5)

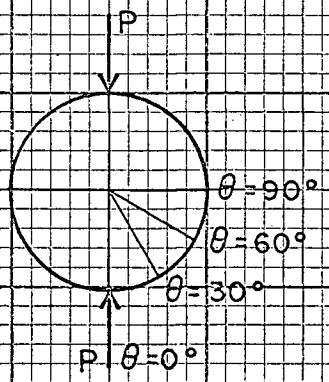

Table (V-I-5) Circular Plate - Two Point Loads

Shear Force/Length, $(N_{\theta\phi}) = \alpha_5(P/R)$ Fig. (V-I-6)

Percentage Error

At θ ; r/R	Elasticity Solution α_5	Statics Matrix Δθ=15° ΔR=.125R	Statics Matrix Δθ=10° ΔR=.0833R	Statics Matrix Δθ=7.5° ΔR=.0625R	Energy Matrix Δθ= 15° ΔR=.125R	Energy Matrix Δθ=10° ΔR=.0833R	Energy Matrix Δθ=7.5° ΔR=.0625R
.25	.5809	- 1.98	- 0.91	- 0.50	- 5.15	- 2.39	- 1.31
30° .50	.5872	3.03	1.62	0.90	0.29	0.48	0.34
.75	.2901	23.34	0.72	- 1.55	23.72	1.58	- 1.21
.25	.5899	- 0.64		- 0.19	- 3.64		- 0.92
45° .50	.3965	3.35		0.60	1.56		0.20
.75	.1099	-50.86		- 2.91	-48.13		- 2.27
.25	.4527	- 0.04	- 0.22	- 0.13	- 2.83	- 1.48	- 0.82
60° .50	.2250	- 1.07	- 0.71	- 0.40	- 2.18	- 1.15	- 0.62
.75	.0467	8.35	- 8.99	- 3.43	12.63	- 8.35	- 2.78

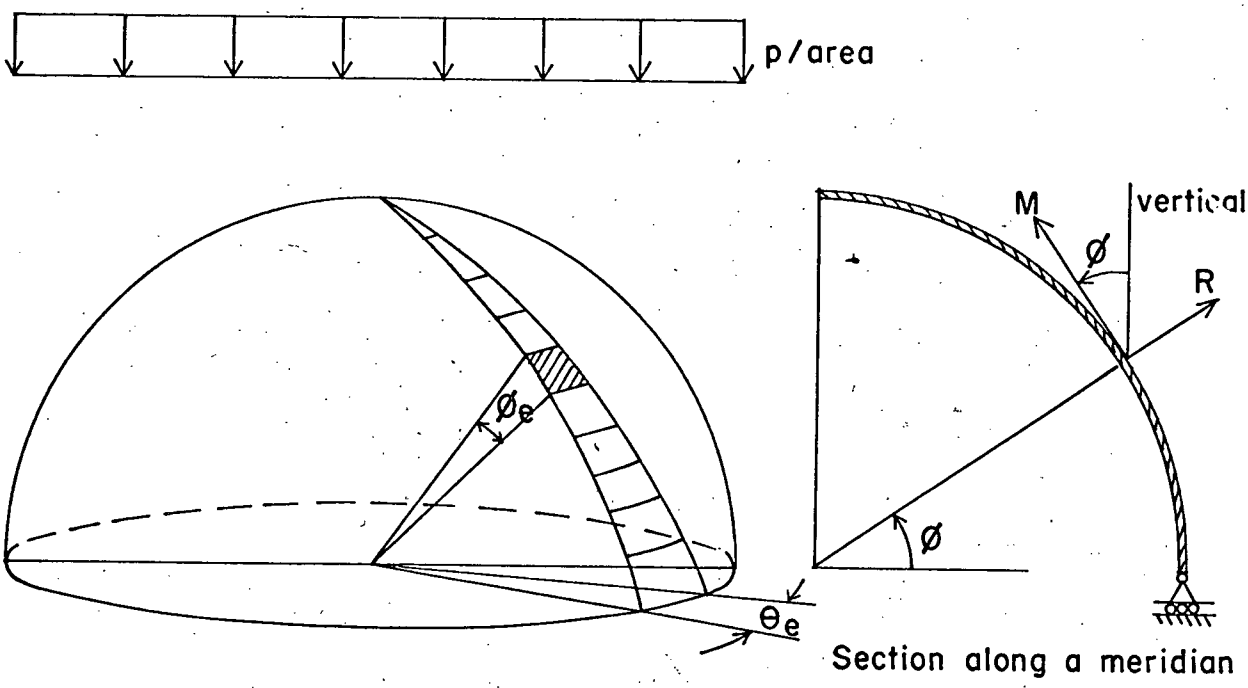

FIGURE V-II-1. HEMISPHERICAL DOME SUBJECTED TO SNOW LOAD

5.4 Example II - Hemispherical Dome Under Snow Load Uniformly Distributed over the Horizontal Projected Area. Fig. (V-II-1)

In this problem, the dome is loaded and supported axisymmetrically. At the base, the dome is free to deflect in the radial directions. The elasticity solution based on the membrane theory[35,36] is obtained for displacements (μ = 0.0 and 0.2) and stresses (independent of μ) and is shown graphically in Figs. (V-II-3 to 6).

In view of the axisymmetry of the boundary and loading conditions of the shell, it is sufficient in the finite element analysis to consider elements bounded by a pair of adjacent meridian lines. The snow load on the horizontal projected area of a shell element is apportioned to the corners according to the laws of statics, Fig. (V-II-2). The vertical load at each node is finally resolved into M and R directions.

Percentage errors in the F.E. solution employing Statics and Energy matrices and using two values of Poisson's ratio (μ = 0.0 and 0.2) are shown in Tables (V-II-1 to 6). For $\theta_e = \phi_e = 2.5°$ element size, excellent accuracy in the calculation of displacements and stresses (error less than a fraction of 1%) is obtained. Higher percentage errors in displacements (3% from Statics matrix and 8% from Energy matrix) and stresses (5% from Statics matrix and 6% from Energy matrix) are noted at the nodes of the triangle element. These errors are attributed to the behaviour of the F.E. model as a cone rather than as a smooth spherical surface at the apex. Rapid convergence of the F.E. results to the elasticity solution is clearly seen on reducing the element size.

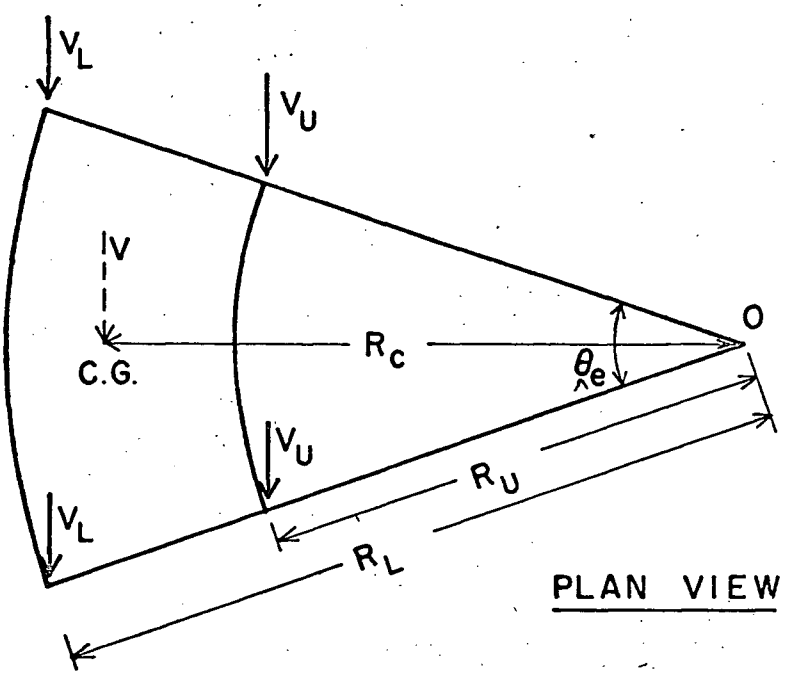

Total vertical load on the element, $V = \frac{1}{2}\theta_e (R_L^2 - R_U^2) p$

For small angle θ_e, distance of C.G. of the load from O,

$$R_c = \frac{2}{3}\left\{\frac{R_L^2 + R_L R_U + R_U^2}{R_L + R_U}\right\}$$

From Statics: $2V_U + 2V_L = V$

and $2V_U \cdot R_U + 2V_L \cdot R_L = V R_C$

Here, V_L and V_U are nodal components of the vertical load on the element

Solving for V_U and V_L

$$V_U = V(R_L - R_C)/2(R_L - R_U)$$

and $$V_L = V(R_C - R_U)/2(R_L - R_U)$$

FIG. (Ⅴ-Ⅱ-2) HEMISPHERICAL DOME SUBJECTED TO SNOW LOAD. CALCULATION OF NODAL LOADS.

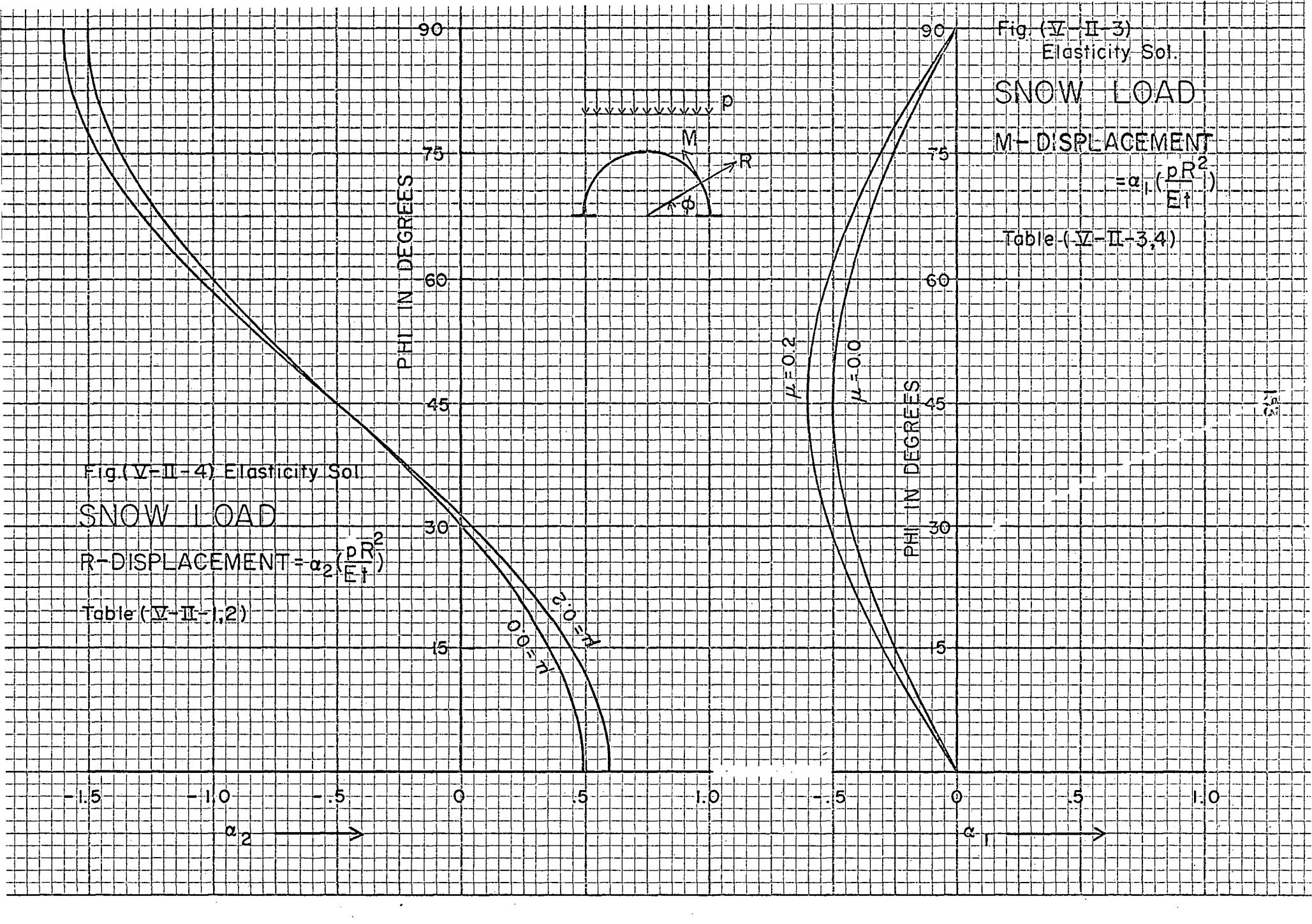

Fig. (V-II-3)
Elasticity Sol.

SNOW LOAD

M-DISPLACEMENT $= \alpha_1 \left(\frac{pR^2}{Et}\right)$

Table (V-II-3,4)

Fig. (V-II-4) Elasticity Sol.

SNOW LOAD

R-DISPLACEMENT $= \alpha_2 \left(\frac{pR^2}{Et}\right)$

Table (V-II-1,2)

Table (V-II-1) Hemispherical Dome - Snow Load

M-Displacement = $\alpha_1(pR^2/Et)$ Fig. (V-II-3)

Poisson's Ratio = 0.0

	ϕ	Elasticity Solution α_1	Percentage Error $\theta_e = \phi_e = 5°$ Statics Matrix	$\theta_e = \phi_e = 5°$ Energy Matrix	$\theta_e = \phi_e = 2.5°$ Statics Matrix	$\theta_e = \phi_e = 2.5°$ Energy Matrix
Base	0.0	0.00000	0.00	0.00	0.00	0.00
	2.5	-0.04358			-0.07	-0.04
	5.0	-0.08682	-0.24	-0.16	-0.06	-0.04
	7.5	-0.12941			-0.06	-0.04
	10.0	-0.17101	-0.24	-0.16	-0.06	-0.04
	12.5	-0.21131			-0.06	-0.04
	15.0	-0.25000	-0.25	-0.17	-0.06	-0.04
	17.5	-0.28679			-0.06	-0.04
	20.0	-0.32139	-0.26	-0.18	-0.06	-0.05
	22.5	-0.35355			-0.06	-0.05
	25.0	-0.38302	-0.27	-0.19	-0.07	-0.05
	27.5	-0.40958			-0.07	-0.05
	30.0	-0.43301	-0.28	-0.20	-0.07	-0.05
	32.5	-0.45315			-0.07	-0.05
	35.0	-0.46985	-0.30	-0.22	-0.08	-0.05
	37.5	-0.48296			-0.08	-0.06
	40.0	-0.49240	-0.32	-0.23	-0.08	-0.06
	42.5	-0.49810			-0.08	-0.06
	45.0	-0.50000	-0.33	-0.25	-0.08	-0.06
	47.5	-0.49810			-0.09	-0.07
	50.0	-0.49240	-0.35	-0.28	-0.09	-0.07
	52.5	-0.48296			-0.09	-0.07
	55.0	-0.46985	-0.37	-0.30	-0.09	-0.07
	57.5	-0.45315			-0.09	-0.08
	60.0	-0.43301	-0.38	-0.32	-0.09	-0.08
	62.5	-0.40958			-0.10	-0.08
	65.0	-0.38302	-0.38	-0.34	-0.09	-0.08
	67.5	-0.35355			-0.09	-0.08
	70.0	-0.32139	-0.36	-0.33	-0.09	-0.08
	72.5	-0.28679			-0.08	-0.07
	75.0	-0.25000	-0.26	-0.24	-0.06	-0.06
	77.5	-0.21131			-0.02	-0.03
	80.0	-0.17101	+0.22	-0.04	+0.05	+0.04
	82.5	-0.12941			0.22	0.22
	85.0	-0.08682	+2.00	+3.00	0.79	0.63
	87.5	-0.04358			1.82	2.89
Apex	90.0	0.00000	0.00	0.00	0.00	0.00

Table (V-II-2) Hemispherical Dome - Snow Load

M-Displacement = $\alpha_1(pR^2/Et)$ Fig. (V-II-3)

Poisson's Ratio = 0.2

	ϕ	Elasticity Solution α_1	Percentage Error $\theta_e = \phi_e = 5°$ Statics Matrix	$\theta_e = \phi_e = 5°$ Energy Matrix	$\theta_e = \phi_e = 2.5°$ Statics Matrix	$\theta_e = \phi_e = 2.5°$ Energy Matrix
Base	0.0	0.00000	0.00	0.00	0.00	0.00
	2.5	-0.05229			-0.06	-0.04
	5.0	-0.10419	-0.24	-0.17	-0.06	-0.04
	7.5	-0.15529			-0.06	-0.04
	10.0	-0.20521	-0.25	-0.17	-0.06	-0.04
	12.5	-0.25357			-0.06	-0.04
	15.0	-0.30000	-0.25	-0.18	-0.06	-0.05
	17.5	-0.34415			-0.07	-0.05
	20.0	-0.38567	-0.26	-0.19	-0.06	-0.05
	22.5	-0.42426			-0.06	-0.05
	25.0	-0.45963	-0.27	-0.20	-0.07	-0.05
	27.5	-0.49149			-0.07	-0.05
	30.0	-0.51962	-0.28	-0.21	-0.07	-0.05
	32.5	-0.54379			-0.07	-0.05
	35.0	-0.56382	-0.29	-0.22	-0.07	-0.06
	37.5	-0.57956			-0.08	-0.06
	40.0	-0.59089	-0.31	-0.24	-0.08	-0.06
	42.5	-0.59772			-0.08	-0.06
	45.0	-0.60000	-0.32	-0.26	-0.08	-0.07
	47.5	-0.59772			-0.08	-0.07
	50.0	-0.59089	-0.34	-0.29	-0.09	-0.07
	52.5	-0.57956			-0.09	-0.08
	55.0	-0.56382	-0.35	-0.31	-0.09	-0.08
	57.5	-0.54379			-0.09	-0.08
	60.0	-0.51962	-0.36	-0.33	-0.09	-0.08
	62.5	-0.49149			-0.09	-0.09
	65.0	-0.45963	-0.36	-0.35	-0.09	-0.09
	67.5	-0.42426			-0.09	-0.09
	70.0	-0.38567	-0.33	-0.35	-0.08	-0.09
	72.5	-0.34415			-0.07	-0.08
	75.0	-0.30000	-0.22	-0.25	-0.05	-0.06
	77.5	-0.25357			-0.01	-0.03
	80.0	-0.20521	+0.27	+0.01	+0.07	+0.03
	82.5	-0.15529			0.23	0.22
	85.0	-0.10419	2.12	3.14	0.81	0.61
	87.5	-0.05229			1.91	3.05
Apex	90.0	0.00000	0.00	0.00	0.00	0.00

Table (V-II-3) Hemispherical Dome - Snow Load

R-Displacement = $\alpha_2(pR^2/Et)$ Fig. (V-II-4)

Poisson's Ratio = 0.0

	ϕ	Elasticity Solution α_2	Percentage Error $\theta_e = \phi_e = 5°$ Statics Matrix	$\theta_e = \phi_e = 5°$ Energy Matrix	$\theta_e = \phi_e = 2.5°$ Statics Matrix	$\theta_e = \phi_e = 2.5°$ Energy Matrix
Base	0.0	0.50000	0.09	0.25	0.02	0.06
	2.5	0.49620			0.02	0.06
	5.0	0.48481	0.10	0.26	0.02	0.07
	7.5	0.46593			0.02	0.07
	10.0	0.43969	0.11	0.27	0.03	0.07
	12.5	0.40631			0.03	0.07
	15.0	0.36603	0.13	0.29	0.03	0.07
	17.5	0.31915			0.04	0.08
	20.0	0.26605	0.18	0.35	0.04	0.09
	22.5	0.20711			0.05	0.10
	25.0	0.14279	0.34	0.53	0.08	0.13
	27.5	0.07358			0.16	0.23
	30.0	0.00000	--	--	--	--
	32.5	-0.07738			-0.17	-0.16
	35.0	-0.15798	-0.36	-0.26	-0.09	-0.07
	37.5	-0.24118			-0.06	-0.03
	40.0	-0.32635	-0.20	-0.08	-0.05	-0.02
	42.5	-0.41284			-0.04	-0.01
	45.0	-0.50000	-0.16	-0.03	-0.04	-0.01
	47.5	-0.58716			-0.04	-0.01
	50.0	-0.67365	-0.14	-0.02	-0.04	-0.01
	52.5	-0.75882			-0.04	-0.00
	55.0	-0.84202	-0.15	-0.02	-0.04	-0.01
	57.5	-0.92262			-0.04	-0.01
	60.0	-1.00000	-0.16	-0.04	-0.04	-0.01
	62.5	-1.07358			-0.04	-0.01
	65.0	-1.14279	-0.18	-0.07	-0.05	-0.02
	67.5	-1.20711			-0.05	-0.02
	70.0	-1.26604	-0.23	-0.09	-0.05	-0.03
	72.5	-1.31915			-0.06	-0.04
	75.0	-1.36603	-0.19	-0.25	-0.07	-0.04
	77.5	-1.40631			-0.07	-0.06
	80.0	-1.43969	-0.54	+0.08	-0.09	-0.05
	82.5	-1.46593			-0.04	-0.16
	85.0	-1.48481	+0.87	-1.53	-0.30	+0.25
	87.5	-1.49620			+1.11	-1.29
Apex	90.0	-1.50000	+1.68	+5.37	+1.67	+5.38

Table (V-II-4) Hemispherical Dome - Snow Load

R-Displacement = $\alpha_2(pR^2/Et)$ Fig. (V-II-4)

Poisson's Ratio = 0.2

	ϕ	Elasticity Solution α_2	Percentage Error $\theta_e = \phi_e = 5°$ Statics Matrix	$\theta_e = \phi_e = 5°$ Energy Matrix	$\theta_e = \phi_e = 2.5°$ Statics Matrix	$\theta_e = \phi_e = 2.5°$ Energy Matrix
Base	0.0	0.60000	0.04	0.17	0.01	0.04
	2.5	0.59581			0.01	0.04
	5.0	0.58329	0.04	0.17	0.01	0.04
	7.5	0.56252			0.01	0.04
	10.0	0.53366	0.05	0.18	0.01	0.04
	12.5	0.49694			0.01	0.04
	15.0	0.45263	0.06	0.19	0.02	0.05
	17.5	0.40107			0.02	0.05
	20.0	0.34265	0.09	0.21	0.02	0.05
	22.5	0.27782			0.03	0.06
	25.0	0.20707	0.17	0.28	0.04	0.07
	27.5	0.13093			0.08	0.10
	30.0	0.05000	+0.84	+0.89	0.20	0.22
	32.5	-0.03512			-0.34	-0.27
	35.0	-0.12378	-0.42	-0.26	-0.11	-0.06
	37.5	-0.21530			-0.07	-0.03
	40.0	-0.30899	-0.21	-0.08	-0.06	-0.02
	42.5	-0.40413			-0.05	-0.01
	45.0	-0.50000	-0.17	-0.04	-0.04	-0.01
	47.5	-0.59587			-0.04	-0.01
	50.0	-0.69101	-0.16	-0.04	-0.04	-0.01
	52.5	-0.78470			-0.04	-0.01
	55.0	-0.87622	-0.16	-0.05	-0.04	-0.01
	57.5	-0.96488			-0.04	-0.02
	60.0	-1.05000	-0.18	-0.07	-0.05	-0.02
	62.5	-1.13093			-0.05	-0.02
	65.0	-1.20707	-0.20	-0.12	-0.05	-0.03
	67.5	-1.27782			-0.05	-0.04
	70.0	-1.34265	-0.25	-0.14	-0.06	-0.04
	72.5	-1.40107			-0.06	-0.05
	75.0	-1.45263	-0.22	-0.33	-0.07	-0.06
	77.5	-1.49694			-0.08	-0.08
	80.0	-1.53366	-0.54	+0.04	-0.10	-0.07
	82.5	-1.56252			-0.05	-0.19
	85.0	-1.58329	+0.74	-1.67	-0.29	+0.26
	87.5	-1.59581			+1.00	-1.35
Apex	90.0	-1.60000	+2.82	+7.96	2.80	+7.90

Fig.(Ⅴ-Ⅱ-5) Elasticity Sol.

SNOW LOAD

P-STRESS $(N_\theta) = \alpha_3 \left(\frac{pR}{2}\right)$

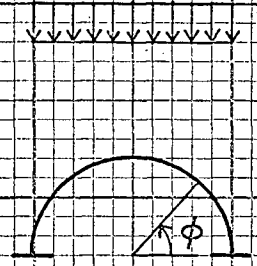

PHI IN DEGREES

90 75 60 45 30 15

-1.0 -.5 0 .5 1.0

α_3

Fig.(Ⅴ-Ⅱ-6) Elasticity Sol.

SNOW LOAD

M STRESS $(N_\phi) = \alpha_4 \left(\frac{pR}{2}\right)$

Table (Ⅴ-Ⅱ-6)

PHI IN DEGREES

90 75 60 45 30 15

-1.0 -.5 0 .5

α_4

Table (V-II-5) Hemispherical Dome - Snow Load

P-Force/Length, $(N_\theta) = \alpha_3(pR/2)$ Fig. (V-II-5)

Percentage Error

ϕ	Elasticity Solution α_3	$\mu = 0.0$ $\theta e = \phi e = 5°$ Statics Matrix	Energy Matrix	$\theta_e = \phi_e = 2.5°$ Statics Matrix	Energy Matrix	$\mu = 0.2$ $\theta_e = \phi_e = 5°$ Statics Matrix	Energy Matrix	$\theta_e = \phi_e = 2.5°$ Statics Matrix	Energy Matrix
0.0	1.0000	-0.48	-0.48	-0.12	-0.12	-0.48	-0.48	-0.12	-0.12
2.5	0.9962			-0.12	-0.12			-0.12	-0.12
5.0	0.9848	-0.48	-0.48	-0.12	-0.12	-0.47	-0.48	-0.12	-0.12
7.5	0.9659			-0.12	-0.12			-0.12	-0.12
10.0	0.9397	-0.47	-0.47	-0.12	-0.12	-0.47	-0.47	-0.12	-0.12
12.5	0.9063			-0.12	-0.12			-0.12	-0.12
15.0	0.8660	-0.46	-0.46	-0.12	-0.12	-0.46	-0.46	-0.12	-0.12
17.5	0.8192			-0.11	-0.11			-0.11	-0.11
20.0	0.7660	-0.45	-0.45	-0.11	-0.11	-0.45	-0.45	-0.11	-0.11
22.5	0.7071			-0.11	-0.11			-0.11	-0.11
25.0	0.6428	-0.42	-0.42	-0.11	-0.11	-0.42	-0.42	-0.11	-0.11
27.5	0.5736			-0.10	-0.10			-0.10	-0.10
30.0	0.5000	-0.37	-0.37	-0.09	-0.09	-0.37	-0.37	-0.10	-0.10
32.5	0.4226			-0.09	-0.09			-0.09	-0.09
35.0	0.3420	-0.27	-0.27	-0.07	-0.07	-0.27	-0.27	-0.07	-0.07
37.5	0.2588			-0.04	-0.04			-0.04	-0.04
40.0	0.1736	+0.07	+0.07	+0.02	+0.02	+0.07	+0.07	+0.02	+0.02
42.5	0.0872			+0.18	+0.18			+0.18	+0.18
45.0	0.0000	--	--	--	--	--	--	--	--
47.5	-0.0872			-0.53	-0.53			-0.53	-0.53
50.0	-0.1736	-1.41	-1.41	-0.36	-0.36	-1.41	-1.41	-0.35	-0.35
52.5	-0.2588			-0.30	-0.30			-0.30	-0.30
55.0	-0.3420	-1.09	-1.09	-0.27	-0.27	-1.09	-1.09	-0.27	-0.27
57.5	-0.4226			-0.27	-0.27			-0.27	-0.27
60.0	-0.5000	-1.04	-1.04	-0.26	-0.26	-1.04	-1.04	-0.26	-0.26
62.5	-0.5736			-0.27	-0.27			-0.27	-0.27
65.0	-0.6428	-1.08	-1.08	-0.27	-0.27	-1.08	-1.08	-0.27	-0.27
67.5	-0.7071			-0.29	-0.29			-0.29	-0.29
70.0	-0.7660	-1.24	-1.24	-0.31	-0.31	-1.24	-1.24	-0.31	-0.31
72.5	-0.8192			-0.35	-0.35			-0.35	-0.35
75.0	-0.8660	-1.64	-1.64	-0.41	-0.41	-1.64	-1.64	-0.41	-0.41
77.5	-0.9063			-0.51	-0.51			-0.51	-0.51
80.0	-0.9397	-2.87	-2.87	-0.70	-0.70	-2.87	-2.87	-0.70	-0.70
82.5	-0.9659			-1.12	-1.12			-1.12	-1.12
85.0	-0.9848	+5.24	+5.24	-2.39	-2.39	+5.24	+5.24	-2.39	=2.39
87.5	-0.9962			+5.02	+5.02			+5.02	+5.02
90.0	-1.0000								

Table (V-II-6) Hemispherical Dome - Snow Load

M-Force/Length, $(N_\phi) = \alpha_4(pR/2)$ Fig. (V-II-6)

Percentage Error

ϕ	Elasticity Solution α_4	$\mu = 0.0$ $\theta_e = \phi_e = 5°$ Statics Matrix	Energy Matrix	$\theta_e = \phi_e = 2.5°$ Statics Matrix	Energy Matrix	$\mu = 0.2$ $\theta_e = \phi_e = 5°$ Statics Matrix	Energy Matrix	$\theta_e = \phi_e = 2.5°$ Statics Matrix	Energy Matrix
0.0	-1.0000	-0.13	-0.13	-0.03	-0.03	-0.13	-0.13	-0.03	
2.5				-0.03	-0.03			-0.03	
5.0		-0.13	-0.13	-0.03	-0.03	-0.13	-0.13	-0.03	
7.5				-0.03	-0.02			-0.03	
10.0		-0.13	-0.13	-0.03	-0.03	-0.13	-0.13	-0.03	
12.5				-0.03	-0.03			-0.03	
15.0		-0.13	-0.12	-0.03	-0.03	-0.14	-0.13	-0.03	
17.5				-0.03	-0.03			-0.04	
20.0		-0.14	-0.12	-0.04	-0.03	-0.14	-0.12	-0.04	
22.5				-0.04	-0.03			-0.04	
25.0		-0.15	-0.12	-0.04	-0.03	-0.15	-0.12	-0.04	
27.5				-0.04	-0.03			-0.04	
30.0		-0.15	-0.12	-0.04	-0.03	-0.15	-0.12	-0.04	
32.5				-0.04	-0.03			-0.04	
35.0		-0.16	-0.12	-0.04	-0.03	-0.16	-0.12	-0.04	
37.5				-0.04	-0.03			-0.04	
40.0		-0.17	-0.12	-0.04	-0.03	-0.17	-0.13	-0.04	
42.5				-0.04	-0.03			-0.05	
45.0		-0.18	-0.13	-0.05	-0.03	-0.18	-0.14	-0.05	
47.5				-0.04	-0.03			-0.05	
50.0		-0.19	-0.15	-0.04	-0.04	-0.19	-0.16	-0.05	
52.5				-0.05	-0.04			-0.05	
55.0		-0.19	-0.17	-0.04	-0.04	-0.21	-0.20	-0.05	
57.5				-0.05	-0.05			-0.05	
60.0		-0.20	-0.23	-0.05	-0.06	-0.22	-0.26	-0.05	
62.5				-0.05	-0.07			-0.06	
65.0		-0.21	-0.32	-0.05	-0.08	-0.24	-0.38	-0.06	
67.5				-0.05	-0.10			-0.06	
70.0		-0.21	-0.51	-0.06	-0.12	-0.26	-0.60	-0.07	
72.5				-0.05	-0.16			-0.06	
75.0		-0.24	-0.88	-0.06	-0.22	-0.33	-1.04	-0.08	
77.5				-0.06	-0.32			-0.09	
80.0		-0.13	-2.22	-0.04	-0.51	-0.32	-2.66	-0.09	
82.5				-0.08	-0.88			-0.17	
85.0		-1.65	-6.18	-0.07	-2.23	-2.36	-7.37	-0.13	
87.5				-1.36	-5.97			-2.08	
90.0		-0.67	-0.67	-0.14	-0.14	-0.67	-0.67	-0.14	

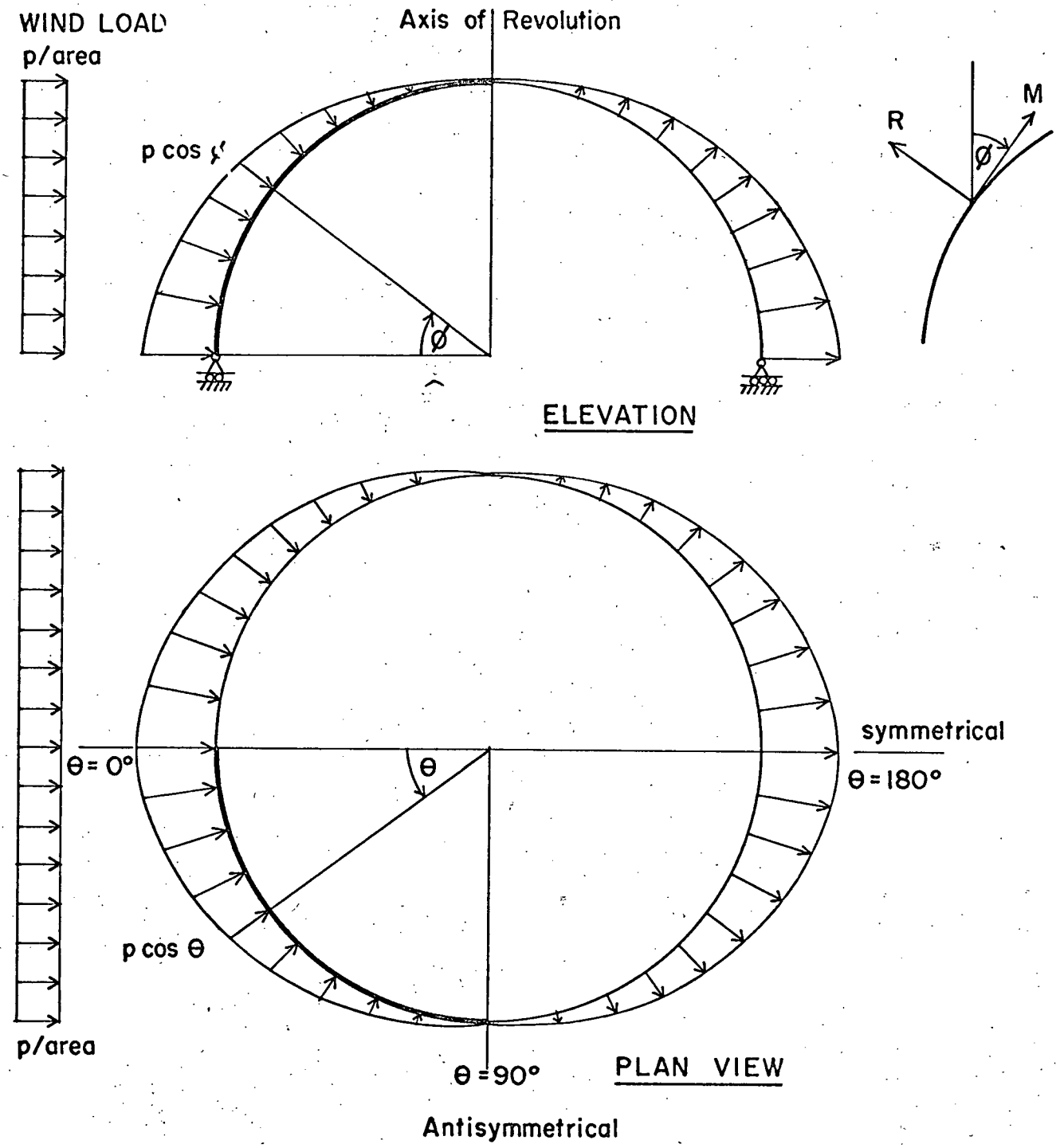

FIGURE V-III-1. HEMISPHERICAL DOME SUBJECTED TO WIND LOAD

5.5 Example III - Hemispherical Dome Subjected to Wind Load Fig. (V-III-1)

The available elasticity solution[35,36] is based on the following assumption of the wind pressure on the dome surface.

$$p_P = 0;\ p_M = 0;\ p_R = -p\ \mathrm{Cos}\phi\ \mathrm{Cos}\theta.$$

Here, p is the intensity of the wind load on a surface normal to the direction of the wind,

and p_P, p_M, p_R are components of the distributed pressures on the shell surface in P, M and R directions respectively.

Corresponding to the above distribution the radial load is symmetrical about $\theta = 0°$ and $\theta = 180°$ meridian planes and antisymmetrical about $\theta = \pm 90°$ meridian planes.

The shell is supported in such a way that the deflections at the base are permitted only in radial directions. By assuming proper boundary conditions along $\theta = 0°$ and $\theta = 90°$ meridians, it is sufficient to solve only one quarter of the dome. Elasticity solution[35,36] for displacements ($\mu = 0.0$ and 0.2) and stresses (independent of μ), based on the membrane theory which neglects flexure, is plotted (Figs. (V-III-2 to 7)) at $\theta = 0°$, 30°, 60° and 90° meridians.

For the finite element analysis, nodal loads in R-directions are calculated by multiplying the intensity of the normal pressure p_R at the node by 1/4 of the areas of all shell elements meeting at that node.

Both Statics and Energy plane stress stiffness matrices are employed to analyse the shell model. Different values of Poisson's ratio and various element sizes are used in the analysis. Percentage errors are calculated and are shown in Tables (V-III-1 to 36). Higher percentage errors in R-displacement and membrane shear, noticed at the nodes of the

triangles, are probably due to the manner of calculation of nodal loads and due to the behaviour of the model as a cone rather than as a spherical surface near the apex. However, here the values of R-displacement and shear are small as compared to their maximum values elsewhere and as such these errors are considered negligible. The stresses and the displacements in the upper part of the shell are obtained with fair accuracy. Larger deviation in R-displacements near the base nodes is noticed. The accuracy of the solution is improved by using smaller sized elements.

In the finite element analysis, errors are introduced due to (i) approximating the continuously curved surface by flat surfaces connected only at the corners, (ii) replacing the continuously varying load by approximate concentrated loads applied at the nodes and (iii) replacing the complicated deflected shape of an element by a simple deflected shape. However, as the element size decreases, the geometry, the loading, the support conditions,and the deflected shape of the model approach closer those of the shell. The errors of the F.E. solution, therefore, are expected to reduce. This is confirmed by the error analysis presented in Tables (V-III-1 to 36).

A further subdivision of the entire shell increases the size of the problem beyond the scope of the present computer program and is unnecessary. In view of the fairly accurate solution obtained for the upper part of the shell, smaller sized elements are only necessary in the base zone. This is conveniently achieved by providing displacement boundary conditions along a parallel circle at which displacements have been calculated with good accuracy. This parallel circle is selected high enough so that the base deflections are unaffected by the small errors in displacements provided along it.

It is observed that the differences in R-displacement at the base nodes between the F.E. and the elasticity solutions are reduced on reduction of the element size but the pattern of deviation, i.e.,the base deflections being too large and the ones one node above being too small, remains unchanged (Fig. (V-III-8)). The cause for this deviation pattern may be explained as follows; loads at the base nodes are determined using the wind intensity at the base, which is somewhat greater than the one over most of the area tributary to the base node. Furthermore, the base loads are shifted vertically down compared to their actual location. Both these causes tend to make the R-deflection at the base in the F.E. solution greater compared to the elasticity solution. The assumed load action in the F.E. solution agrees closely with the elasticity solution with regard to $\sum P_R$ condition (i.e. sum of the forces in radial direction) but differs from it substantially in $\sum M_p$ condition (i.e. sum of the moments about P-axis) in view of the vertical shift of the load. This inconsistency between the two solutions might be removed by the application of an equivalent balancing moment made up of two equal forces applied in opposite directions at the base node and at the node one step up. Such couple of forces would evidently decrease the R-deflection at the base and increase it at the next node up. Presumably the action of these forces would restore the deflections of the F.E. solution to the elasticity level. Without such action, the base R-deflections will be greater and the deflections one step up smaller than the deflections found by the elasticity. It is reminded that the comparison of the two deflections just concluded, refers to the membrane solution.

The results presented in Tables (V-III-1 to 36) show that for $\theta_e = \phi_e = 10^\circ$ element size ($\mu = 0.0$ and 0.2), the membrane F.E. solution differs from the elasticity solution by 2% in P and M displacements by 4% in

R-displacements and in stress by 3.5% using Statics matrix and by 5.5% using Energy matrix. In the above, the base nodes and the nodes at which values of displacements or stresses are small are excluded.

The supposedly exact elasticity solution[35,36] used in the preceding discussion assumes the absence of flexural stresses and this is not the case in the structure under consideration. In view of the bottom edge of the shell carrying radially directed loads and not being restrained in R-direction, some flexural stresses are induced near the base zone and the load there is partially carried by flexure.[39] The elasticity membrane solution[35,36] is therefore somewhat erroneous in the base zone. Away from the base the flexural stresses quickly die out as is a general condition in the shells of revolution having positive gaussian curvatures in the two principal directions.

To study the effect of flexure in the shell, the finite elements were endowed with both plane stress and flexure properties. Due to the increased degrees of freedom at each node, the size of the problem is increased. To be within the scope of the present computer program, only the base zone of the shell is analysed in two cases. The displacement and rotation boundary conditons are provided at $\phi = 30°$ for $\theta_e = \phi_e = 5°$ element size in one case and at $\phi = 15°$ and $\theta = 45°$ for $\theta_e = \phi_e = 2.5°$ element size in the other. It is assumed that near the new boundary, the displacements found in the membrane solution and the rotations implied in them are essentially correct. The flexure solution is carried out in three stages. In the first stage, displacements at all nodes are calculated using the membrane theory alone. In the second stage which includes flexure, P and M rotations of various nodes are found which would effect their moment equilibrium in the presence of deflections determined in the first

stage. Finally, in the third stage, the displacements and rotations in the base zone are calculated using the combined membrane and flexure theory while providing at the new boundary the displacements and rotations from the second stage of the solution. The percentage deviations in displacements and membrane stresses of the flexure F.E. solution from the elasticity membrane solution[35,36] are shown in Tables (V-III-1 to 36). These results are for a thin shell (radius R = 100.0 in.; thickness t = 1.0 in.). The differences in results of displacements and stresses calculated by membrane and by flexure solutions show the effect of flexure. These differences are small. The flexure stresses are then largely the participation stresses having virtually no effect on the load carrying capacity of the shell except near the base where there is small effect present. In spite of this the unit flexural stresses (#/in^2) may be significant and may cause the shell to crack. The bending moments/length along $\theta = 0°$ meridian are shown in Table (V-III-37).

In order to study the effect of flexure in a thicker shell (radius = 100.0 in.; thickness = 5.0 in.), the deviations in R-displacements and bending moments (at $\theta = 0°$ meridian; for $\mu = 0.2$ and $\theta_e = \phi_e = 5°$ element size) are calculated. Table (V-III-37) shows that on increasing the thickness of the shell, larger bending moments/length are induced. The small differences in the R-displacements in the membrane and flexure solutions shown in Table (V-III-38) suggest that the effect of flexure on the load carrying capacity of the shell on increasing the thickness (from t = 1.0 in. to t = 5.0 in.) is small. Furthermore, the flexure effects are restricted at the base zone ($\phi = 0°$ to $\phi = 35°$) above which the shell action is essentially membrane.

The overall results presented in the Tables (V-III-1 to 36) show that the solution is obtained with good accuracy for both values of Poisson's ratio (0.0 and 0.2) by using either Statics or Energy stiffness matrices. However, better accuracy is noticed from the use of Statics matrices.

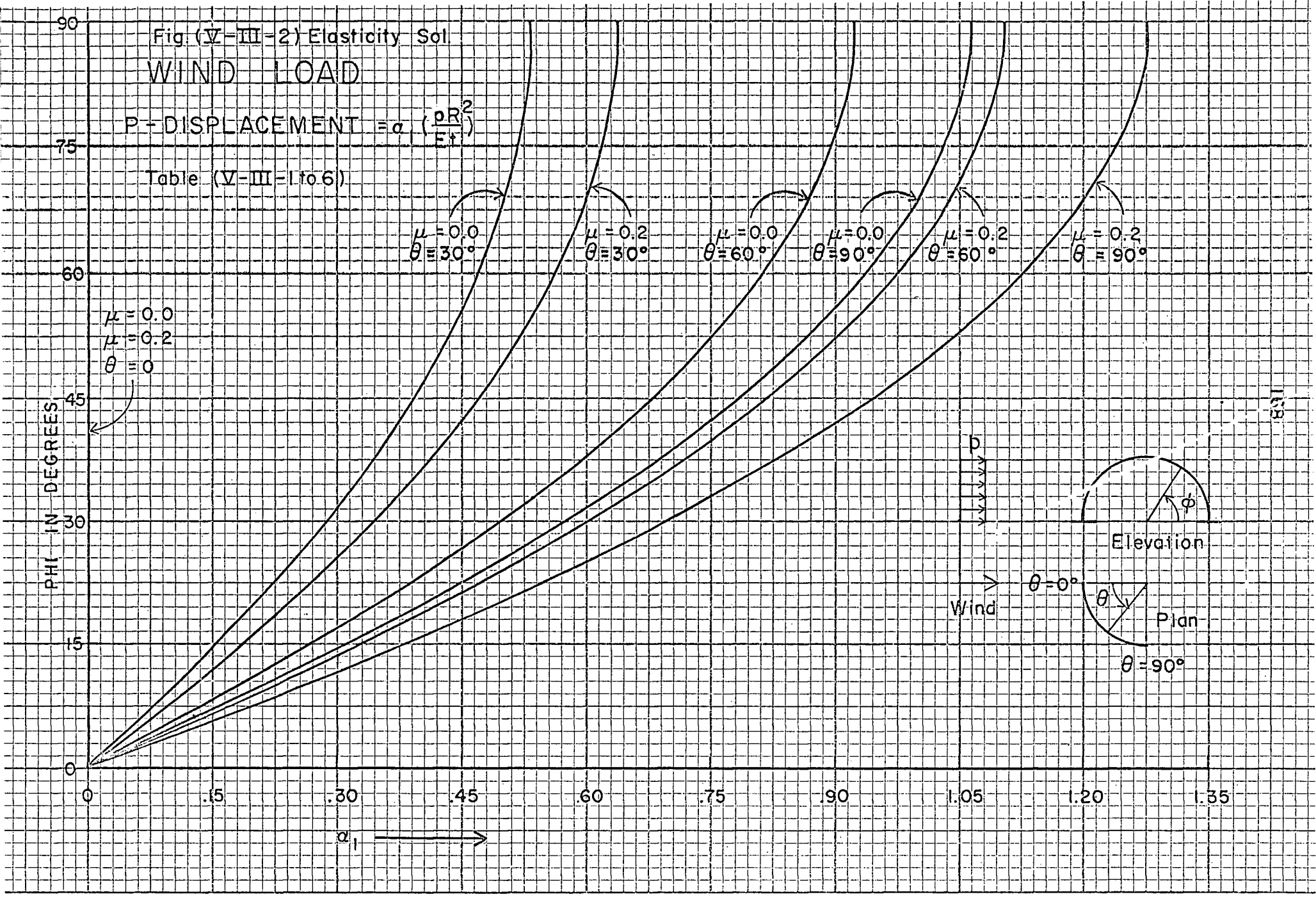
Fig (V-III-2) Elasticity Sol.
WIND LOAD
P - DISPLACEMENT = α (pR²/Et)
Table (V-III-1 to 6)
μ = 0.0
θ = 30°
μ = 0.2
θ = 30°
μ = 0.0
θ = 60°
μ = 0.0
θ = 90°
μ = 0.2
θ = 60°
μ = 0.2
θ = 90°
μ = 0.0
μ = 0.2
θ = 0
PHI IN DEGREES
90
75
60
45
30
15
0
0
.15
.30
.45
.60
.75
.90
1.05
1.20
1.35
α1
p
φ
Elevation
Wind
θ = 0°
θ
Plan
θ = 90°

Table (V-III-1) Hemispherical Dome - Wind Load

P-Displacement = $\alpha_1(pR^2/Et)$ Fig. (V-III-2)

μ = 0.0; R/t = 100.0; θ = 30° meridian (Fig. (V-III-1))

Percentage Error

		← Membrane →								Flexure	
ϕ	Elasticity Solution α_1	$\theta_e=\phi_e=15°$		$\theta_e=\phi_e=10°$		$\theta_e=\phi_e=5°$		$\theta_e=\phi_e=2.5°$		$\theta_e=\phi_e$ =5°	$\theta_e=\phi_e$ =2.5°
		Stat	Engy	Stat	Engy	Stat	Engy	Stat	Engy	Stat	Stat
0.0	0.0000	0.00	0.00	0.00	0.00	0.00	0.00	0.00	0.00	0.00	0.00
2.5	0.0286							0.00	0.00		0.00
5.0	0.0563					0.36	0.36	0.18	0.18	0.35	0.18
7.5	0.0832							0.00	0.00		0.00
10.0	0.1092			1.83	1.83	0.18	0.18	0.00	0.00	0.09	0.00
12.5	0.1345							0.00	0.00		0.00
15.0	0.1589	4.03	4.15			0.06	0.06	0.00	0.00	0.06	0.00
17.5	0.1826										
20.0	0.2055			1.07	1.07	0.05	0.05			0.05	
22.5	0.2277										
25.0	0.2491					0.04	0.04			0.04	
27.5	0.2698										
30.0	0.2898	2.24	2.31	0.93	0.97	0.00	0.00			0.00	
35.0	0.3275										
40.0	0.3622			0.86	0.83						
45.0	0.3939	1.98	1.98								
50.0	0.4224			0.78	0.76						
55.0	0.4478										
60.0	0.4700	1.64	1.53	0.72	0.66						
65.0	0.4889										
70.0	0.5044			0.67	0.56						
75.0	0.5165	1.55	1.36								
80.0	0.5252			0.67	0.51						
85.0	0.5304										
90.0											

Stat. - Statics matrix

Engy. - Energy matrix

Table (V-III-2) Hemispherical Dome - Wind Load

P-Displacement $= \alpha_1 (pR^2/Et)$ Fig. (V-III-2)
$\mu = 0.2$; $R/t = 100.0$; $\theta = 30°$ meridian (Fig. (V-III-1))

Percentage Error

		← Membrane →								Flexure	
ϕ	Elasticity Solution	$\theta_e=\phi_e=15°$		$\theta_e=\phi_e=10°$		$\theta_e=\phi_e=5°$		$\theta_e=\phi_e=2.5°$		$\theta_e=\phi_e=5°$	$\theta_e=\phi_e=2.5°$
	α_1	Stat	Engy	Stat	Engy	Stat	Engy	Stat	Engy	Stat	Stat
0.0°	0.0000	0.00	0.00	0.00	0.00	0.00	0.00	0.00	0.00	0.00	0.00
2.5°	0.0343							0.29	0.29		0.29
5.0°	0.0676					0.30	0.30	0.00	0.00	0.15	0.00
7.5°	0.0998							0.00	0.00		0.10
10.0°	0.1311			1.45	1.45	0.08	0.08	0.00	0.00	0.08	0.00
12.5°	0.1613							0.06	0.06		0.06
15.0°	0.1907	3.30	3.46			0.05	0.05	0.00	0.00	0.05	0.00
17.5°	0.2191										
20.0°	0.2466			0.93	0.93	0.04	0.04			0.04	
22.5°	0.2732										
25.0°	0.2990					0.00	0.00			0.00	
27.5°	0.3238										
30.0°	0.3478	1.93	2.01	0.81	0.83	0.00	0.00			0.00	
35.0°	0.3930										
40.0°	0.4346			0.74	0.76						
45.0°	0.4726	1.69	1.74								
50.0°	0.5069			0.67	0.67						
55.0°	0.5374										
60.0°	0.5640	1.37	1.35	0.62	0.60						
65.0°	0.5866										
70.0°	0.6053			0.56	0.50						
75.0°	0.6198	1.24	1.10								
80.0°	0.6303			0.54	0.40						
85.0°	0.6365										
90.0°											

Stat. - Statics matrix

Engy. - Energy matrix

Table (V-III-3) Hemispherical Dome - Wind Load

P-Displacement = $\alpha_1(pR^2/Et)$ Fig. (V-III-2)

μ = 0.0; R/t = 100.0; θ = 60° meridian (Fig. (V-III-1))

Percentage Error

		← Membrane →								Flexure	
ϕ	Elasticity Solution	$\theta_e=\phi_e=15°$		$\theta_e=\phi_e=10°$		$\theta_e=\phi_e=5°$		$\theta_e=\phi_e=2.5°$		$\theta_e=\phi_e$ =5°	$\theta_e=\phi_e$ =2.5°
	α_1	Stat	Engy	Stat	Engy	Stat	Engy	Stat	Engy	Stat	Stat
0.0	0.0000	0.00	0.00	0.00	0.00	0.00	0.00	0.00	0.00	0.00	
2.5	0.0496							0.00	0.00		
5.0	0.0976					0.31	0.31	0.00	0.00	0.21	
7.5	0.1441							0.00	0.00		
10.0	0.1892			1.74	1.74	0.11	0.11	0.00	0.00	0.11	
12.5	0.2329							0.00	0.00		
15.0	0.2752	3.96	4.11			0.11	0.11	0.00	0.00	0.07	
17.5	0.3162										
20.0	0.3560			1.01	1.01	0.03	0.03			0.03	
22.5	0.3944										
25.0	0.4315					0.02	0.02			0.02	
27.5	0.4674										
30.0	0.5019	2.19	2.23	0.92	0.92	0.00	0.00			0.00	
35.0	0.5672										
40.0	0.6274			0.81	0.80						
45.0	0.6822	1.92	1.91								
50.0	0.7317			0.75	0.72						
55.0	0.7757										
60.0	0.8141	1.60	1.49	0.70	0.64						
65.0	0.8467										
70.0	0.8736			0.66	0.56						
75.0	0.8946	1.53	1.34								
80.0	0.9097			0.66	0.51						
85.0	0.9188										
90.0											

Stat. - Statics matrix

Engy. - Energy matrix

Table (V-III-4) Hemispherical Dome - Wind Load

P-Displacement = $\alpha_1(pR^2/Et)$ Fig. (V-III-2)

μ = 0.2; R/t = 100.0; θ = 60° meridian (Fig. (V-III-1))

Percentage Error

		← Membrane →								Flexure	
ϕ	Elasticity Solution	$\theta_e=\phi_e=15°$		$\theta_e=\phi_e=10°$		$\theta_e=\phi_e=5°$		$\theta_e=\phi_e=2.5°$		$\theta_e=\phi_e$ =5°	$\theta_e=\phi_e$ =2.5°
	α_1	Stat	Engy	Stat	Engy	Stat	Engy	Stat	Engy	Stat	Stat
0.0°	0.0000	0.00	0.00	0.00	0.00	0.00	0.00	0.00	0.00	0.00	
2.5°	0.0595							0.00	0.00		
5.0°	0.1171					0.26	0.26	0.00	0.00	0.17	
7.5°	0.1729							0.00	0.00		
10.0°	0.2270			1.45	1.45	0.09	0.09	0.00	0.00	0.09	
12.5°	0.2795							0.00	0.00		
15.0°	0.3303	3.24	3.36			0.06	0.06	0.00	0.00	0.06	
17.5°	0.3795										
20.0°	0.4271			0.87	0.91	0.05	0.05			0.05	
22.5°	0.4733										
25.0°	0.5178					0.02	0.02			0.02	
27.5°	0.5608										
30.0°	0.6023	1.86	1.94	0.78	0.81	0.00	0.00			0.00	
35.0°	0.6807										
40.0°	0.7528			0.70	0.72						
45.0°	0.8186	1.63	1.67								
50.0°	0.8780			0.65	0.65						
55.0°	0.9308										
60.0°	0.9769	1.33	1.30	0.60	0.57						
65.0°	1.0161										
70.0°	1.0484			0.55	0.49						
75.0°	1.0736	1.21	1.08								
80.0°	1.0916			0.54	0.41						
85.0°	1.1025										
90.0°											

Stat. - Statics matrix

Engy. - Energy matrix

Table (V-III-5) Hemispherical Dome - Wind Load

P-Displacement $=\alpha_1(pR^2/Et)$ (Fig. (V-III-2)

$\mu = 0.0$; $R/t = 100.0$; $\theta = 90°$ meridian (Fig. (V-III-1))

Percentage Error

		← Membrane →								Flexure	
$\phi°$	Elasticity Solution	$\theta_e=\phi_e=15°$		$\theta_e=\phi_e=10°$		$\theta_e=\phi_e=5°$		$\theta_e=\phi_e=2.5°$		$\theta_e=\phi_e=5°$	$\theta_e=\phi_e=2.5°$
	α_1	Stat	Engy	Stat	Engy	Stat	Engy	Stat	Engy	Stat	Stat
0.0	0.0000	0.00	0.00	0.00	0.00	0.00	0.00	0.00	0.00	0.00	
2.5	0.0572							0.18	0.18		
5.0	0.1127					0.27	0.27	0.00	0.00	0.18	
7.5	0.1664							0.00	0.00		
10.0	0.2185			1.56	1.60	0.05	0.05	0.00	0.00	0.05	
12.5	0.2689							0.00	0.00		
15.0	0.3178	3.65	3.78			0.06	0.06	0.00	0.00	0.03	
17.5	0.3682										
20.0	0.4110			0.90	0.93	0.02	0.02			0.02	
22.5	0.4554										
25.0	0.4983					0.00	0.00			0.00	
27.5	0.5397										
30.0	0.5796	2.02	2.07	0.83	0.83	0.00	0.00				
35.0	0.6550										
40.0	0.7244			0.76	0.75						
45.0	0.7877	1.83	1.80								
50.0	0.8449			0.72	0.69						
55.0	0.8957										
60.0	0.9400	1.55	1.44	0.68	0.63						
65.0	0.9777										
70.0	1.0088			0.64	0.55						
75.0	1.0330	1.52	1.34								
80.0	1.0504			0.67	0.51						
85.0	1.0609										
90.0											

Stat. - Statics matrix

Engy. - Energy matrix

Table (V-III-6) Hemispherical Dome - Wind Load

P-Displacement = $\alpha_1(pR^2/Et)$ Fig. (V-III-2)

$\mu = 0.2$; $R/t = 100.0$; $\theta = 90°$ meridian (Fig. (V-III-1))

Percentage Error

		← Membrane →								Flexure	
ϕ	Elasticity Solution	$\theta_e=\phi_e=15°$		$\theta_e=\phi_e=10°$		$\theta_e=\phi_e=5°$		$\theta_e=\phi_e=2.5°$		$\theta e=\phi e$ =5°	$\theta e=\phi e$ =2.5°
	α_1	Stat	Engy	Stat	Engy	Stat	Engy	Stat	Engy	Stat	Stat
0.0°	0.0000	0.00	0.00	0.00	0.00	0.00	0.00	0.00	0.00	0.00	
2.5°	0.0687							0.00	0.00		
5.0°	0.1352					0.22	0.22	0.00	0.00	0.15	
7.5°	0.1997							0.00	0.00		
10.0°	0.2621			1.30	1.30	0.08	0.08	0.04	0.00	0.08	
12.5°	0.3227							0.00	0.00		
15.0°	0.3814	2.94	3.07			0.03	0.03	0.00	0.00	0.03	
17.5°	0.4382										
20.0°	0.4932			0.77	0.79	0.02	0.02			0.02	
22.5°	0.5465										
25.0°	0.5979					0.02	0.02			0.02	
27.5°	0.6476										
30.0°	0.6955	1.70	1.77	0.71	0.73	0.00	0.00			0.00	
35.0°	0.7860										
40.0°	0.8693			0.64	0.67						
45.0°	0.9453	1.51	1.57								
50.0°	1.0138			0.61	0.61						
55.0°	1.0748										
60.0°	1.1280	1.29	1.25	0.58	0.55						
65.0°	1.1733										
70.0°	1.2105			0.55	0.48						
75.0°	1.2397	1.20	1.07								
80.0°	1.2605			0.54	0.41						
85.0°	1.2731										
90.0°											

Stat. - Statics matrix

Engy. - Energy matrix

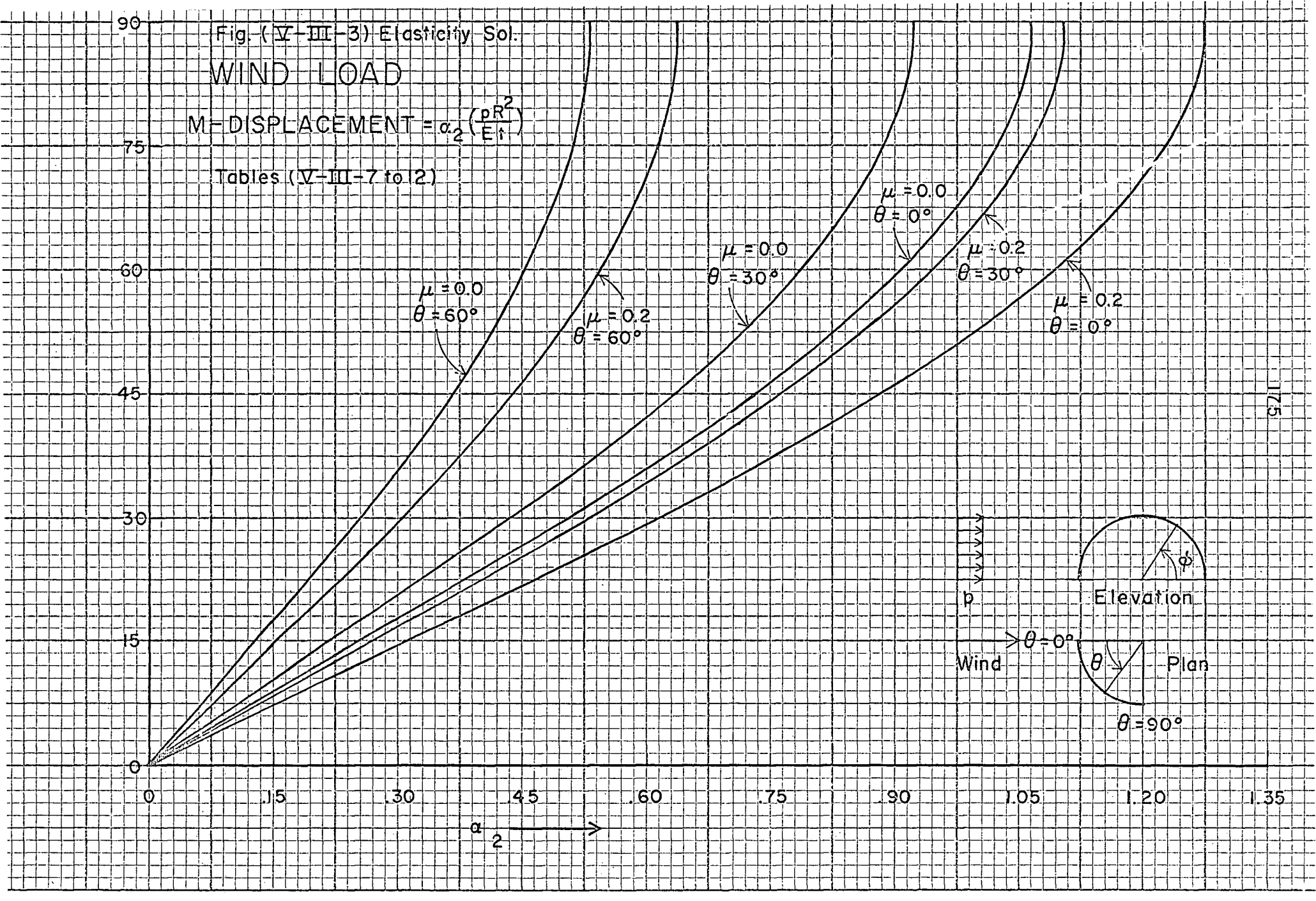
Fig. (V-III-3) Elasticity Sol.
WIND LOAD
M=DISPLACEMENT = $\alpha_2 \left(\frac{pR^2}{Et}\right)$
Tables (V-III-7 to 12)
μ = 0.0
θ = 0°
μ = 0.0
θ = 30°
μ = 0.2
θ = 30°
μ = 0.2
θ = 0°
μ = 0.0
θ = 60°
μ = 0.2
θ = 60°
90
75
60
45
30
15
0
0
.15
.30
.45
.60
.75
.90
1.05
1.20
1.35
α_2
p
Elevation
Φ
Wind
θ = 0°
θ
Plan
θ = 90°
1125

Table (V-III-7) Hemispherical Dome - Wind Load

M-Displacement = $\alpha_2(pR^2/Et)$ Fig. (V-III-3)

μ = 0.0; R/t = 100.0; θ = 0° meridian (Fig. (V-III-1))

Percentage Error

		← Membrane →								Flexure	
ϕ	Elasticity Solution	$\theta_e=\phi_e=15°$		$\theta_e=\phi_e=10°$		$\theta e=\phi e=5°$		$\theta_e=\phi e=2.5°$		$\theta e=\phi e$ =5°	$\theta_e=\phi_e$ =2.5°
	α_2	Stat	Engy	Stat	Engy	Stat	Engy	Stat	Engy	Stat	Stat
0.0°	0.0000	0.00	0.00	0.00	0.00	0.00	0.00	0.00	0.00	0.00	0.00
2.5°	0.0436							1.38	1.38		0.92
5.0°	0.0873					2.52	2.52	0.34	0.34	2.29	0.46
7.5°	0.1308							0.23	0.23		0.31
10.0°	0.1744			5.33	5.62	0.63	0.63	0.06	0.06	0.92	0.06
12.5°	0.2177							0.05	0.05		0.05
15.0°	0.2609	7.44	8.20			0.38	0.38	0.00	0.00	0.38	0.00
17.5°	0.3039										
20.0°	0.3465			1.65	1.91	0.17	0.17			0.17	
22.5°	0.3887										
25.0°	0.4304					0.07	0.07			0.07	
27.5°	0.4716										
30.0°	0.5120	2.12	2.79	1.15	1.41	0.00	0.00			0.00	
35.0°	0.5906										
40.0°	0.6653			0.77	1.04						
45.0°	0.7355	1.51	2.14								
50.0°	0.8005			0.60	0.86						
55.0°	0.8596										
60.0°	0.9121	1.12	1.71	0.48	0.72						
65.0°	0.9576										
70.0°	0.9955			0.44	0.64						
75.0°	1.0254	0.61	0.93								
80.0°	1.0470			0.28	0.33						
85.0°	1.0600										
90.0°	1.0644	0.97	0.89	0.46	0.34						

Stat. - Statics matrix

Engy. - Energy matrix

Table (V-III-8) Hemispherical Dome - Wind Load

M-Displacement = $\alpha_2(pR^2/Et)$ Fig. (V-III-3)

$\mu = 0.2$; $R/t = 100.0$; $\theta = 0°$ meridian (Fig. (V-III-1))

Percentage Error

		← Membrane →								Flexure	
ϕ	Elasticity Solution	$\theta_e=\phi_e=15°$		$\theta_e=\phi_e=10°$		$\theta_e=\phi_e=5°$		$\theta_e=\phi_e=2.5°$		$\theta_e=\phi_e$ =5°	$\theta_e=\phi_e$ =2.5°
	α_2	Stat	Engy	Stat	Engy	Stat	Engy	Stat	Engy	Stat	Stat
0.0°	0.0000	0.00	0.00	0.00	0.00	0.00	0.00	0.00	0.00	0.00	0.00
2.5°	0.0524							1.15	1.15		0.76
5.0°	0.1047					2.48	2.48	0.38	0.38	2.29	0.48
7.5°	0.1570							0.19	0.19		0.25
10.0°	0.2092			5.12	5.40	0.62	0.62	0.10	0.10	0.91	0.14
12.5°	0.2613							0.04	0.04		0.04
15.0°	0.3131	7.09	7.79			0.35	0.35	0.00	0.00	0.38	0.00
17.5°	0.3647										
20.0°	0.4158			1.54	1.78	0.17	0.17			0.17	
22.5°	0.4665										
25.0°	0.5165					0.06	0.06			0.06	
27.5°	0.5659										
30.0°	0.6144	1.99	2.56	1.06	1.30	0.00	0.00			0.00	
35.0°	0.7087										
40.0°	0.7984			0.70	0.94						
45.0°	0.8826	1.34	1.92								
50.0°	0.9606			0.53	0.78						
55.0°	1.0315										
60.0°	1.0946	0.95	1.49	0.41	0.64						
65.0°	1.1491										
70.0°	1.1946			0.39	0.57						
75.0°	1.2304	0.50	0.73								
80.0°	1.2564			0.24	0.26						
85.0°	1.2720										
90.0°	1.2773	0.78	0.66	0.38	0.25						

Stat. - Statics matrix

Engy. - Energy matrix

Table (V-III-9) Hemispherical Dome - Wind Load

M-Displacement = $\alpha_2(pR^2/Et)$ Fig. (V-III-3)

μ = 0.0; R/t = 100.0; θ = 30° meridian (Fig. (V-III-1))

Percentage Error

		← Membrane →								Flexure	
ϕ	Elasticity Solution	$\theta_e=\phi_e=15°$		$\theta_e=\phi_e=10°$		$\theta_e=\phi_e=5°$		$\theta_e=\phi_e=2.5°$		$\theta_e=\phi_e$ =5°	$\theta_e=\phi_e$ =2.5°
	α_2	Stat	Engy	Stat	Engy	Stat	Engy	Stat	Engy	Stat	Stat
0.0°	0.0000	0.00	0.00	0.00	0.00	0.00	0.00	0.00	0.00	0.00	0.00
2.5°	0.0378							1.32	1.32		0.79
5.0°	0.0756					2.51	2.51	0.27	0.27	2.25	0.53
7.5°	0.1133							0.18	0.18		0.26
10.0°	0.1510			5.30	5.63	0.66	0.66	0.07	0.07	0.93	0.13
12.5°	0.1886							0.00	0.00		0.00
15.0°	0.2260	7.39	8.14			0.35	0.35	0.00	0.00	0.35	0.00
17.5°	0.2632										
20.0°	0.3001			1.63	1.87	0.17	0.17			0.17	
22.5°	0.3366										
25.0°	0.3728					0.05	0.05			0.05	
27.5°	0.4084										
30.0°	0.4434	2.16	2.77	1.13	1.40	0.00	0.00			0.00	
35.0°	0.5114										
40.0°	0.5762			0.76	1.02						
45.0°	0.6370	1.48	2.10								
50.0°	0.6933			0.58	0.85						
55.0°	0.7444										
60.0°	0.7899	1.10	1.70	0.47	0.71						
65.0°	0.8293										
70.0°	0.8621			0.44	0.65						
75.0°	0.8880	0.61	0.92								
80.0°	0.9067			0.29	0.34						
85.0°	0.9180										
90.0°											

Stat. - Statics matrix

Engy. - Energy matrix

Table (V-III-10) Hemispherical Dome - Wind Load

M-Displacement = $\alpha_2(pR^2/Et)$ Fig. (V-III-3)

$\mu = 0.2$; $R/t = 100.0$; $\theta = 30°$ Meridian (Fig. (V-III-1))

Percentage Error

		← Membrane →								Flexure	
ϕ	Elasticity Solution	$\theta_e=\phi_e=15°$		$\theta_e=\phi_e=10°$		$\theta_e=\phi_e=5°$		$\theta_e=\phi_e=2.5°$		$\theta_e=\phi_e$ =5°	$\theta_e=\phi_e$ =2.5°
	α_2	Stat	Engy	Stat	Engy	Stat	Engy	Stat	Engy	Stat	Stat
0.0°	0.0000	0.00	0.00	0.00	0.00	0.00	0.00	0.00	0.00	0.00	0.00
2.5°	0.0453							1.33	1.33		0.88
5.0°	0.0907					2.43	2.43	0.33	0.33	2.01	0.44
7.5°	0.1360							0.15	0.15		0.22
10.0°	0.1812			5.08	5.41	0.61	0.61	0.11	0.11	0.94	0.11
12.5°	0.2263							0.04	0.04		0.04
15.0°	0.2712	7.04	7.74			0.33	0.33	0.00	0.00	0.37	0.00
17.5°	0.3158										
20.0°	0.3601			1.53	1.78	0.17	0.17			0.17	
22.5°	0.4040										
25.0°	0.4473					0.07	0.07			0.07	
27.5°	0.4901										
30.0°	0.5321	1.96	2.54	1.05	1.30	0.00	0.00			0.00	
35.0°	0.6137										
40.0°	0.6914			0.69	0.94						
45.0°	0.7644	1.32	1.90								
50.0°	0.8319			0.53	0.77						
55.0°	0.8933										
60.0°	0.9479	0.94	1.48	0.41	0.63						
65.0°	0.9952										
70.0°	1.0345			0.39	0.57						
75.0°	1.0656	0.50	0.72								
80.0°	1.0880			0.25	0.27						
85.0°	1.1016										
90.0°											

Stat. - Statics matrix

Engy. - Energy matrix

Table (V-III-11) Hemispherical Dome - Wind Load

M-Displacement = $\alpha_2(pR^2/Et)$ Fig. (V-III-3)

μ= 0.0; R/t = 100.0; θ = 60° meridian (Fig. (V-III-1))

Percentage Error

ϕ	Elasticity Solution	Membrane								Flexure	
		$\theta_e=\phi_e=15°$		$\theta_e=\phi_e=10°$		$\theta_e=\phi_e=5°$		$\theta_e=\phi_e=2.5°$		$\theta_e=\phi_e$ =5°	$\theta_e=\phi_e$ =2.5°
	α_2	Stat	Engy	Stat	Engy	Stat	Engy	Stat	Engy	Stat	Stat
0.0°	0.0000	0.00	0.00	0.00	0.00	0.00	0.00	0.00	0.00	0.00	
2.5°	0.0218							1.38	1.38		
5.0°	0.0436					2.52	2.52	0.46	0.46	2.29	
7.5°	0.0654							0.31	0.31		
10.0°	0.0872			5.23	5.62	0.57	0.57	0.12	0.12	0.92	
12.5°	0.1089							0.00	0.00		
15.0°	0.1305	7.28	8.05			0.31	0.31	0.00	0.00	0.31	
17.5°	0.1519										
20.0°	0.1733			1.56	1.79	0.12	0.12			0.12	
22.5°	0.1944										
25.0°	0.2152					0.05	0.05			0.05	
27.5°	0.2358										
30.0°	0.2560	2.07	2.70	1.09	1.37	0.00	0.00			0.00	
35.0°	0.2953										
40.0°	0.3327			0.72	0.99						
45.0°	0.3678	1.41	2.04								
50.0°	0.4003			0.55	0.82						
55.0°	0.4298										
60.0°	0.4561	1.05	1.64	0.44	0.68						
65.0°	0.4788										
70.0°	0.4977			0.44	0.64						
75.0°	0.5127	0.61	0.92								
80.0°	0.5235			0.29	0.34						
85.0°	0.5300										
90.0°											

Stat. - Statics matrix

Engy. - Energy matrix

Table (V-III-12) Hemispherical Dome - Wind Load

M-Displacement = $\alpha_2(pR^2/Et)$ Fig. (V-III-3)

μ = 0.2; R/t = 100.0; θ = 60° meridian (Fig. (V-III-1))

Percentage Error

ϕ	Elasticity Solution	← Membrane →								Flexure	
		$\theta_e=\phi_e$=15°		$\theta_e=\phi_e$=10°		$\theta_e=\phi_e$=5°		$\theta_e=\phi_e$=2.5°		$\theta_e=\phi_e$ =5°	$\theta_e=\phi_e$ =2.5°
	α_2	Stat	Engy	Stat	Engy	Stat	Engy	Stat	Engy	Stat	Stat
0.0°	0.0000	0.00	0.00	0.00	0.00	0.00	0.00	0.00	0.00	0.00	
2.5°	0.0262							1.15	1.15		
5.0°	0.0524					2.29	2.29	0.19	0.19	2.10	
7.5°	0.0785							0.25	0.26		
10.0°	0.1046			5.07	5.35	0.67	0.67	0.10	0.10	0.96	
12.5°	0.1306							0.08	0.08		
15.0°	0.1566	6.90	7.60			0.32	0.32	0.00	0.00	0.32	
17.5°	0.1823										
20.0°	0.2079			1.49	1.73	0.14	0.14			0.14	
22.5°	0.2332										
25.0°	0.2583					0.04	0.04			0.04	
27.5°	0.2829										
30.0°	0.3072	1.89	2.44	1.01	1.27	0.00	0.00			0.00	
35.0°	0.3543										
40.0°	0.3992			0.65	0.90						
45.0°	0.4413	1.25	1.84								
50.0°	0.4803			0.50	0.75						
55.0°	0.5158										
60.0°	0.5473	0.90	1.43	0.38	0.60						
65.0°	0.5746										
70.0°	0.5973			0.37	0.55						
75.0°	0.6152	0.49	0.72								
80.0°	0.6282			0.24	0.26						
85.0°	0.6360										
90.0°											

Stat. - Statics matrix

Engy. - Energy matrix

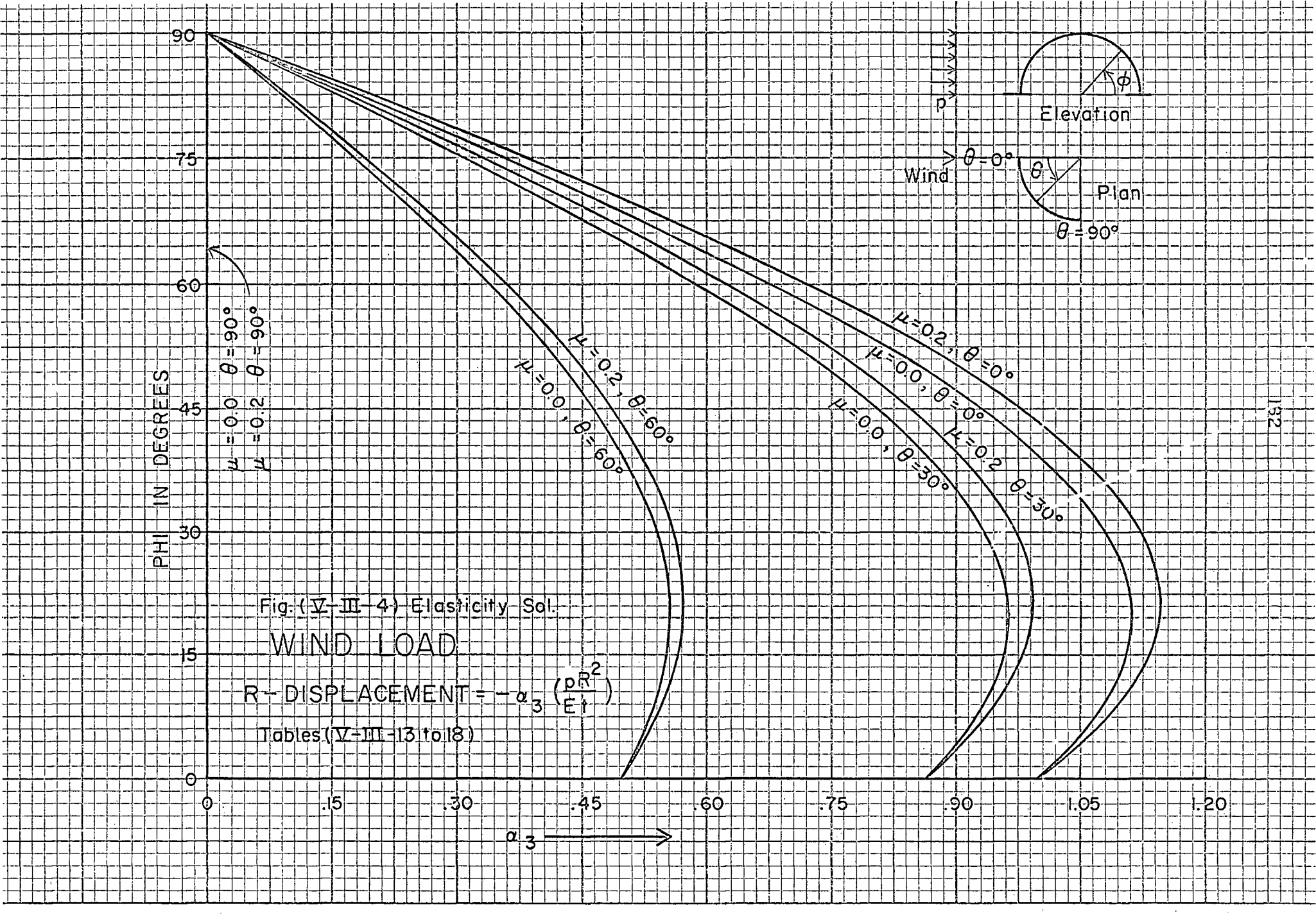
90
75
60
45
30
15
0
PHI IN DEGREES
0
.15
.30
.45
.60
.75
.90
1.05
1.20
α_3
$\mu = 0.0$ $\theta = 90°$
$\mu = 0.2$ $\theta = 90°$
$\mu = 0.2$, $\theta = 60°$
$\mu = 0.0$, $\theta = 60°$
$\mu = 0.2$, $\theta = 0°$
$\mu = 0.0$, $\theta = 0°$
$\mu = 0.2$ $\theta = 30°$
$\mu = 0.0$, $\theta = 30°$
p
Wind
$\theta = 0°$
θ
$\theta = 90°$
Plan
ϕ
Elevation
Fig. (V-III-4) Elasticity Sol.
WIND LOAD
R - DISPLACEMENT = $-\alpha_3 \left(\frac{pR^2}{Et}\right)$
Tables (V-III-13 to 18)
132

Table (V-III-13) Hemispherical Dome - Wind Load

R-Displacement = $-\alpha_3(pR^2/Et)$ Fig. (V-III-4)

$\mu = 0.0$; $R/t = 100.0$; $\theta = 0°$ meridian (Fig. (V-III-1))

Percentage Error

		Membrane								Flexure	
ϕ	Elasticity Solution	$\theta_e=\phi_e=15°$		$\theta_e=\phi_e=10°$		$\theta_e=\phi_e=5°$		$\theta_e=\phi_e=2.5°$		$\theta_e=\phi_e=5°$	$\theta_e=\phi_e=2.5°$
	α_3	Stat	Engy	Stat	Engy	Stat	Engy	Stat	Engy	Stat	Stat
0.0°	1.0000	23.96	24.87	16.28	16.64	8.06	8.10	4.08	4.09	4.84	1.46
2.5°	1.0272							-1.20	-1.20		0.52
5.0°	1.0506					-2.33	-2.31	0.19	0.19	0.27	-0.02
7.5°	1.0701							-0.17	-0.16		-0.21
10.0°	1.0859			-4.23	-4.13	0.41	0.42	-0.06	-0.06	-0.70	-0.19
12.5°	1.0980							-0.12	-0.11		-0.11
15.0°	1.1062	-5.93	-5.81			-0.29	-0.28	0.00	0.00	-0.33	0.00
17.5°	1.1108										
20.0°	1.1117			1.23	1.36	-0.04	-0.04			-0.13	
22.5°	1.1089										
25.0°	1.1025					-0.10	-0.11			-0.15	
27.5°	1.0927										
30.0°	1.0793	2.48	2.73	-0.10	-0.04	0.00	0.00			0.00	
35.0°	1.0425										
40.0°	0.9927			0.36	0.38						
45.0°	0.9308	-0.07	-0.22								
50.0°	0.8576			0.32	0.21						
55.0°	0.7741										
60.0°	0.6813	2.29	1.67	0.19	-0.32						
65.0°	0.5805										
70.0°	0.4728			1.44	0.30						
75.0°	0.3595	-8.23	-16.63								
80.0°	0.2420			-8.21	-16.58						
85.0°	0.1217										
90.0°	0.0000	0.00	0.00	0.00	0.00						

Stat. - Statics matrix

Engy. - Energy matrix

Table (V-III-14) Hemispherical Dome - Wind Load

R-Displacement = $-\alpha_3(pR^2/Et)$ Fig. (V-III-4)

$\mu = 0.2$; $R/t = 100.0$; $\theta = 0°$ meridian (Fig. (V-III-1))

Percentage Error

		Membrane								Flexure	
ϕ	Elasticity Solution	$\theta_e=\phi_e=15°$		$\theta_e=\phi_e=10°$		$\theta_e=\phi_e=5°$		$\theta_e=\phi_e=2.5°$		$\theta_e=\phi_e=5°$	$\theta_e=\phi_e=2.5°$
	α_3	Stat	Engy	Stat	Engy	Stat	Engy	Stat	Engy	Stat	Stat
0.0°	1.0000	22.8	23.75	15.55	15.91	7.70	7.74	3.90	3.90	4.64	1.44
2.5°	1.0328							-1.16	-1.16		0.48
5.0°	1.0614					-2.24	-2.23	0.17	0.17	0.24	-0.05
7.5°	1.0859							-0.18	-0.18		-0.24
10.0°	1.1062			-4.07	-3.95	0.35	0.36	-0.08	-0.07	-0.70	-0.23
12.5°	1.1223							-0.13	-0.13		-0.12
15.0°	1.1343	-5.73	-5.58			-0.30	-0.30	0.00	0.00	-0.34	0.00
17.5°	1.1422										
20.0°	1.1461			1.11	1.25	-0.06	-0.06			-0.15	
22.5°	1.1459										
25.0°	1.1418					-0.13	-0.13			-0.17	
27.5°	1.1338										
30.0°	1.1220	2.22	2.52	-0.13	-0.05	0.00	0.00			0.00	
35.0°	1.0871										
40.0°	1.0380			0.33	0.38						
45.0°	0.9755	-0.10	-0.16								
50.0°	0.9005			0.29	0.22						
55.0°	0.8142										
60.0°	0.7176	1.98	1.53	0.20	-0.25						
65.0°	0.6121										
70.0°	0.4989			1.24	0.28						
75.0°	0.3797	-6.79	-14.35								
80.0°	0.2557			-6.76	-14.29						
85.0°	0.1287										
90.0°	0.0000	0.00	0.00	0.00	0.00						

Stat. - Statics matrix

Engy. - Energy matrix

Table (V-III-15) Hemispherical Dome - Wind Load

R-Displacement = $-\alpha_3(pR^2/Et)$ Fig. (V-III-4)

$\mu = 0.0$; $R/t = 100.0$; $\theta = 30°$ meridian (Fig. (V-III-1))

Percentage Error

		← Membrane →								Flexure	
ϕ	Elasticity Solution	$\theta_e=\phi_e=15°$		$\theta_e=\phi_e=10°$		$\theta_e=\phi_e=5°$		$\theta_e=\phi_e=2.5°$		$\theta_e=\phi_e=5°$	$\theta_e=\phi_e=2.5°$
	α_3	Stat	Engy	Stat	Engy	Stat	Engy	Stat	Engy	Stat	Stat
0.0°	0.8660	23.89	24.79	16.26	16.62	8.05	8.10	4.08	4.09	4.83	1.51
2.5°	0.8896							-1.20	-1.20		0.52
5.0°	0.9098					-2.34	-2.33	0.20	0.20	0.26	-0.03
7.5°	0.9268							-0.17	-0.17		-0.23
10.0°	0.9405			-4.24	-4.15	0.42	0.43	-0.06	-0.06	-0.71	-0.20
12.5°	0.9509							-0.12	-0.12		-0.08
15.0°	0.9580	-5.98	-5.87			-0.28	-0.27	0.00	0.00	-0.32	0.00
17.5°	0.9620										
20.0°	0.9627			1.22	1.34	-0.04	-0.04			-0.11	
22.5°	0.9603										
25.0°	0.9548					-0.13	-0.13			-0.15	
27.5°	0.9463										
30.0°	0.9347	2.42	2.67	-0.13	-0.06	0.00	0.00			0.00	
35.0°	0.9028										
40.0°	0.8597			0.34	0.36						
45.0°	0.8061	-0.14	-0.29								
50.0°	0.7427			0.30	0.19						
55.0°	0.6704										
60.0°	0.5900	2.24	1.63	0.19	-0.34						
65.0°	0.5027										
70.0°	0.4094			1.44	0.29						
75.0°	0.3114	-8.28	-16.70								
80.0°	0.2096			-8.19	-16.65						
85.0°	0.1054										
90.0°	0.0000	0.00	0.00	0.00	0.00						

Stat. - Statics matrix

Engy. - Energy matrix

Table (V-III-16) Hemispherical Dome - Wind Load

R-Displacement = $-\alpha_3(pR^2/Et)$ Fig. (V-III-4)

$\mu = 0.2$; $R/t = 100.0$; $\theta = 30°$ meridian (Fig. (V-III-1))

Percentage Error

		← Membrane →								Flexure	
ϕ	Elasticity Solution	$\theta_e=\phi_e=15°$		$\theta_e=\phi_e=10°$		$\theta_e=\phi_e=5°$		$\theta_e=\phi_e=2.5°$		$\theta_e=\phi_e$ =5°	$\theta_e=\phi_e$ =2.5°
	α_3	Stat	Engy	Stat	Engy	Stat	Engy	Stat	Engy	Stat	Stat
0.0°	0.8660	22.78	23.68	15.53	15.90	7.69	7.74	3.89	3.90	4.63	1.45
2.5°	0.8944							-1.16	-1.16		0.49
5.0°	0.9192					-2.26	-2.25	0.16	0.17	0.24	-0.05
7.5°	0.9404							-0.18	-0.18		-0.23
10.0°	0.9580			-4.08	-3.97	0.36	0.37	-0.07	-0.07	-0.70	-0.22
12.5°	0.9719							-0.12	-0.12		-0.10
15.0°	0.9823	-5.77	-5.63			-0.30	-0.29	0.00	0.00	-0.34	0.00
17.5°	0.9892										
20.0°	0.9925			1.09	1.23	-0.07	-0.07			-0.14	
22.5°	0.9924										
25.0°	0.9888					-0.14	-0.15			-0.17	
27.5°	0.9819										
30.0°	0.9716	2.17	2.47	-0.14	-0.06	0.00	0.00			0.00	
35.0°	0.9415										
40.0°	0.8990			0.29	0.35						
45.0°	0.8448	-0.15	-0.23								
50.0°	0.7799			0.27	0.21						
55.0°	0.7051										
60.0°	0.6214	1.95	1.50	0.19	-0.26						
65.0°	0.5301										
70.0°	0.4321			1.23	0.28						
75.0°	0.3288	-6.84	-14.42								
80.0°	0.2215			-6.80	-14.43						
85.0°	0.1114										
90.0°	0.0000	0.00	0.00	0.00	0.00						

Stat. - Statics matrix

Engy. - Energy matrix

Table (V-III-17) Hemispherical Dome - Wind Load

R-Displacement = $-\alpha_3(pR^2/Et)$ Fig. (V-III-4)

$\mu = 0.0$; $R/t = 100.0$; $\theta = 60°$ meridian (Fig. (V-III-1))

Percentage Error

		← Membrane →								Flexure	
ϕ	Elasticity Solution	$\theta_e=\phi_e=15°$		$\theta_e=\phi_e=10°$		$\theta_e=\phi_e=5°$		$\theta_e=\phi_e=2.5°$		$\theta_e=\phi_e=5°$	$\theta_e=\phi_e=2.5°$
	α_3	Stat	Engy	Stat	Engy	Stat	Engy	Stat	Engy	Stat	Stat
0.0°	0.5000	23.54	24.44	16.08	16.44	8.04	8.08	4.08	4.08	4.80	
2.5°	0.5136							-1.21	-1.21		
5.0°	0.5253					-2.36	-2.34	0.19	0.19	0.25	
7.5°	0.5351							-0.17	-0.17		
10.0°	0.5430			-4.37	-4.27	0.39	0.41	-0.07	-0.07	-0.74	
12.5°	0.5490							-0.11	-0.11		
15.0°	0.5531	-6.16	-6.06			-0.33	-0.31	0.00	0.00	-0.36	
17.5°	0.5554										
20.0°	0.5558			1.06	1.19	-0.05	-0.05			-0.13	
22.5°	0.5544										
25.0°	0.5513					-0.15	-0.16			-0.16	
27.5°	0.5463										
30.0°	0.5396	2.15	2.41	-0.28	-0.20	0.00	0.00			0.00	
35.0°	0.5212										
40.0°	0.4964			0.18	0.20						
45.0°	0.4654	-0.39	-0.56								
50.0°	0.4288			0.14	0.02						
55.0°	0.3870										
60.0°	0.3407	2.00	1.32	0.03	-0.50						
65.0°	0.2902										
70.0°	0.2364			1.23	0.13						
75.0°	0.1798	-8.56	-17.02								
80.0°	0.1210			-8.51	-17.03						
85.0°	0.0609										
90.0°	0.0000	0.00	0.00	0.00	0.00						

Stat. - Statics matrix

Engy. - Energy matrix

Table (V-III-18) Hemispherical Dome - Wind Load

R-Displacement = $-\alpha_3(pR^2/Et)$ Fig. (V-III-4)

μ - 0.2; R/t = 100.0; θ = 60° meridian (Fig. (V-III-1))

Percentage Error

		← Membrane →								Flexure	
ϕ	Elasticity Solution	$\theta_e=\phi_e=15°$		$\theta_e=\phi_e=10°$		$\theta_e=\phi_e=5°$		$\theta_e=\phi_e=2.5°$		$\theta_e=\phi_e$ =5°	$\theta_e=\phi_e$ =2.5°
	α_3	Stat	Engy	Stat	Engy	Stat	Engy	Stat	Engy	Stat	Stat
0.0°	0.5000	22.48	23.38	15.38	15.74	7.68	7.74	3.90	3.90	4.62	
2.5°	0.5164							-1.16	-1.16		
5.0°	0.5307					-2.26	-2.26	0.17	0.17	0.21	
7.5°	0.5429							-0.17	-0.17		
10.0°	0.5531			-4.19	-4.09	0.34	0.34	-0.07	-0.07	-0.72	
12.5°	0.5611							-0.11	-0.11		
15.0°	0.5671	-5.94	-5.78			-0.32	-0.32	0.00	0.00	-0.35	
17.5°	0.5711										
20.0°	0.5730			0.94	1.08	-0.07	-0.07			-0.16	
22.5°	0.5730										
25.0°	0.5709					-0.18	-0.18			-0.19	
27.5°	0.5669										
30.0°	0.5610	1.91	2.19	-0.30	-0.21	0.00	0.00			0.00	
35.0°	0.5436										
40.0°	0.5190			0.15	0.21						
45.0°	0.4878	-0.41	-0.49								
50.0°	0.4503			0.11	0.04						
55.0°	0.4071										
60.0°	0.3588	1.70	1.23	0.06	-0.39						
65.0°	0.3060										
70.0°	0.2495			1.04	0.12						
75.0°	0.1898	-7.06	-14.65								
80.0°	0.1279			-6.96	-14.54						
85.0°	0.0643										
90.0°	0.0000	0.00	0.00	0.00	0.00						

Stat. - Statics matrix

Engy. - Energy matrix

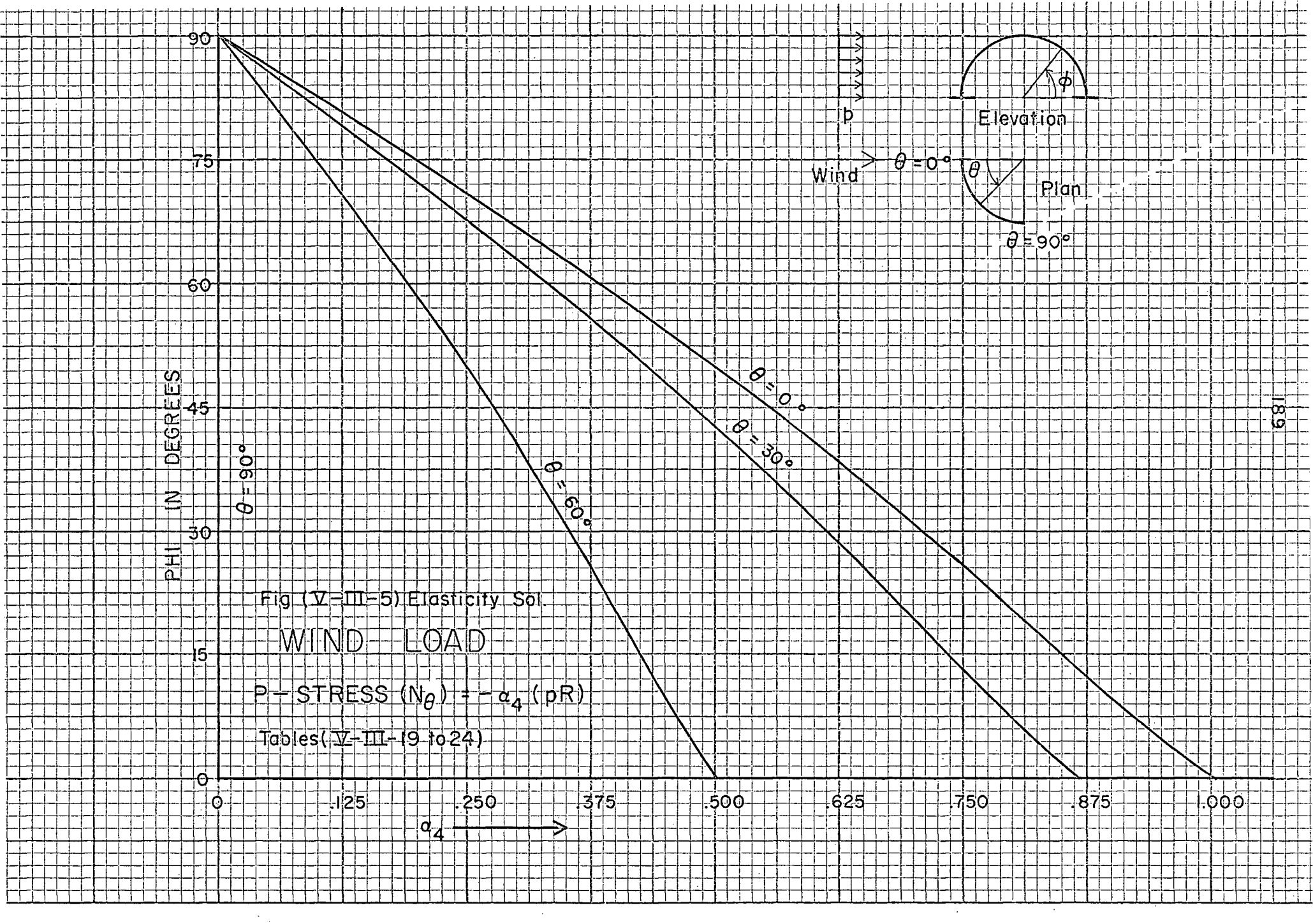
90
75
60
45
30
15
0
PHI IN DEGREES
θ=90°
θ=60°
θ=30°
θ=0°
0
.125
.250
.375
.500
.625
.750
.875
1.000
α4
Fig (V-III-5) Elasticity Sol.
WIND LOAD
P-STRESS (Nθ) = -α4 (pR)
Tables (V-III-19 to 24)
p
Wind
θ=0°
Elevation
φ
θ
Plan
θ=90°

Table (V-III-19) Hemispherical Dome - Wind Load

P-Force/length, $(N_\theta) = -\alpha_4(pR)$ Fig. (V-III-5)

$\mu = 0.0$; $R/t = 100.0$; $\theta = 0°$ meridian (Fig. (V-III-1))

Percentage Error

		← Membrane →								Flexure	
ϕ	Elasticity Solution	$\theta_e=\phi_e=15°$		$\theta_e=\phi_e=10°$		$\theta_e=\phi_e=5°$		$\theta_e=\phi_e=2.5°$		$\theta_e=\phi_e$ =5°	$\theta_e=\phi_e$ =2.5°
	α_4	Stat	Engy	Stat	Engy	Stat	Engy	Stat	Engy	Stat	Stat
0.0°	1.0000	-1.76	-1.76	-0.72	-0.72	-0.35	-0.38	-0.13	-0.13	-1.51	-1.27
2.5°	0.972							-0.13	-0.14		0.61
5.0°	0.945					-0.32	-0.35	-0.13	-0.14	0.91	0.04
7.5°	0.920							-0.13	-0.14		-0.21
10.0°	0.895			-0.79	-0.79	-0.30	-0.34	-0.13	-0.14	-0.63	-0.24
12.5°	0.871							-0.14	-0.15		-0.14
15.0°	0.847	-1.91	-1.91			-0.31	-0.35			-0.53	
17.5°	0.824										
20.0°	0.800			-0.84	-0.84	-0.28	-0.32			-0.29	
22.5°	0.777										
25.0°	0.753					-0.28	-0.33			-0.25	
27.5°	0.730										
30.0°	0.706	-1.96	-1.96	-0.84	-0.84						
35.0°	0.656										
40.0°	0.605			-0.84	-0.84						
45.0°	0.552	-1.90	-1.90								
50.0°	0.497			-0.80	-0.80						
55.0°	0.440										
60.0°	0.381	-1.58	-1.58	-0.69	-0.69						
65.0°	0.321										
70.0°	0.258			-0.32	-0.32						
75.0°	0.195	1.15	1.15								
80.0°	0.130			2.53	2.53						
85.0°	0.065										
90.0°	0.000										

Stat. - Statics matrix

Engy. - Energy matrix

Table (V-III-20) Hemispherical Dome - Wind Load

P-Force/Length, $(N_\theta) = -\alpha_4(pR)$ Fig. (V-III-5)

$\mu = 0.2$; $R/t = 100.0$; $\theta = 0°$ meridian (Fig. (V-III-1))

Percentage Error

		← Membrane →								Flexure	
ϕ	Elasticity Solution	$\theta_e=\phi_e=15°$		$\theta_e=\phi_e=10°$		$\theta_e=\phi_e=5°$		$\theta_e=\phi_e=2.5°$		$\theta_e=\phi_e=5°$	$\theta_e=\phi_e=2.5°$
	α_4	Stat	Engy	Stat	Engy	Stat	Engy	Stat	Engy	Stat	Stat
0.0°	1.000	-1.76	-1.76	-0.72	-0.72	-0.35	-0.38	-0.12	-0.13	-1.45	-1.18
2.5°	0.972							-0.12	-0.13		0.60
5.0°	0.945					-0.32	-0.35	-0.13	-0.13	+0.87	0.02
7.5°	0.920							-0.13	-0.14		-0.23
10.0°	0.895			-0.79	-0.79	-0.31	-0.34	-0.13	-0.14	-0.62	-0.25
12.5°	0.871							-0.13	-0.14		-0.15
15.0°	0.847	-1.91	-1.91			-0.31	-0.35			-0.53	
17.5°	0.824										
20.0°	0.800			-0.84	-0.84	-0.28	-0.32			-0.32	
22.5°	0.777										
25.0°	0.753					-0.28	-0.33			-0.28	
27.5°	0.730										
30.0°	0.706	-1.96	-1.96	-0.84	-0.84						
35.0°	0.656										
40.0°	0.605			-0.84	-0.84						
45.0°	0.552	-1.90	-1.90								
50.0°	0.497			-0.80	-0.80						
55.0°	0.440										
60.0°	0.381	-1.58	-1.58	-0.69	-0.69						
65.0°	0.321										
70.0°	0.258			-0.32	-0.31						
75.0°	0.195	1.15	1.15								
80.0°	0.130			2.53	2.53						
85.0°	0.065										
90.0°	0.000										

Stat. - Statics matrix

Engy. - Energy matrix

Table (V-III-21) Hemispherical Dome - Wind Load

P-Force/Length, $(N_\theta) = -\alpha_4(pR)$ Fig. (V-III-5)

$\mu = 0.0$; $R/t = 100.0$; $\theta = 30°$ meridian (Fig. (V-III-1))

Percentage Error

		← Membrane →								Flexure	
ϕ	Elasticity Solution	$\theta_e=\phi_e=15°$		$\theta_e=\phi_e=10°$		$\theta_e=\phi_e=5°$		$\theta_e=\phi_e=2.5°$		$\theta_e=\phi_e$ =5°	$\theta_e=\phi_e$ =2.5°
	α_4	Stat	Engy	Stat	Engy	Stat	Engy	Stat	Engy	Stat	Stat
0.0°	0.866										
2.5°	0.842							-0.13	-0.14		0.62
5.0°	0.818					-0.33	-0.36	-0.13	-0.14	0.90	0.02
7.5°	0.796							-0.13	-0.14		-0.23
10.0°	0.775			-0.81	-0.81	-0.30	-0.34	-0.13	-0.14	-0.63	-0.24
12.5°	0.754							-0.14	-0.15		-0.14
15.0°	0.734	-1.95	-1.95			-0.30	-0.34			-0.53	
17.5°	0.713										
20.0°	0.693			-0.86	-0.86	-0.29	-0.33			-0.31	
22.5°	0.673										
25.0°	0.653					-0.28	-0.33			-0.27	
27.5°	0.632										
30.0°	0.611	-1.99	-1.99	-0.86	-0.86						
35.0°	0.568										
40.0°	0.524			-0.85	-0.85						
45.0°	0.478	-1.91	-1.91								
50.0°	0.431			-0.80	-0.80						
55.0°	0.381										
60.0°	0.330	-1.54	-1.54	-0.67	-0.67						
65.0°	0.278										
70.0°	0.224			-0.27	-0.27						
75.0°	0.169	1.30	1.30								
80.0°	0.113			2.64	2.64						
85.0°	0.057										
90.0°											

Stat. - Statics matrix

Engy. - Energy matrix

Table (V-III-22) Hemispherical Dome - Wind Load

P-Force/Length, $(N_\theta) = -\alpha_4(pR)$ Fig. (V-III-5)

$\mu = 0.2$; $R/t = 100.0$; $\theta = 30°$ meridian (Fig. (V-III-1))

Percentage Error

		← Membrane →								Flexure	
ϕ	Elasticity Solution	$\theta_e=\phi_e=15°$		$\theta_e=\phi_e=10°$		$\theta_e=\phi_e=5°$		$\theta_e=\phi_e=2.5°$		$\theta_e=\phi_e=5°$	$\theta_e=\phi_e=2.5°$
	α_4	Stat	Engy	Stat	Engy	Stat	Engy	Stat	Engy	Stat	Stat
0.0°	0.866										
2.5°	0.842							-0.13	-0.13		0.60
5.0°	0.818					-0.33	-0.36	-0.13	-0.13	0.86	0.01
7.5°	0.796							-0.13	-0.14		-0.24
10.0°	0.775			-0.81	-0.81	-0.31	-0.34	-0.13	-0.14	-0.62	-0.25
12.5°	0.754							-0.13	-0.14		-0.14
15.0°	0.734	-1.95	-1.95			-0.31	-0.34			-0.53	
17.5°	0.713										
20.0°	0.693			-0.86	-0.86	-0.29	-0.33			-0.32	
22.5°	0.673										
25.0°	0.653					-0.29	-0.34			-0.28	
27.5°	0.632										
30.0°	0.611	-1.99	-1.99	-0.86	-0.86						
35.0°	0.568										
40.0°	0.524			-0.85	-0.85						
45.0°	0.478	-1.91	-1.91								
50.0°	0.431			-0.80	-0.80						
55.0°	0.381										
60.0°	0.330	-1.54	-1.54	-0.67	-0.67						
65.0°	0.278										
70.0°	0.224			-0.27	-0.27						
75.0°	0.169	1.30	1.30								
80.0°	0.113			2.64	2.64						
85.0°	0.057										
90.0°	0.000										

Stat. - Statics matrix

Engy. - Energy matrix

Table (V-III-23) Hemispherical Dome - Wind Load

P-Force/Length, $(N_\theta) = -\alpha_4(pR)$ Fig. (V-III-5)

$\mu = 0.0$; $R/t = 100.0$; $\theta = 60°$ meridian (Fig. (V-III-1))

Percentage Error

		← Membrane →								Flexure	
ϕ	Elasticity Solution	$\theta_e=\phi_e=15°$		$\theta_e=\phi_e=10°$		$\theta_e=\phi_e=5°$		$\theta_e=\phi_e=2.5°$		$\theta_e=\phi_e$ =5°	$\theta_e=\phi_e$ =2.5°
	α_4	Stat	Engy	Stat	Engy	Stat	Engy	Stat	Engy	Stat	Stat
0.0°	0.500										
2.5°	0.486							-0.14	-0.14		
5.0°	0.473					-0.35	-0.38	-0.13	-0.14	0.88	
7.5°	0.460							-0.14	-0.15		
10.0°	0.447			-0.90	-0.90	-0.33	-0.36	-0.14	-0.15	-0.65	
12.5°	0.435							-0.15	-0.16		
15.0°	0.424	-2.12	-2.12			-0.34	-0.38			-0.56	
17.5°	0.412										
20.0°	0.400			-0.93	-0.93	-0.31	-0.35			-0.33	
22.5°	0.389										
25.0°	0.377					-0.31	-0.36			-0.29	
27.5°	0.365										
30.0°	0.353	-2.08	-2.08	-0.90	-0.90						
35.0°	0.328										
40.0°	0.303			-0.87	-0.87						
45.0°	0.276	-1.90	-1.90								
50.0°	0.249			-0.78	-0.78						
55.0°	0.220										
60.0°	0.191	-1.38	-1.38	-0.59	-0.59						
65.0°	0.160										
70.0°	0.129			-0.12	-0.13						
75.0°	0.097	1.77	1.77								
80.0°	0.065			2.96	2.94						
85.0°	0.033										
90.0°											

Stat. - Statics matrix

Engy. - Energy matrix

Table (V-III-24) Hemispherical Dome - Wind Load

P-Force/Length, $(N_\theta) = -\alpha_4(pR)$ Fig. (V-III-5)

$\mu = 0.2$; R/t = 100.0; $\theta = 60°$ meridian (Fig. (V-III-1))

Percentage Error

		Membrane								Flexure	
ϕ	Elasticity Solution	$\theta_e=\phi_e=15°$		$\theta_e=\phi_e=10°$		$\theta_e=\phi_e=5°$		$\theta_e=\phi_e=2.5°$		$\theta_e=\phi_e=5°$	$\theta_e=\phi_e=2.5°$
	α_4	Stat	Engy	Stat	Engy	Stat	Engy	Stat	Engy	Stat	Stat
0.0°	0.500										
2.5°	0.486							-0.13	-0.14		
5.0°	0.473					-0.35	-0.38	-0.13	-0.14	0.84	
7.5°	0.460							-0.14	-0.15		
10.0°	0.447			-0.90	-0.90	-0.33	-0.36	-0.14	-0.15	-0.65	
12.5°	0.435							-0.15	-0.16		
15.0°	0.424	-2.12	-2.12			-0.34	-0.38			-0.56	
17.5°	0.412										
20.0°	0.400			-0.93	-0.93	-0.31	-0.35			-0.35	
22.5°	0.389										
25.0°	0.377					-0.32	-0.36			-0.31	
27.5°	0.365										
30.0°	0.353	-2.08	-2.08	-0.90	-0.90						
35.0°	0.328										
40.0°	0.303			-0.87	-0.87						
45.0°	0.276	-1.91	-1.91								
50.0°	0.249			-0.78	-0.78						
55.0°	0.220										
60.0°	0.191	-1.38	-1.38	-0.59	-0.59						
65.0°	0.160										
70.0°	0.129			-0.13	-0.12						
75.0°	0.097	1.77	1.77								
80.0°	0.065			2.96	2.94						
85.0°	0.033										
90.0°	0.000										

Stat. - Statics matrix

Engy. - Energy matrix

Fig. (V-III-7) Elasticity Sol.

WIND LOAD

SHEAR STRESS ($N_{\theta\phi}$) = $+\alpha_6(pR)$

Tables (V-III-30 to 36)

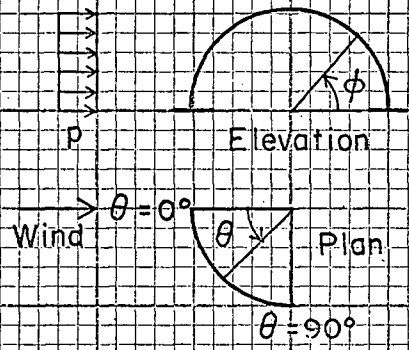

Fig. (V-III-6) Elasticity Sol.

WIND LOAD

M-STRESS (N_ϕ) = $-\alpha_5(pR)$

Tables (V-III-25 to 30)

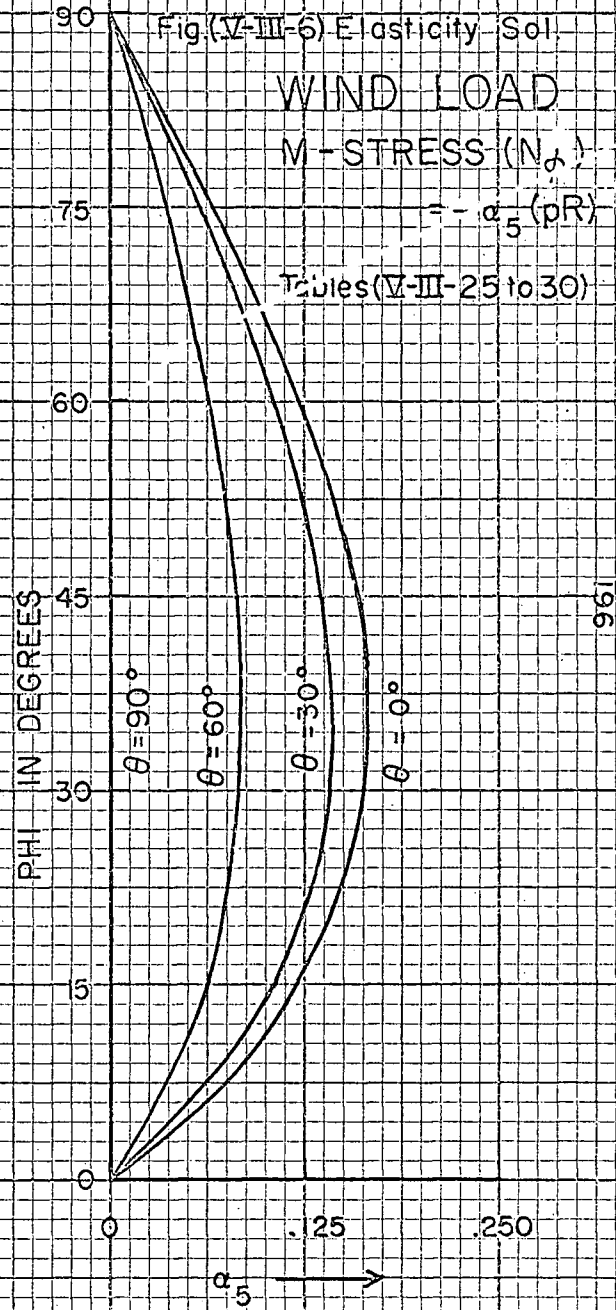

196

Table (V-III-25) Hemispherical Dome - Wind Load

M-Force/Length, $(N_\phi) = -\alpha_5(pR)$ Fig. (V-III-6)

$\mu = 0.0$; $R/t = 100.0$; $\theta = 0°$ meridian (Fig. (V-III-1))

Percentage Error

		← Membrane →								Flexure	
ϕ	Elasticity Solution	$\theta_e=\phi_e=15°$		$\theta_e=\phi_e=10°$		$\theta_e=\phi_e=5°$		$\theta_e=\phi_e=2.5°$		$\theta_e=\phi_e=5°$	$\theta_e=\phi_e=2.5°$
	α_5	Stat	Engy	Stat	Engy	Stat	Engy	Stat	Engy	Stat	Stat
0.0°	0.000	0.00	0.00	0.00	0.00	0.00	0.00	0.00	0.00	0.00	0.00
2.5°	0.027							2.61	2.90		3.04
5.0°	0.051					0.51	1.08	1.35	1.49	-0.14	1.51
7.5°	0.072							0.92	1.02		1.01
10.0°	0.090			-1.89	-1.96	0.07	0.39	0.72	0.80	-0.42	0.79
12.5°	0.106							0.61	0.67		0.69
15.0°	0.119	-4.39	-4.62			-0.17	0.08	0.51	0.57	-0.45	0.56
17.5°	0.130										
20.0°	0.139			-1.40	-1.55	-0.15	0.07			-0.45	
22.5°	0.147										
25.0°	0.153					-0.23	-0.03			-0.54	
27.5°	0.157										
30.0°	0.160	-3.33	-3.95	-1.79	-2.06	-0.37	-0.17			-0.47	
35.0°	0.163										
40.0°	0.161			-1.93	-2.44						
45.0°	0.155	-4.95	-6.46								
50.0°	0.146			-2.40	-3.39						
55.0°	0.133										
60.0°	0.119	-8.00	-13.12	-3.10	-5.18						
65.0°	0.102										
70.0°	0.084			-6.67	-12.50						
75.0°	0.064	-4.44	-12.63								
80.0°	0.043			-2.76	-11.60						
85.0°	0.022										
90.0°	0.000										

Stat. - Statics matrix

Engy. - Energy matrix

Table (V-III-26) Hemispherical Dome - Wind Load

M-Force/Length, $(N_\phi) = -\alpha_5(pR)$ Fig. (V-III-6)

$\mu = 0.2$; $R/t = 100.0$; $\theta = 0°$ meridian (Fig. (V-III-1))

Percentage Error

		← Membrane →								Flexure	
ϕ	Elasticity Solution	$\theta_e=\phi_e=15°$		$\theta_e=\phi_e=10°$		$\theta_e=\phi_e=5°$		$\theta_e=\phi_e=2.5°$		$\theta_e=\phi_e=5°$	$\theta_e=\phi_e=2.5°$
	α_5	Stat	Engy	Stat	Engy	Stat	Engy	Stat	Engy	Stat	Stat
0.0°	0.000	0.00	0.00	0.00	0.00	0.00	0.00	0.00	0.00	0.00	0.00
2.5°	0.027							2.53	2.79		2.86
5.0°	0.051					0.55	1.08	1.31	1.45	-0.12	1.41
7.5°	0.072							0.88	0.99		0.93
10.0°	0.090			-1.83	-1.90	0.10	0.40	0.69	0.77	-0.40	0.73
12.5°	0.106							0.57	0.64		0.62
15.0°	0.119	-4.29	-4.53			-0.14	0.09	0.44	0.51	-0.41	0.47
17.5°	0.130										
20.0°	0.139			-1.39	-1.54	-0.12	0.08			-0.41	
22.5°	0.147										
25.0°	0.153					-0.20	-0.01			-0.38	
27.5°	0.157										
30.0°	0.160	-3.35	-4.00	-1.79	-2.07	-0.34	-0.16			-0.35	
35.0°	0.163										
40.0°	0.161			-1.96	-2.49						
45.0°	0.155	-5.08	-6.65								
50.0°	0.146			-2.49	-3.52						
55.0°	0.133										
60.0°	0.119	-8.37	-13.70	-3.32	-5.47						
65.0°	0.102										
70.0°	0.084			-7.12	-13.15						
75.0°	0.064	-8.79	-17.78								
80.0°	0.043			-7.27	-16.95						
85.0°	0.022										
90.0°	0.000										

Stat. - Statics matrix

Engy. - Energy matrix

Table (V-III-27) Hemispherical Dome - Wind Load

M-Force/Length, $(N_\phi) = -\alpha_5(pR)$ Fig. (V-III-6)

$\mu = 0.0$; $R/t = 100.0$; $\theta = 30°$ meridian (Fig. (V-III-1))

Percentage Error

		← Membrane →								Flexure	
ϕ	Elasticity Solution	$\theta_e=\phi_e=15°$		$\theta_e=\phi_e=10°$		$\theta_e=\phi_e=5°$		$\theta_e=\phi_e=2.5°$		$\theta_e=\phi_e$ =5°	$\theta_e=\phi_e$ =2.5°
	α_5	Stat	Engy	Stat	Engy	Stat	Engy	Stat	Engy	Stat	Stat
0.0°	0.000	0.00	0.00	0.00	0.00	0.00	0.00	0.00	0.00	0.00	0.00
2.5°	0.024							2.58	2.84		2.97
5.0°	0.044					0.41	0.63	1.33	1.47	-0.20	1.67
7.5°	0.062							0.92	1.01		1.20
10.0°	0.078			-2.05	-2.12	0.06	0.04	0.71	0.78	-0.44	0.90
12.5°	0.091							0.59	0.67		0.72
15.0°	0.103	-4.75	-4.98			-0.15	-0.17	0.53	0.58	-0.43	0.59
17.5°	0.113										
20.0°	0.121			-1.54	-1.69	-0.24	-0.19			-0.46	
22.5°	0.127										
25.0°	0.132					-0.30	-0.25			-0.49	
27.5°	0.136										
30.0°	0.139	-3.64	-4.26	-1.92	-2.20	-0.39	-0.30			-0.39	
35.0°	0.141										
40.0°	0.139			-2.08	-2.59						
45.0°	0.134	-5.30	-6.82								
50.0°	0.126			-2.55	-3.54						
55.0°	0.116										
60.0°	0.103	-8.46	-13.60	-3.29	-5.37						
65.0°	0.088										
70.0°	0.072			-6.87	-12.71						
75.0°	0.055	-5.16	-13.38								
80.0°	0.037			-3.42	-12.30						
85.0°	0.019										
90.0°											

Stat. - Statics matrix

Engy. - Energy matrix

Table (V-III-28) Hemispherical Dome - Wind Load

M-Force/Length, $(N_\phi) = -\alpha_5(pR)$ Fig. (V-III-6)

$\mu = 0.2$; $R/t = 100.0$; $\theta = 30°$ meridian (Fig. (V-III-1))

Percentage Error

		← Membrane →								Flexure	
ϕ	Elasticity Solution	$\theta_e=\phi_e=15°$		$\theta_e=\phi_e=10°$		$\theta_e=\phi_e=5°$		$\theta_e=\phi_e=2.5°$		$\theta_e=\phi_e=5°$	$\theta_e=\phi_e=2.5°$
	α_5	Stat	Engy	Stat	Engy	Stat	Engy	Stat	Engy	Stat	Stat
0.0°	0.000	0.00	0.00	0.00	0.00	0.00	0.00	0.00	0.00	0.00	0.00
2.5°	0.024							2.50	2.75		2.75
5.0°	0.044					0.45	0.97	1.27	1.42	-0.20	1.54
7.5°	0.062							0.87	0.96		1.08
10.0°	0.078			-2.00	-2.07	0.09	0.39	0.67	0.76	-0.44	0.89
12.5°	0.091							0.55	0.62		0.63
15.0°	0.103	-4.66	-4.89			-0.11	0.12	0.46	0.53	-0.43	0.50
17.5°	0.113										
20.0°	0.121			-1.53	-1.68	-0.21	-0.01			-0.45	
22.5°	0.127										
25.0°	0.132					-0.26	-0.08			-0.45	
27.5°	0.136										
30.0°	0.139	-3.66	-4.31	-1.92	-2.20	-0.35	-0.17			-0.38	
35.0°	0.141										
40.0°	0.139			-2.11	-2.64						
45.0°	0.134	-5.43	-7.00								
50.0°	0.126			-2.63	-3.67						
55.0°	0.116										
60.0°	0.103	-8.84	-14.71	-3.51	-5.67						
65.0°	0.088										
70.0°	0.072			-7.33	-13.37						
75.0°	0.055	-9.48	-18.51								
80.0°	0.037			-7.97	-17.65						
85.0°	0.019										
90.0°	0.000										

Stat. - Statics matrix

Engy. - Energy matrix

Table (V-III-29) Hemispherical Dome - Wind Load

M-Force/Length, $(N_\phi) = -\alpha_5(pR)$ Fig. (V-III-6)

$\mu = 0.0$; $R/t = 100.0$; $\theta = 60°$ meridian (Fig. (V-III-1))

Percentage Error

		← Membrane →								Flexure	
ϕ	Elasticity Solution	$\theta_e=\phi_e=15°$		$\theta_e=\phi_e=10°$		$\theta_e=\phi_e=5°$		$\theta_e=\phi_e=2.5°$		$\theta_e=\phi_e=5°$	$\theta_e=\phi_e=2.5°$
	α_5	Stat	Engy	Stat	Engy	Stat	Engy	Stat	Engy	Stat	Stat
0.0°	0.000	0.00	0.00	0.00	0.00	0.00	0.00	0.00	0.00	0.00	
2.5°	0.014							2.42	2.64		
5.0°	0.026					0.08	0.63	1.25	1.41	-0.66	
7.5°	0.036							0.86	0.97		
10.0°	0.045			-3.25	-3.31	-0.27	0.04	0.67	0.76	-0.73	
12.5°	0.053							0.59	0.65		
15.0°	0.059	-6.95	-7.17			-0.40	-0.17	0.52	0.59	-0.64	
17.5°	0.065										
20.0°	0.070			-2.44	-2.58	-0.40	-0.19			-0.62	
22.5°	0.073										
25.0°	0.076					-0.45	-0.25			-0.61	
27.5°	0.079										
30.0°	0.080	-5.47	-6.11	-2.76	-3.03	-0.51	-0.30			-0.61	
35.0°	0.081										
40.0°	0.080			-2.91	-3.42						
45.0°	0.077	-7.19	-8.72								
50.0°	0.073			-3.44	-4.44						
55.0°	0.067										
60.0°	0.059	-10.71	-15.87	-4.31	-6.38						
65.0°	0.051										
70.0°	0.042			-8.17	-14.03						
75.0°	0.032	-8.19	-16.48								
80.0°	0.022			-5.00	-13.89						
85.0°	0.011										
90.0°	0.000										

Stat. - Statics matrix

Engy. - Energy matrix

Table (V-III-30) Hemispherical Dome - Wind Load

M-Force/Length, $(N_\phi) = -\alpha_5(pR)$ Fig. (V-III-6)

$\mu = 0.2$; $R/t = 100.0$; $\theta = 60°$ meridian (Fig. (V-III-1))

Percentage Error

		← Membrane →								Flexure	
ϕ	Elasticity Solution	$\theta_e=\phi_e=15°$		$\theta_e=\phi_e=10°$		$\theta_e=\phi_e=5°$		$\theta_e=\phi_e=2.5°$		$\theta_e=\phi_e=5°$	$\theta_e=\phi_e=2.5°$
	α_5	Stat	Engy	Stat	Engy	Stat	Engy	Stat	Engy	Stat	Stat
0.0°	0.000	0.00	0.00	0.00	0.00	0.00	0.00	0.00	0.00	0.00	
2.5°	0.014							2.35	2.57		
5.0°	0.026					0.08	0.63	1.21	1.37	-0.63	
7.5°	0.036							0.83	0.95		
10.0°	0.045			-3.18	-3.25	-0.25	0.07	0.65	0.73	-0.71	
12.5°	0.053							0.57	0.65		
15.0°	0.059	-6.84	-7.06			-0.39	-0.15	0.56	0.61	-0.62	
17.5°	0.065										
20.0°	0.070			-2.43	-2.58	-0.37	-0.17			-0.60	
22.5°	0.073										
25.0°	0.076					-0.41	-0.24			-0.63	
27.5°	0.079										
30.0°	0.080	-5.50	-6.15	-2.76	-3.03	-0.45	-0.27			-0.61	
35.0°	0.081										
40.0°	0.080			-2.94	-3.47						
45.0°	0.077	-7.31	-8.90								
50.0°	0.073			-3.52	-4.56						
55.0°	0.067										
60.0°	0.059	-11.08	-16.43	-4.53	-6.68						
65.0°	0.051										
70.0°	0.042			-8.63	-14.67						
75.0°	0.032	-12.38	-21.45								
80.0°	0.022			-9.58	-19.26						
85.0°	0.011										
90.0°	0.000										

Stat. - Statics matrix

Engy. - Energy matrix

Table (V-III-31) Hemispherical Dome - Wind Load

Membrane Shear, $(N_{\theta\phi}) = \alpha_6(pR)$ Fig. (V-III-7)

$\mu = 0.0$; $R/t = 100.0$; $\theta = 30°$ meridian (Fig. (V-III-1))

Percentage Error

		← Membrane →								Flexure	
ϕ	Elasticity Solution	$\theta e=\phi e=15°$		$\theta e=\phi e=10°$		$\theta e=\phi e=5°$		$\theta e=\phi e=2.5°$		$\theta e=\phi e=5°$	$\theta e=\phi e=2.5°$
	α_6	Stat	Engy	Stat	Engy	Stat	Engy	Stat	Engy	Stat	Stat
0.0°	0.333	-0.78	-0.80	-0.31	-0.31	-0.24	-0.24	-0.06	-0.06	-0.22	-0.06
2.5°	0.312							-0.03	-0.05		0.05
5.0°	0.293					-0.14	-0.22	-0.03	-0.06	-0.12	0.03
7.5°	0.275							-0.04	-0.05		-0.01
10.0°	0.259			-0.02	-0.32	-0.17	-0.24	-0.04	-0.05	-0.22	-0.04
12.5°	0.244							-0.05	-0.06		-0.07
15.0°	0.229	-0.31	-0.93			-0.20	-0.25			-0.21	
17.5°	0.216										
20.0°	0.204			-0.17	-0.41	-0.25	-0.28			-0.24	
22.5°	0.192										
25.0°	0.181					-0.28	-0.29			-0.32	
27.5°	0.170										
30.0°	0.160	-0.68	-1.15	-0.26	-0.47						
35.0°	0.142										
40.0°	0.125			-0.29	-0.47						
45.0°	0.109	-0.70	-1.14								
50.0°	0.095			-0.24	-0.41						
55.0°	0.081										
60.0°	0.069	0.03	-0.57	0.02	-0.19						
65.0°	0.056										
70.0°	0.045			1.01	0.61						
75.0°	0.033	-13.11	-0.21								
80.0°	0.022			-11.99	1.14						
85.0°	0.011										
90.0°	0.000										

Stat. - Statics matrix

Engy. - Energy matrix

Table (V-III-32) Hemispherical Dome - Wind Load

Membrane Shear, $(N_{\theta\phi}) = \alpha_6(pR)$ Fig. (V-III-7)

$\mu = 0.2$; $R/t = 100.0$; $\theta = 30°$ meridian (Fig. (V-III-1))

Percentage Error

		← Membrane →								Flexure	
ϕ	Elasticity Solution	$\theta_e=\phi_e=15°$		$\theta_e=\phi_e=10°$		$\theta_e=\phi_e=5°$		$\theta_e=\phi_e=2.5°$		$\theta_e=\phi_e=5°$	$\theta_e=\phi_e=2.5°$
	α_6	Stat	Engy	Stat	Engy	Stat	Engy	Stat	Engy	Stat	Stat
0.0°	0.333	-0.79	-0.79	-0.31	-0.31	-0.23	-0.23	-0.06	-0.06	-0.21	0.00
2.5°	0.312							-0.04	-0.05		0.03
5.0°	0.293					-0.15	-0.22	-0.03	-0.05	-0.13	0.00
7.5°	0.275							-0.04	-0.05		-0.03
10.0°	0.259			-0.15	-0.40	-0.17	-0.23	-0.04	-0.05	-0.22	-0.05
12.5°	0.244							-0.03	-0.05		-0.06
15.0°	0.229	-0.62	-1.16			-0.21	-0.25			-0.21	-0.19
17.5°	0.216										
20.0°	0.204			-0.26	-0.48	-0.24	-0.28			-0.23	
22.5°	0.192										
25.0°	0.181					-0.27	-0.29			-0.30	
27.5°	0.170										
30.0°	0.160	-0.93	-1.42	-0.39	-0.61						
35.0°	0.142										
40.0°	0.125			-0.45	-0.67						
45.0°	0.109	-1.11	-1.66								
50.0°	0.095			-0.43	-0.67						
55.0°	0.081										
60.0°	0.069	-0.54	-1.30	-0.22	-0.50						
65.0°	0.056										
70.0°	0.045			0.67	0.23						
75.0°	0.033	-7.95	3.87								
80.0°	0.022			-6.52	5.65						
85.0°	0.011										
90.0°	0.000										

Stat. - Statics matrix

Engy. - Energy matrix

Table (V-III-33) Hemispherical Dome - Wind Load

Membrane Shear, $(N_{\theta\phi}) = \alpha_6(pR)$ Fig. (V-III-7)

$\mu = 0.0$; $R/t = 100.0$; $\theta = 60°$ meridian (Fig. (V-III-1))

Percentage Error

		← Membrane →								Flexure	
ϕ	Elasticity Solution	$\theta_e=\phi_e=15°$		$\theta_e=\phi_e=10°$		$\theta_e=\phi_e=5°$		$\theta_e=\phi_e=2.5°$		$\theta_e=\phi_e$ =5°	$\theta_e=\phi_e$ =2.5°
	α_6	Stat	Engy	Stat	Engy	Stat	Engy	Stat	Engy	Stat	Stat
0.0°	0.577	-0.88	-0.88	-0.36	-0.36	-0.24	-0.24	-0.06	-0.07	-0.21	
2.5°	0.541							-0.03	-0.06		
5.0°	0.508					-0.15	-0.33	-0.04	-0.06	-0.12	
7.5°	0.477							-0.03	-0.05		
10.0°	0.449			-0.07	-0.37	-0.18	-0.25	-0.03	-0.05	-0.22	
12.5°	0.422							-0.03	-0.04		
15.0°	0.398	-0.39	-1.01			-0.20	-0.25			-0.20	
17.5°	0.374										
20.0°	0.353			-0.19	-0.44	-0.23	-0.26			-0.20	
22.5°	0.332										
25.0°	0.313					-0.26	-0.27			-0.25	
27.5°	0.295										
30.0°	0.278	-0.68	-1.15	-0.25	-0.46						
35.0°	0.246										
40.0°	0.217			-0.24	-0.43						
45.0°	0.190	-0.55	-0.99								
50.0°	0.165			-0.12	-0.30						
55.0°	0.141										
60.0°	0.119	0.47	-0.15	0.24	0.03						
65.0°	0.098										
70.0°	0.077			1.43	1.01						
75.0°	0.057	-11.77	1.20								
80.0°	0.038			-11.32	1.87						
85.0°	0.019										
90.0°	0.000										

Stat. - Statics matrix

Engy. - Energy matrix

Table (V-III-34) Hemispherical Dome - Wind Load

Membrane Shear, $(N_{\theta\phi}) = \alpha_6(pR)$ Fig. (V-III-7)

$\mu = 0.2$; $R/t = 100.0$; $\theta = 60°$ meridian (Fig. (V-III-1))

Percentage Error

		← Membrane →								Flexure	
ϕ	Elasticity Solution	$\theta_e=\phi_e=15°$		$\theta_e=\phi_e=10°$		$\theta_e=\phi_e=5°$		$\theta_e=\phi_e=2.5°$		$\theta_e=\phi_e$ =5°	$\theta_e=\phi_e$ =2.5°
	α_6	Stat	Engy	Stat	Engy	Stat	Engy	Stat	Engy	Stat	Stat
0.0°	0.577	-0.88	-0.88	-0.36	-0.36	-0.23	-0.23	-0.06	-0.06	-0.21	
2.5°	0.541							-0.04	-0.06		
5.0°	0.508					-0.17	-0.23	-0.04	-0.05	-0.14	
7.5°	0.477							-0.03	-0.05		
10.0°	0.449			-0.19	-0.44	-0.18	-0.24	-0.03	-0.05	-0.23	
12.5°	0.422							-0.03	-0.04		
15.0°	0.397	-0.70	-1.24			-0.21	-0.25			-0.21	
17.5°	0.374										
20.0°	0.353			-0.28	-0.50	-0.23	-0.27			-0.21	
22.5°	0.332										
25.0°	0.313					-0.26	-0.28			-0.24	
27.5°	0.295										
30.0°	0.278	-0.93	-1.41	-0.39	-0.60						
35.0°	0.246										
40.0°	0.217			-0.40	-0.62						
45.0°	0.190	-0.95	-1.51								
50.0°	0.165			-0.31	-0.56						
55.0°	0.141										
60.0°	0.119	-0.09	-0.88	0.01	-0.28						
65.0°	0.098										
70.0°	0.077			1.09	0.64						
75.0°	0.057	-6.61	5.28								
80.0°	0.038			-5.87	6.37						
85.0°	0.019										
90.0°	0.000										

Stat. - Statics matrix

Engy. - Energy matrix

Table (V-III-35) Hemispherical Dome - Wind Load

Membrane Shear, $(N_{\theta\phi}) = \alpha_6(pR)$ Fig. (V-III-7)

$\mu = 0.0$; $R/t = 100.0$; $\theta = 90°$ meridian (Fig. (V-III-1))

Percentage Error

		← Membrane								Flexure	
ϕ	Elasticity Solution	$\theta_e=\phi_e=15°$		$\theta_e=\phi_e=10°$		$\theta_e=\phi_e=5°$		$\theta_e=\phi_e=2.5°$		$\theta_e=\phi_e=5°$	$\theta_e=\phi_e=2.5°$
	α_6	Stat	Engy	Stat	Engy	Stat	Engy	Stat	Engy	Stat	Stat
0.0°	0.667	-1.28	-1.28	-0.57	-0.57	-0.31	-0.31	-0.08	-0.09	-0.27	
2.5°	0.625							-0.04	-0.06		
5.0°	0.586					-0.18	-0.26	-0.04	-0.06	-0.15	
7.5°	0.551							-0.03	-0.05		
10.0°	0.518			-0.15	-0.45	-0.20	-0.26	-0.03	-0.04	-0.23	
12.5°	0.487							-0.01	-0.03		
15.0°	0.459	-0.47	-1.10			-0.20	-0.25			-0.19	
17.5°	0.432										
20.0°	0.407			-0.19	-0.44	-0.20	-0.23			-0.16	
22.5°	0.384										
25.0°	0.362					-0.19	-0.20			-0.14	
27.5°	0.341										
30.0°	0.321	-0.52	-1.00	-0.17	-0.38						
35.0°	0.284										
40.0°	0.250			-0.07	-0.26						
45.0°	0.219	-0.11	-0.56								
50.0°	0.190			0.15	-0.03						
55.0°	0.163										
60.0°	0.137	1.28	0.66	0.63	0.44						
65.0°	0.113										
70.0°	0.089			1.98	1.57						
75.0°	0.066	-9.88	3.14								
80.0°	0.044			-10.81	2.42						
85.0°	0.022										
90.0°	0.000										

Stat. - Statics matrix

Engy. - Energy matrix

Table (V-III-36) Hemispherical Dome - Wind Load

Membrane Shear, $(N_{\theta\phi}) = \alpha_6(pR)$ Fig. (V-III-7)

$\mu = 0.2$; $R/t = 100.0$; $\theta = 90°$ meridian (Fig. (V-III-1))

Percentage Error

		← Membrane →								Flexure	
ϕ	Elasticity Solution	$\theta_e=\phi_e=15°$		$\theta_e=\phi_e=10°$		$\theta_e=\phi_e=5°$		$\theta_e=\phi_e=2.5°$		$\theta_e=\phi_e=5°$	$\theta_e=\phi_e=2.5°$
	α_6	Stat	Engy	Stat	Engy	Stat	Engy	Stat	Engy	Stat	Stat
0.0°	0.667	-1.30	-1.30	-0.58	-0.58	-0.30	-0.30	-0.08	-0.08	-0.26	
2.5°	0.625							-0.05	-0.06		
5.0°	0.586					-0.20	-0.27	-0.04	-0.06	-0.16	
7.5°	0.551							-0.03	-0.05		
10.0°	0.518			-0.27	-0.53	-0.20	-0.25	-0.03	-0.04	-0.24	
12.5°	0.487							-0.02	-0.04		
15.0°	0.459	-0.78	-1.32			-0.20	-0.25			-0.21	
17.5°	0.432										
20.0°	0.407			-0.29	-0.51	-0.20	-0.23			-0.18	
22.5°	0.384										
25.0°	0.362					-0.18	-0.20			-0.20	
27.5°	0.341										
30.0°	0.321	-0.78	-1.27	-0.31	-0.52						
35.0°	0.284										
40.0°	0.250			-0.23	-0.45						
45.0°	0.219	-0.51	-1.08								
50.0°	0.190			-0.04	-0.28						
55.0°	0.163										
60.0°	0.137	0.71	-0.09	0.41	0.12						
65.0°	0.113										
70.0°	0.089			1.66	1.19						
75.0°	0.066	-4.73	7.22								
80.0°	0.044			-5.49	6.79						
85.0°	0.022										
90.0°	0.000										

Stat. - Statics matrix

Engy. - Energy matrix

Table (V-III-37) Hemispherical Dome - Wind Load

Bending Moments; M_θ, M_ϕ (Kip-inch/inch)

At $\theta = 0°$ Meridian; $\theta_e = \phi_e = 5°$ Element Size

Radius = 100.0 inch; p = 0.001 Ksi

E = 1000.0 Ksi; $\mu = 0.2$

	Thickness = 1.0 in.		Thickness = 5.0 in.	
$\phi°$	M_θ	M_ϕ	M_θ	M_ϕ
0°	-0.00006	0.00000	-0.00211	0.00000
5°	-0.00002	0.00034	-0.00203	0.00036
10°	-0.00007	0.00001	-0.00210	-0.00039
15°	-0.00010	-0.00014	-0.00223	-0.00131
20°	-0.00010	-0.00013	-0.00233	-0.00198
25°	-0.00010	-0.00010	-0.00234	-0.00232
30°	-0.0009	-0.00009	-0.00229	-0.00239
35°	-0.00008	-0.00008	-0.00218	-0.00229
40°	-0.00008	-0.00008	-0.00204	-0.00212
45°	-0.00007	-0.00007	-0.00187	-0.00192
50°	-0.00007	-0.00007	-0.00169	-0.00171
55°	-0.00006	-0.00006	-0.00151	-0.00151
60°	-0.00005	-0.00005	-0.00132	-0.00131
65°	-0.00004	-0.00004	-0.00111	-0.00093
70°	-0.00003	-0.00004	-0.00090	-0.00086
75°	-0.00003	-0.00002	-0.00068	-0.00063
80°	-0.00002	-0.00000	-0.00020	-0.00017
85°	-0.00000	-0.00000	-0.00000	-0.00000
90°				

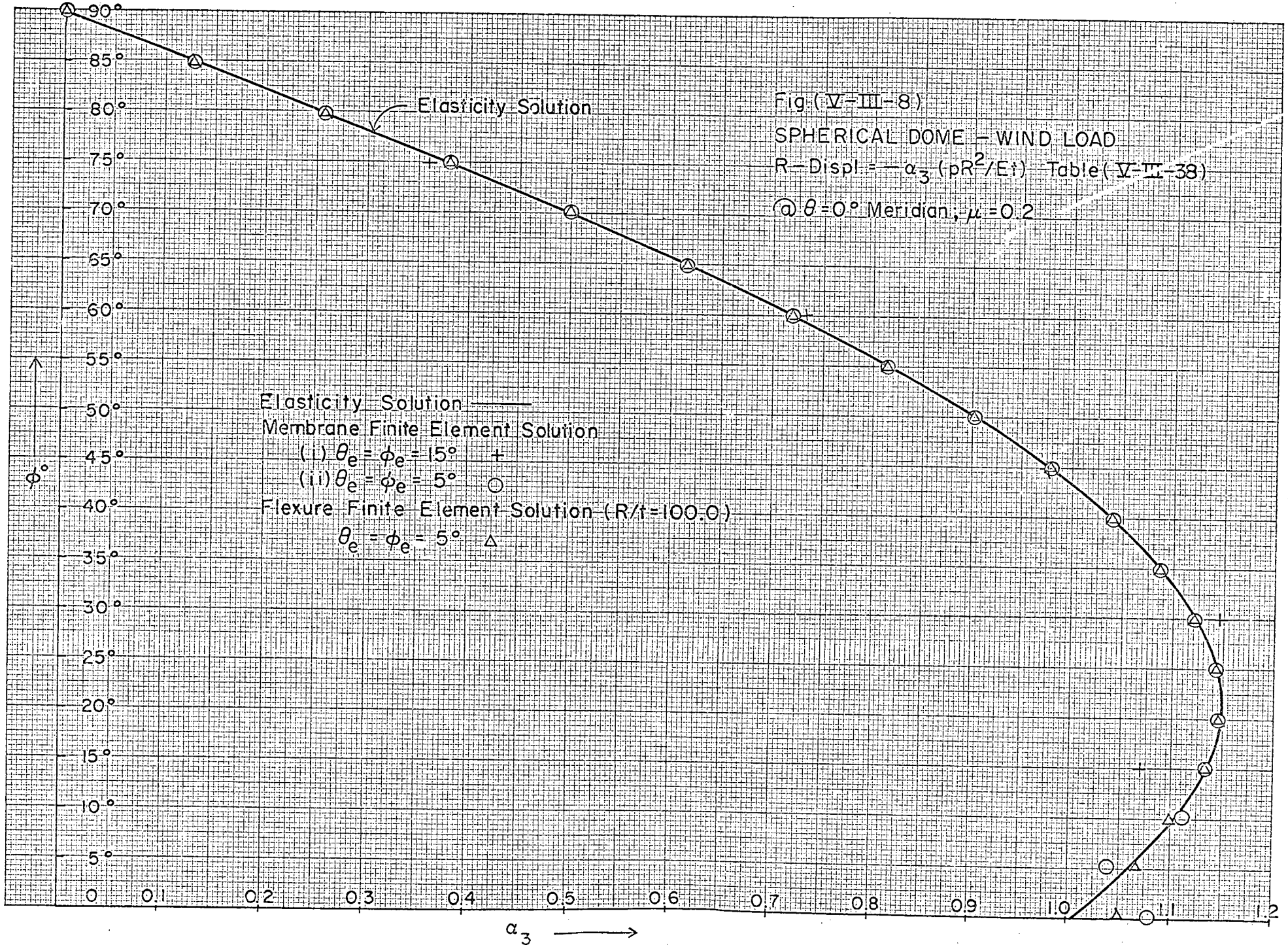
Fig (V-III-8)
SPHERICAL DOME - WIND LOAD
R-Displ = $-\alpha_3 (pR^2/Et)$ Table (V-III-38)
@ $\theta = 0°$ Meridian, $\mu = 0.2$
Elasticity Solution
Elasticity Solution ——
Membrane Finite Element Solution
(i) $\theta_e = \phi_e = 15°$ +
(ii) $\theta_e = \phi_e = 5°$ ○
Flexure Finite Element Solution (R/t=100.0)
$\theta_e = \phi_e = 5°$ △
$\phi°$
α_3
90° 85° 80° 75° 70° 65° 60° 55° 50° 45° 40° 35° 30° 25° 20° 15° 10° 5° 0
0.1 0.2 0.3 0.4 0.5 0.6 0.7 0.8 0.9 1.0 1.1 1.2 +
210

Table (V-III-38) Hemispherical Dome - Wind Load

R-Diaplacement = $-\alpha_3(\gamma R/Et)$; Fig. (V-III-8)

At $\theta = 0°$ Meridian; $\theta_e = \phi_e = 5°$ Element Size.

$\mu = 0.2$; Radius = 100.0 in.; Thickness = t in.

		F.E. Solution α_3		
	Elasticity Sol.	Membrane Sol.	Flexure Sol.	
$\phi°$	α_3	t=1.0, 5.0 in.	t=1.0 in.	t= 5.0 in.
0	1.0000	1.0786	1.0475	1.034
5	1.0614	1.0385	1.0646	1.0735
10	1.1062	1.1111	1.0990	1.1055
15	1.1343	1.1321	1.1309	1.129
20	1.1461	1.1461	1.1454	1.140
25	1.1418	1.1414	1.1414	1.137
30	1.1220	1.1218	1.1215	1.119
35	1.0871	1.0871	1.0867	1.0855
40	1.0380	1.0381	1.0378	1.0375
45	0.9755	0.9756	0.9754	0.9755
50	0.09005	0.9006	0.9005	0.9005
55	0.8142	0.8142	0.8142	0.8143
60	0.7176	0.7176	0.7176	0.7175
65	0.6121	0.6120	0.6121	0.612
70	0.4989	0.4987	0.4989	0.499
75	0.3797	0.3794	0.3793	0.3795
80	0.2557	0.2552	0.2551	0.255
85	0.1287	0.1286	0.1287	0.1285
90	0.0000	0.0000	0.0000	0.0000

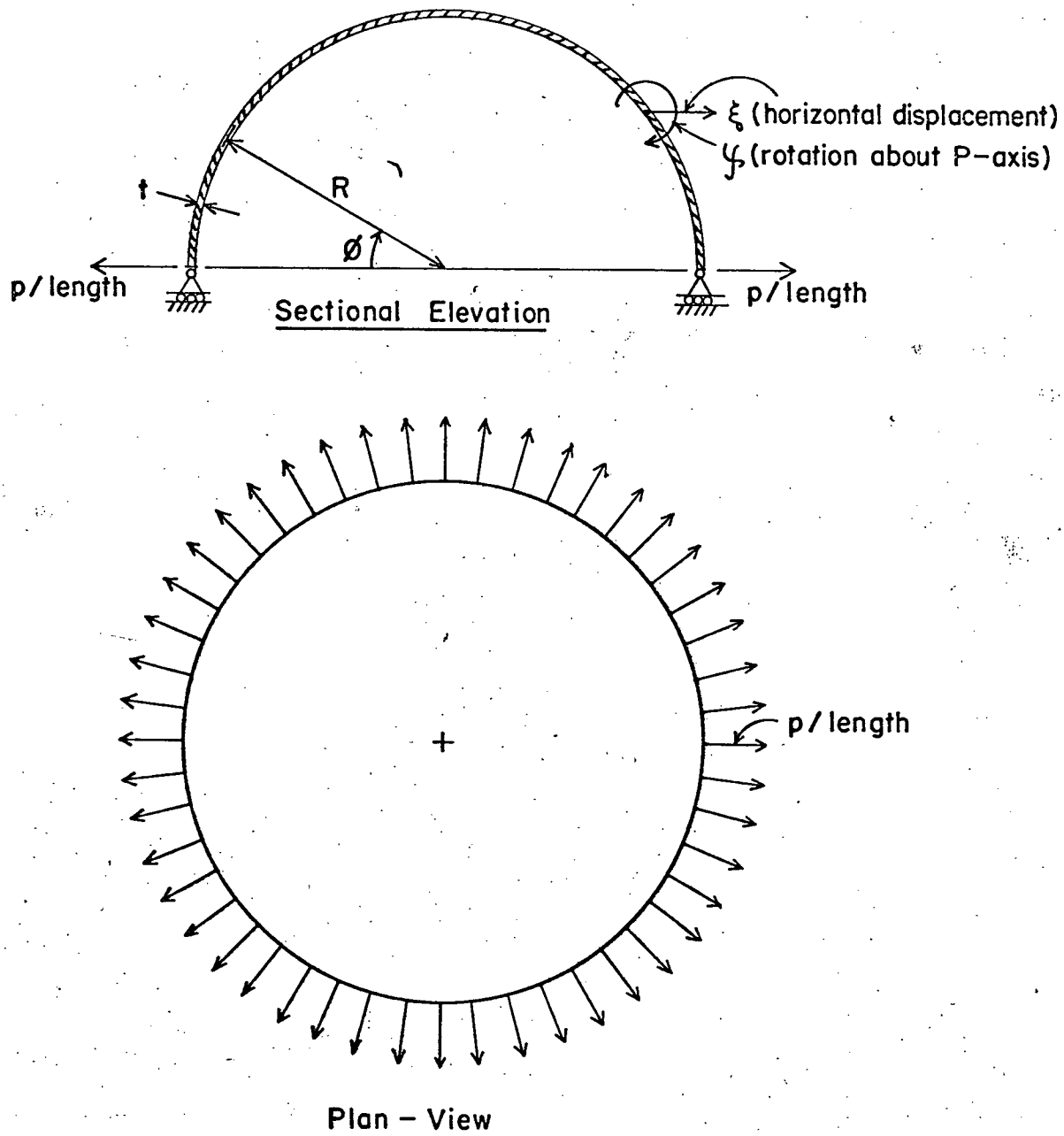

FIGURE V-IV-1. HEMISPHERICAL DOME SUBJECTED TO RADIAL LOAD ALONG THE ENTIRE EDGE.

5.6 Example IV Hemispherical Dome Subjected to Radial Load Applied Along the Entire Edge. Fig. (V-IV-1)

In the elasticity solution of this problem[35] allowing for flexure, the displacements, rotations, stresses, and moments are calculated for various values of (i) radius to thickness ratio (100.0 and 500.0), and (ii) Poisson's ratio (0.0 and 0.2). These are shown in Figs. (V-IV-2 to 25). Severe displacement and stress gradients are noticed in the base zone. These functions oscillate exponentially and die out at some distance from the base. As the R/t ratio increases, the height of the zone gets smaller and gradients steeper.

The shell is axisymmetrically loaded and is self supported. In view of the axisymmetry of the problem, it is sufficient in the finite element analysis to consider only the elements bounded by a pair of adjacent meridian lines. Statics type plane stress and flexure element stiffness matrices are used in the computation of results. Due to the presence of high displacement and stress gradients, it is necessary to use small sized elements to obtain a fair representation of the displacements and stresses. Since the membrane and flexure stresses die out at a comparatively short distance from the base, it is sufficient to analyse a model extending somewhat beyond the distance at which force-free boundary conditions may be applied.

Percentage error in the finite element solution using various element sizes for μ = 0.0 and 0.2 and R/t = 100.0 and 500.0 is calculated and shown in Tables (V-IV-1 to 24). Excellent results are obtained in the region of interest and remarkable convergence to the true solution is noticed on reduction of the element size. Higher percentage errors occur

at points where either the function changes sign or the value of the function is small compared to its value elsewhere. As expected, a higher percentage error is observed in stresses than in displacements.

For $\theta_e = \phi_e = 0.5°$ element size and radius to thickness ratio (R/t) of 100.0 the displacements, rotations, and stresses calculated by the F.E. solution differ from the elasticity solution by 2%. M_θ moment is calculated with an error of 5%. For R/t = 500.0, higher errors in the order of 5% are observed.

Fig. (V-IV-2) Elasticity Sol.

EDGE R FORCE

HORIZONTAL DISP. $(\xi) = \alpha_1 \left(\frac{R_p}{E_t}\right)$

$R/t = 100$
$\mu = 0.0$
} Table (V-IV-1)

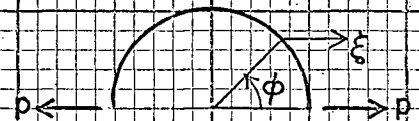

PHI IN DEGREES

30
25
20
15
10
5
0

0 3.0 6.0 9.0 12.0 15.0 18.0 21.0 24.0 27.0

α_1 ⟶

215

Table (V-IV-1) Hemispherical Dome - Radial Load Along the Edge

Horizontal Displacement, (ξ) = α_1(pR/Et)

μ = 0.0; R/t = 100.0 (Fig. (V-IV-2))

	Elasticity Solution	Percentage Error				Elasticty Solution	Percentage Error				Elasticity Solution	Percentage Error		
ϕ°	α_1	$\theta_e=\phi_e$ =2°	$\theta_e=\phi_e$ =1°	$\theta_e=\phi_e$ =0.5°	ϕ	α_1	$\theta_e=\phi_e$ =2°	$\theta_e=\phi_e$ =1°	$\theta_e=\phi_e$ =0.5°	ϕ	α_1	$\theta_e=\phi_e$ =2°	$\theta_e=\phi_e$ =1°	$\theta_e=\phi_e$ =0.5°
0.0	26.3215	- 1.67	-0.37	-0.11	8.5	-1.3761			0.79	17.0	-0.3664		1.93	1.92
0.5	23.3101			-0.12	9.0	-1.5669		2.41	0.79	17.5	-0.2879			1.96
1.0	20.3671		-0.30	-0.11	9.5	-1.6808			0.82	18.0	-0.2189	-2.88	1.32	1.97
1.5	17.5477			-0.11	10.0	-1.7309	7.38	2.19	0.86	18.5	-0.1591			1.89
2.0	14.8935	-1.21	-0.26	-0.10	10.5	-1.7293			0.91	19.0	-0.1080		-0.42	1.65
2.5	12.4331			-0.09	11.0	-1.6868		2.14	0.97	19.5	-0.0651			1.01
3.0	10.1850		-0.26	-0.08	11.5	-1.6128			1.04	20.0	-0.0295	-58.3	-9.95	-1.31
3.5	8.1589			-0.07	12.0	-1.5156	6.11	2.16	1.10	20.5	-0.0008			-32.10
4.0	6.3570	-1.91	-0.36	-0.07	12.5	-1.4024			1.19	21.0	0.0219		21.10	9.91
4.5	4.7761			-0.07	13.0	-1.2792		2.20	1.27	21.5	0.0393			7.39
5.0	3.4081		-0.70	-0.09	13.5	-1.1510			1.35	22.0	0.0521	36.54	10.72	6.80
5.5	2.2416			-0.14	14.0	-1.0219	5.05	2.23	1.43	22.5	0.0610			6.69
6.0	1.2629	-10.52	-2.18	-0.31	14.5	-0.8953			1.52	23.0	0.0664		8.95	6.79
6.5	0.4564			-1.09	15.0	-0.7736		2.24	1.61	23.5	0.0692			7.03
7.0	-0.1941		16.50	3.25	15.5	-0.6588			1.70	24.0	0.0696	22.44	8.39	7.33
7.5	-0.7053			1.10	16.0	-0.5521	3.03	2.16	1.78	24.5	0.0683			7.23
8.0	-1.0940	13.05	3.26	0.85	16.5	-0.4545			1.86	25.0	0.0656		8.24	8.18

Fig. (V-IV-3) Elasticity Sol.

EDGE R FORCE

HORIZONTAL DISP. $(\xi) = \alpha_1 \left(\frac{Rp}{Et}\right)$

$R/t = 100$
$\mu = 0.2$
} Table (V-IV-2)

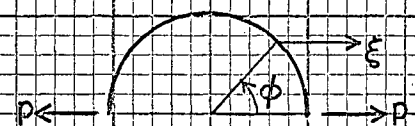

PHI IN DEGREES

30
25
20
15
10
5
0

0 3.0 6.0 9.0 12.0 15.0 18.0 21.0 24.0 27.0

α ⟶

Table (V-IV-2) Hemispherical Dome - Radial Load Along the Edge

Horizontal Displacement, $(\xi) = \alpha_1(pR/Et)$

$\mu = 0.2$; $R/t = 100.0$ (Fig. (V-IV-3))

	Elasticity Solution	Percentage Error				Elasticity Solution	Percentage Error				Elasticity Solution	Percentage Error		
$\phi°$	α_1	$\theta_e=\phi_e$ =2°	$\theta_e=\phi_e$ =1°	$\theta_e=\phi_e$ =0.5°	$\phi°$	α_1	$\theta_e=\phi_e$ =2°	$\theta_e=\phi_e$ =1°	$\theta_e=\phi_e$ =0.5°	$\phi°$	α_1	$\theta_e=\phi_e$ =2°	$\theta_e=\phi_e$ =1°	$\theta_e=\phi_e$ =0.5°
0.0	26.0542	-1.69	-0.42	-0.16	8.5	-1.3149			0.49	17.0	-0.3912		2.04	1.88
0.5	23.1021			-0.15	9.0	-1.5167		2.23	0.54	17.5	-0.3113			1.94
1.0	20.2162		-0.34	-0.14	9.5	-1.6415			0.61	18.0	-0.2405	-1.72	1.60	1.97
1.5	17.4500			-0.13	10.0	-1.7022	7.22	2.05	0.67	18.5	-0.1789			1.94
2.0	14.8431	-1.22	-0.28	-0.11	10.5	-1.7105			0.75	19.0	-0.1258		0.36	1.79
2.5	12.4238			-0.09	11.0	-1.6771		2.02	0.82	19.5	-0.0808			1.37
3.0	10.2099		-0.26	-0.06	11.5	-1.6112			0.90	20.0	-0.0432	-36.40	-4.99	0.11
3.5	8.2110			-0.04	12.0	-1.5211	5.99	2.06	0.98	20.5	-0.0125			-7.41
4.0	6.4298	-1.81	-0.32	-0.01	12.5	-1.4139			1.07	21.0	0.0121		32.96	14.87
4.5	4.8633			0.02	13.0	-1.2956		2.12	1.16	21.5	0.0313			8.26
5.0	3.5041		-0.57	0.05	13.5	-1.1713			1.25	22.0	0.0458	40.12	11.22	7.14
5.5	2.3416			0.08	14.0	-1.0452	5.04	2.18	1.35	22.5	0.0561			6.86
6.0	1.3627	-9.16	-1.69	0.10	14.5	-0.9206			1.43	23.0	0.0629		9.01	6.89
6.5	0.5526			0.05	15.0	-0.8001		2.22	1.53	23.5	0.0668			7.08
7.0	-0.1043		26.2	1.07	15.5	-0.6857			1.62	24.0	0.0683	22.87	8.38	7.37
7.5	-0.6239			0.44	16.0	-0.5788	3.27	2.19	1.71	24.5	0.0679			7.73
8.0	-1.0223	13.23	3.05	0.45	16.5	-0.4805			1.80	25.0	0.0659		8.23	7.90

Fig. (V-IV-4) Elasticity Sol.

EDGE R FORCE

HORIZONTAL DISP. $(\xi) = \alpha_1 \left(\frac{Rp}{Et}\right)$

$R/t = 500$
$\mu = 0.0$
} Table (V-IV-3)

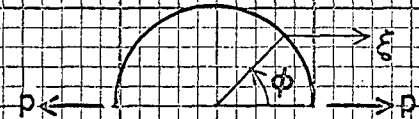

PHI IN DEGREES

30
25
20
15
10
5
0

0 8 16 24 32 40 48 56 64 72

α_1 ⟶

219

Table (V-IV-3) Hemispherical Dome - Radial Load Along the Edge

Horizontal Displacement, $(\xi) = \alpha_1(pR/Et)$

$\mu = 0.0$; $R/t = 500.0$ (Fig. (V-IV-4))

	Elasticity Solution	Percentage Error				Elasticity Solution	Percentage Error				Elasticity Solution	Percentage Error		
$\phi°$	α_1	$\theta_e=\phi_e$ =2°	$\theta_e=\phi_e$ =1°	$\theta_e=\phi_e$ =0.5°	$\phi°$	α_1	$\theta_e=\phi_e$ =2°	$\theta_e=\phi_e$ =1°	$\theta_e=\phi_e$ =0.5°	$\phi°$	α_1	$\theta_e=\phi_e$ =2°	$\theta_e=\phi_e$ =1°	$\theta_e=\phi_e$ =0.5°
0.0	58.8566	-8.36	-2.16	-0.53	8.5	-0.2512			4.24	17.0	-0.0070		38.17	9.59
0.5	44.0317			-0.45	9.0	-0.0512		-93.9	-25.6	17.5	-0.0063			8.10
1.0	30.6669		-1.58	-0.42	9.5	0.0733			18.71	18.0	-0.0053		25.82	6.83
1.5	19.5407			-0.52	10.0	0.1402		36.22	9.30	18.5	-0.0042			5.48
2.0	10.8905	-9.39	-3.31	-0.88	10.5	0.1656			6.93	19.0	-0.0030		14.21	3.87
2.5	4.6052			-2.15	11.0	0.1638		21.27	5.79	19.5	-0.0021			1.52
3.0	0.3768		-94.3	-27.35	11.5	0.1460			5.03	20.0	-0.0013		-6.53	-2.36
3.5	-2.1894			4.70	12.0	0.1203	69.20	14.85	4.40	20.5	-0.0007			
4.0	-3.4993	40.46	10.85	2.78	12.5	0.0927			3.77	21.0	-0.0002			
4.5	-3.9242			2.21	13.0	0.0667		8.00	3.00	21.5	0.0000			
5.0	-3.7767		7.39	1.92	13.5	0.0444			1.92	22.0	0.0002			
5.5	-3.3021			1.70	14.0	0.0265	-35.5	-5.99	0.11	22.5	0.0003			
6.0	-2.6807	25.13	5.51	1.49	14.5	0.0131			-3.83	23.0	0.0003			
6.5	-2.0352			1.21	15.0	0.0038		-94.1	-20.9	23.5	0.0003			
7.0	-1.4414		2.56	0.81	15.5	-0.0021			43.26	24.0	0.0002			
7.5	-0.9392			0.16	16.0	-0.0054		71.48	16.61	24.5	0.0002			
8.0	-0.5432	-17.09	-5.50	-1.09	16.5	-0.0068			11.81	25.0	0.0001			

Fig. (V-IV-5) Elasticity Sol.

EDGE R FORCE

HORIZONTAL DISP. $(\xi) = \alpha_1 \left(\frac{Rp}{Et}\right)$

$R/t = 500$
$\mu = 0.2$
} Table (V-IV-4)

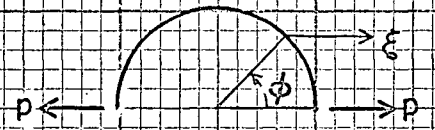

PHI IN DEGREES

30
25
20
15
10
5
0

0 8 16 24 32 40 48 56 64

α_1 ⟶

Table (V-IV-4) Hemispherical Dome - Radial Load Along the Edge

Horizontal Displacement, $(\xi) = \alpha_1 (pR/Et)$

$\mu = 0.2$; $R/t = 500.0$ (Fig. (V-IV-5))

	Elasticity Solution	Percentage Error				Elasticity Solution	Percentage Error				Elasticity Solution	Percentage Error		
ϕ°	α_1	$\theta_e=\phi_e$ =2°	$\theta_e=\phi_e$ =1°	$\theta_e=\phi_e$ =0.5°	ϕ°	α_1	$\theta_e=\phi_e$ =2°	$\theta_e=\phi_e$ =1°	$\theta_e=\phi_e$ =0.5°	ϕ°	α_1	$\theta_e=\phi_e$ =2°	$\theta_e=\phi_e$ =1°	$\theta_e=\phi_e$ =0.5°
0.0	58.2590	-8.22	-2.13	-0.54	8.5	-0.2918			-3.28	17.0	-0.0070		40.32	9.83
0.5	43.7273			-0.45	9.0	-0.0811		-63.8	-15.18	17.5	-0.0066			8.16
1.0	30.6028		-1.55	-0.42	9.5	0.0535			24.71	18.0	-0.0056		27.16	6.79
1.5	19.6416			-0.51	10.0	0.1288		39.0	9.94	18.5	-0.0045			5.38
2.0	11.0812	-9.02	-3.15	-0.84	10.5	0.1610			7.13	19.0	-0.0034		16.37	3.71
2.5	4.8237			-1.96	11.0	0.1640		21.75	5.88	19.5	-0.0024			1.22
3.0	0.5789		-66.35	-16.99	11.5	0.1493			5.10	20.0	-0.0015	-33.12		-2.69
3.5	-2.0298			4.85	12.0	0.1255	70.63	15.27	4.48	20.5	-0.0009			
4.0	-3.3931	40.61	10.89	2.77	12.5	0.0985			3.88	21.0	-0.0004			
4.5	-3.8712			2.18	13.0	0.0724		8.95	3.20	21.5	-0.0001			
5.0	-3.7693		7.32	1.89	13.5	0.0495			2.27	22.0	0.0001			
5.5	-3.3292			1.68	14.0	0.0308	-19.15	-2.79	0.80	22.5	0.0002			
6.0	-2.7303	24.91	5.52	1.48	14.5	0.0164			-2.09	23.0	0.0003			
6.5	-2.0962			1.23	15.0	0.0062		-60.24	-11.16	23.5	0.0003			
7.0	-1.5048		2.80	0.87	15.5	-0.0005				24.0	0.0002			
7.5	-0.9984			0.29	16.0	-0.0045		85.75	19.40	24.5	0.0002			
8.0	-0.5942	-12.37	-4.24	-0.77	16.5	-0.0065			12.52	25.0	0.0001			

Fig. (V-IV-6) Elasticity Sol.

EDGE R FORCE

P ROTATION (φ) $= -\alpha_2 \left(\frac{p}{Et}\right)$

R/t = 100
μ = 0.0
} Table (V-IV-5)

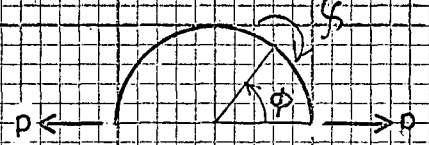

PHI IN DEGREES

30
25
20
15
10
5
0

0 50 100 150 200 250 300 350 400

α_2 ⟶

Table (V-IV-5) Hemispherical Dome - Radial Load Along the Edge

P-Rotation, $(\chi) = -\alpha_2(p/Et)$

$\mu = 0.0$; $R/t = 100.0$ (Fig. (V-IV-6))

	Elasticity Solution	Percentage Error				Elasticity Solution	Percentage Error				Elasticity Solution	Percentage Error		
ϕ°	α_2	$\theta_e=\phi_e$ =2°	$\theta_e=\phi_e$ =1°	$\theta_e=\phi_e$ =0.5°	ϕ°	α_2	$\theta_e=\phi_e$ =2°	$\theta_e=\phi_e$ =1°	$\theta_e=\phi_e$ =0.5°	ϕ°	α_2	$\theta_e=\phi_e$ =2°	$\theta_e=\phi_e$ =1°	$\theta_e=\phi_e$ =0.5°
0.0	346.409	-3.30	-0.73	-0.12	8.5	27.317			-0.10	17.0	-9.866		3.95	2.88
0.5	342.180			-0.08	9.0	17.660		-1.02	-0.47	17.5	-8.760			2.97
1.0	330.771		-0.40	-0.04	9.5	9.570			-1.43	18.0	-7.675	7.63	3.94	3.05
1.5	313.924			0.00	10.0	2.915	-37.5	-12.14	-6.42	18.5	-6.632			3.15
2.0	293.152	-1.04	-0.15	0.03	10.5	-2.442			9.54	19.0	-5.647		3.85	3.24
2.5	269.748			0.06	11.0	-6.643		7.29	4.09	19.5	-4.731			3.35
3.0	244.803		0.05	0.10	11.5	-9.825			3.11	20.0	-3.892	4.93	3.60	3.45
3.5	219.221			0.13	12.0	-12.124	12.55	4.65	2.73	20.5	-3.134			3.54
4.0	193.732	0.23	0.21	0.15	12.5	-13.665			2.57	21.0	-2.458		2.95	3.62
4.5	168.919			0.18	13.0	-14.569		4.09	2.50	21.5	-1.862			3.73
5.0	145.225		0.33	0.20	13.5	-14.944			2.49	22.0	-1.345	-4.77	1.40	3.81
5.5	122.978			0.22	14.0	-14.891	9.68	3.93	2.51	22.5	-0.903			3.76
6.0	102.405	0.75	0.39	0.23	14.5	-14.499			2.54	23.0	-0.530		-4.28	3.60
6.5	83.645			0.23	15.0	-13.846		3.91	2.60	23.5	-0.221			2.67
7.0	66.768		0.34	0.22	15.5	-13.002			2.65	24.0	0.030			19.67
7.5	51.785			0.17	16.0	-12.025	8.76	3.93	2.73	24.5	0.228			7.54
8.0	38.659	-0.43	0.06	0.08	16.5	-10.966			2.80	25.0	0.381		17.82	6.98

Fig. (V-IV-7) Elasticity Sol.

EDGE R FORCE

P – ROTATION (ς) = $-\alpha_2 \left(\frac{p}{Et}\right)$

R/t = 100

μ = 0.2

} Table (V-IV-6)

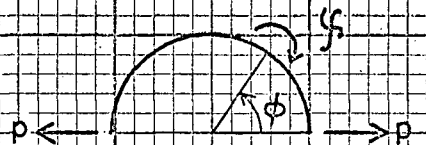

PHI IN DEGREES

30
25
20
15
10
5
0

0 50 100 150 200 250 300 350 400

α_2 →

Table (V-IV-6) Hemispherical Dome - Radial Load Along the Edge

P-Rotation, $(\chi) = -\alpha_2(p/Et)$

$\mu = 0.2$; $R/t = 100.0$ (Fig. (V-IV-7))

Elasticity Solution		Percentage Error			Elasticity Solution		Percentage Error			Elasticity Solution		Percentage Error		
$\phi°$	α_2	$\theta_e=\phi_e$ =2°	$\theta_e=\phi_e$ =1°	$\theta_e=\phi_e$ =0.5°	$\phi°$	α_2	$\theta_e=\phi_e$ =2°	$\theta_e=\phi_e$ =1°	$\theta_e=\phi_e$ =0.5°	$\phi°$	α_2	$\theta_e=\phi_e$ =2°	$\theta_e=\phi_e$ =1°	$\theta_e=\phi_e$ =0.5°
0.0	339.410	-3.29	-0.77	-0.17	8.5	28.562			-0.06	17.0	-10.041		3.91	2.82
0.5	335.347			-0.13	9.0	18.914		-0.88	-0.36	17.5	-8.967			2.91
1.0	324.373		-0.44	-0.09	9.5	10.792			-1.10	18.0	-7.904	7.67	3.93	3.01
1.5	308.148			-0.06	10.0	4.073	-25.1	-8.12	-4.10	18.5	-6.876			3.09
2.0	288.114	-1.09	-0.20	-0.02	10.5	-1.373			15.35	19.0	-5.898		3.86	3.19
2.5	265.507			0.01	11.0	-5.681		8.04	4.38	19.5	-4.982			3.30
3.0	241.372		-0.01	0.04	11.5	-8.981			3.15	20.0	-4.138	5.30	3.67	3.40
3.5	216.578			0.08	12.0	-11.403	12.75	4.72	2.72	20.5	-3.370			3.50
4.0	191.829	0.15	0.15	0.10	12.5	-13.069			2.54	21.0	-2.681		3.16	3.58
4.5	167.688			0.13	13.0	-14.095		4.07	2.46	21.5	-2.070			3.66
5.0	144.588		0.27	0.16	13.5	-14.587			2.44	22.0	-1.535	-2.61	1.95	3.76
5.5	122.850			0.18	14.0	-14.643	9.58	3.88	2.45	22.5	-1.074			3.76
6.0	102.699	0.68	0.33	0.19	14.5	-14.349			2.49	23.0	-0.682		-1.92	3.61
6.5	84.277			0.20	15.0	-13.784		3.86	2.54	23.5	-0.354			2.94
7.0	67.657		0.29	0.19	15.5	-13.016			2.60	24.0	-0.084	0.95	-51.4	-2.38
7.5	52.856			0.16	16.0	-12.104	8.67	3.88	2.66	24.5	0.133			10.00
8.0	39.846	-0.34	0.05	0.08	16.5	-11.098			2.74	25.0	0.302		20.8	8.15

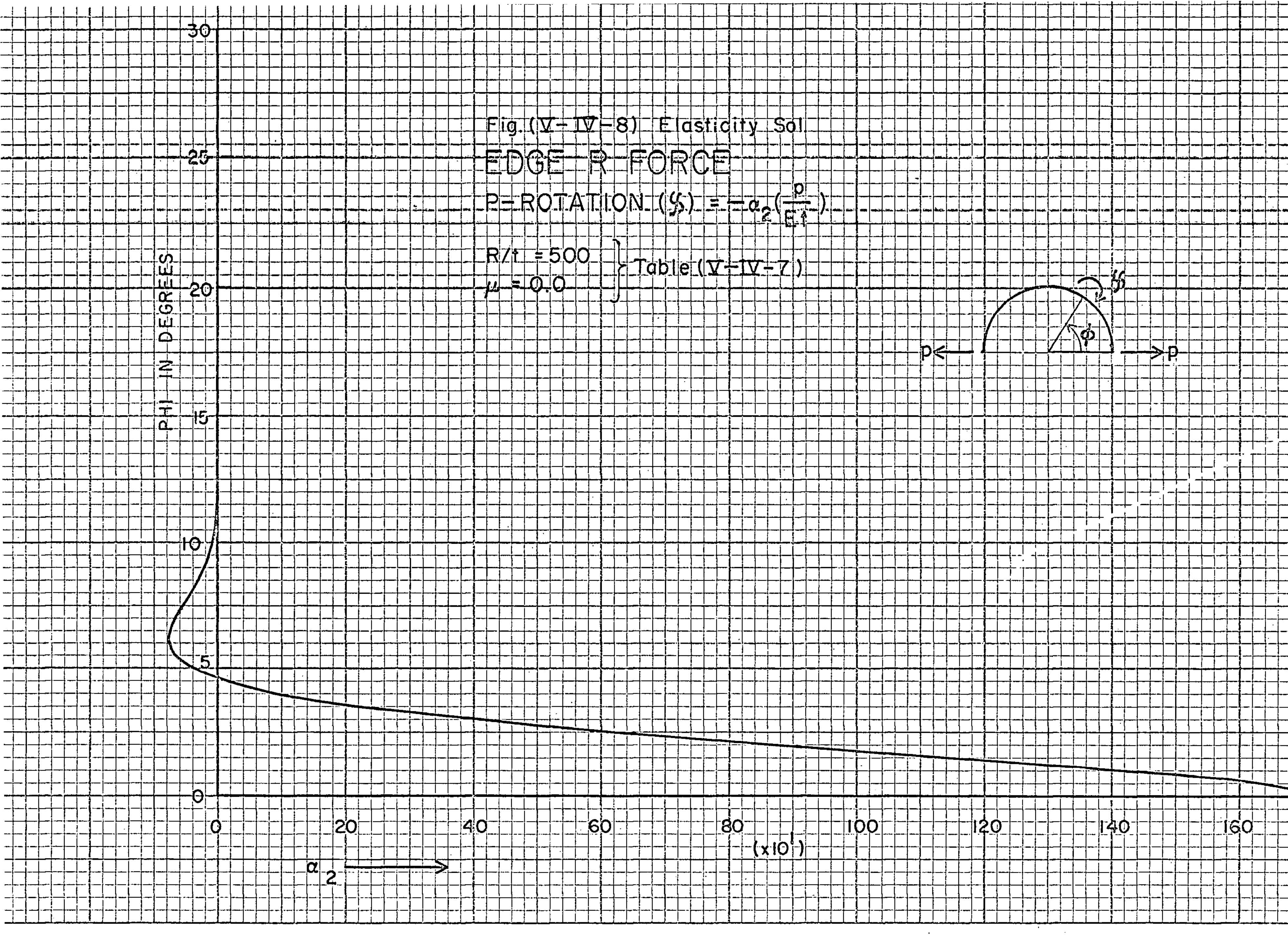

Fig. (V-IV-8) Elasticity Sol
EDGE R FORCE
P-ROTATION (ψ) = $-\alpha_2(\frac{p}{Et})$
R/t = 500
μ = 0.0
Table (V-IV-7)
PHI IN DEGREES
α_2
(x10^1)
0
5
10
15
20
25
30
20
40
60
80
100
120
140
160
p
p
ϕ
ψ

Table (V-IV-7) Hemispherical Dome - Radial Load Along the Edge

P-Rotation, $(\chi) = -\alpha_2(p/Et)$

$\mu = 0.0$; $R/t = 500.0$ (Fig. (V-IV-8)))

	Elasticity Solution	Percentage Error				Elasticity Solution	Percentage Error				Elasticity Solution	Percentage Error		
$\phi°$	α_2	$\theta_e=\phi_e$ =2°	$\theta_e=\phi_e$ =1°	$\theta_e=\phi_e$ =0.5°	$\phi°$	α_2	$\theta_e=\phi_e$ =2°	$\theta_e=\phi_e$ =1°	$\theta_e=\phi_e$ =0.5°	$\phi°$	α_2	$\theta_e=\phi_e$ =2°	$\theta_e=\phi_e$ =1°	$\theta_e=\phi_e$ =0.5°
0.0	1732.046	-16.02	-4.27	-1.06	8.5	-28.172			1.59	17.0	-0.036			55.8
0.5	1636.122			-0.62	9.0	-18.479		2.60	0.97	17.5	-0.105			19.91
1.0	1411.794		-1.24	-0.31	9.5	-10.794			-0.23	18.0	-0.135		53.00	14.27
1.5	1133.527			-0.09	10.0	-5.095	-46.70	-14.70	-3.21	18.5	-0.139			11.77
2.0	851.378	3.18	0.30	0.06	10.5	-1.165			-21.01	19.0	-0.127		35.24	10.19
2.5	595.696			0.13	11.0	1.305		82.43	21.40	19.5	-0.107			8.99
3.0	381.935		0.55	0.08	11.5	2.650			10.52	20.0	-0.085		24.25	7.64
3.5	215.068			-0.19	12.0	3.184		29.06	7.98	20.5	-0.062			6.33
4.0	93.284	-2.26	-4.12	-1.27	12.5	3.179			6.79	21.0	-0.042		10.80	4.72
4.5	10.899			-16.30	13.0	2.852		20.66	6.00	21.5	-0.026			1.59
5.0	-39.506		19.35	5.38	13.5	2.365			5.36	22.0	-0.014		-24.14	-3.29
5.5	-65.633			3.40	14.0	1.832	74.15	14.72	4.69	22.5	-0.005			
6.0	-74.569	42.17	10.40	2.86	14.5	1.327			3.89	23.0	0.001			
6.5	-72.308			2.59	15.0	0.889		5.94	2.78	23.5	0.004			
7.0	-63.577		8.64	2.41	15.5	0.536			0.88	24.0	0.006			
7.5	-51.866			2.22	16.0	0.270	-90.54	-20.44	-3.26	24.5	0.006			
8.0	-39.568	34.89	6.77	1.97	16.5	0.084			-19.93	25.0	0.006			

Fig. (V-IV-9) Elasticity Sol.

EDGE R FORCE

P = ROTATION (φ) = $-\alpha_2 \left(\frac{p}{E}\right)$

R/t = 500
μ = 0.2
} Table (V-IV-8)

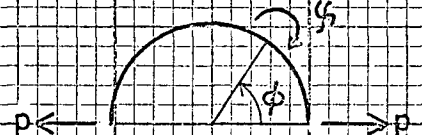

PHI IN DEGREES

30
25
20
15
10
5
0

0 20 40 60 80 100 120 140 160

α_2 ⟶ ($\times 10^1$)

Table (V-IV-8) Hemispherical Dome - Radial Load Along the Edge

P-Rotation, $(\chi) = -\alpha_2(p/Et)$

$\mu = 0.2$; $R/t = 500.0$ (Fig. (V-IV-9))

	Elasticity Solution	Percentage Error				Elasticity Solution	Percentage Error				Elasticity Solution	Percentage Error		
$\phi°$	α_2	$\theta_e=\phi_e$ =2°	$\theta_e=\phi_e$ =1°	$\theta_e=\phi_e$ =0.5°	$\phi°$	α_2	$\theta_e=\phi_e$ =2°	$\theta_e=\phi_e$ =1°	$\theta_e=\phi_e$ =0.5°	$\phi°$	α_2	$\theta_e=\phi_e$ =2°	$\theta_e=\phi_e$ =1°	$\theta_e=\phi_e$ =0.5°
0.0	1697.052	-15.74	-4.20	-1.06	8.5	-29.426			1.64	17.0	-0.001			
0.5	1604.798			-0.62	9.0	-19.698		3.12	1.10	17.5	-0.084			24.66
1.0	1388.463		-1.24	-0.32	9.5	-11.873			0.09	18.0	-0.125		58.16	15.70
1.5	1119.182			-0.11	10.0	-5.977	-31.75	-10.33	-2.24	18.5	-0.137			12.78
2.0	845.046	2.94	0.26	0.04	10.5	-1.832			-12.15	19.0	-0.131		36.95	10.90
2.5	595.467			0.11	11.0	0.845			31.28	19.5	-0.114			9.74
3.0	385.674		0.55	0.08	11.5	2.371			11.43	20.0	-0.092		26.15	8.65
3.5	220.837			-0.17	12.0	3.050		30.20	8.28	20.5	-0.070			7.42
4.0	99.560	-1.26	-3.52	-1.10	12.5	3.154			6.92	21.0	-0.049		14.17	5.87
4.5	16.639			-10.03	13.0	2.899		21.07	6.11	21.5	-0.032			3.29
5.0	-34.902		20.78	5.79	13.5	2.456			5.46	22.0	-0.019		-12.13	-2.66
5.5	-62.403			3.44	14.0	1.943	76.16	15.33	4.83	22.5	-0.009			
6.0	-72.689	41.60	10.35	2.85	14.5	1.440			4.11	23.0	-0.002			
6.5	-71.590			2.57	15.0	0.993		7.60	3.13	23.5	0.003			
7.0	-63.754		8.57	2.39	15.5	0.625			1.57	24.0	0.005			
7.5	-52.650			2.21	16.0	0.340	-66.54	-12.36	-1.46	24.5	0.006			
8.0	-40.695	34.49	6.83	1.98	16.5	0.135			-10.55	25.0	0.006			

Fig. (V-IV-10) Elasticity Sol.

EDGE R FORCE

P STRESS $(N_\theta) = \alpha_3(p)$

R/t = 100
μ = 0.0
} Table (V-IV-9)

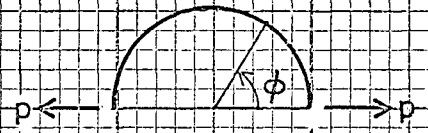

2311

PHI IN DEGREES

30
25
20
15
10
5
0

0 4 8 12 16 20 24 28 32

α_3 ⟶

Table (V-IV-9) Hemispherical Dome - Radial Load Along the Edge

P-Force/Length, $(N_\theta) = \alpha_3(p)$

$\mu = 0.0$; $R/t = 100.0$ (Fig. (V-IV-10))

	Elasticity Solution	Percentage Error				Elasticity Solution	Percentage Error				Elasticity Solution	Percentage Error		
$\phi°$	α_3	$\theta_e=\phi_e$ =2°	$\theta_e=\phi_e$ =1°	$\theta_e=\phi_e$ =0.5°	$\phi°$	α_3	$\theta_e=\phi_e$ =2°	$\theta_e=\phi_e$ =1°	$\theta_e=\phi_e$ =0.5°	$\phi°$	α_3	$\theta_e=\phi_e$ =2°	$\theta_e=\phi_e$ =1°	$\theta_e=\phi_e$ =0.5°
0.0	26.321	-2.05	-0.48	-0.15	8.5	-1.391			-0.31	17.0	-0.383		3.67	2.35
0.5	23.311			-0.06	9.0	-1.586		-0.88	-0.02	17.5	-0.302			2.51
1.0	20.370		0.09	-0.01	9.5	-1.704			0.19	18.0	-0.230	8.79	4.12	2.65
1.5	17.554			0.05	10.0	-1.758	-0.98	0.18	0.36	18.5	-0.168			2.80
2.0	14.903	1.82	0.59	0.12	10.5	-1.759			0.52	19.0	-0.114		4.63	2.90
2.5	12.445			0.19	11.0	-1.718		0.87	0.66	19.5	-0.069			2.91
3.0	10.199		1.17	0.28	11.5	-1.646			0.80	20.0	-0.031	6.54	5.49	2.49
3.5	8.174			0.38	12.0	-1.549	2.99	1.43	0.93	20.5	-0.001			-40.70
4.0	6.373	6.93	1.93	0.51	12.5	-1.436			1.06	21.0	0.023		4.60	5.84
4.5	4.791			0.67	13.0	-1.313		1.91	1.20	21.5	0.042			5.43
5.0	3.421		3.21	0.89	13.5	-1.184			1.33	22.0	0.056	14.59	5.50	5.50
5.5	2.252			1.24	14.0	-1.053	5.50	2.37	1.47	22.5	0.066			5.76
6.0	1.270	25.50	6.86	1.95	14.5	-0.925			1.61	23.0	0.072		6.06	6.07
6.5	0.459			4.57	15.0	-0.801		2.80	1.75	23.5	0.075			6.46
7.0	-0.196		-31.2	-8.64	15.5	-0.684			1.90	24.0	0.076	14.93	6.60	6.90
7.5	-0.711			-1.78	16.0	-0.574	7.42	3.23	2.05	24.5	0.075			7.38
8.0	-1.105	-13.39	-3.23	-0.76	16.5	-0.474			2.20	25.0	0.072		7.13	7.90

Fig. (V-IV-11) Elasticity Sol.

EDGE R FORCE

P — STRESS $(N_\theta) = \alpha_3(p)$

R/t = 100

μ = 0.2

} Table (V-IV-10)

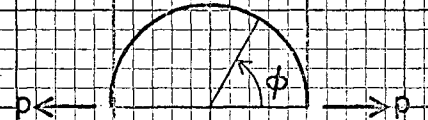

PHI IN DEGREES

30
25
20
15
10
5
0

0 4 8 12 16 20 24 28 32

α_3 →

Table (V-IV-10) Hemispherical Dome - Radial Load Along the Edge

P-Force/Length, $(N_\theta) = \alpha_3(p)$

$\mu = 0.2$; $R/t = 100.0$ (Fig. (V-IV-11))

	Elasticity Solution	Percentage Error				Elasticity Solution	Percentage Error				Elasticity Solution	Percentage Error		
ϕ°	α_3	$\theta_e=\phi_e$ =2°	$\theta_e=\phi_e$ =1°	$\theta_e=\phi_e$ =0.5°	ϕ°	α_3	$\theta_e=\phi_e$ =2°	$\theta_e=\phi_e$ =1°	$\theta_e=\phi_e$ =0.5°	ϕ°	α_3	$\theta_e=\phi_e$ =2°	$\theta_e=\phi_e$ =1°	$\theta_e=\phi_e$ =0.5°
0.0	26.054	-2.11	-0.58	-0.25	8.5	-1.335			-0.65	17.0	-0.409		3.60	2.27
0.5	23.104			-0.10	9.0	-1.541		-1.15	-0.29	17.5	-0.326			2.43
1.0	20.221		0.04	-0.04	9.5	-1.670			-0.04	18.0	-0.253	8.65	4.09	2.58
1.5	17.458			0.03	10.0	-1.734	-1.34	-0.02	0.16	18.5	-0.188			2.73
2.0	14.854	1.72	0.54	0.10	10.5	-1.745			0.34	19.0	-0.133		4.66	2.85
2.5	12.437			0.19	11.0	-1.713		0.71	0.50	19.5	-0.085			2.91
3.0	10.225		1.12	0.29	11.5	-1.648			0.65	20.0	-0.045	8.12	5.63	2.73
3.5	8.226			0.40	12.0	-1.559	2.70	1.29	0.79	20.5	-0.013			0.60
4.0	6.445	6.68	1.88	0.54	12.5	-1.451			0.93	21.0	0.014		2.73	7.19
4.5	4.876			0.73	13.0	-1.333		1.79	1.07	21.5	0.034			5.67
5.0	3.515		3.14	0.98	13.5	-1.207			1.22	22.0	0.050	14.25	5.09	5.59
5.5	2.349			1.38	14.0	-1.079	5.23	2.25	1.36	22.5	0.061			5.78
6.0	1.366	23.6	6.54	2.16	14.5	-0.952			1.50	23.0	0.069		5.79	6.06
6.5	0.551			4.68	15.0	-0.830		2.70	1.65	23.5	0.073			6.42
7.0	-0.110		-58.4	-19.7	15.5	-0.712			1.80	24.0	0.075	14.54	6.38	6.83
7.5	-0.635			-2.75	16.0	-0.603	7.18	3.15	1.95	24.5	0.075			7.29
8.0	-1.038	-14.7	-3.81	-1.26	16.5	-0.501			2.11	25.0	0.073		6.96	7.78

Fig. (V-IV-12) Elasticity Sol.

EDGE R FORCE

P- STRESS $(N_\theta) = \alpha_3(p)$

R/t = 500

μ = 0.0

} Table (V-IV-11)

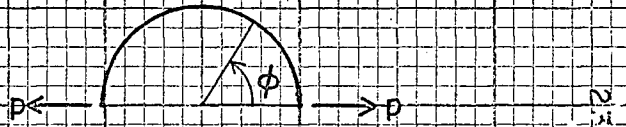

PHI IN DEGREES

30
25
20
15
10
5
0

0 8 16 24 32 40 48 56 64

α_3 →

Table (V-IV-11) Hemispherical Dome - Radial Load Along the Edge

P-Force/Length, $(N_\theta) = \alpha_3(p)$

$\mu = 0.0$; R/t = 500.0 (Fig. (V-IV-12))

	Elasticity Solution	Percentage Error				Elasticity Solution	Percentage Error				Elasticity Solution	Percentage Error		
$\phi°$	α_3	$\theta_e=\phi_e$ =2°	$\theta_e=\phi_e$ =1°	$\theta_e=\phi_e$ =0.5°	$\phi°$	α_3	$\theta_e=\phi_e$ =2°	$\theta_e=\phi_e$ =1°	$\theta_e=\phi_e$ =0.5°	$\phi°$	α_3	$\theta_e=\phi_e$ =2°	$\theta_e=\phi_e$ =1°	$\theta_e=\phi_e$ =0.5°
0.0	58.8566	-9.25	-2.58	-0.71	8.5	-0.2540			1.99	17.0	-0.0073		30.23	7.66
0.5	44.0334			0.09	9.0	-0.0519		0.53	-0.52	17.5	-0.0067			7.07
1.0	30.6716		2.64	0.77	9.5	0.0744			5.32	18.0	-0.0056		25.01	6.45
1.5	19.5474			1.57	10.0	0.1423	43.98	14.85	4.29	18.5	-0.0044			5.84
2.0	10.8971	35.42	10.62	2.72	10.5	0.1684			4.15	19.0	-0.0032		19.38	4.89
2.5	4.6096			5.28	11.0	0.1669		14.33	4.14	19.5	-0.0022			3.44
3.0	0.3773			46.31	11.5	0.1489			4.15	20.0	-0.0013	52.37	7.18	0.22
3.5	-2.1935			-4.89	12.0	0.1230	65.45	14.05	4.16	20.5	-0.0007			
4.0	-3.5078	-37.3	-6.66	-1.45	12.5	0.0949			4.11	21.0	-0.0002			
4.5	-3.9364			-0.23	13.0	0.0684		12.71	3.99	21.5	0.0000			
5.0	-3.7911		1.20	0.47	13.5	0.0456			3.71					
5.5	-3.3174			0.96	14.0	0.0273	54.28	7.74	3.10					
6.0	-2.6955	16.77	4.74	1.34	14.5	0.0136			1.61					
6.5	-2.0484			1.65	15.0	0.0040		-36.36	-5.58					
7.0	-1.4522		7.00	1.90	15.5	-0.0022			21.45					
7.5	-0.9473			2.09	16.0	-0.0056		44.80	10.62					
8.0	-0.5486	46.80	8.21	2.17	16.5	-0.0071			8.65					

Fig. (V-IV-13) Elasticity Sol.

EDGE R FORCE

P - STRESS $(N_\theta) = \alpha_3(p)$

R/t = 500

μ = 0.2

} Table (V-IV-12)

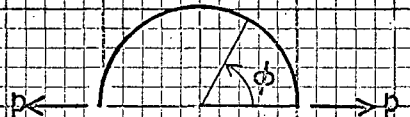

PHI IN DEGREES

30
25
20
15
10
5
0

0 8 16 24 32 40 48 56 64

α_3 →

Table (V-IV-12) Hemispherical Dome - Radial Load Along the Edge

P-Force/Length, $(N_\theta) = \alpha_3(p)$

$\mu = 0.2$; $R/t = 500.0$ (Fig. (V-IV-13))

	Elasticity Solution	Percentage Error				Elasticity Solution	Percentage Error				Elasticity Solution	Percentage Error		
$\phi°$	α_3	$\theta_e=\phi_e$ =2°	$\theta_e=\phi_e$ =1°	$\theta_e=\phi_e$ =0.5°	$\phi°$	α_3	$\theta_e=\phi_e$ =2°	$\theta_e=\phi_e$ =1°	$\theta_e=\phi_e$ =0.5°	$\phi°$	α_3	$\theta_e=\phi_e$ =2°	$\theta_e=\phi_e$ =1°	$\theta_e=\phi_e$ =0.5°
0.0	58.2590	-9.09	-2.54	-0.71	8.5	-0.2948			2.07	17.0	-0.0073		30.96	7.83
0.5	43.7299			0.07	9.0	-0.0818		4.09	0.83	17.5	-0.0069			7.04
1.0	30.6083		2.53	0.74	9.5	0.0545			5.84	18.0	-0.0059		25.34	6.50
1.5	19.6484			1.51	10.0	0.1311	41.15	14.75	4.24	18.5	-0.0048			5.80
2.0	11.0871	33.91	10.17	2.61	10.5	0.1640			4.06	19.0	-0.0036		20.33	4.90
2.5	4.8267			4.98	11.0	0.1673		14.05	4.04	19.5	-0.0025			3.35
3.0	0.5775			30.30	11.5	0.1525			4.07	20.0	-0.0016	67.15	10.42	0.12
3.5	-2.0360			-5.39	12.0	0.1284	63.27	13.83	4.08	20.5	-0.0009			
4.0	-3.4039	-38.91	-7.14	-1.60	12.5	0.1010			4.05	21.0	-0.0004			
4.5	-3.8854			-0.33	13.0	0.0744		12.75	3.97	21.5	-0.0001			
5.0	-3.7856		0.93	0.39	13.5	0.0509			3.74	22.0	0.0001			
5.5	-3.3461			0.88	14.0	0.0317	55.91	8.77	3.25	22.5	0.0003			
6.0	-2.7464	15.57	4.48	1.27	14.5	0.0170			2.18	23.0	0.0003			
6.5	-2.1105			1.58	15.0	0.0064		-16.29	-1.67	23.5	0.0003			
7.0	-1.5164		6.73	1.84	15.5	-0.0006			69.48	24.0	0.0003			
7.5	-1.0072			2.03	16.0	-0.0047		50.76	11.80	24.5	0.0002			
8.0	-0.5999	44.12	8.01	2.15	16.5	-0.0067			8.95	25.0	0.0002			

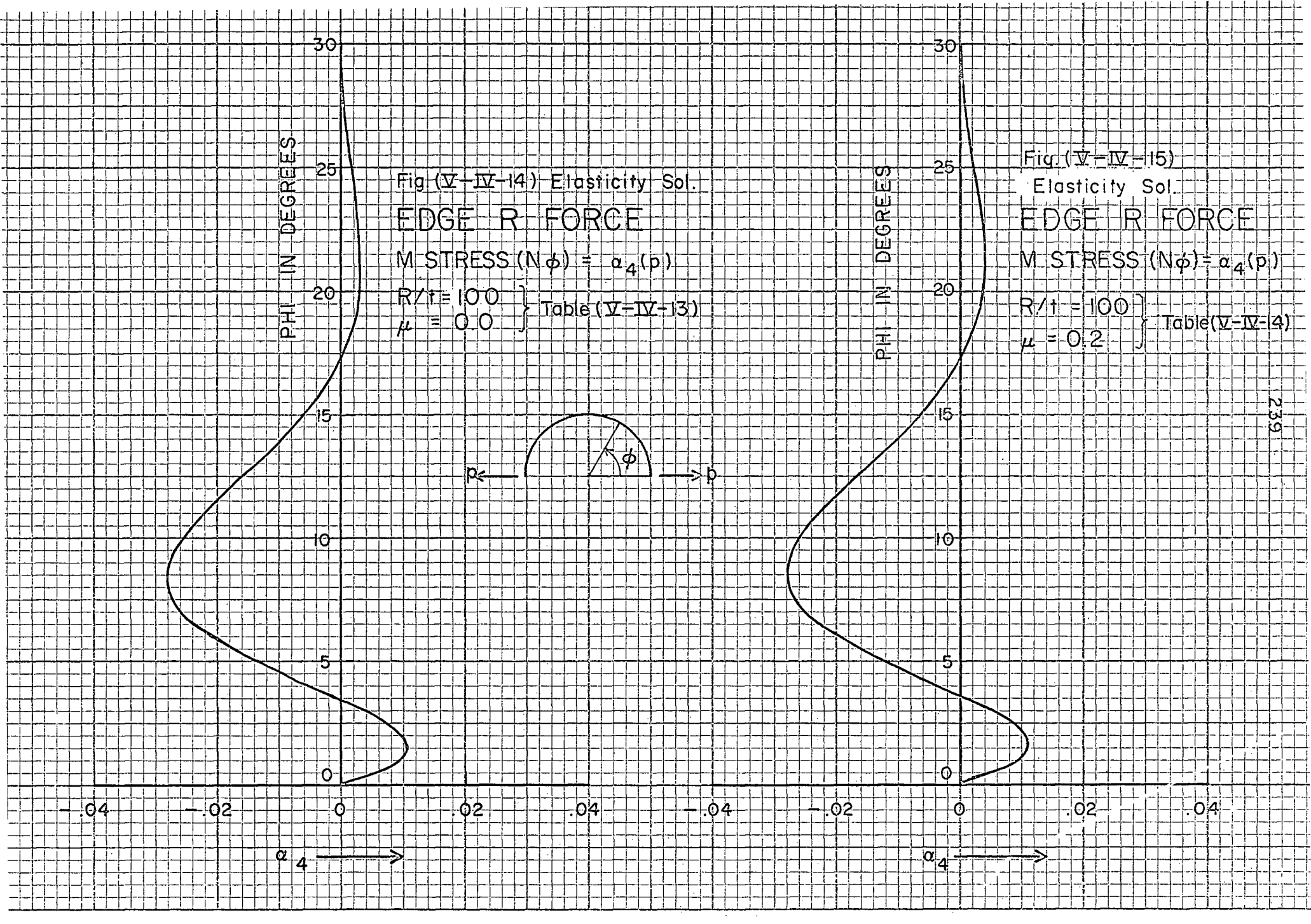
Fig (V-IV-14) Elasticity Sol.
EDGE R FORCE
M STRESS (Nφ) = α4(p)
R/t = 100
μ = 0.0
Table (V-IV-13)
PHI IN DEGREES
30
25
20
15
10
5
0
R
p
φ
-.04
-.02
0
.02
.04
α4
Fig. (V-IV-15)
Elasticity Sol.
EDGE R FORCE
M STRESS (Nφ) = α4(p)
R/t = 100
μ = 0.2
Table (V-IV-14)
PHI IN DEGREES
30
25
20
15
10
5
0
-.04
-.02
0
.02
.04
α4

Table (V-IV-13) Hemispherical Dome - Radial Load Along the Edge

M-Force/Length, $(N_\phi) = \alpha_4(p)$

$\mu = 0.0$; R/t = 100.0 (Fig. (V-IV-14))

	Elasticity Solution	Percentage Error				Elasticity Solution	Percentage Error				Elasticity Solution	Percentage Error		
$\phi°$	α_4	$\theta_e=\phi_e$ =2°	$\theta_e=\phi_e$ =1°	$\theta_e=\phi_e$ =0.5°	$\phi°$	α_4	$\theta_e=\phi_e$ =2°	$\theta_e=\phi_e$ =1°	$\theta_e=\phi_e$ =0.5°	$\phi°$	α_4	$\theta_e=\phi_e$ =2°	$\theta_e=\phi_e$ =1°	$\theta_e=\phi_e$ =0.5°
0.0	0.0000	0.00	0.00	0.00	8.5	-0.0276			1.05	17.0	-0.0002		-64.7	-9.5
0.5	0.0068			-1.05	9.0	-0.0272		1.55	1.11	17.5	0.0007			6.22
1.0	0.0103		0.07	-0.68	9.5	-0.0263			1.17	18.0	0.0015	36.91	11.84	3.82
1.5	0.0112			-0.65	10.0	-0.0250	3.68	1.68	1.23	18.5	0.0021			3.64
2.0	0.0100	1.79	0.19	-0.71	10.5	-0.0235			1.28	19.0	0.0026		8.63	3.63
2.5	0.0073			-1.14	11.0	-0.0216		1.76	1.34	19.5	0.0030			3.42
3.0	0.0036		-0.11	-2.65	11.5	-0.0197			1.41	20.0	0.0032	19.32	7.45	3.42
3.5	-0.0007			17.75	12.0	-0.0176	3.37	1.75	1.44	20.5	0.0034			3.57
4.0	-0.0052	-0.32	1.07	2.21	12.5	-0.0154			1.52	21.0	0.0034		7.13	3.49
4.5	-0.0097			1.37	13.0	-0.0133		1.71	1.58	21.5	0.0034			3.55
5.0	-0.0139		1.02	1.06	13.5	-0.0112			1.59	22.0	0.0033	15.73	6.82	3.24
5.5	-0.0177			0.98	14.0	-0.0092	1.23	1.36	1.66	22.5	0.0032			3.13
6.0	-0.0209	2.35	1.15	0.94	14.5	-0.0073			1.71	23.0	0.0030		6.88	3.15
6.5	-0.0235			0.95	15.0	-0.0056		0.52	1.68	23.5	0.0028			2.78
7.0	-0.0255		1.29	0.95	15.5	-0.0040			1.52	24.0	0.0025	13.62	6.89	2.24
7.5	-0.0268			0.99	16.0	-0.0026	-12.03	-2.07	1.29	24.5	0.0023			1.65
8.0	-0.0275	3.26	1.43	1.04	16.5	-0.0013			0.85	25.0	0.0020		6.78	0.83

Table (V-IV-14) Hemispherical Dome - Radial Load Along the Edge

M-Force/Length, $(N_\phi) = \alpha_4(p)$

$\mu = 0.2$; R/t = 100.0 (Fig. (V-IV-15))

	Elasticity Solution	Percentage Error				Elasticity Solution	Percentage Error				Elasticity Solution	Percentage Error		
$\phi°$	α_4	$\theta_e=\phi_e$ =2°	$\theta_e=\phi_e$ =1°	$\theta_e=\phi_e$ =0.5°	$\phi°$	α_4	$\theta_e=\phi_e$ =2°	$\theta_e=\phi_e$ =1°	$\theta_e=\phi_e$ =0.5°	$\phi°$	α_4	$\theta_e=\phi_e$ =2°	$\theta_e=\phi_e$ =1°	$\theta_e=\phi_e$ =0.5°
0.0	0.0000	0.00	0.00	0.00	8.5	-0.0279			1.02	17.0	-0.0006		-20.89	-0.71
0.5	0.0069			-0.76	9.0	-0.0276		1.48	1.07	17.5	0.0004			6.74
1.0	0.0104		0.16	-0.40	9.5	-0.0268			1.12	18.0	0.0013	43.5	14.29	4.29
1.5	0.0113			-0.39	10.0	-0.0256	3.57	1.59	1.20	18.5	0.0019			3.56
2.0	0.0102	1.78	0.26	-0.43	10.5	-0.0241			1.27	19.0	0.0025		8.75	3.35
2.5	0.0075			-0.64	11.0	-0.0223		1.66	1.31	19.5	0.0029			3.65
3.0	0.0039		0.54	-1.27	11.5	-0.0204			1.40	20.0	0.0032	19.56	7.57	3.37
3.5	-0.0004			14.15	12.0	-0.0183	3.39	1.74	1.45	20.5	0.0033			3.46
4.0	-0.0049	-0.93	0.77	1.48	12.5	-0.0162			1.55	21.0	0.0034		7.01	3.28
4.5	-0.0094			1.02	13.0	-0.0140		1.68	1.56	21.5	0.0034			3.55
5.0	-0.0137		0.82	0.81	13.5	-0.0119			1.55	22.0	0.0034	15.86	6.95	3.40
5.5	-0.0175			0.80	14.0	-0.0099	1.53	1.45	1.63	22.5	0.0033			3.22
6.0	-0.0208	2.16	1.01	0.80	14.5	-0.0080			1.82	23.0	0.0031		6.90	3.10
6.5	-0.0235			0.80	15.0	-0.0062		0.83	1.78	23.5	0.0029			3.00
7.0	-0.0255		1.18	0.87	15.5	-0.0045			1.85	24.0	0.0027	13.99	6.98	2.69
7.5	-0.0269			0.89	16.0	-0.0030	-8.98	-1.25	1.84	24.5	0.0024			1.84
8.0	-0.0277	3.09	1.30	0.95	16.5	-0.0017			1.28	25.0	0.0022		6.73	1.54

Fig.(V-IV-16) Elasticity Sol.

EDGE R FORCE

M-STRESS (N_ϕ) = $\alpha_4(p)$

R/t = 500, μ = 0.0 } Table(V-IV-15)

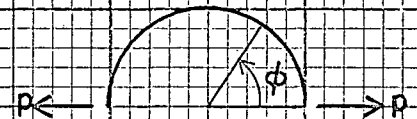

Fig.(V-IV-17) Elasticity Sol.

EDGE R FORCE

M - STRESS (N_ϕ) = $\alpha_4(p)$

R/t = 500, μ = 0.2 } Table(V-IV-16)

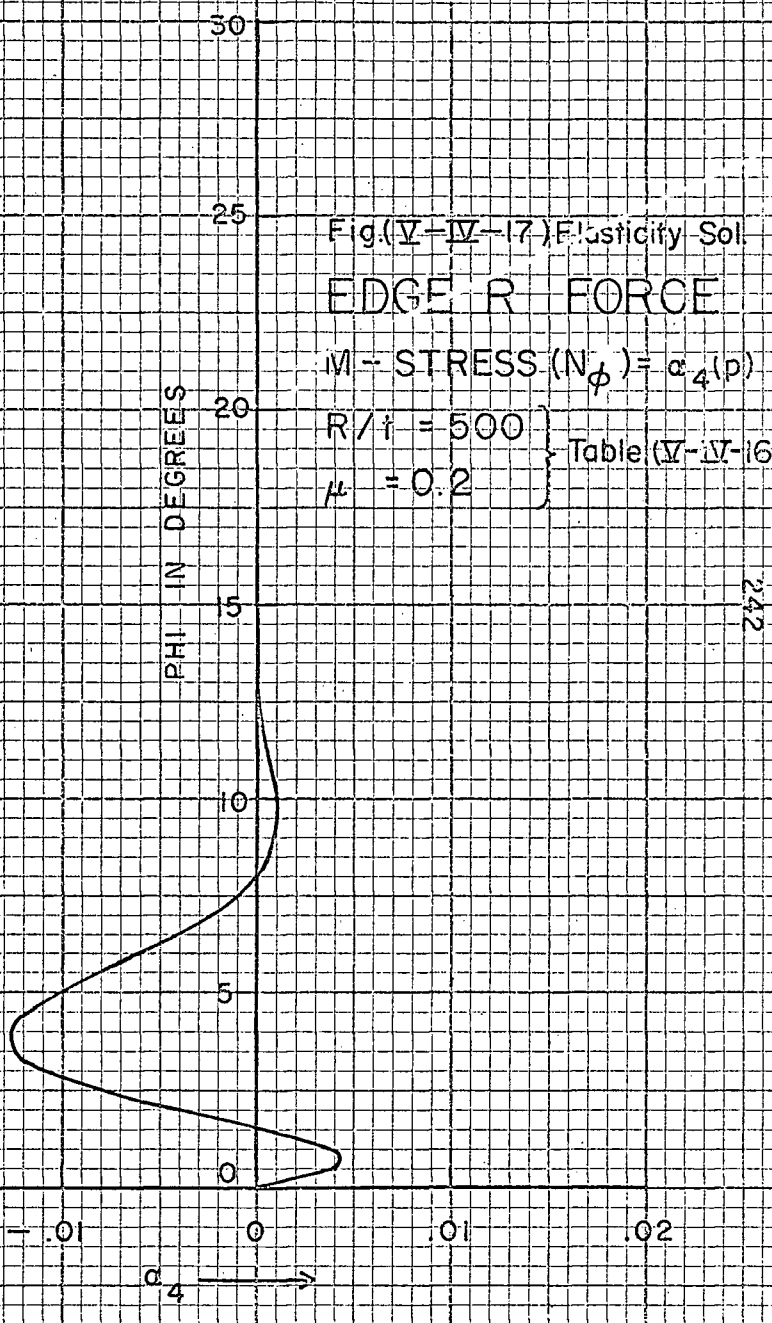

Table (V-IV-15) Hemispherical Dome - Radial Load Along the Edge

M-Force/Length, $(N_\phi) = \alpha_4(p)$

$\mu = 0.0$; $R/t = 500.0$ (Fig. (V-IV-16))

	Elasticity Solution	Percentage Error				Elasticity Solution	Percentage Error		
$\phi°$	α_4	$\theta_e=\phi_e$ =2°	$\theta_e=\phi_e$ =1°	$\theta_e=\phi_e$ =0.5°	$\phi°$	α_4	$\theta_e=\phi_e$ =2°	$\theta_e=\phi_e$ =1°	$\theta_e=\phi_e$ =0.5°
0.0	0.0000	0.00	0.00	0.00	8.5	0.0011			-2.10
0.5	0.0048			-1.66	9.0	0.0014		16.95	-2.27
1.0	0.0040		2.40	-1.74	9.5	0.0015			-3.13
1.5	0.0003			-34.23	10.0	0.0014	67.23	12.19	-3.58
2.0	-0.0042	-5.93	0.97	2.72	10.5	0.0012			-5.55
2.5	-0.0082			1.70	11.0	0.0010		6.98	-8.02
3.0	-0.0109		2.97	1.69	11.5	0.0007			-11.81
3.5	-0.0121			1.72	12.0	0.0005	23.80	-2.00	-18.60
4.0	-0.0121	15.78	3.74	1.75	12.5	0.0003			
4.5	-0.0110			1.83	13.0	0.0002			
5.0	-0.0093		3.66	1.89	13.5	0.0000			
5.5	-0.0072			2.07	14.0	0.0000			
6.0	-0.0051	14.22	2.12	2.37					
6.5	-0.0032			2.81					
7.0	-0.0015		-7.55	4.06					
7.5	-0.0003			12.67					
8.0	0.0006		40.17	-4.75					

Table (V-IV-16) Hemispherical Dome - Radial Load Along the Edge

M-Force/Length, $(N_\phi) = \alpha_4(p)$

$\mu = 0.2$; $R/t = 500.0$ (Fig. (V-IV-17)

	Elasticity Solution	Percentage Error				Elasticity Solution	Percentage Error		
$\phi°$	α_4	$\theta_e=\phi_e$ =2°	$\theta_e=\phi_e$ =1°	$\theta_e=\phi_e$ =0.5°	$\phi°$	α_4	$\theta_e=\phi_e$ =2°	$\theta_e=\phi_e$ =1°	$\theta_e=\phi_e$ =0.5°
0.0	0.0000	0.00	0.00	0.00	8.5	0.0011			-1.02
0.5	0.0048			-1.24	9.0	0.0014		18.13	0.07
1.0	0.0041		2.39	-1.21	9.5	0.0015			-0.20
1.5	0.0004			-13.33	10.0	0.0014	67.66	13.33	-1.21
2.0	-0.0041	-6.80	0.41	2.12	10.5	0.0012			-2.26
2.5	-0.0081			1.56	11.0	0.0010		9.02	-4.71
3.0	-0.0109		2.74	1.54	11.5	0.0008			-7.05
3.5	-0.0122			1.59	12.0	0.0005	30.73	3.09	-10.36
4.0	-0.0123	15.17	3.56	1.63	12.5	0.0004			
4.5	-0.0113			1.71	13.0	0.0002			
5.0	-0.0096		3.57	1.84	13.5	0.0001			
5.5	-0.0075			2.01	14.0	0.0000			
6.0	-0.0054	14.03	1.96	2.09					
6.5	-0.0034			2.32					
7.0	-0.0018		-6.40	2.58					
7.5	-0.0005			4.04					
8.0	0.0005		48.12	-2.50					

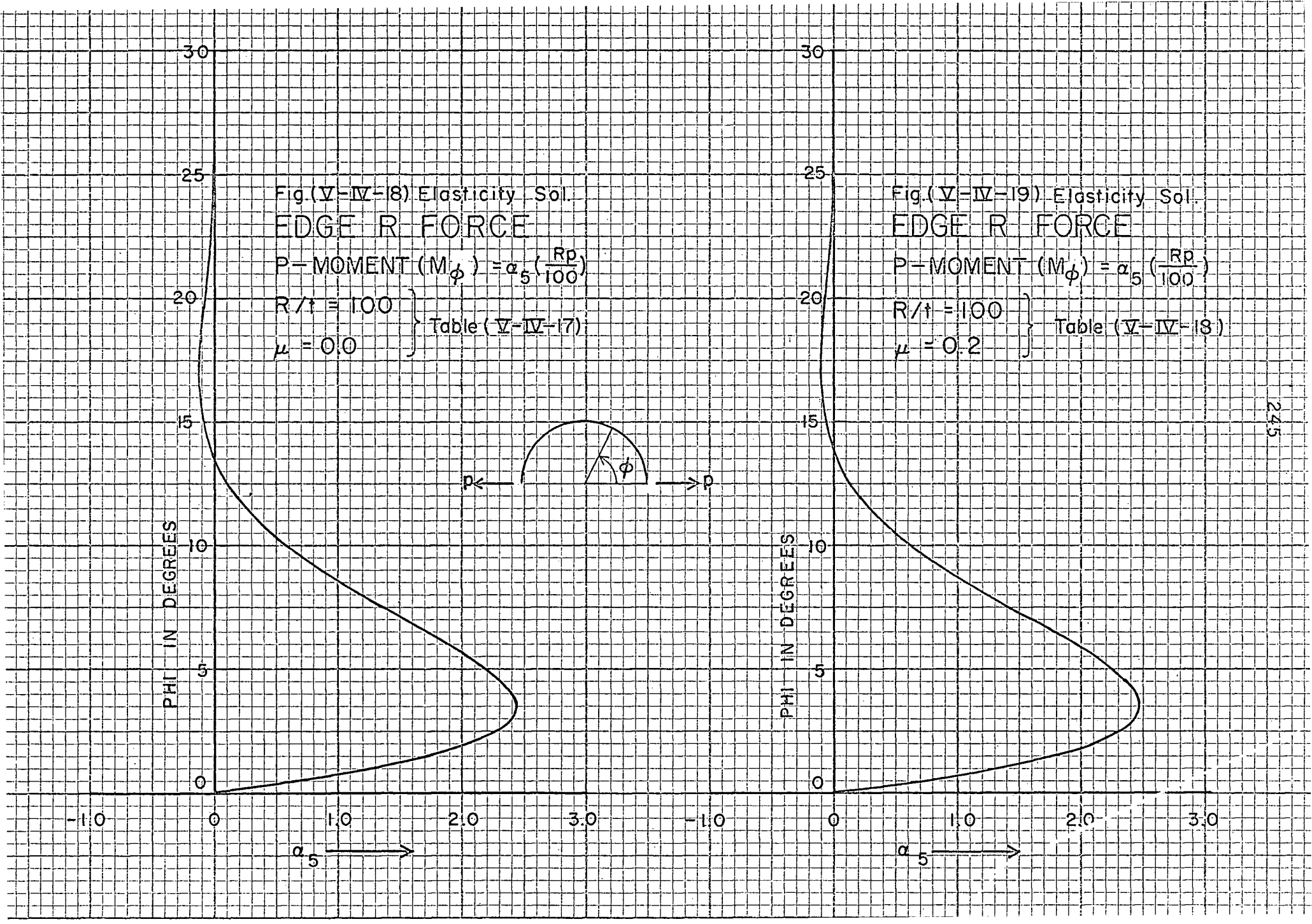
Fig.(V-IV-18) Elasticity Sol.
EDGE R FORCE
P-MOMENT (M_ϕ) = $\alpha_5 (\frac{Rp}{100})$
R/t = 100
μ = 0.0
Table (V-IV-17)
Fig.(V-IV-19) Elasticity Sol.
EDGE R FORCE
P-MOMENT (M_ϕ) = $\alpha_5 (\frac{Rp}{100})$
R/t = 100
μ = 0.2
Table (V-IV-18)
p
p
φ
PHI IN DEGREES
PHI IN DEGREES
30
25
20
15
10
5
0
-1.0
0
1.0
2.0
3.0
α_5
α_5
22.5

Table (V-IV-17) Hemispherical Dome - Radial Load Along the Edge

P-Moment/Length, $(M_\phi) = \alpha_5(pR/100)$

$\mu = 0.0$; $R/t = 100.0$ (Fig. (V-IV-18))

	Elasticity Solution	Percentage Error				Elasticity Solution	Percentage Error				Elasticity Solution	Percentage Error		
$\phi°$	α_5	$\theta_e=\phi_e$ =2°	$\theta_e=\phi_e$ =1°	$\theta_e=\phi_e$ =0.5°	$\phi°$	α_5	$\theta_e=\phi_e$ =2°	$\theta_e=\phi_e$ =1°	$\theta_e=\phi_e$ =0.5°	$\phi°$	α_5	$\theta_e=\phi_e$ =2°	$\theta_e=\phi_e$ =1°	$\theta_e=\phi_e$ =0.5°
0.0	0.0000	0.00	0.00	0.00	8.5	1.0008			0.46	17.0	-0.1058		4.82	2.37
0.5	0.7763			0.05	9.0	0.8453		0.59	0.51	17.5	-0.1050			2.45
1.0	1.3750		0.07	0.02	9.5	0.7019			0.56	18.0	-0.1019	12.80	4.67	2.55
1.5	1.8185			0.03	10.0	0.5713	-0.32	0.48	0.60	18.5	-0.0970			2.65
2.0	2.1282	0.62	0.16	0.04	10.5	0.4541			0.64	19.0	-0.0909		4.64	2.76
2.5	2.3243			0.05	11.0	0.3503		0.16	0.68	19.5	-0.0839			2.87
3.0	2.4255		0.25	0.07	11.5	0.2596			0.69	20.0	-0.0763	10.54	4.65	2.99
3.5	2.4488			0.09	12.0	0.1814	-7.19	-0.76	0.68	20.5	-0.0685			3.12
4.0	2.4098	1.15	0.34	0.11	12.5	0.1149			0.58	21.0	-0.0607		4.66	3.25
4.5	2.3222			0.14	13.0	0.0594		-5.01	0.21	21.5	-0.0531			3.39
5.0	2.1979		0.43	0.17	13.5	0.0139			-2.74	22.0	-0.0457	7.93	4.62	3.56
5.5	2.0474			0.20	14.0	-0.0226	78.81	18.28	3.73	22.5	-0.0388			3.76
6.0	1.8796	1.41	0.50	0.24	14.5	-0.0511			2.49	23.0	-0.0325		4.47	4.02
6.5	1.7021			0.28	15.0	-0.0725		6.69	2.25	23.5	-0.0266			4.36
7.0	1.5210		0.57	0.32	15.5	-0.0878			2.22	24.0	-0.0213	2.51	4.06	4.86
7.5	1.3413			0.36	16.0	-0.0979	17.41	5.26	2.24	24.5	-0.0167			5.62
8.0	1.1669	1.16	0.60	0.41	16.5	-0.1037			2.29	25.0	-0.0125		3.09	6.85

Table (V-IV-18) Hemispherical Dome - Radial Load Along the Edge

P-Moment/Length, $(M_\phi) = \alpha_5(pR/100)$

$\mu = 0.2$; $R/t = 100.0$ (Fig. (V-IV-19))

	Elasticity Solution	Percentage Error				Elasticity Solution	Percentage Error				Elasticity Solution	Percentage Error		
$\phi°$	α_5	$\theta_e=\phi_e$ =2°	$\theta_e=\phi_e$ =1°	$\theta_e=\phi_e$ =0.5°	$\phi°$	α_5	$\theta_e=\phi_e$ =2°	$\theta_e=\phi_e$ =1°	$\theta_e=\phi_e$ =0.5°	$\phi°$	α_5	$\theta_e=\phi_e$ =2°	$\theta_e=\phi_e$ =1°	$\theta_e=\phi_e$ =0.5°
0.0	0.0000	0.00	0.00	0.00	8.5	1.0393			0.48	17.0	-0.1065		5.29	2.78
0.5	0.7772			0.04	9.0	0.8818		0.61	0.52	17.5	-0.1067			2.83
1.0	1.3784		0.08	0.02	9.5	0.7360			0.56	18.0	-0.1043	13.27	5.06	2.90
1.5	1.8256			0.03	10.0	0.6029	-0.20	0.48	0.58	18.5	-0.1000			2.97
2.0	2.1397	0.63	0.18	0.05	10.5	0.4829			0.61	19.0	-0.0943		4.96	3.06
2.5	2.3405			0.06	11.0	0.3762		0.14	0.61	19.5	-0.0876			3.16
3.0	2.4465		0.28	0.08	11.5	0.2825			0.59	20.0	-0.0802	10.93	4.94	3.25
3.5	2.4745			0.11	12.0	0.2013	-6.40	-0.79	0.50	20.5	-0.0725			3.35
4.0	2.4398	1.16	0.37	0.14	12.5	0.1321			0.28	21.0	-0.0647		4.91	3.46
4.5	2.3558			0.17	13.0	0.0738		-4.50	-0.32	21.5	-0.0569			3.59
5.0	2.2345		0.46	0.20	13.5	0.0257			-3.10	22.0	-0.0495	8.41	4.83	3.72
5.5	2.0864			0.24	14.0	-0.0132		34.73	9.90	22.5	-0.0424			3.91
6.0	1.9202	1.43	0.54	0.28	14.5	-0.0439			3.98	23.0	-0.0357		4.66	4.13
6.5	1.7436			0.32	15.0	-0.0673		7.97	3.17	23.5	-0.0296			4.41
7.0	1.5626		0.60	0.36	15.5	-0.0845			2.90	24.0	-0.0241	3.54	4.23	4.83
7.5	1.3824			0.40	16.0	-0.0962	18.44	5.92	2.79	24.5	-0.0191			5.43
8.0	1.2070	1.20	0.63	0.44	16.5	-0.1032			2.77	25.0	-0.0147		3.29	6.44

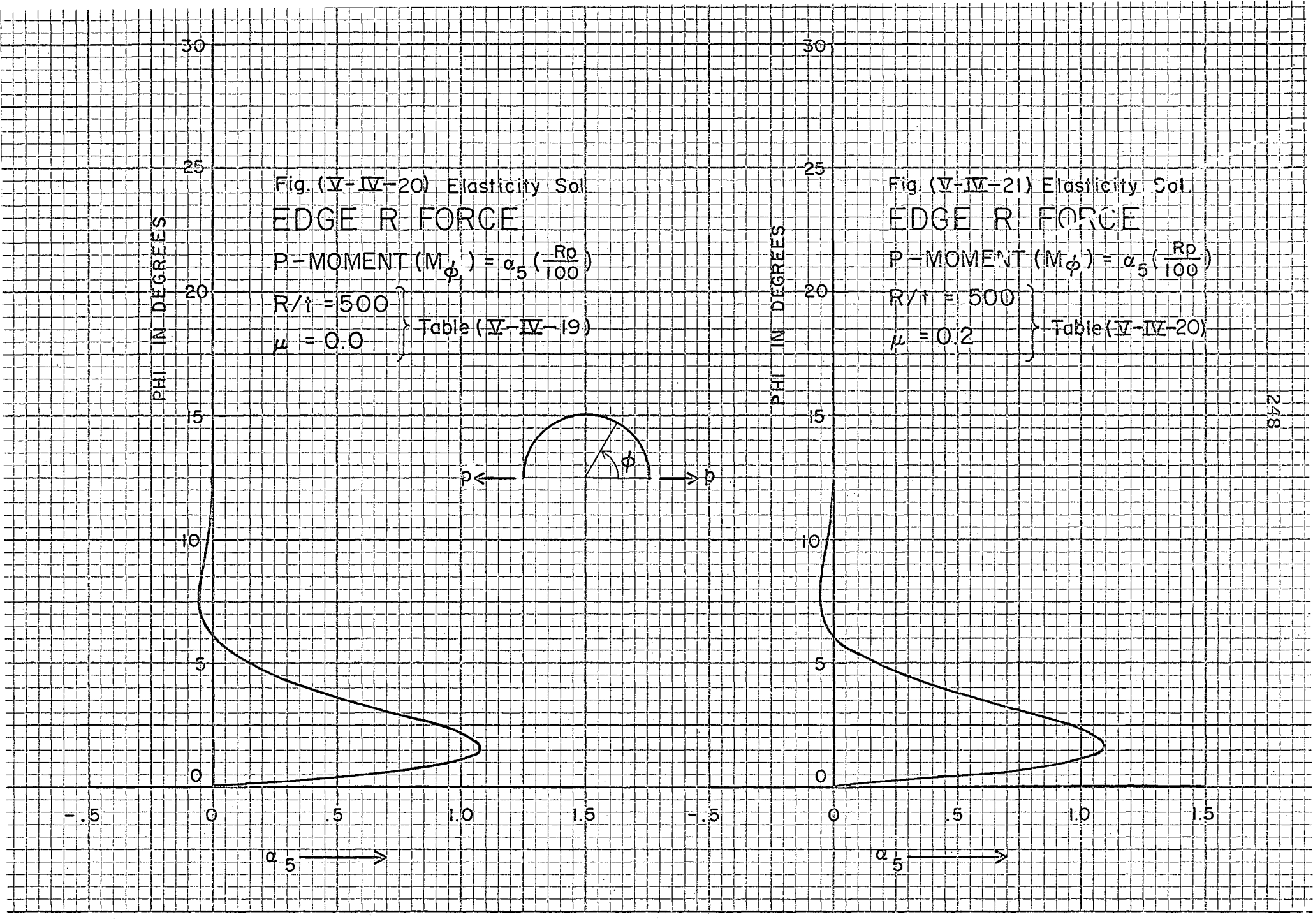
Fig. (V-IV-20) Elasticity Sol
EDGE R FORCE
P-MOMENT (M_{ϕ}) = $\alpha_5 (\frac{Rp}{100})$
R/t = 500
μ = 0.0
Table (V-IV-19)
PHI IN DEGREES
30
25
20
15
10
5
0
-.5
0
.5
1.0
1.5
α_5
p
p
ϕ
Fig. (V-IV-21) Elasticity Sol
EDGE R FORCE
P-MOMENT (M_{ϕ}) = $\alpha_5 (\frac{Rp}{100})$
R/t = 500
μ = 0.2
Table (V-IV-20)
PHI IN DEGREES
30
25
20
15
10
5
0
-.5
0
.5
1.0
1.5
α_5

Table (V-IV-19) Hemispherical Dome - Radial Load Along the Edge

P-Moment/Length, $(M_\phi) = \alpha_5(pR/100)$

$\mu = 0.0$; $R/t = 500.0$ (Fig. (V-IV-20))

	Elasticity Solution	Percentage Error				Elasticity Solution	Percentage Error				Elasticity Solution	Percentage Error		
$\phi°$	α_5	$\theta_e=\phi_e$ =2°	$\theta_e=\phi_e$ =1°	$\theta_e=\phi_e$ =0.5°	$\phi°$	α_5	$\theta_e=\phi_e$ =2°	$\theta_e=\phi_e$ =1°	$\theta_e=\phi_e$ =0.5°	$\phi°$	α_5	$\theta_e=\phi_e$ =2°	$\theta_e=\phi_e$ =1°	$\theta_e=\phi_e$ =0.5°
0.0	0.0000	0.00	0.00	0.00	8.5	-0.0406			3.24	17.0	0.0003		-5.71	0.86
0.5	0.6676			0.16	9.0	-0.0333		9.94	2.80	17.5	0.0002			
1.0	0.9990		0.85	0.24	9.5	-0.0255			2.35	18.0	0.0001			
1.5	1.0953			0.32	10.0	-0.0182	25.46	5.11	1.75	18.5	0.0000			
2.0	1.0412	5.65	1.46	0.37	10.5	-0.0120			0.85					
2.5	0.9025			0.40	11.0	-0.0071		-6.04	-0.83					
3.0	0.7275		1.48	0.38	11.5	-0.0034			-4.53					
3.5	0.5486			0.29	12.0	-0.0008		-93.8	-23.90					
4.0	0.3855	4.53	0.33	0.10	12.5	0.0008			29.10					
4.5	0.2486			-0.29	13.0	0.0016		52.7	13.41					
5.0	0.1414		-4.63	-1.11	13.5	0.0020			9.40					
5.5	0.0628			-3.44	14.0	0.0020		29.21	7.87					
6.0	0.0093		-94.2	-26.4	14.5	0.0018			6.87					
6.5	-0.0236			10.61	15.0	0.0015		20.60	6.42					
7.0	-0.0409		22.49	5.76	15.5	0.0012			5.08					
7.5	-0.0471			4.40	16.0	0.0009	46.16	10.70	3.84					
8.0	-0.0460	60.62	13.94	3.69	16.5	0.0006			2.24					

Table (V-IV-20) Hemispherical Dome - Radial Load Along the Edge

P-Moment/Length, $(M_\phi) = \alpha_5(pR/100)$

$\mu = 0.2$; $R/t = 500.0$ (Fig. (V-IV-21))

	Elasticity Solution	Percentage Error				Elasticity Solution	Percentage Error				Elasticity Solution	Percentage Error		
$\phi°$	α_5	$\theta_e=\phi_e$ =2°	$\theta_e=\phi_e$ =1°	$\theta_e=\phi_e$ =0.5°	$\phi°$	α_5	$\theta_e=\phi_e$ =2°	$\theta_e=\phi_e$ =1°	$\theta_e=\phi_e$ =0.5°	$\phi°$	α_5	$\theta_e=\phi_e$ =2°	$\theta_e=\phi_e$ =1°	$\theta_e=\phi_e$ =0.5°
0.0	0.0000	0.00	0.00	0.00	8.5	-0.0421			3.32	17.0	0.0004		-2.32	0.70
0.5	0.6695			0.16	9.0	-0.0350		10.15	2.89	17.5	0.0002			
1.0	1.0051		0.83	0.23	9.5	-0.0272			2.46	18.0	0.0001			
1.5	1.1062			0.31	10.0	-0.0198	27.43	5.67	1.91	18.5	0.0000			
2.0	1.0561	5.50	1.43	0.37	10.5	-0.0134			1.05	19.0	0.0000			
2.5	0.9202			0.39	11.0	-0.0082		-3.91	-0.31					
3.0	0.7461		1.47	0.38	11.5	-0.0042			-3.15					
3.5	0.5667			0.30	12.0	-0.0014	-90.43	-62.9	-14.03					
4.0	0.4020	4.61	0.41	0.12	12.5	0.0004			52.33					
4.5	0.2626			-0.24	13.0	0.0015		59.73	15.34					
5.0	0.1525		-4.08	-0.99	13.5	0.0020			10.25					
5.5	0.0709			-3.00	14.0	0.0021		30.82	8.54					
6.0	0.0148	38.69	-65.9	-16.63	14.5	0.0019			7.38					
6.5	-0.0205			12.42	15.0	0.0016		21.23	6.38					
7.0	-0.0396		23.48	6.10	15.5	0.0013			5.31					
7.5	-0.0472			4.54	16.0	0.0010	54.43	12.47	4.33					
8.0	-0.0470	60.77	14.15	3.81	16.5	0.0007			3.58					

Fig.(V-IV-22) Elasticity Sol.

EDGE R FORCE

M-MOMENT (M_θ) = $\alpha_6 \left(\frac{Rp}{100}\right)$

R/t = 100

μ = 0.0

} Table(V-IV-21)

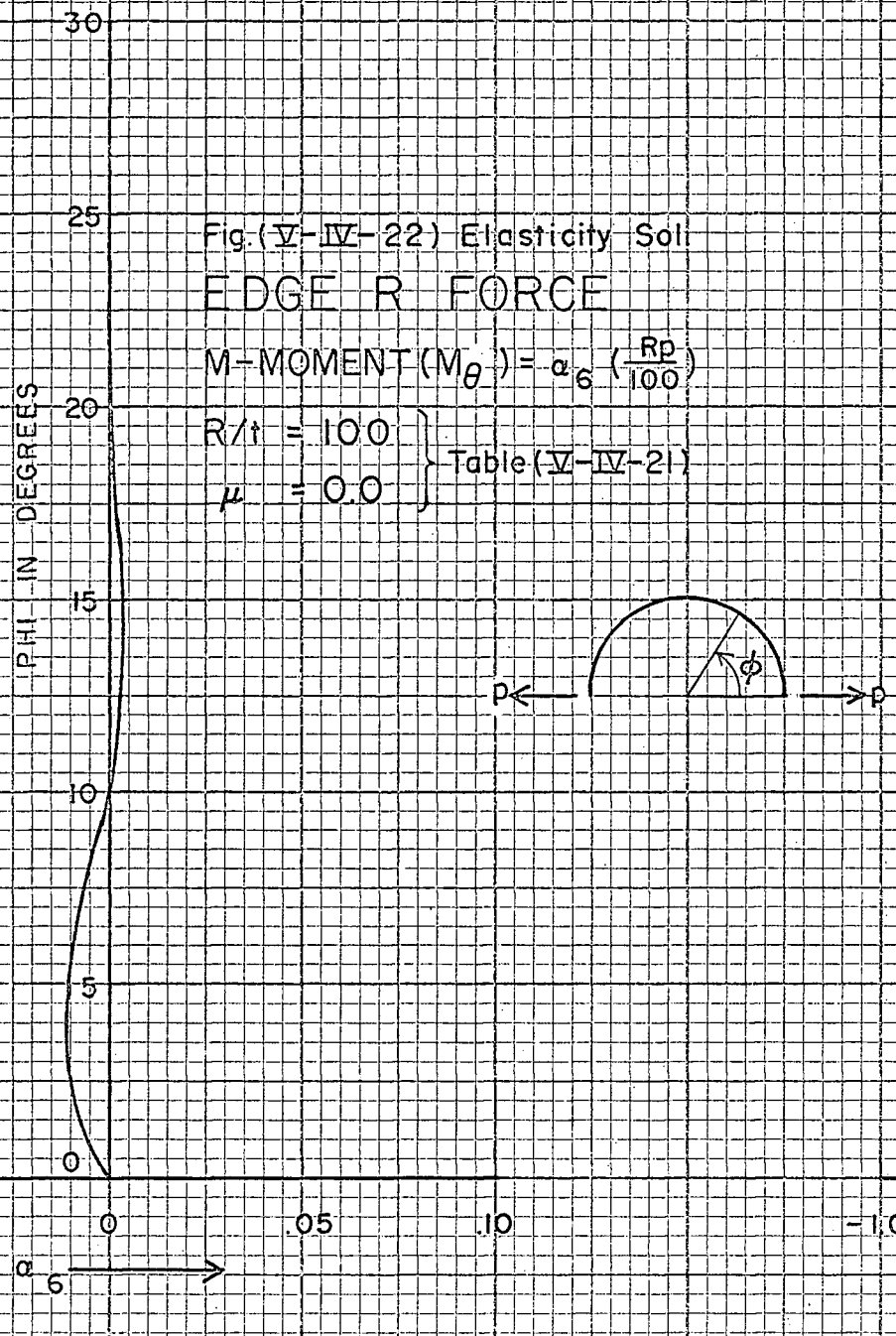

Fig.(V-IV-23) Elasticity Sol.

EDGE R FORCE

M-MOMENT (M_θ) = $\alpha_6 \left(\frac{Rp}{100}\right)$

R/t = 100

μ = 0.2

} Table(V-IV-22)

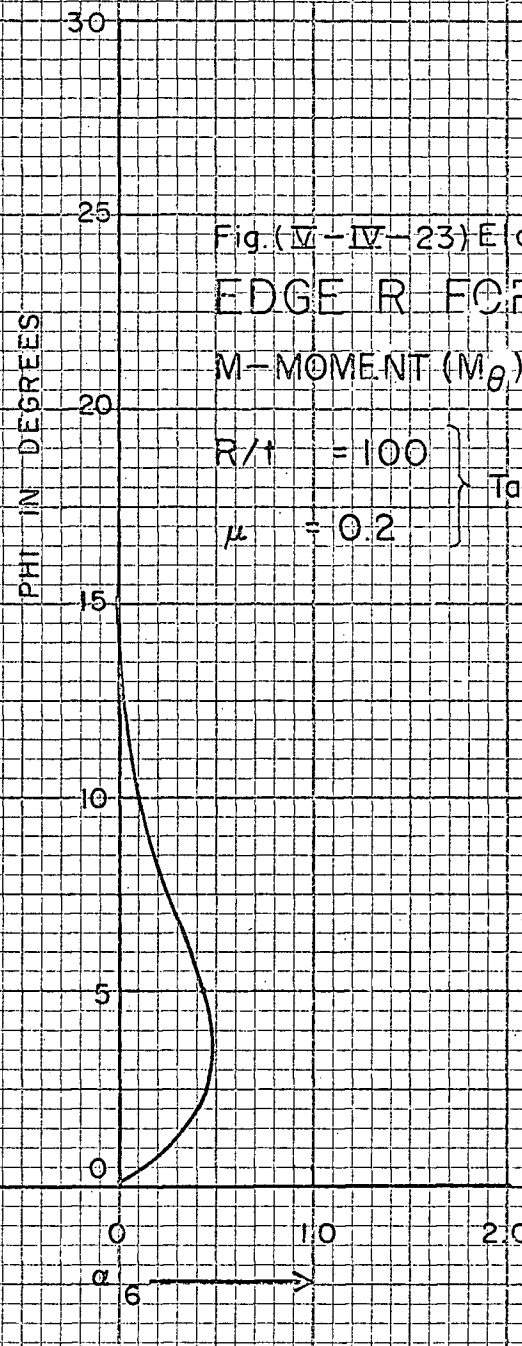

Table (V-IV-21) Hemispherical Dome - Radial Load Along the Edge

M-Moment/Length, $(M_\theta) = \alpha_6(pR/100)$

$\mu = 0.0$; $R/t = 100.0$ (Fig. (V-IV-22))

	Elasticity Solution	Percentage Error				Elasticity Solution	Percentage Error				Elasticity Solution	Percentage Error		
$\phi°$	α_6	$\theta_e=\phi_e$ =2°	$\theta_e=\phi_e$ =1°	$\theta_e=\phi_e$ =0.5°	$\phi°$	α_6	$\theta_e=\phi_e$ =2°	$\theta_e=\phi_e$ =1°	$\theta_e=\phi_e$ =0.5°	$\phi°$	α_6	$\theta_e=\phi_e$ =2°	$\theta_e=\phi_e$ =1°	$\theta_e=\phi_e$ =0.5°
0.0	0.0000	0.00	0.00	0.00	8.5	-0.0034			1.73	17.0	0.0025		3.59	2.91
0.5	-0.0025			-1.36	9.0	-0.0023		10.00	2.23	17.5	0.0023			3.04
1.0	-0.0048		-5.59	-0.87	9.5	-0.0013			3.53	18.0	0.0021	8.99	4.28	3.12
1.5	-0.0069			-0.67	10.0	-0.0004		47.21	7.91	18.5	0.0018			3.35
2.0	-0.0085	-15.8	-4.06	-0.76	10.5	0.0004			-7.10	19.0	0.0016		5.31	3.70
2.5	-0.0098			-0.64	11.0	0.0011		-15.09	-1.48	19.5	0.0014			3.57
3.0	-0.0107		-2.66	-0.53	11.5	0.0017			-0.24	20.0	0.0012	16.27	6.36	4.24
3.5	-0.0112			-0.25	12.0	0.0021	-26.37	-4.93	0.42	20.5	0.0010			4.08
4.0	-0.0113	-6.58	-1.40	-0.19	12.5	0.0025			1.03	21.0	0.0008		7.09	4.30
4.5	-0.0111			-0.07	13.0	0.0028		-1.61	1.18	21.5	0.0006			5.41
5.0	-0.0106		-0.18	0.11	13.5	0.0030			1.37	22.0	0.0004	29.56	10.00	6.44
5.5	-0.0099			0.26	14.0	0.0031	-6.31	0.23	1.68	22.5	0.0003			7.10
6.0	-0.0090	3.08	1.14	0.45	14.5	0.0031			1.95	23.0	0.0002		12.10	6.84
6.5	-0.0079			0.64	15.0	0.0031		1.46	2.07	23.5	0.0001			12.50
7.0	-0.0068		2.77	0.85	15.5	0.0030			2.35	24.0	0.0000	0.00	0.00	0.00
7.5	-0.0057			1.07	16.0	0.0029	2.51	2.58	2.51	24.5	-0.0001			
8.0	-0.0045	18.67	4.99	1.26	16.5	0.0027			2.47	25.0	-0.0001			

Table (V-IV-22) Hemispherical Dome - Radial Load Along the Edge

M-Moment/Length, $(M_\theta) = \alpha_6(pR/100)$

$\mu = 0.2$; $R/t = 100.0$ (Fig. (V-IV-23))

	Elasticity Solution	Percentage Error				Elasticity Solution	Percentage Error				Elasticity Solution	Percentage Error		
$\phi°$	α_6	$\theta_e=\phi_e$ =2°	$\theta_e=\phi_e$ =1°	$\theta_e=\phi_e$ =0.5°	$\phi°$	α_6	$\theta_e=\phi_e$ =2°	$\theta_e=\phi_e$ =1°	$\theta_e=\phi_e$ =0.5°	$\phi°$	α_6	$\theta_e=\phi_e$ =2°	$\theta_e=\phi_e$ =1°	$\theta_e=\phi_e$ =0.5°
0.0	0.0000	0.00	0.00	0.00	8.5	0.2042			4.25	17.0	-0.0186		32.2	31.0
0.5	0.1529			-0.58	9.0	0.1738		4.58	3.72	17.5	-0.0189			28.6
1.0	0.2708		-4.04	1.67	9.5	0.1456			2.99	18.0	-0.0186	33.28	28.13	26.7
1.5	0.3581			2.61	10.0	0.1199	7.38	3.15	2.01	18.5	-0.0180			25.1
2.0	0.4192	-10.22	0.57	3.21	10.5	0.0968			0.65	19.0	-0.0171		25.40	23.76
2.5	0.4580			3.67	11.0	0.0762		0.19	-1.26	19.5	-0.0160			22.44
3.0	0.4783		2.53	4.03	11.5	0.0581			-4.05	20.0	-0.0147	29.27	22.95	21.18
3.5	0.4834			4.33	12.0	0.0424	0.98	-6.42	-8.32	20.5	-0.0134			19.90
4.0	0.4763	-0.03	3.74	4.58	12.5	0.0289			-15.6	21.0	-0.0120		20.47	18.64
4.5	0.4597			4.79	13.0	0.0176		-27.11	-27.9	21.5	-0.0107			17.23
5.0	0.4359		4.56	4.94	13.5	0.0082			-71.4	22.0	-0.0093	24.27	17.54	15.74
5.5	0.4070			5.05	14.0	0.0005				22.5	-0.0081			13.92
6.0	0.3747	4.61	5.09	5.10	14.5	-0.0056				23.0	-0.0069		13.43	11.90
6.5	0.3404			5.10	15.0	-0.0103		63.6	62.9	23.5	-0.0058			9.67
7.0	0.3053		5.32	5.02	15.5	-0.0138			47.3	24.0	-0.0048	13.53	7.52	6.68
7.5	0.2704			4.87	16.0	-0.0162	42.4	39.9	39.2	24.5	-0.0039			3.20
8.0	0.2365	7.15	5.20	4.61	16.5	-0.0178			34.3	25.0	-0.0031		-2.21	-1.24

Fig. (V-IV-24) Elasticity Sol.

EDGE R FORCE

M-MOMENT (M_θ) = $\alpha_6 \left(\frac{Rp}{100}\right)$

R/t = 500

μ = 0.0

} Table (V-IV-23)

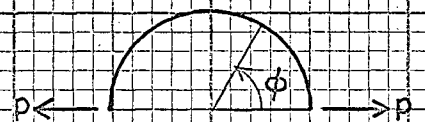

Fig. (V-IV-25) Elasticity Sol.

EDGE R FORCE

M-MOMENT (M_θ) = $\alpha_6 \left(\frac{Rp}{100}\right)$

R/t = 500

μ = 0.2

} Table (V-IV-24)

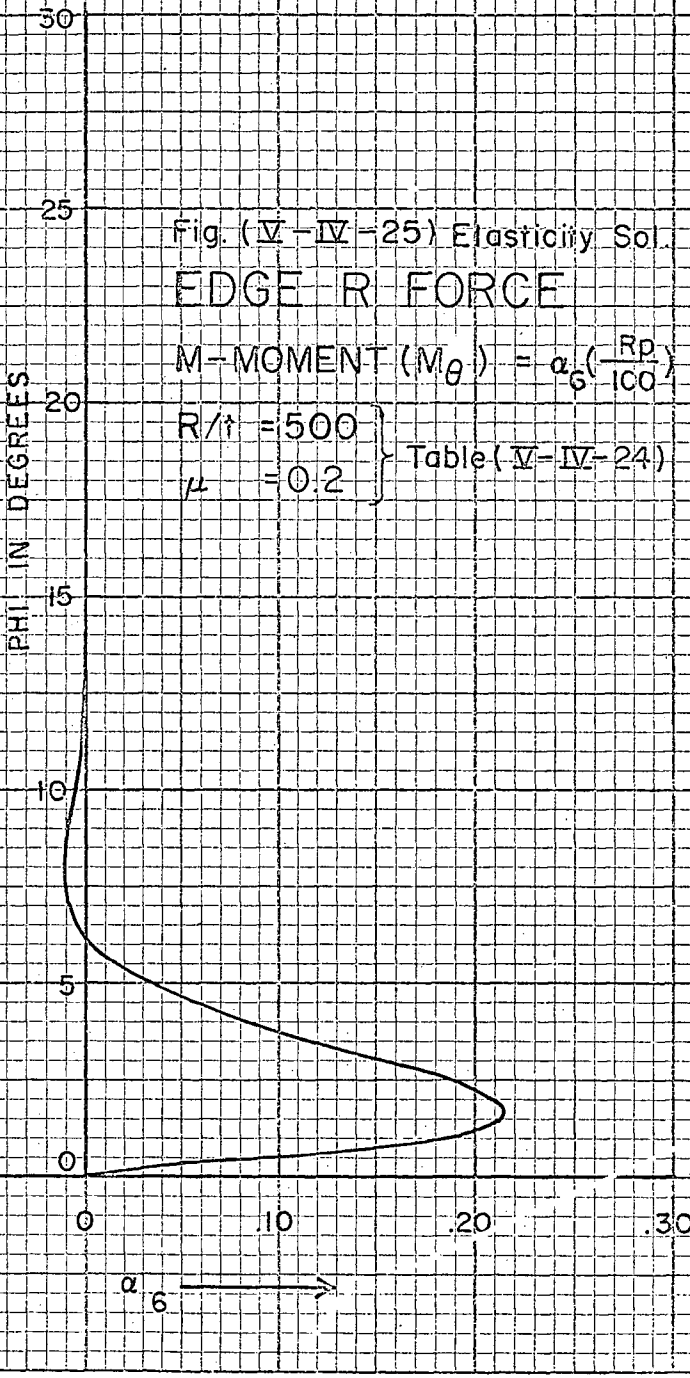

Table (V-IV-23) Hemispherical Dome - Radial Load Along the Edge

M-Moment/Length, $(M_\theta) = \alpha_6(pR/100)$

$\mu = 0.0$; $R/t = 500.0$ (Fig. (V-IV-24))

	Elasticity Solution	Percentage Error				Elasticity Solution	Percentage Error		
$\phi°$	α_6	$\theta_e=\phi_e$ =2°	$\theta_e=\phi_e$ =1°	$\theta_e=\phi_e$ =0.5°	$\phi°$	α_6	$\theta_e=\phi_e$ =2°	$\theta_e=\phi_e$ =1°	$\theta_e=\phi_e$ =0.5°
0.0	0.0000	0.00	0.00	0.00	8.5	0.0001			3.60
0.5	-0.0005			-7.50	9.0	0.0001		15.00	2.00
1.0	-0.0008		-17.9	-4.51	9.5	0.0001			6.67
1.5	-0.0010			-2.93	10.0	0.0000			
2.0	-0.0010	-29.2	-5.76	-1.11					
2.5	-0.0009			0.00					
3.0	-0.0007		8.21	1.94					
3.5	-0.0004			5.00					
4.0	-0.0002		45.00	10.45					
4.5	+0.0000			76.7					
5.0	0.0001		-73.3	-20.0					
5.5	0.0002			-6.19					
6.0	0.0003	-82.3	-15.0	-2.69					
6.5	0.0003			0.37					
7.0	0.0003		-1.54	0.00					
7.5	0.0002			0.00					
8.0	0.0002	24.74	5.26	0.00					

Table (V-IV-24) Hemispherical Dome - Radial Load Along the Edge

M-Moment/Length, $(M_\theta) = \alpha_6(pR/100)$

$\mu = 0.2$; $R/t = 500.0$ (Fig. (V-IV-25))

	Elasticity Solution	Percentage Error				Elasticity Solution	Percentage Error				Elasticity Solution	Percentage Error		
$\phi°$	α_6	$\theta_e=\phi_e$ =2°	$\theta_e=\phi_e$ =1°	$\theta_e=\phi_e$ =0.5°	$\phi°$	α_6	$\theta_e=\phi_e$ =2°	$\theta_e=\phi_e$ =1°	$\theta_e=\phi_e$ =0.5°	$\phi°$	α_6	$\theta_e=\phi_e$ =2°	$\theta_e=\phi_e$ =1°	$\theta_e=\phi_e$ =0.5°
0.0	0.0000	0.00	0.00	0.00	8.5	-0.0083			6.10	17.0	0.0001		4.44	-1.11
0.5	0.1334			-7.50	9.0	-0.0069		12.36	5.74	17.5	0.0000			
1.0	0.2002		-14.33	-2.87	9.5	-0.0054			5.30	18.0	0.0000			
1.5	0.2202			-1.09	10.0	-0.0039	50.41	11.65	4.61					
2.0	0.2102	-22.33	-3.53	-0.05	10.5	-0.0027			3.72					
2.5	0.1831			0.66	11.0	-0.0016		7.38	1.52					
3.0	0.1485		1.56	1.19	11.5	-0.0009			-2.79					
3.5	0.1129			1.57	12.0	-0.0003	4.67	-23.00	-16.33					
4.0	0.0802	16.24	5.15	1.81	12.5	0.0001								
4.5	0.0525			1.85	13.0	0.0003		52.59	27.78					
5.0	0.0306		8.22	1.55	13.5	0.0004			19.19					
5.5	0.0144			0.24	14.0	0.0004		30.75	14.00					
6.0	0.0032		15.25	-9.10	14.5	0.0004			13.24					
6.5	-0.0038			13.46	15.0	0.0003		25.31	10.94					
7.0	-0.0077		9.71	8.16	15.5	0.0002			12.00					
7.5	-0.0092			7.00	16.0	0.0002	95.8	21.05	8.95					
8.0	-0.0092	28.56	11.63	6.42	16.5	0.0001			9.23					

CHAPTER VI

DISCUSSION

In deriving the element stiffness matrix by the statics approach, prorating of boundary stresses into equivalent forces at the immediately adjacent corners results in an asymmetric stiffness matrix. Asymmetry of the stiffness matrix contradicts Betti's reciprocal theorem - valid for all linearly elastic bodies subject to superposition. However, the approach has the following advantages:

(i) The procedure of prorating the edge stresses to yield nodal forces is clearly defined.

(ii) The process is formulated as a sequence of operations on matrices composed of relatively simple expressions. This makes it possible to derive the stiffness matrix in an explicit algebric form.

and

(iii) The significance of a nodal force is more than being merely a number of computation. The nodal force is statically equivalent to the adjoining edge stresses. The edges which are not adjacent to the corner point do not contribute towards the nodal force at the corner in question.

However, it is important to note that in conditons of uniform stress or bending, the nodal forces do satisfy Betti's reciprocal theorem

irrespective of the size and exact shape of the trapezoidal element. As the element size decreases, the state of stress in the vicinity of an element becomes more and more uniform. Thus, in the limit the reciprocal theorem is in fact satisfied. It is also worth noting that when a trapezoid is reduced to a rectangle, the asymmetry of the plane stress and flexure matrices disappears. Apparently, the asymmetry of the stiffness matrices reflects the lack of symmetry of the trapezoid element itself about one of its axes.

In order to simplify the computation work, the asymmetric matrix is made symmetrical by averaging the matrix and its transpose. The terms of the resultant symmetric matrix satisfy the equilibrium requirements. The process of averaging is thus equivalent to introducing additional self equilibrating nodal forces in each mode.

The energy approach uses a systematic procedure for stiffness matrix computation and in all cases yields a symmetric matrix. However, the approach suffers from the following drawbacks:

(i) For complicated shapes of a finite element, evaluation of the component matrix

$$[H] = \iint_{area} [G]^T [D] [G] dxdy$$

required in the calculation of the stiffness matrix (Eqns. (II-27,b) and (III-25), is not always possible without using the computer.

and

(ii) Matrix multiplication to obtain element stiffness matrix (Eqns. (II-27,b) and (III-25)),

$$[K] = [A^{-1}]^T [H] [A^{-1}]$$

involves long expressions and thus, invariably needs to be done in the computer. In such a case, the stiffness coefficients are merely numbers and as such have no physical significance.

Using the statics approach, a symmetric stiffness matrix for a rectangular element in flexure was independently derived elsewhere.[23,37] It was observed that, in general, the Statics matrix will yield better results than the Energy stiffness matrices.[17,27]

Errors in the finite element analysis of a shell are due to approximating the curved shell surface by flat elements, replacing the distributed load by approximately calculated nodal loads and preserving the continuity of the model at the nodes only. However, as the element size decreases, the model imitates the shell conditions more closely thereby reducing the errors.

In shells with positive curvatures in both principal directions and with the load of distributed nature, the load carrying stresses are the membrane stresses except near the supports whose reactions develop components in R-direction. In this case flexural stresses may take on some load carrying function, even though it may be comparatively minor. Thus, normally the flexure stresses are simply the participation stresses having little or no effect on the load carrying capacity of the structure. In spite of this minor role of flexure, the unit flexural stresses (#/in^2) may be quite significant and may cause a nonreinforced or reinforced concrete or stone shell to crack. The shell also is likely to develop significant flexure stresses near concentrated or sharply localised loads. The thinner the shell is (i.e. the greater the radius to thickness ratio is) the smaller the region is near the support or near the localized load within which the

flexure stress is significant. In this region, smaller sized elements possessing both plane stress and flexure properties must be used in order to obtain a reasonably good representation of displacements and stresses. In regions father away from the boundaries or localized loads, the shell action is largely membrane. In this region elements of larger size are fully acceptable.

The shell is first analysed with elements of fairly large size. The region which needs to be finely subdivided is separated from the rest of the shell by the boundaries whose displacements at the nodes have already been calculated fairly accurately. The finely subdivided region is analysed by assigning the calculated displacements at the boundaries. The displacements at the intermediate nodes of the boundaries are interpolated. In cases when flexure properties of the elements must be used a three stage solution, described earlier, is suggested. The size of mesh necessary to obtain a reasonable representation of displacements and stresses is not directly obvious. It depends on the problem and is determined largely by judgement.

Calculation of shell stresses by the displacement method is cumbersome. Calculation based on statics and consisting in distributing the nodal forces over the tributary areas provides fairly accurate results in regions where stress gradients are not very steep. Where steep stress gradients are present, small element size improves the results. In general, higher percentage error in stresses than in displacements is expected.

Results of the numerical analysis on a variety of problems confirm the suitability of flat elements for solving problems involving shells of revolution with positive curvatures. Stresses and displacements are

calculated with good accuracy by using either Statics or Energy stiffness matrices. From the error analysis of the various problems presented, convergence of displacements and stresses to their exact elasticity values is indicated on reduction of the element size. It is expected that the method is equally applicable to the general case of shells of revolution which includes structures with reversed curvature.

CONCLUSION

A circular plate subjected to a pair of diametrically opposite point loads and a spherical shell subjected to snow load, wind load, and radial edge load are analysed with good accuracy for both membrane and flexure stresses using flat equilateral trapezoids and isosceles triangle elements. The method may be applied to a shell of revolution of an arbitrary shape subjected to any loading and provided with any boundary conditions, with an expectation of results of comparable precision.

Three values of Poisson's ratio (0.0, 0.2 and 1/3) are used in solution involving Statics and Energy stiffness matrices. There is no reason to doubt the applicability of the method with other values of Poisson's ratio.

In the spherical shell supporting a load of distributed nature, the load carrying stresses are the membrane stresses except near sharply localised loads or near the supports having reaction in R-direction where the flexural stresses become to some extent the load carrying stresses. Similar load carrying behaviour may be expected from a shell of revolution having positive curvatures in both principal directions.

In the problems analysed, the Statics and Energy stiffness matrices provide, on the whole, comparable accuracy.

In regions of rapidly changing displacements and stresses, small sized elements are necessary to obtain a fair accuracy of the results.

On reduction of the element size, the errors in stresses and in displacements decrease consistently. Convergence to the exact elasticity values is expected on further decrease of fineness of mesh without limit, apart from possible effects of the rounding off errors of the computer.

REFERENCES

1. Fletcher, B., "A History of Architecture," Seventeenth edition, Athlone Press, 1961, pp 197-199.

2. Anon, "Dome Shell Roofs," AIA file: 4-a, Published by Portland Cement Association, Chicago, Illinois.

3. Meyer, R.R., and Harmon, M.B., "Conical Segment Method for Analysing Open Crown Shells of Revolution for Edge Loadings," AIAA Journal, Vol. 1, No. 4, April 1963, pp 886-891.

4. Grafton, P.E., and Strome, D.R., "Analysis of Axisymmetric Shells by the Direct Stiffness Method," AIAA Journal, Vol. 1, No. 10, October 1963, pp 2342-2347.

5. Popov, E.P., Penzien, J., and Lu, Z.A., "Finite-Element Solution for Axisymmetrical Shells," ASCE Eng. Mech. Div. Journal, October 1964, pp 119-145.

6. Jones, R.E., and Strome, D.R., "Direct Stiffness Method of Analysis of Shells of Revolution Utilizing Curved Elements," AIAA Journal, Vol. 4, No. 9, September 1966, pp 1519-1525.

7. Percy, J.H., Pian, T.H.H., Klein, S., and Navaratna, D.R., "Application of Matrix Displacement Method to Linear Elastic Analysis of Shells of Revolution," AIAA paper No. 65-142, January 1965.

8. Jones, R.E., and Strome, D.R., "A Survey of Analysis of Shells by Displacement Method," AFFDL-TR-66-80, 'Matrix Methods in Structural Mechanics', November 1966, pp 205-219.

9. Turner, M.J., Clough, R.W., Martin, H.C., and Topp, L.J., "Stiffness and Deflection Analysis of Complex Structures," Journal of Aeronautical Sciences, Vol. 23, No. 9, September 1956, pp 805-854.

10. Greene, B.E., Strome, D.R., and Weikel, R.C., "Application of the Stiffness Method to the Analysis of Shell Structures," ASME paper No. 61-AV-58, March 1961.

11. Adini, A., "Analysis of Shell Structures by the Finite Element Method," Ph.D. Dissertation, University of California, Berkeley, California, 1961.

12. Antebi, J., Rossow, E.C., Shah, I.K., and Shah, J.M., "Computer Analysis of the F-111 Wing Assembly," ASCE Struct. Div. Journal, December 1966, pp 405-425.

13. Gallagher, R.H., "A Correlation Study of Methods of Matrix Structural Analysis," The MacMillan Co. 1964.

14. Clough, R.W., "The Finite Element Method in Structural Mechanics," Chapter 7, 'Stress Analysis' edited by Zienkiewicz and Holister, John Wiley and Sons Ltd., 1965.

15. Jones, R.E., "A Generalization of the Direct Stiffness Method of Structural Analysis," AIAA Journal, Vol. 2, No. 5, May 1964, pp 821-826.

16. Melosh, R.J., "Development of the Stiffness Method to Define Bounds on Elastic Behaviour of Structures," Ph.D. Thesis, Department of Civil Engineering, Univ. of Washington, Seattle, June 1962.

17. Melosh, R.J., "Basis for Derivation of Matrices for the Direct Stiffness Method," AIAA Journal, July 1963, pp 1631-1637.

18. Irons, B.M., and Draper, K.J., "Inadequacy of Nodal Connections in a Stiffness Solution for Plate Bending," AIAA Journal, Technical Note, May 1965, page 961.

19. DeVeubeke, B.F., "Duality between displacement and equilibrium methods with a view to obtaining upper and lower bounds to static influence coefficients," Proc. 14th Meeting of AGARD 'Structures and Material Panel'. Paris, July 1962, AGARDograph 72.

20. Clough, R.W., "The Finite Element Method in Plane Stress Analysis," Proc. 2nd ASCE Conference on Electronic Computation, Pittsburg, Pa., September 1960, pp 345-377.

21. Bazeley, G.P., Cheung, Y.K., Irons, R.M., and Zienkiewicz, O.C., "Triangular Elements in Plate Bending - Conforming and Nonconforming Solutions," AFFDL-TR-66-80, November 1966, pp 547-576.

22. Zienkiewicz, O.C., "The Finite Element Method in Structural and Continuum Mechanics," McGraw Hill, 1967. pp 21-25.

23. Hrennikoff, A., "The Finite Element Method Applied to Plane Stress and Bending of Plates," Lecture notes.

23a. Hrennikoff, A., "The Finite Element Method in Application to Plane Stress," Vol. 28, I.A.B.S.E., to be Published in 2nd half of 1968 volume.

24. Timoshenko, S., and Goodier, J.N., "Theory of Elasticity," 2nd edition, McGraw Hill, 1951.

25. Perlis, S., "Theory of Matrices," Addison-Wesley Publishing Co., 1958 page 86.

26. Timoshenko, S., and Woinowsky-Kreiger, S., "Theory of Plates and Shells." McGraw Hill Book Co., second edition, 1959.

27. Zienkiewicz, O.C., and Cheung, Y.K., "The finite element method for analysis of elastic, isotropic and orthotropic slabs," Proc. Inst. Civil Engrs. (London), 28, April 1964, pp 471-487.

28. Tocher, J.L., "Analysis of Plate Bending Using Triangular Elements," Ph.D. Dissertation, Univ. of California, Berkeley, 1962.

29. Gallagher, R.H., and Huff, R.D., "Derivation of the Force-Displacement Properties of Triangular and Quadrilateral Orthotropic Plates in Plane Stress and Bending," Bell Aerosystems Co., Report No. D2114-950005, 1964.

30. Shah, J.M., "A Finite Element Technique for the Analysis of Thin Shells and Plates," Simpson-Gumpertz and Heger Inc., Cambridge Massachusetts, 1966.

31. Tezcan, S.S., discussion of "Simplified Formulation of Stiffness Matrices," by P.M. Wright, Journal of the Struct. Div. ASCE, Vol. 89, No. ST 6, December 1963, pp 445-449.

32. Faddeeva, V.N., "Computational Methods of Linear Algebra," Dover Publication, 1959, pp 81-85.

33. Hrennikoff, A., and Tezcan, S.S., "Analysis of Cylindrical Shells by the Finite Element Method," 'Symposium on Problems of Interdependence of Design and Construction of Large Span Shells for Industrial and Civic Buildings,' USSR, Lenningrad, 6-9 September 1966.

34. Muskhelishvili, N.I., "Some Basic Problems of the Mathematical Theory of Elasticity," Translated from the Russian by J.R.M. Radok, P. Noordhoff Ltd., 1963, pp 330-338.

35. "BETON=KALENDER", Taschenbuck fur Beton und Stahlbetonbau sowie die Verwandten Facher, Zweiter Teil, Berlin 1958, pp 56-96.

36. Flugge, W., "Stresses in Shells," Second Printing, Springer-Verlag, Berlin, 1962.

37. Agrawal, K.M. and Hooley, R.F., "Finite Element Solution of a Plate Bending Problem," Publication Pending.

38. Turner, M.J., Clough, R.W., Martin, H.C., and Topp, L.J., "Stiffness and Deflection Analysis of Complex Structures," Journal of the Aeronautical Sciences, Vol. 23, No. 9, September 1956, pp 805-823.

39. Pfluger, A., "Elementary Statics of Shells," 2nd Edition, McGraw-Hill Book Co., 1961.

APPENDIX

BRIEF DESCRIPTION OF COMPUTER PROGRAMS AND FLOW DIAGRAMS

Description of PR-I: This program is intended to read the structure data from cards, to assign deformation numbers to the joints, to assign corner numbers to the elements, to calculate code nos. of each element, and to calculate stiffness matrix in element coordinates, transformation matrix and transformed stiffness matrix of each typical element. The above information is stored in Tapes 3 and 4. PR-I calls two subroutines; SM3 and SM4. These subroutines calculate element stiffness matrix in element coordinates, transformation matrix and transformed stiffness matrix for triangular and trapezoidal elements respectively. These subroutines employ either Statics or Energy stiffness matrices. For analysing a membrane shell, subroutines using only the plane stress properties of the finite element are used. For a shell having flexure properties these subroutines are simply externally replaced by those which include both plane stress and flexure properties of the finite element.

SIMPLIFIED FLOW DIAGRAM

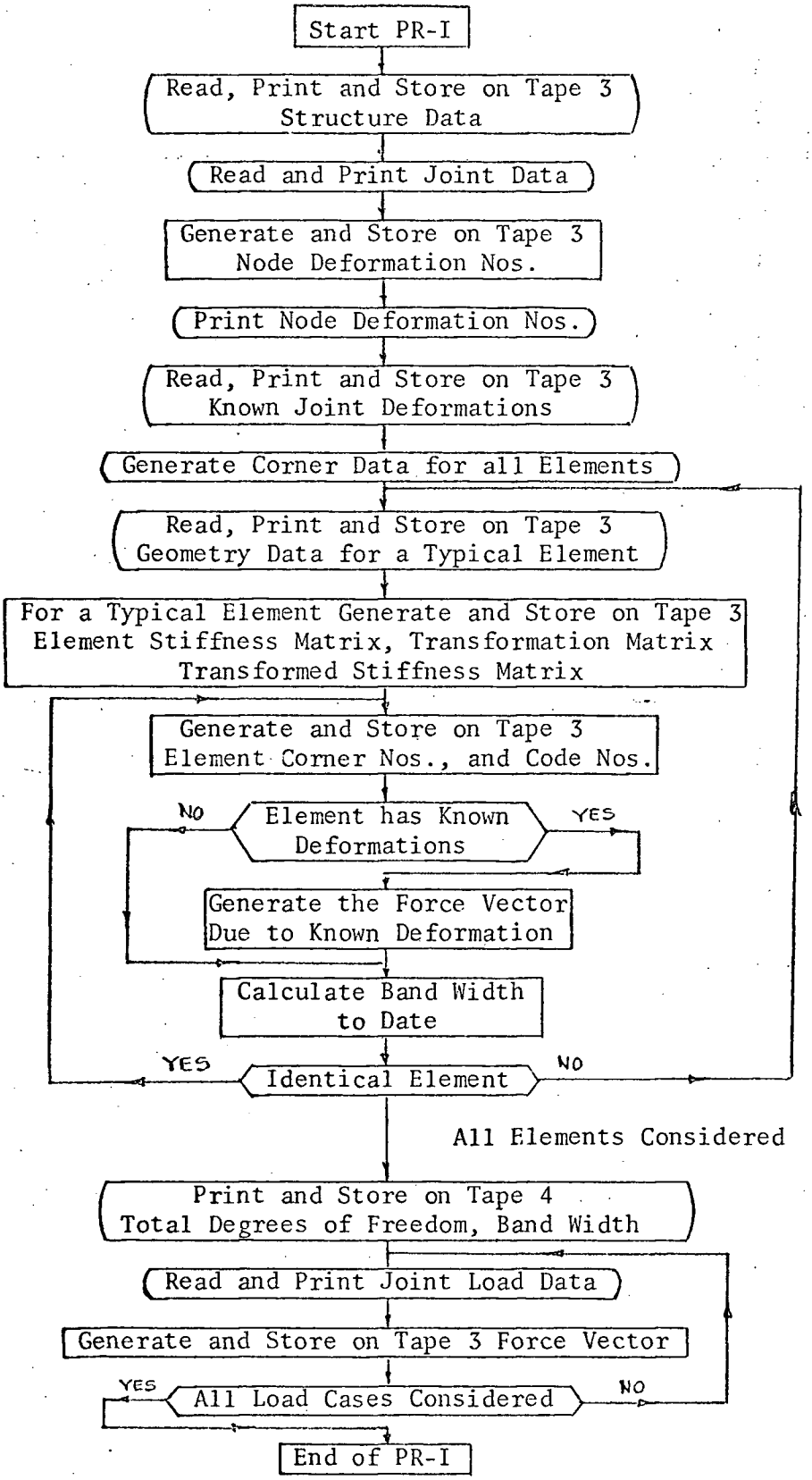

Description of PR-II: This program is intended to read the structure data from tapes 3 and 4, generate the structure stiffness matrix and solve the system of simultaneous linear equations by Choleski's method. The Choleski's method of solution was originally programmed by Dr. R. F. Hooley for ALP II - a program for solving two dimensional frames on IBM 1620.

The system of simultaneous equations are solved for all load cases and the deformation vectors are written on tape 4.

No data is required to execute the program.

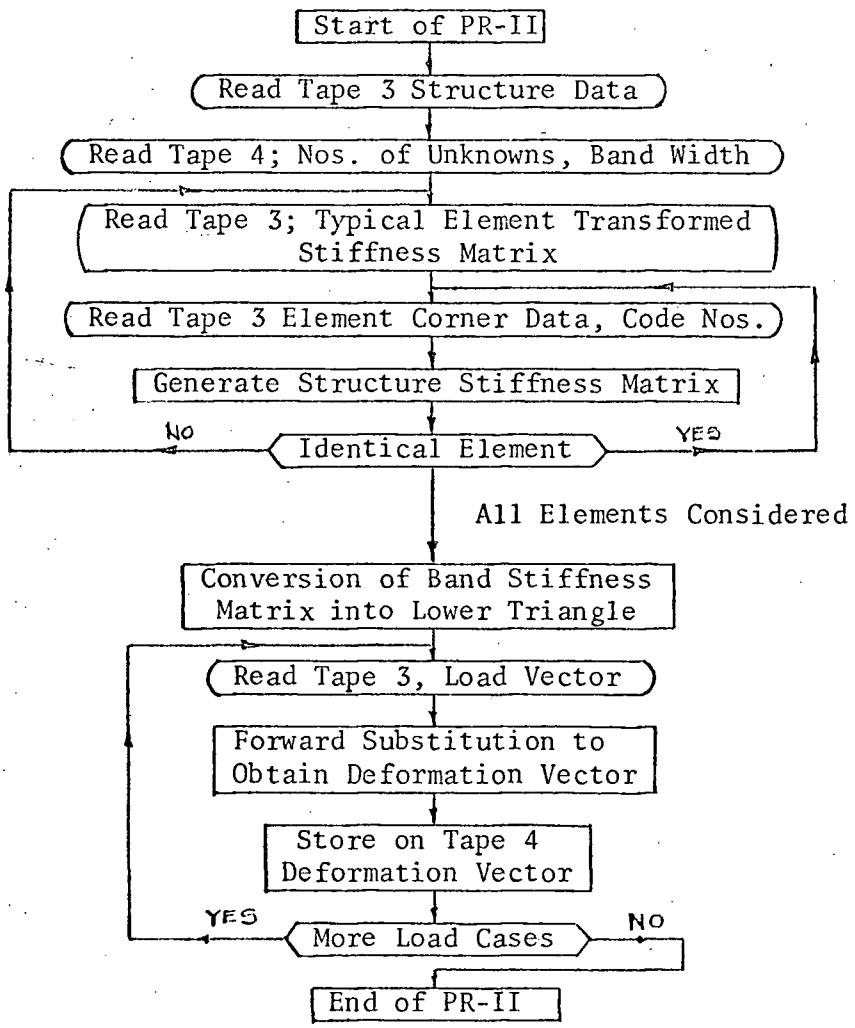

Description of PR-III: This program is intended to read structure data and shell deformation data from tapes 3 and 4, assign deformations to various joints and calculate nodal forces in various elements. Deformations at various joints and element nodal forces are obtained as printed out-put and are also stored on disk 10.

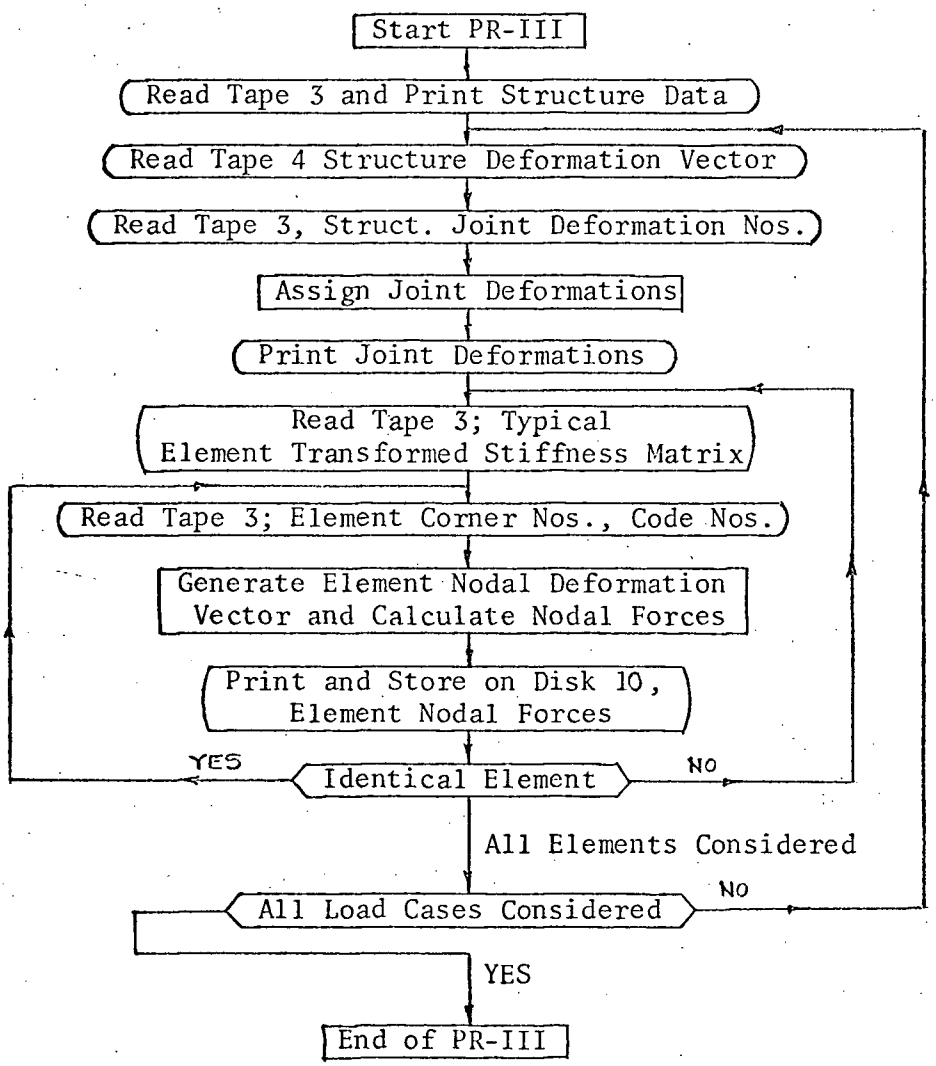

Description of PR-IV This program is intended to read the nodal force concentrations from tape 10 (calculated and stored there by PR-III). Elements connecting a particular joint are supplied as data to calculate stress resultants at that joint.